

Impacts of water residence time on lake thermal structure: implications for management and climate change



Freya Olsson BSc

This thesis is submitted for the degree of Doctor of Philosophy

2021

Lancaster University

Lancaster Environment Centre



UK Centre for
Ecology & Hydrology



Declaration

I declare that this thesis has not been submitted in support of an application for another degree at this or any other university. It is the result of my own work and includes nothing that is the outcome of work done in collaboration except where specifically indicated. Many of the ideas in this thesis were the product of discussion with my supervisors; Ian Jones, Eleanor Mackay, Phil Barker, Bryan Spears, Sian Davies, and Ruth Hall.

Signed:

Date: 29/09/2021

Freya Olsson BSc

Lancaster University, UK

Statement of authorship

Chapters 4-7 are presented in the style of papers, one has been published and one is under review. FO is first author on all data chapters, carrying out the data collection, completing the data analysis, running the hydrodynamic modelling experiments, and co-designing the studies.

Abstract

Lakes provide globally important ecosystem services. However, the dual threats of eutrophication and climate change threaten lakes' ability to provide these services. Water residence time (WRT), the ratio between lake volume and discharge, is important for lake functioning, affecting nutrient loading, time available for biogeochemical processes, and flushing of biota. WRT manipulations have been proposed as a novel management intervention to restore eutrophic lakes by inhibiting seasonal stratification and thereby preventing hypolimnetic anoxia and associated internal loading. However, the impact of WRT on lake thermal structure is not well understood, and the contribution of inflows to lake heat budgets are often overlooked. Changes to WRT are also relevant in a climate change context. River flow changes, driven by evaporation and precipitation changes, are projected for more than three-quarters of the landmass. This thesis uses long-term and high-frequency data from a small UK lake, alongside hydrodynamic modelling to examine the extent to which management and climate-induced WRT changes could affect lake thermal structure and subsequent impacts on lake function.

Results reveal that annual WRT changes impact lake temperatures year-round, with the direction of change seasonal. Shorter WRT caused cooling in the summer and warming in the winter. Annual WRT reductions failed to inhibit stratification, only weakening stability, and hypolimnetic anoxia persisted. However, results showed that reductions in WRT were enhancing deep-water oxygenation and that strategic sub-seasonal management could potentially control internal loading. WRT changes during the summer stratified period were associated with short-term reductions in water column stability, increased vertical mixing, and replenishment of deep-water oxygen. Results also highlighted that in the northwest of England, river flow changes are likely to be exacerbating air temperature warming impacts on lakes. Failing to account for future WRT changes could be underestimating the impact of climate change, in a multitude of short-residence time lakes.

Acknowledgements

Firstly, I would like to say a huge thank you to my supervisory team (Bryan, Phil, Sian, and Ruth) for their support over the last four years, their help has been invaluable to my PhD research and my development as a researcher. I am particularly grateful to Ian Jones and Ellie Mackay for their constant encouragement and assistance, without which this PhD would not have been possible, I feel so fortunate to have had you as supervisors.

This research would not have been possible without the financial input from the NERC Envision Doctoral Training Partnership.

I am also grateful to the members of the Lakes Ecosystem Group at UKCEH who have been a great group to be part of throughout my PhD journey. They have provided me with invaluable technical expertise, as well as a good chat, and moral support. I would also like to thank the UKCEH Inorganic Analytical Chemistry team for their extensive training and allowing me to use their lab facilities. A special thanks is reserved for Binoti Tanna, for her patience and conversation during the long days in the lab.

I am thankful to the numerous volunteers who came out in all weathers to assist with my fieldwork. Vincent, Ellen, Kate, Jade, Lise, Emma, Katie, Liz, Daniel, Victoria, Zoe, Abi, Greer, Elena, and Nye – thank you! Thanks also to the Environment Agency and South Cumbrian Rivers' Trust for providing river flow and water quality data vital for the completion of this project.

Finally, I would like to thank my friends and family for their help and support throughout my PhD. In particular, I would like to thank Giles Exley, Charlotte Smith, and Ben Taylor for keeping me sane and being an integral part of making this PhD experience a good one. To my mum and dad, I will be forever grateful for your confidence in me as well as your unwavering support, love, and wisdom, I couldn't have done this without you.

Contents

Chapter 1	Introduction	16
1.1	Thesis focus	18
1.2	Thesis structure.....	20
Chapter 2	Background and context	21
2.1	Overview	21
2.2	Importance of lake systems	21
2.3	Water residence time	22
2.4	Lake physics and heat fluxes	36
2.5	Climate change impacts on lake thermal dynamics.....	46
2.6	Deep water oxygen dynamics and internal loading.....	50
2.7	Lake management.....	55
2.8	Summary	59
Chapter 3	Methodology and site description	61
3.1	Study site.....	61
3.2	Field monitoring – primary data	67
3.3	Field monitoring – secondary data	70
3.4	Modelling methods.....	74
Chapter 4	Can reductions in water residence time be used to disrupt seasonal stratification and control internal loading in a eutrophic monomictic lake?	77
4.1	Abstract.....	77
4.2	Introduction	78
4.3	Methods and materials.....	81
4.4	Results.....	88
4.5	Discussion.....	94
4.6	Conclusions	98
4.7	Supplementary information for Chapter 4	99

Chapter 5	Annual water residence time effects on thermal structure: a potential lake restoration measure?.....	114
5.1	Abstract	114
5.2	Introduction.....	114
5.3	Methods	117
5.4	Results	124
5.5	Discussion	129
5.6	Conclusions.....	133
5.7	Supplementary information for Chapter 5.....	134
Chapter 6	Hypolimnetic reoxygenation during seasonal anoxia is related to inflow events in a small temperate lake.....	139
6.1	Abstract	139
6.2	Introduction.....	139
6.3	Methods	142
6.4	Results	147
6.5	Discussion	159
6.6	Conclusions.....	163
6.7	Supplementary information for Chapter 6.....	164
Chapter 7	Dual climate threats of air temperature and inflow change impact the thermal structure of small temperate lakes	170
7.1	Abstract	170
7.2	Introduction.....	170
7.3	Materials and methods	173
7.4	Results	179
7.5	Discussion	188
7.6	Conclusions.....	193
7.7	Supplementary information for Chapter 7.....	194
Chapter 8	Discussion	200

8.1	WRT impacts on lake thermal dynamics.....	201
8.2	WRT as a management tool.....	207
8.3	Impacts of climate change on lake temperatures	212
8.4	Methods.....	217
Chapter 9	Conclusions and future work	224
9.1	Thesis conclusions.....	224
9.2	Areas of potential future research.....	226
Bibliography	228

List of Tables

Table 2.1 Example of sources of surface, groundwater, and atmospheric components of the lake water budget	25
Table 2.2 Lake mixing regime types (after Lewis 1983), plus the additional classification of meromictic.	42
Table 3.1 Morphometric characteristics of the three basins of Elterwater (from Goldsmith et al., 2003; Maberly et al., 2016)	61
Table 3.2 Percentage (%) missing in the 2012-2019 meteorological data and the linear regression between Blelham and Windermere buoy data variables (2012-2019)	73
Table 3.3 The maximum, minimum and final parameters values, optimised during the auto-calibration route. Model performance statistics for the calibration (2018) and validation (2019) periods reported as root mean squared error, Nash-Sutcliffe efficiency and mean absolute error.....	76
Table 4.1 Hydromorphometric and physiochemical comparison of Impact and Control sites. Data from 2015 Lakes Tour (Maberly et al., 2016) and Haworth et al. (2003).	82
Table 4.2 The maximum, minimum and final parameters values, optimised during the auto-calibration route. Model performance statistics for the calibration (2018) and validation (2019) periods reported as root mean squared error, Nash-Sutcliffe efficiency and mean absolute error.....	87
Table 4.3 Summary of the water residence time, water temperatures and stratification metrics for the two modelled scenarios (2016-2019 with and with intervention) compared with the natural variability in parameters (2012-2019 without intervention). Values show the mean and the range (minimum – maximum).	90
Table 4.4 Before-After-Control-Impact (BACI) analysis results using a two-way Analysis of Variance including the effect of the interaction of Period (Before and After) and season on mean difference between lakes (Elterwater – Blelham). Where a significant interaction was found, post-hoc analysis of contrasts was done to look at Period effect in individual seasons. Bold face and asterisks denote significant results at the 0.05 (*) level.	93
Table 5.1 Data collected at Elterwater and Blelham Tarn for model boundary conditions ..	119
Table 5.2 Parameters optimised during the calibration route. The maximum, minimum and final parameter values are shown.....	121
Table 5.3 Seasonal mean discharge, water residence time (WRT), inflow-lake temperature differences, extreme low (Q95) and high (Q5) flow percentiles and advective (Q_{adv}) and total	

surface heat (Q_{surf_tot}) fluxes in Elterwater inner basin under unchanged conditions. Values in brackets show the median values of flow parameters.....	124
Table 7.1 Hydromorphometric characteristics of the inner basin of Elterwater (Elterwater-IB). Data from 2015 Lakes Tour (Maberly et al., 2016) and Haworth et al. (2003).....	173
Table 7.2 The maximum, minimum and final parameters values, optimised during the auto-calibration route. Model performance statistics for the calibration (2018) and validation (2019) periods reported as root mean squared error, Nash-Sutcliffe efficiency and mean absolute error.	176

List of Figures

Figure 1.1 Structure of the thesis chapters.....	20
Figure 2.1 Relationship between rates of growth (τ_{growth}) and loss (τ_{loss}) determines the effect of WRT on phytoplankton biomass (B^*). Orange = where loss > growth, blue = growth > loss. Moving horizontally across the graph from left to right indicates increasing WRT (T^*_{tran}).	34
Figure 2.2 Reservoir zooplankton community is controlled by the direct dilution and transport effects of WRT (right side) and by modification of environmental quality and biotic interactions (left side) (Threlkeld, 1982).	35
Figure 2.3 Components of the heat exchange between a lake and the environment (from Schmid and Read, 2021).....	37
Figure 2.4 Conceptual temperature profile during a stratified period, comprised of an isothermal epilimnion (mixed layer), the cooler mixed hypolimnion, separated by a metalimnion, with a steep temperature gradient.	41
Figure 2.5 Relationship between water temperature and water density. Maximum density is at 3.94 °C. Water densities calculated using rLakeAnalyzer R package (version 1.11.4.1; Read et al., 2011).....	41
Figure 2.6 Influence of the euphotic depth (Z_{eu}) and mixed layer (Z_{mix}) on the vertical distribution of phytoplankton biomass (modified from Thornton et al., 1990).	45
Figure 3.1 Map of Elterwater with its major inflow and outflows labelled. Approximate location of the flow diversion, implemented in 2016, is shown with a dashed line.....	62
Figure 3.2 Average climate at Newton Rigg meteorological station. Points show mean values and error bars are ± 1 standard deviation of climate variable measured. N represents the number of monthly measurements from the period 1960 – 2021. Sunshine duration data were collected from 1960 – 1981 only.....	63
Figure 3.3 Daily average water temperatures measured in the inner basin of Elterwater from May 2015 to December 2020.....	64
Figure 3.4 A) Chlorophyll a and B) total phosphorus concentrations in Elterwater’s three basins (inner, middle and outer) for the period 2012-2019. Dashed lines show the mean (chlorophyll and TP) and maximum (chlorophyll only) concentrations for eutrophic class (OECD). Data available on the UK Lakes Portal (at https://eip.ceh.ac.uk/apps/lakes/detail.html#wbid=29222) which uses Environment Agency water quality data from the Water Quality Archive (Beta) published under an Open Government Licence.	65

Figure 3.5 Photographs of the off-take structure (left) on the Great Langdale Beck and the discharge of the pipeline into a field drain which discharges into Elterwater inner basin (right).	67
Figure 3.6 Observations of the relationship between gauged outflow (River Brathay) and pipeline discharge. Blue line represents the fitted GAM model.	72
Figure 3.7 A) Prediction of water temperature based on the 12-hour rolling average air temperature. Points show observations and blue line the fitted linear model. B) Predicted vs observed inflow water temperatures using the linear model fit. Red line shows the 1-1 line.	72
Figure 4.1 Different aspects of the stratification → anoxia → internal P loading sequence are targeted by different in-lake restoration methods.....	79
Figure 4.2 Map of Elterwater with its major inflow and outflows labelled. Approximate location of the flow diversion, implemented in 2016, is shown with a dashed line and sampling locations with yellow circles.....	81
Figure 4.3 a) change in volume averaged water column temperature in each season, b) water temperature changes at different depths with the intervention. Positive values indicate warming and negative values cooling, compared to water temperatures without the intervention.	89
Figure 4.4 a) Total phosphorus, b) soluble reactive phosphorus and c) chlorophyll a concentrations in Elterwater-IB (impact) and Blelham (control) sites before and after intervention, annually and grouped by season.	91
Figure 4.5 a) average annual chlorophyll a dynamics (shading shows +/- 1 SE) and b) cumulative chlorophyll accumulation for each year before and after restoration at the control (Blelham) and impact (Elterwater-inner basin) lakes.....	92
Figure 4.6 Approximate volume of Elterwater-IB that is anoxic (< 2 mg L ⁻¹ , solid line) and concentration of biological available phosphorus (dashed lines) in the surface (0.5 m) and hypolimnion (6 m) based on profiles collected from May 2018 - December 2019.....	94
Figure 4.7 Diagnostic plots for two-ANOVAs fitted to water chemistry variables	104
Figure 5.1 Map of Elterwater. The main inflow (Great Langdale Beck) and outflow (River Brathay) are shown alongside the restoration diversion (dashed line). Elterwater inner basin, the modelled system, is highlighted.	118
Figure 5.2 A-D: Modelled and observed water temperatures for the calibration and validation periods. E-F model error, as the residual between observed and modelled water temperature.	122

Figure 5.3 Controls on the advective heat flux during the baseline scenario (2018) A) discharge and WRT and B) inflow-lake temperature difference. 125

Figure 5.4 A) General Additive Model fit to three-day average values comparing the advective heat flux (Q_{adv}) for 2018 at different annual water residence times and B) a General Additive Model fit to three-day average values of the baseline advective flux (Q_{adv}) and the total lake surface heat flux (Q_{surf_tot}), including labels of the impact of the advective flux on the total lake surface heat flux. The duration of the longest continuous stratified period under unmodified conditions is also shown..... 126

Figure 5.5 Change in volume averaged lake temperature across different seasons. Dotted lines represent unchanged AWRT. 127

Figure 5.6 A) Change to the length of the longest continuous stratified period. B) Dates of onset and overturn at different AWRT. The solid black lines indicate the period of continuous stratification. The grey shading covers June and July, which are stratified under all AWRTs tested. C) Percentage change to stratification strength (as Schmidt stability) during June and July. Dotted lines represent unchanged AWRT..... 128

Figure 5.7 A) Occurrence of inverse stratification, converted into days, at each AWRT; B) total occurrence of normal stratification, converted to days. Dashed lines indicate the unmodified AWRT..... 129

Figure 5.8 Conceptualisation of the timings of different management strategies proposed for Elterwater. Labelled numbers relate to the periods discussed in the text. Dashed line shows a smooth of the Schmidt stability under unmodified conditions. 133

Figure 6.1 Study site – Elterwater inner basin in the northwest of England, UK, with the location of the monitoring buoy indicated by the red circle. The dashed line shows the approximate location of the pipeline installed in 2016 to divert part of the main inflow into the inner basin from the Great Langdale Beck into the inner basin. 143

Figure 6.2 Identified dissolved oxygen replenishment events (green points) during the seasonal anoxic periods in 2018 and 2019 (DO no longer continuously $> 1 \text{ mg L}^{-1}$)..... 148

Figure 6.3 Inflow discharge during the two periods alongside the identified dissolved oxygen replenishment events at 5 m (points). 149

Figure 6.4 Total surface heat flux during the two periods alongside the identified dissolved oxygen replenishment events at 5 m (points). Negative surface heat flux represents surface cooling and positive heat flux surface warming..... 150

Figure 6.5 Wind power during the two periods alongside the identified dissolved oxygen replenishment events at 5 m (points). 151

Figure 6.6 Schmidt stability during the two periods alongside the identified dissolved oxygen replenishment events at 5 m (points).....	152
Figure 6.7 Vertical turbulent diffusivity (K_z) and inflow discharge during the two periods alongside the identified dissolved oxygen replenishment events at 5 m (points).	153
Figure 6.8 Proportion of days during the two identified periods in which there is a dissolved oxygen replenishment event at 5 m (as identified above) associated with different levels of A) inflow discharge, B) wind power, C) total surface heat flux, and D) Schmidt stability. Number of events are shown in the circles.	154
Figure 6.9 Relationship between inflow discharge and A) Schmidt stability flux, B) K_z , C) total surface heat flux, and D) wind power during the stratified periods. Green highlighted points indicate the dissolved oxygen replenishment events identified at 5 m. The results (R value, a significance) of the Spearman's Rank Correlation on differenced data are also shown above.	155
Figure 6.10 Identified high-discharge inflow events (blue) and dissolved oxygen replenishment events (green) during the seasonal anoxic periods in 2018 and 2019 (DO no longer continuously $> 1 \text{ mg L}^{-1}$).	156
Figure 6.11 Downwards flux of oxygen (black line) from 4 to 5 m during the seasonal anoxic period. The change in oxygen at 5 is also shown (green dashed) and the identified oxygen events at 5 m (points).	157
Figure 6.12 A) Water column and inflow (dashed) temperatures and B) Inflow intrusion depth estimated as the depth of the water column of equal density to the inflow during the two periods alongside the identified dissolved oxygen replenishment events at 5 m (points). ..	158
Figure 6.13 Chlorophyll a concentration at different depths in the water column. Concentrations at 5 m are shown with the black line. B) estimated photic depth (1% of surface light), and C) proportion of days during the two identified periods in which there is a dissolved oxygen replenishment event at 5 m. Green points on panels A and B show the dates of DO replenishment events at 5 m.	159
Figure 7.1 Map of Elterwater. The main inflow (Great Langdale Beck) and outflow (River Brathay) are shown alongside the pipeline diversion constructed in 2016 (dashed line). Elterwater inner basin, the modelled system, is highlighted.	174
Figure 7.2 Change in surface water temperature (SWT) for A) air temperature (T) change, individually, B) discharge (Q) change, individually and C) the combined effect of change in air temperature and discharge. Values represent the difference from unmodified air temperature and flow conditions. Grey shading on A) and B) shows ± 1 standard deviation around the mean.	180

Figure 7.3 The air-temperature equivalent change in surface water temperature (SWT) caused by discharge reductions in summer (A) and discharge increases in winter (B) for each air temperature scenario. Only discharge scenarios that induced lake warming are included (reductions in summer and increases in winter). The effect of discharge changes alongside a 4 °C air temperature warming (and 3.5 °C & -50% Q in summer) were beyond the temperature-only effect at 4 °C so cannot be interpolated. 181

Figure 7.4 Change in bottom water temperature (BWT) for A) air temperature (T) change, individually, B) discharge (Q) change, individually and C) the combined effect of changes in air temperature and discharge. Values represent the difference from unmodified air temperature and flow conditions. Grey shading on A) and B) show ± 1 standard deviation around the mean. 182

Figure 7.5 Change in summer Schmidt stability for each A) air temperature (T) change, individually, B) discharge (Q) change, individually and C) the combined effects of changes in air temperature and discharge. Values represent the difference from unmodified air temperature and flow conditions. Grey shading on A) and B) show ± 1 standard deviation around the mean. D) Air-temperature equivalent change in summer water column stability caused by discharge reductions for each air temperature scenario. The effect of discharge changes alongside a 4 °C air temperature warming (and 3.5 °C & -50% Q in summer) were beyond the temperature-only effect at 4 °C so could not be interpolated. 183

Figure 7.6 Change in length of the summer stratified period for each A) air temperature (T) changes, individually, B) discharge (Q) change, individually and C) the combined effect of air temperature and discharge changes. Values represent the difference from unmodified air temperature and flow conditions. Grey shading on A) and B) show ± 1 standard deviation around the mean..... 184

Figure 7.7 Change in the dates of onset and overturn of the summer-stratified period for A) air temperature (T) change and B) discharge (Q) changes. Panels C) and D) show the combined effects of air temperature and discharge changes on stratification onset and overturn dates, respectively. Values represent the difference from unmodified air temperature and flow conditions. Grey shading on A) and B) show ± 1 standard deviation around the mean. 185

Figure 7.8 Change in inverse stratification occurrence (number of hours) for each A) air temperature (T) change, individually, B) discharge (Q) changes, individually and C) the combined effect of air temperature and discharge changes. Values represent the difference from unmodified air temperature and flow conditions. Grey shading on A) and B) show ± 1 standard deviation around the mean 186

Figure 7.9 Change in summer mixed depth across different temperature and discharge scenarios using two different methods. Method 1 uses a modified version of rLakeAnalyzer and Method 2 uses a density difference of 0.1 kg m^{-3} to define the mixed depth. Negative values indicate a shallowing of the mixed depth and positive values a deepening. 187

Figure 7.10 Comparison of changes in lake surface water temperatures with and without the inclusion of changes to the inflow temperature in a) summer and b) winter. Difference represents the additional warming when the inflow temperature warming is included. 188

Figure 8.1 Common themes between data Chapters 4 -7 and the understanding generated from the conclusions of each. Numbers in brackets correspond to the sections of the discussion in which these themes are primarily discussed. 201

Figure 8.2 Theoretical impact of inflow discharge changes investigated in this thesis on lake functioning through its impact on the advective heat flux and lake heat budget. The theoretical system is shown in black with inferred responses (dashed). The processes impacted by management (blue) and climate change (purple) are also shown. 202

Figure 8.3 Suggested workflow to investigate and implement a success WRT manipulation restoration scheme, based on lessons learned in this thesis. 212

Figure 8.4 Example of how differential warming of lakes and rivers and reduced flow could impact the temperature difference between the lake and its inflow (arrow) and the potential depth of neutral buoyancy (depth of river intrusion)..... 215

Chapter 1 Introduction

Despite covering less than 2% of the global surface area (Messenger et al., 2016), lakes provide a number of essential ecosystem services to millions of people (Reynaud and Lanzasova, 2017; Schallenberg et al., 2013). Lakes deliver important provisioning services including fisheries and drinking water (Deines et al., 2017). Estimates suggest the global lake fishery harvest to be 8.4 million tonnes per year (Deines et al., 2017), which is 40% of total fisheries production, providing a vital protein source globally (Lynch et al., 2016). Cultural services provided by lakes include recreation, tourism, and navigation (Schallenberg et al., 2013). Across only 14 EU member states, blue-space recreation is estimated to be worth €631 billion (approximately £540 billion) per year (Börger et al., 2021). Lakes also provide support and regulatory services on global and regional scales (Downing et al., 2021). Processes including denitrification (Harrison et al., 2009; Seitzinger et al., 2006), carbon cycling (Evans et al., 2017; Toming et al., 2020), and long-term sequestration of nutrients and sediments (Harrison et al., 2009; Mendonça et al., 2017) and play a key role in biogeochemical cycles that regulate nutrient availability (Downing, 2010; Holgerson and Raymond, 2016; Toming et al., 2020), exemplified as their role as carbon sinks. Lakes are estimated to bury as much carbon in their sediments as that buried by the whole ocean over the same period (Mendonça et al., 2017; Raymond et al., 2013). Lakes are also crucial biodiversity hotspots (Tickner et al., 2020), providing habitat for one third of global vertebrate species (Strayer and Dudgeon, 2010) and large numbers of endemic species (Collen et al., 2014).

The ability of lakes to deliver these important ecosystem services is being degraded by excess anthropogenic nutrient addition and consequent eutrophication (Downing et al., 2021; Schallenberg et al., 2013). Eutrophication is a widespread and persistent problem (Smith and Schindler, 2009), characterised by excess algal growth, low oxygen conditions and increased turbidity. Eutrophication has socio-economic and environmental implications including additional water treatment costs, potential health threats for animals and humans, as well as recreation and tourism losses, estimated to amount to £173 million per year in the UK (Jones et al., 2020). Additionally, eutrophication increases greenhouse gas emissions, globally estimated to cost up to \$81 trillion (£59 trillion) between 2015 and 2050 (Downing et al., 2021) based on the global social cost.

A key water quality problem associated with eutrophication is the development of anoxia in the deep waters or hypolimnion. Hypolimnetic anoxia is particularly prevalent in stratifying, productive lakes during the summer stratified period, when the hypolimnion becomes isolated

from the atmosphere due to the development of a thermocline (Boehrer and Schultze, 2008). Anoxia at the sediment-water interface induces changes to redox conditions that result in the internal loading of nutrients into the overlying water (Mortimer, 1942; Nürnberg, 1984). This adds further nutrients to the water column, which can exacerbate primary production and introducing additional oxygen demand, driving a positive feedback for water quality degradation and the associated socio-economic impacts.

Internal loading is thought to be the primary mechanism preventing lake recovery following eutrophication (Does et al., 1992; Søndergaard et al., 2003; Van Liere and Gulati, 1992). Despite efforts to reduce external inputs of nutrients from lake catchments, water quality problems persist (McCrackin et al., 2017) and in-lake restoration methods are increasingly required to restore degraded lakes (Huser et al., 2016b; Lürling and Mucci, 2020; Zamparas and Zacharias, 2014). In-lake methods targeting internal loading of nutrients have used various chemical and physical methods (Huser et al., 2016b; Lürling et al., 2020), with mixed success and variable longevity (Huser et al., 2016a; Lürling and Mucci, 2020). The lack of consistent success in tackling the problem using existing approaches means that novel restoration measures are required to combat internal loading of nutrients. In addition, it is increasingly recognised that measures targeting the issue require a lake-specific understanding of the restoration requirements and different lakes are likely to require different approaches. One proposed method, recently initiated at Elterwater in the English Lake District, is to inhibit summer stratification by reducing the water residence time and therefore reduce anoxia and subsequent internal nutrient loading.

Water residence time the amount of time water spends within a lake basin (Andradóttir et al., 2012; Kalff, 2002; Monsen et al., 2002). It is typically thought of as the ratio between the lake's volume and the throughflow discharge (Kalff, 2002; Straškraba and Hocking, 2002). Water residence time is an important parameter to consider in the understanding of lake functioning, important for nutrient and sediment loading (Jones and Elliott, 2007; Rangel et al., 2012; Vollenweider, 1975), time available metabolic and biogeochemical processes to occur (Catalán et al., 2016; Evans et al., 2017; León et al., 2016) and flushing of biota (phytoplankton and zooplankton) from the lake (Havens et al., 2017, 2016; Reynolds et al., 2012). However, little is known about the importance of water residence time in affecting lake stratification and water temperatures, particularly the use of water residence time manipulation as a strategy to manage stratification duration.

As well as eutrophication, climate change is also a stressor on lakes and projected to have various negative impacts on lake ecosystems (Jeppesen et al., 2015; Myers et al., 2017; Woolway et al., 2020). Understanding water residence time dynamics is also important in the context of future climate change, as changes to river flows are projected for large proportions of the global landmass (Arnell and Gosling, 2013; van Vliet et al., 2013). Previous research addressing climate change impacts on lakes has primarily focused on air temperature warming. However, other large scale changes in climate, including wind stilling (Stetler et al., 2020; Woolway et al., 2019a), solar dimming and brightening (Schmid and Köster, 2016) and changes to the water cycle, in terms of precipitation and evapotranspiration (Roderick et al., 2014), will also have impacts relevant to lake functioning. Changes to the water cycle will modify river flows and therefore the rate of throughflow and water residence times of lake systems (Barontini et al., 2009; Kay et al., 2020). The importance of changes to water residence times on lake temperatures has not been widely considered (Woolway et al., 2020). These changes are especially relevant for smaller, shorter-residence time lakes where throughflow importance is likely to be larger.

Short-residence time lakes (< 100 days) are globally numerous, accounting for more than 375,000 or 1 in 4 lakes (Messenger et al., 2016). These short-residence time lakes are likely to be the most affected by water residence time changes. Of particular interest in these are smaller lakes as other external drivers of thermal structure, such as wind forcing, are likely to be less influential (Read et al., 2012). These smaller (< 1km²), short residence time lakes amount to more than 330,000 or 1 in 5 lakes (Messenger et al., 2016).

1.1 Thesis focus

The research project was focused on improving our understanding of the role of water residence time changes in impacting lake physical structures and wider ecosystem effects. This has been carried out by assessing the impact of a water residence time-focused restoration measure at Elterwater, investigating the impact of theoretical water residence time changes on temperature and stratification, exploring the role of short term flow events on vertical mixing and reoxygenation and considering the impacts of future flows on water residence time and lake physical structure. The impact of water residence times on lake stratification is not well understood, and the contribution of inflows to lake heat budgets often omitted or overlooked, therefore requiring a more thorough assessment.

This thesis uses a combination of long-term monitoring data, high-frequency sensor data, and hydrodynamic modelling to investigate the following knowledge gaps:

1. Understand how changes to water residence time on different timescales impact the thermal structure of a short-residence time lake and subsequent deep-water oxygen dynamics,
2. Investigate how water residence time manipulations could be used in the management of eutrophic lake systems
3. Explore how climate-related change in river discharge, and consequent lake water residence time, might interact with air temperature rises to impact lake temperatures.

The following objectives will be addressed to achieve these aims:

1. Evaluate the impact of the 2016 Elterwater restoration project, a novel implementation of water residence time management, on lake thermal structure, nutrient, and chlorophyll *a* concentrations using modelling and long-term data records (Chapter 4)
2. Use a systematic modelling approach, that maintains natural flow variability, to determine the effect of modifying annual water residence time on annual, seasonal, and short-term thermal dynamics (Chapter 5)
3. Explore the impact of episodic reductions in water residence time and hypolimnetic dissolved oxygen replenishment during the seasonal anoxic period (Chapter 6)
4. Discuss how management strategies can be optimised to enhance lake mixing to increase deep-water oxygen concentration during important times of year (Chapters 5 and 6)
5. Examine how discharge changes may interact with air temperature under future climate change to impact lake temperatures and stratification (Chapter 7)
6. Demonstrate the additional effects of inflow warming on lake thermal structure (Chapter 7)

1.2 Thesis structure

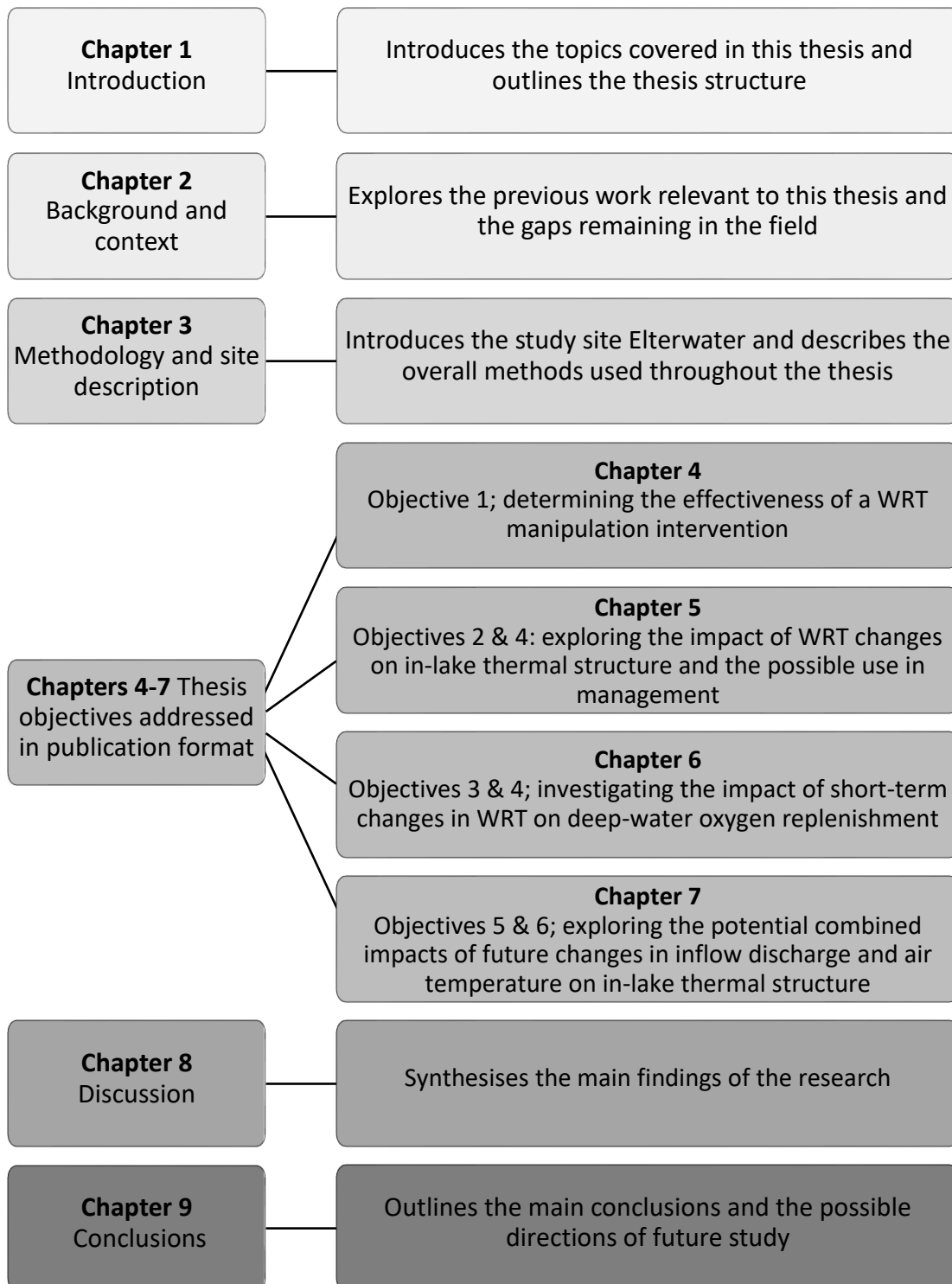


Figure 1.1 Structure of the thesis chapters

The results in Chapters 4 -7 are presented in the style of papers and are published, are under review, or are in preparation for submission at academic journals.

Chapter 2 Background and context

2.1 Overview

The primary aim of this project is to understand the impacts of water residence time (WRT) changes on lake ecosystem functioning, with a particular focus on lake temperatures and stratification. This chapter will provide the background and context in which the novel findings of this thesis sit. The chapter will begin by describing the concept of lake water residence time (WRT) and provide an overview of current understanding on its effects in lakes. The importance of lake temperatures and stratification to lake functioning will also be explored followed by a discussion of the current knowledge of the potential climate change impacts on lake thermal structure. Next, the review will briefly explore the relationship between lake thermal structure and deep-water oxygen dynamics and consequent internal nutrient loading. Finally, the current status of management measures taken to control internal loading will be discussed.

2.2 Importance of lake systems

Water is a key resource for human populations. Of all the water on earth, about 2.5% is freshwater, stored in rivers, glaciers, groundwater, wetlands and lakes (Shiklomanov, 1998). As the main source for human consumption and the most easily accessible, surface freshwater (rivers, lakes, and ponds) accounts for <0.3% of the earth's freshwater, with most freshwater stored as ice (~69%) and groundwater (~30%) (Shiklomanov, 1998), with lakes estimated to cover < 2% of the earth's surface (Messenger et al., 2016). As well as being used for drinking water, these surface freshwater resources provide other important ecosystem services. Lakes provide ecosystem services in the form of fisheries, recreation, irrigation water, and flood control (Börger et al., 2021; Deines et al., 2017; Schallenberg et al., 2013). This important resource requires sustainable and careful management.

As well as the anthropogenic needs for lake freshwater, lakes are key systems for biogeochemical processing (Messenger et al., 2016). Lakes provide support and regulatory services on global and regional scales (Downing et al., 2021). Lakes play a key role in biogeochemical cycles that regulate nutrient availability (Downing, 2010; Holgerson and Raymond, 2016; Toming et al., 2020), exemplified by their role as carbon sinks in which they bury as much carbon in their sediments as that buried by the whole ocean over the same period (Mendonça et al., 2017; Raymond et al., 2013). Lakes are also biodiversity hotspots

(Tickner et al., 2020), providing habitat for one third of global vertebrate species (Strayer and Dudgeon, 2010) and large numbers of endemic species (Collen et al., 2014).

Small lakes are often overlooked but represent a large contribution to lake numbers globally (Downing et al., 2006; Messenger et al., 2016; Verpoorter et al., 2014). Quantified most recently in the HydroLAKES database (Messenger et al., 2016), using geo-spatial methods to calculate the surface area, volume, and residence times of global lakes, the smallest class of lakes (0.1 – 1 km) were estimated to account for 87% of lakes (> 1.2 million). Even smaller lakes (< 0.1 km), not quantified in this method, may represent an even greater number of freshwater systems. Much higher estimates from Verpoorter *et al.* (2014), found that out of the 117 million lakes larger than 0.002 km², 90 million (77%) were less than 0.01 km². In this thesis, estimates from HydroLAKES (Messenger et al., 2016) are used, due to the availability of residence time estimates.

Increasingly, small freshwater systems are being acknowledged as crucial for understanding global carbon budgets, habitat availability, and biogeochemical cycling (Downing, 2010; Holgerson and Raymond, 2016; Scheffer et al., 2006). Estimates suggest that small lakes contribute disproportionately to the emissions of carbon dioxide and methane, contributing 15.1 % of CO₂ and 40.6 % of CH₄ despite comprising of only 8.6 % of lake area globally (Holgerson and Raymond, 2016). Increased rates of cycling and emissions are likely due to higher perimeter to surface area ratio, greater loading per volume, greater rates of water column mixing, and shorter WRTs (Holgerson and Raymond, 2016). Furthermore, small lakes are also represent important nitrogen sinks, processing 16% more N than large lakes (Harrison et al., 2009). As the climate continues to warm, thawing permafrost is also likely to create more of these small systems, further increasing greenhouse gas emissions (Burke et al., 2019; Holgerson and Raymond, 2016). The greater extent of littoral zones (per area) in small lakes also provide important habitat for fish and invertebrates (Downing, 2010; Scheffer et al., 2006).

2.3 Water residence time

2.3.1 Defining and characterising transport timescales in lake systems

Timescales of transport and mixing of lakes are important characteristics of aquatic systems. The rate of transport of water, and associated components, through a lake controls the biogeochemical and physical processes that act to structure lake ecosystems and control their functionality (Andradóttir et al., 2012; Jørgensen, 2002; Kalff, 2002; León et al., 2016; Rueda

et al., 2006). Therefore, it is important to understand the factors that control transport and calculate estimates of timescales accurately.

Water residence time (WRT) can be defined as the “average time to refill a basin if it were emptied” (Kalff, 2002) or alternatively the “average length of time water remains within the boundaries of an aquatic system” (Andradóttir et al., 2012; Messenger et al., 2016; Rueda et al., 2006). In measuring and defining this parameter an aquatic system there is inconsistency. Differences in definitions for the same syntax, using different syntax in comparable ways and failing to define terms at all, make quantitative comparisons difficult. Various terms are used when referring to lake water residence time, including: instantaneous and hydraulic residence time, water retention time, flushing rate, exposure time, water age and water renewal time, all used to highlight different aspects on the transport timescale. Furthermore, water residence time can refer to the throughflow of water at different timescales, from instantaneous to annual average depending on the processes and phenomena being investigated.

2.3.2 WRT and its controls

The most commonly used and simplest derivation of transport timescales in a lake system is the ratio between lake volume and volumetric flow rate, from here referred to as water residence time (WRT), τ_w . Changes to either the lake volume (V) and/or the discharge (Q) will have implications for WRT (Straškraba and Hocking, 2002).

$$\tau_w = \frac{V}{Q} \quad (2.1)$$

The interaction of lake inflows, outflows and water level determines the residence time of the water within a lake system.

2.3.2.1 Lake volume

Lake morphology is an important determinant of the volume component of WRT. Larger, deeper lakes, with large water volumes tend to have longer residence times than small, shallower lakes (Beaver et al., 2013; Messenger et al., 2016). The volume of a lake can be dependent on its formation history. Alpine zones and rift valleys with deep lakes tend to hold more water than areas with shallower lakes formed by continental glaciers or by fluvial processes (Messenger et al., 2016). Although important, the volume of a lake does not always give an accurate description of the likely WRT of a lake. Some large lakes exhibit shorter WRT than small lakes due to large rivers discharging into them (Messenger et al., 2016).

In studies of the effects of WRT for a particular lake, volume is often assumed to be constant (Londe et al., 2016; Pilotti et al., 2014). This simplification is often needed as data on changes

to lake volume is not readily available and infrequently measured during monitoring, relying on bathymetric maps. Subsequently, authors simply divide the lake volume by the annual, monthly, or daily discharge values (Londe et al., 2016; Pilotti et al., 2014). Where V has not been measured, using rate of inflow and outflow would allow for a change of volume to be accounted for (Straškraba and Hocking, 2002). Equation 2 shows how inflow (Q_{in}) and outflow (Q_{out}) rates could be used to determine WRT, over a shorter period of time (Straškraba and Hocking, 2002).

$$WRT = \frac{V^i}{(\sum Q_{in}^i + Q_{out}^i)/2} \quad (2.2)$$

Where the index i refers to the individual measurements. V = lake volume in m^3 and Q = flow rate in $m^3 d^{-1}$ for the inflow and the flow. Further simplifications to estimate lake volume without a hypsographic curve or detailed bathymetry include using *mean depth* \times *surface area* or $\frac{1}{2}$ *maximum depth* \times *surface area* (e.g. Messenger et al., 2016).

However, constant volume does not always reflect reality. In some lakes, the water volume within a system is variable over seasonal timescales. In reservoirs, managed drawdowns occur (Andradóttir et al., 2012) and in natural lakes a lack of rainfall or drought conditions can result in the lake level dropping, altering the total water volume (Gophen, 2003). If possible volume should be considered when assessing the impacts of WRT, as in some cases, the depth of the water may be a more significant component of WRT, than the flow rate, in driving some ecological processes (Beklioglu et al., 2007).

2.3.2.2 Discharge

The discharge through a lake is determined by its water budget. The discharge component comprises of inputs from surface water, groundwater, and direct precipitation as well as outputs to surface flows, groundwater recharge and evaporation back to the atmosphere (Table 2.1). The relative importance of the interaction between a lake and each of these three sources is dependent on the characteristics of the catchment, including geology, land use and soil characteristics and the local climate (Wetzel, 2001a; Winter, 2004). Direct precipitation will represent a larger percentage of inputs if the lake has a very large surface area compared to its catchment. For example, Lake Victoria, Africa's largest lake (maximum depth = 81 m), receives more than 84% of its inflow from direct precipitation (Wetzel 2001). Overall, the precipitation into the catchment is the primary driver of inflows into lakes, as it will travel as surface and subsurface flows that eventually discharge into lakes. Heavy rainfall and overall wetter climate will drive larger inputs into the lake from all sources. Regional and local climate

will also be important in determining the relative loss to the atmosphere with greater evaporation in warm, less humid conditions. Losses via evaporation will also be higher in lakes which have large emergent vegetation biomass, as water is lost through transpiration by the plants. However, where there are other outflows to the groundwater and surface water, evapotranspiration is often negligible proportion (Kalff, 2002).

Table 2.1 Example of sources of surface, groundwater, and atmospheric components of the lake water budget

Source	Inputs	Outputs
Surface water	Channelised (rivers, streams, ditches) and unchannelised (overland flow/surface runoff)	Channelised outflows
Groundwater	Subsurface flow. Often in near-shore areas clear of fine sediment	Seepage and groundwater recharge
Atmosphere	Precipitation (direct onto lake surface)	Evapotranspiration (determined by air temperature and humidity, also from aquatic emergent plants), highly seasonal and dependent on local climate

The surface water contribution to lakes is highly variable between systems (Wetzel, 2001; Kalff, 2003), accounting for none to most of the inflowing water. Surface water contributions are highly dependent on catchment characteristics such as catchment slope, soil type and vegetation cover. If the catchment slope is steep, surface inflows will generally contribute a greater proportion to the lake system (Winter, 2004). In England, the upland lakes of the Cumbrian fells, in which this thesis' study site is based, are dominated by streams due to the steep slopes and impermeable geology of the region. A catchment's land-cover is also an important influence of the proportion of run-off entering lakes. Where land-cover is dominated by forest or woodland, surface runoff will be reduced, due to increases in transpiration from the trees and increased infiltration promoted by the root systems of the forest (Kalff, 2002).

Groundwater contributions and losses can be highly variable depending on the lake and its catchment. Groundwater and subsurface flow will generally represent a greater proportion of

a lake's input in lowland catchments where the topography is less steep (Winter, 2004) and where soils are deeper and sandy (Kalff, 2002). The rate of seepage loss is also affected by the permeability of the geology and the hydraulic characteristics of the sediment (Winter, 2004). Groundwater forms the major flow into and out of karst and doline lakes in limestone regions, lakes below the water table, and those with glacial till beds (Wetzel, 2001).

Overall, catchment size is a key feature for understanding the Q component of the WRT calculation. In the same geographic location, larger lake catchments receive higher quantities of precipitation than smaller catchments (Beaver et al., 2013; Messenger et al., 2016). This results in more runoff and a greater volume of water, and associated solutes, entering the lake; replacing water in the lake more quickly (Kalff, 2002). Combined with this, the size of the lake relative to these input is going to affect the WRT. Therefore, lake area to catchment area ratio (LA:CA) is cited as the basic driver of WRT (Ambrosetti et al., 2003; George and Hurley, 2003); the higher the LA:CA the shorter the WRT. This can explain why some small lakes have much longer WRTs than volume alone may suggest (Messenger et al., 2016). Within the same catchment, temporal variability in WRTs will occur due to periods of high rainfall, precipitation and run off from the catchment and during low rainfall periods (Coppens et al., 2016; Özen et al., 2010; Reynolds et al., 2012) or due to abstraction upstream (Döll et al., 2009).

2.3.3 Spatial and temporal heterogeneity of WRTs

There are multiple assumptions made with the use of (2.1). Firstly, the equation assumes that lakes are instantly and fully mixed when inflow is added (Monsen et al., 2002; Rueda et al., 2006), and are acting as idealised completely stirred tank reactors (CSTRs) (Monsen et al., 2002; Pilotti et al., 2014). This is unrealistic in real lakes, especially in stratifying lakes, where density stratification prevents vertical mixing (Andradóttir et al., 2012; Rueda Valdivia, 2006; Straškraba and Hocking, 2002). Irregularities in the morphometry of the lake surface may be differentially affected by throughflow (Monsen et al., 2002). Irregularities, such as bays and lateral arms, may not be affected by the main currents and flows (Castellano et al., 2010; Zhang and Shen, 2015). Spatial variability in flow, currents and heating (leading to stratification and changes in the volume influenced by throughflows), means that water within different parts of the lake will have different WRTs (Ambrosetti et al., 2003; Kalff, 2002; Monsen et al., 2002).

Further to this, there is vertical heterogeneity in lake WRT due to the stratification process and differential interactions with inflowing water (Kalinin et al., 2016). Often, water in the hypolimnion of a stratified lake can remain in the lake much longer than epilimnetic water

(Kalinin et al., 2016; Pilotti et al., 2014; Rueda et al., 2006). During stratification, water in the epilimnion is isolated (Castellano et al., 2010) and will not become mixed with deeper lake water, giving the epilimnion a much shorter WRT than the lake average (Ambrosetti et al., 2003; Castellano et al., 2010; George and Hurley, 2003; Kalinin et al., 2016). The outflow of a natural lake system takes the warmer epilimnetic waters (León et al., 2016; Rueda et al., 2006), further extending the WRT in the hypolimnion. Modifications of (2.1) have been proposed which adapt the calculation to account for stratification (George and Hurley, 2003) by using only the epilimnion volume in calculating WRT during summer.

Conversely, if inflowing water is significantly colder (i.e. snow melt in alpine areas), it may intrude into the water column (Ambrosetti et al., 2003; Pilotti et al., 2014) due to its higher density than the resident water. This may flush the hypolimnion of a stratified lake at a quicker rate than the overlying water (León et al., 2016). Therefore, the intrusion depth of inflowing waters and the length and strength of stratification are significant drivers of the vertical heterogeneity in WRTs (Ambrosetti et al., 2003; Pilotti et al., 2014).

WRT is not a static characteristic of a lake. With variability in discharge and volume, WRT is dynamic over seasonal, annual and inter-annual time scales (Andradóttir et al., 2012; Rueda et al., 2006). To account for temporal variability, studies frequently use daily, monthly or seasonal average discharge values when calculating WRT rather than an annual value (Andradóttir et al., 2012; León et al., 2016). The seasonal patterns of precipitation, the main driver of Q , vary between regions. In some regions precipitation peaks correspond to a wet summer (e.g. Soares *et al.*, 2012), in others, precipitation is higher in winter (e.g. Nöges *et al.*, 2011). Therefore, the overall climate of a region will influence the likely temporal variability in WRT. At a longer time scale, WRT will also show natural inter-annual and longer term variability, related to drought and flood (Beaver et al., 2013; Gophen, 2003) especially in areas affected by climatic oscillations like El Niño (Havens et al., 2017).

Due to the assumptions outlined above and the spatial and temporal heterogeneity with a lake, the V/Q ratio is often referred to as “theoretical water residence time” (Ambrosetti et al., 2003; Castellano et al., 2010; Messenger et al., 2016; Pilotti et al., 2014). Even this theoretical water residence time can help with basic understanding of how differences in the morphological characteristics of lakes and their watersheds, and their location in areas with different hydro-meteorological conditions, will cause changes in the transport and mixing process of lakes (Ambrosetti et al., 2003; Monsen et al., 2002). However, if the aim is to gain a greater understanding of the impacts of changes in WRT on a lake, an annually averaged

theoretical WRT is likely to be inadequate to capture the full heterogeneity within the system (Andradóttir et al., 2012; Castellano et al., 2010; Messenger et al., 2016).

2.3.4 Importance of WRT to lake functioning

WRT influences the spatial, both horizontal and vertical, and temporal patterns in lake characteristics and functioning as well as controlling the time available for metabolic reactions and biogeochemical processes to occur within the lake.

2.3.4.1 Physical

Described further in Section 2.4, inflows contribute to the lake's heat budget. Therefore, changes to the inflow discharge, and consequent WRT, can have impacts on lake temperatures. However, the contribution of inflows is not often considered and is often omitted from considerations of lake heat budgets, especially in larger lakes (e.g. Fink *et al.*, 2014), despite the fact that the contribution of inflows to the lake heat budget can be important in determining in-lake temperatures (Råman Vinnå et al., 2018).

The impact of changing flow on in-lake temperature dynamics, through changes to the advective heat flux (see Section 2.4), has not been widely considered previously. Observations have focused on comparisons between lakes of different WRT and on the short-term impacts of extreme episodic inflow events. Some studies have also drawn comparisons between lakes of different residence time in the same region or between years/periods of different prevailing hydrological conditions (Brasil et al., 2016; León et al., 2016; Obertegger et al., 2007; Tarczyńska et al., 2001). Cooler water temperatures and shorter periods of summer stratification are observed alongside shorter WRTs (León et al., 2016). Field observations also suggest that large episodic inflow events (e.g. storms) temporarily increase the inflow cooling effect (M. R. Andersen et al., 2020), although in-lake changes cannot fully be attributable to WRT changes as high inflow often co-occurs with increased wind speed and reduced surface heating.

Modelling studies have looked at short vs long WRT scenarios in reservoirs and found that shorter WRTs are associated with weaker and shorter periods of summer stratification (Li et al., 2018; Straškraba and Hocking, 2002; Yang et al., 2020). These studies investigated the impact of changes to constant flow rates in managed reservoirs, unrealistic in natural lakes, where inflow rates vary considerably on a temporal scale (Section 2.3.3). The modelling also mostly considered limited scenarios, high vs low flow conditions, and failed to investigate WRT impacts on lake temperature systematically.

The understanding of WRT impacts on lake temperatures is poor and requires further, more systematic investigation, than has previously occurred. Specifically, understanding natural

seasonality in WRT and the contribution of the inflow to the heat budget is needed to understand how WRT modifications may affect lake temperatures in a management and climate change context.

WRT can affect lake water clarity, although the impact of WRT changes will depend on the primary driver of clarity (dissolved organic carbon vs phytoplankton; Rose *et al.*, 2017). On the one hand observations and modelling have shown water clarity improvements at shorter WRTs (Jørgensen, 2002). This is thought to be associated with a reduction in the biovolume of phytoplankton within the water column, which are a main contributor to the transparency in natural lake systems. In a modelling study on Lake Glum (surface area = 0.5 km², mean depth = 1.6 m), a reduction in the annual WRT from six to four months resulted in an increase in the minimum transparency of the lake from 18cm to 70cm (Jørgensen, 2002). Similarly, observations from Lake Veluwe, a shallow non-stratifying lake, showed increased summer transparency when WRT was artificially shortened (Jagtman *et al.*, 1992). However, a switch to diatom dominance from cyanobacteria resulted in a higher turnover rate and relatively more detritus in the water column compared to a cyanobacterial dominated lake (Jagtman *et al.*, 1992), limiting the improvement in water clarity. This shows that composition as well as biomass of the phytoplankton community is important in determining transparency.

Conversely, water clarity may decrease with episodic reductions in WRT and increases in flow (Beaver *et al.*, 2013; Mitrovic *et al.*, 2011; Rennella and Quirós, 2006; Rose *et al.*, 2017). This is associated with changes to the suspended solids concentration within the water column. Within reservoirs, field studies have found that in the lentic zone, characterised by longer WRT, and when lentic conditions prevail across a year, transparency is higher than in the lotic zone and during shorter WRT periods (Rennella and Quirós, 2006; Soares *et al.*, 2012). Reservoir field observations showed increases in transparency during drought periods and lowest transparency values occurring during a flood (Beaver *et al.*, 2013), caused by the run off from the catchment bringing in sediment and the disturbance of bottom sediments by increased inflow and mixing. Generally, lower clarity lakes have been shown to be less sensitive to changes in meteorological conditions, changing less between wet and dry years than higher clarity lakes (Rose *et al.*, 2017). Extreme episodic events that reduce WRTs, can also rapidly reduce lake water clarity by flushing material into lakes (Rose *et al.*, 2017).

2.3.4.2 Chemical

In-lake phosphorus concentration is a function of the external phosphorus (P) loading and the retention of P controlled by the WRT (Cooke *et al.*, 2005). The Vollenweider model describes

the relationship between nutrient input/output and the within-lake concentration of phosphorus under equilibrium (Vollenweider, 1976, 1975). Within this model, this relationship changes with nutrient load and with WRT as it is the WRT which determines the extent of nutrient retention or flushing in the system.

$$P = \frac{L_p / q_s}{(1 + \sqrt{\tau_w})}$$

This equation states that in-lake concentration of phosphorus (P) is a function of the annual load (L_p), the water discharge (q_s) and WRT (τ_w). The retention of any nutrient load that enters the lake depends on WRT. As WRT increases, nutrients are increasingly likely to be retained in the lake via sedimentation. When WRTs are shorter, nutrient concentration in the inflows have less time to be altered before being exported via the outflow.

The external source of nutrients will also modify how lakes respond to changes in WRT. Where nutrients are derived from diffuse sources, such as catchment sources, a reduction in WRT will increase the loading of nutrients (Elliott and Defew, 2012; Jones and Elliott, 2007; Rangel et al., 2012). On the other hand, when nutrients are derived from point sources, which can include waste water treatment works or in-lake sediment sources, a reduction in WRT will reduce in-lake concentrations due to dilution effects (Elliott et al., 2009; Jones and Elliott, 2007; Schindler, 2006; Wagner and Zalewski, 2000).

Even though the internal load can often exceed the external sources of nutrients (Schindler, 2006), studies looking at the natural fluctuation of internal load with changes in WRT are infrequent. As with external loads, the impact of WRT on internal loading is likely to depend on the dominant process driving internal loading in a lake. In many shallow lakes, sediment entrainment is the dominant process causing internal loading. Reduced WRTs have been linked to greater sediment entrainment, especially close to the inflow and in littoral zones (Jones and Welch, 1990; Marsden, 1989). However, resuspension of particles may not necessarily lead to an increased release of phosphorus (Søndergaard et al., 2003), as this will be dependent on the chemical conditions of the water and uptake by biota (Søndergaard et al., 2003). As well as increases in the upward flux with decreasing WRT, a decrease in the downward flux may contribute to the net increase in internal loading. Reducing the WRT may reduce the sedimentation of P and retention within the sediments (Uttormark and Hutchins, 1980). However, at Moses Lake, a weakly stratifying dendritic lake, this was deemed insignificant in comparison to the contribution of the upwards flux to the overall increase in internal loading following reductions in WRT (Jones and Welch, 1990).

In other lakes sediment P release is mediated by redox conditions at the sediment water interface (see section 2.6). WRT changes that modify deep-water oxygen conditions have the potential to moderate this redox-related P-release. Reductions in the length and strength of the stratified period, and the associated seasonal anoxia, may reduce internal loading. As the influence of WRT changes on stratification is not widely understood, this relationship can only be inferred at present. Therefore, the effect that changes in WRT have on the internal load within a lake will be dependent on the dominant processes. Similar to the external load, the source and processes driving internal load will be differentially affected by changes in WRT.

Loading of dissolved organic carbon from the catchment is closely coupled to WRT, with higher DOC loads at shorter WRT (Toming et al., 2020; Zwart et al., 2017), promoting heterotrophy in these systems (Zwart et al., 2017). This is especially true for extreme precipitation events, that reduce WRT and can contribute up to 58% of the seasonal flux of DOC (Zwart et al., 2017). Despite greater loading in short WRT lakes, retention and mineralisation rates are often lower, which potentially dampens the effect of extreme precipitation events on heterotrophic carbon fluxes (Zwart et al., 2017).

2.3.4.3 WRT moderates process rates

Importantly WRT can drive the rate of biogeochemical processes, even if the direction is not consistent. A large meta-analysis of 82, predominantly European and North American, water bodies showed that the effect of WRT was to moderate the rate of organic carbon production and consumption, with the trophic status determining the source-sink status of the lake (Evans et al., 2017). Similarly, denitrification rates were modified by WRT, larger proportions of N were removed at longer WRTs (Harrison et al., 2009; Seitzinger et al., 2006). Longer WRT slowed the increase in total N in waterbodies acting as N sinks, but accelerated the removal from the waterbodies acting as N sources (Tong et al., 2019).

2.3.5 Biological

WRTs can impact phytoplankton in multiple ways. They can directly modify phytoplankton biomass through direct flushing and advective losses. If WRTs are increased above growth rates, species cannot persist as they are removed from the lake (Elliott and Defew, 2012), potentially selecting for species with faster growth rates over slower growing species. This is evident in the absence of slow growing algal species, such as *Microcystis* and *Ceratium* (Reynolds et al., 2012) and an increase in fast growing species such as *Stephanodiscus sp.*, at shorter WRTs (Elliott and Defew, 2012; Reynolds et al., 2012). This switch has been both modelled (Elliott and Defew, 2012) and observed (Beaver et al., 2013). The main change in

phytoplankton community composition is switch to a cyanobacteria-dominated communities at longer WRTs (Elliott, 2010; Elliott and Defew, 2012; Saito et al., 2013; Soares et al., 2012). Greater cyanobacteria biomass has been recorded during low flow conditions, such as during droughts, when WRT is longer (Beaver et al., 2013; Reynolds et al., 2012; Romo et al., 2013; Soares et al., 2012). At these times, the vertical stability and stratification of the water body is also increased (see 2.3.4.1) favouring the growth of cyanobacteria (Mitrovic et al., 2011; Nöges et al., 2011; Romo et al., 2013). Romo *et al.* (2013) observed across a year that blooms in cyanobacteria are often during summer, when WRTs are longest. However, other factors, such as light, nutrient load and temperature are also likely to be contributing to this, improving summer growing conditions. Obertegger *et al.* (2007) showed a negative correlation between biomass of zooplankton-edible algae ($\leq 30 \mu\text{m}$), mainly composed of diatoms, with WRT, perhaps showing increase dominance by the largely inedible cyanobacteria within the community at longer WRTs.

To account for losses and prevent biomass reductions, species may increase their growth rate. Calculations by Reynolds *et al.*, (2012) found that if the WRT of Grasmere decreased from 65 to 28 days then the growth rate of the phytoplankton species will need to increase from 0.0155 day^{-1} to 0.036 day^{-1} . Furthermore, when the WRT is reduced to 9 days, the growth rate needs to be > 0.118 to simply overcome dilution, before accounting for losses from sinking, grazing and mortality (Reynolds et al., 2012; Reynolds and Lund, 1988).

Additionally, phytoplankton communities may be affected by WRTs by the changes caused to lake conditions. Where WRT changes modify nutrient concentrations, light conditions, or thermal structure (as described above), phytoplankton species will be consequently impacted. Species adapted to specific conditions may benefit at the expense of other species. For example, if light conditions are reduced due to increased loading of DOC from the catchment, low-light adapted species may dominate over others. Where nutrient loads are increased with shorter WRTs, this may promote additional growth, if the rate of flushing is below that of the growth rate. Field observations of a positive WRT-biomass relationship suggest that longer WRTs promote algal growth, due to increased stability of the water column (Londe et al., 2016), less advective loss of algal cells (León et al., 2016; Londe et al., 2016; Lucas et al., 2009; Mitrovic et al., 2011; Rangel et al., 2012) and reduced flushing of nutrients from the system (Elliott et al., 2009; Gophen, 2003; Jones and Elliott, 2007; Rangel et al., 2012; Reynolds et al., 2012). This means the time available for utilisation of these nutrients is longer, enhancing growth (Jones et al., 2011).

The source of the nutrients to the system can affect the impact of WRT on phytoplankton. Changes in WRT caused different responses when nutrients inputs were dominated by diffuse or point sources (Elliott et al., 2009; Jones et al., 2011; Jones and Elliott, 2007). The PROTECH model, which simulates the responses of phytoplankton to environmental change, including WRT, was used to investigate these differential impacts. The model showed that when the nutrient load was fixed but WRT decreased (i.e. if nutrients were from a point source) there was a predicted decrease in phytoplankton biomass (Elliott et al., 2009; Jones et al., 2011; Jones and Elliott, 2007) due to dilution of nutrients and washout of phytoplankton cells (Jones et al., 2011). Conversely, when nutrients were mainly from diffuse sources, there was little change in phytoplankton biomass in response to WRT changes (Elliott et al., 2009; Jones et al., 2011) as increased nutrient input was offset by increases in advective losses and sedimentation (Elliott et al., 2009; Jones et al., 2011).

As well as phytoplankton biomass, the duration and timing of the blooms is affected by changes in WRT (Elliott, 2010; Jones et al., 2011; Jones and Elliott, 2007). Modelling studies, have shown that at shorter WRTs the onset of the spring bloom is later (Jones et al., 2011; Jones and Elliott, 2007). However, Elliott, Jones & Page (2009) found that at the shortest WRTs (<18 days) the onset was brought forward with little changes as the WRT lengthened. This difference may be due to be initial populations present within the lakes and other site-specific limiting factors controlling growth. Longer WRTs also extended the duration of the bloom into the year (Elliott, 2010; Elliott et al., 2009; Jones and Elliott, 2007). Jones & Elliott (2007) demonstrated that at longer WRTs the algal blooms could be extended by up to 150 days.

Similarly to patterns reported for other biogeochemical process rates, Lucas *et al.*, (2009) suggest that WRT acts to moderate the rates of change in biomass, rather than causing the directional change itself. They argue that it is the growth-loss relationship which is vital in determining the effect of WRT on phytoplankton biomass. Where growth rates exceeds loss rates, any increase in WRT will amplify the net biomass increase, whereas when loss processes exceed growth, increased WRT will amplify net loss of biomass (Figure 2.1). This theoretical model summarises the diversity of relationships seen between phytoplankton and WRT (Lucas et al., 2009).

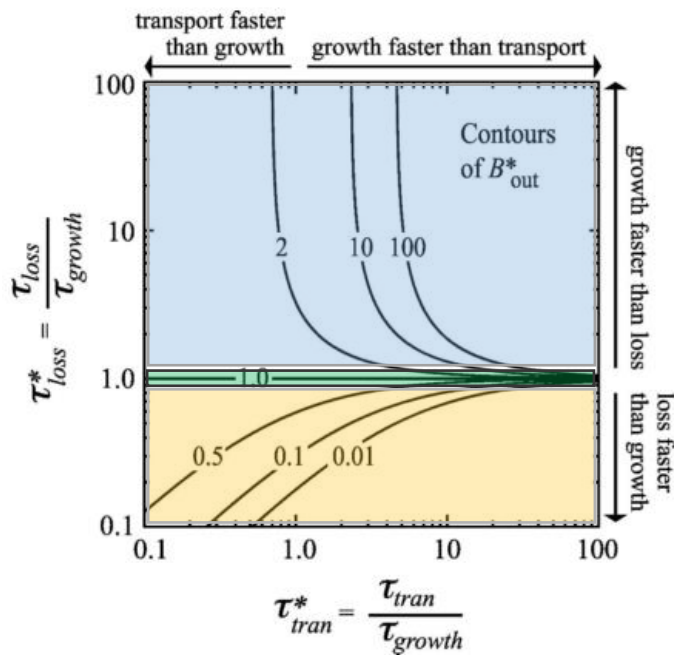


Figure 2.1 Relationship between rates of growth (τ_{growth}) and loss (τ_{loss}) determines the effect of WRT on phytoplankton biomass (B^*). Orange = where loss > growth, blue = growth > loss. Moving horizontally across the graph from left to right indicates increasing WRT (T^*_{tran}).

Although not studied in the same detail or at the same frequency as phytoplankton response, it is noted that zooplankton are susceptible to depletion during increased flows and when WRTs are short (Beaver et al., 2013; Rangel et al., 2012; Reynolds et al., 2012). Zooplankton abundance and composition can be affected by WRT in a combination of ways (Figure 2.2; Threlkeld, 1982; Beaver *et al.*, 2013):

1. **Non-selective washout** of species occurs when zooplankton are unable to compensate for losses with higher growth rate, affecting abundance. Direct wash-out affects zooplankton in a similar way to phytoplankton in causing advective losses at short WRTs (Beaver et al., 2013; Obertegger et al., 2007). Additionally in zooplankton, washout affects the different life-stages of the zooplankton in different ways, with juveniles more susceptible to shorter WRTs than adults (Obertegger et al., 2007). This would decrease population numbers due to poor recruitment (Obertegger et al., 2007). Similar to the dominance of certain phytoplankton, zooplankton species with a shorter reproductive time are able to off-set their flushing losses, allowing them to dominate (Rennella and Quirós, 2006). This accounts for the increase representation of rotifers and some smaller, quick growing cladocera at short WRTs (Obertegger et al., 2007; Rennella and Quirós, 2006).
2. Modification to the local conditions influence zooplankton through **abiotic control**, including changes to food availability in the form of phytoplankton. WRT also controls

abiotic conditions, such as transparency which have been shown to affect reproductive success in certain cladocera (Threlkeld, 1982). However, this impact was shown to be a temporary response to a short-term change rather than a strategic response over a longer period (Threlkeld, 1982). These changes may affect abundance, if growing conditions become unsuitable, and community structure, if species are differentially affected.

3. **Species-specific responses** to WRT will favour selection of some species over others causing community composition changes.

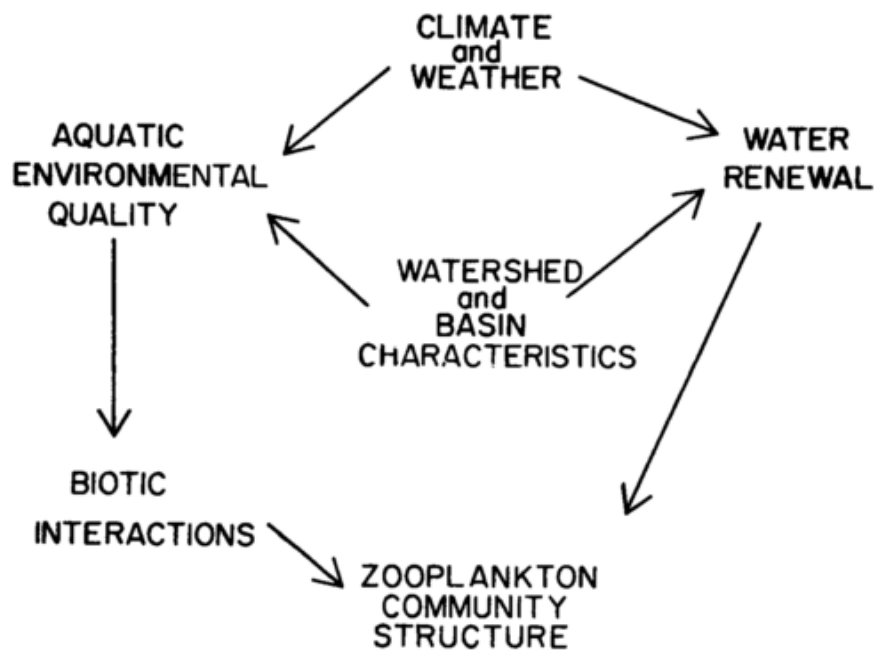


Figure 2.2 Reservoir zooplankton community is controlled by the direct dilution and transport effects of WRT (right side) and by modification of environmental quality and biotic interactions (left side) (Threlkeld, 1982).

The dominant control of WRT on zooplankton is unclear. Threlkeld (1982) suggests that WRT effects zooplankton through modification of lake conditions (food availability, light climate, temperature etc.), independent of flushing effect, which then influence zooplankton population dynamics. This conclusion is drawn from the relationship between WRT and transparency, which would influence productivity and thus food availability. However, it has also been suggested that mechanical losses are more important in controlling zooplankton dynamics than food availability (Beaver et al., 2013). This is exemplified in reservoir *Daphnia* populations which exhibited reductions in biomass even when food resources increase (Beaver et al., 2013). These differing conclusions suggest that the dominant control is likely to be dependent on the species in question.

Crustacean and copepods show decreases in biomass and abundance with shorter WRTs (Obertegger et al., 2007; Rennella and Quirós, 2006). The magnitude of the summer peaks in all zooplankton and copepods were greater during the dry summers when WRTs were longer compared to wetter summers (Rennella and Quirós, 2006). Calanoid copepod densities were found to be higher in longer WRT systems and up to 9 times lower in shorter WRT systems (2.6 L^{-1} compared to 18.7 L^{-1}) (Doubek et al., 2019). Calanoid taxa may be particularly influenced by shorter residence times because of the longer generation time and the time taken for individuals to reach sexual maturity (Doubek et al., 2019). Conversely, evidence shows that rotifers are not affected by changes WRT (Obertegger et al., 2007; Rennella and Quirós, 2006) and their biomass is generally controlled through exploitative competition with crustaceans for phytoplankton (Obertegger et al., 2007). Dominance of rotifers at shorter WRTs may be due to the relative decrease in crustacean or the release of rotifers from competition with crustaceans for resources. The balance between rotifer and cladocera dominance was quantified by Obertegger *et al.* (2007). They identified a critical WRT in Lake Tovel, a short-residence time karstic lake in Italy as 193 days as the switch between cladocera and rotifer dominance (Obertegger et al., 2007), although it is likely that this is variable across different systems.

2.4 Lake physics and heat fluxes

Water temperature and stratification dynamics in lakes are determined by the lake's heat budget and the balance between heat losses and gains, mostly occurring at the lake's surface (Schmid and Read, 2021; Woolway et al., 2015b). The surface heat flux is made up of the incoming long-wave (Q_{lin}), outgoing longwave (Q_{lout}), incoming short-wave (Q_{sin}), and the sensible (Q_h) and latent (evaporative, Q_e) heat fluxes (Schmid and Read, 2021), with additional heat fluxes from advection (Q_{adv}) and lake sediments (Q_{sed}) (see Figure 2.3).

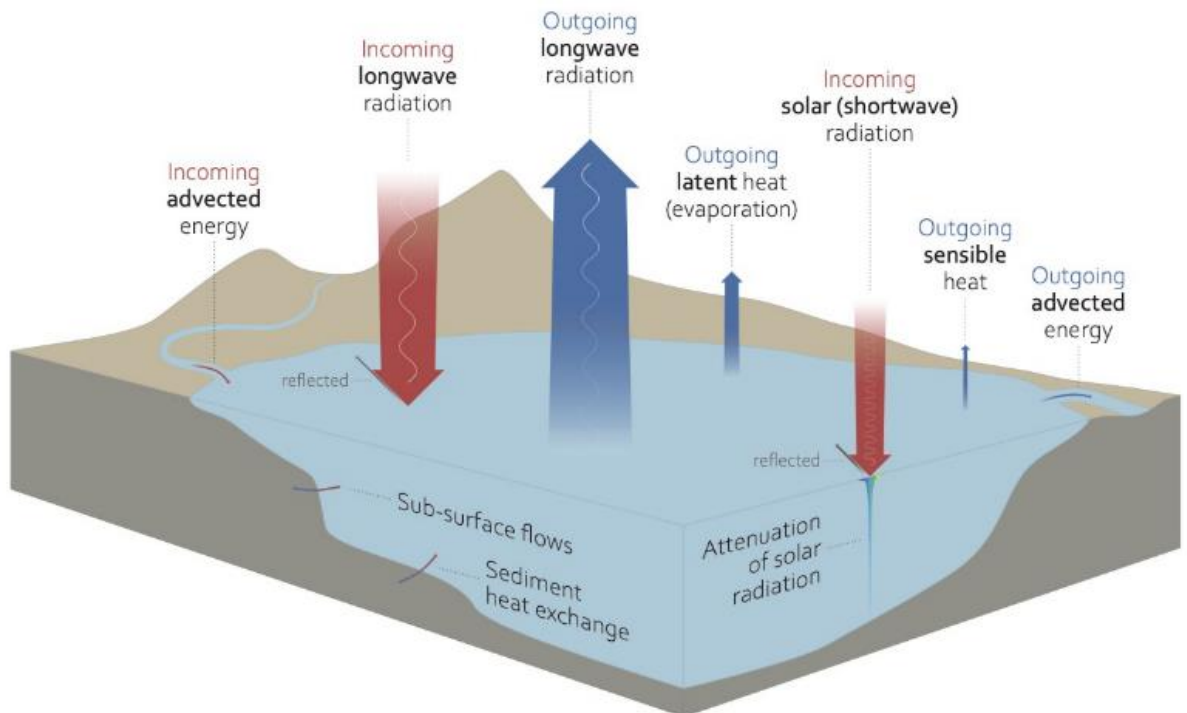


Figure 2.3 Components of the heat exchange between a lake and the environment (from Schmid and Read, 2021)

In this thesis, positive heat fluxes will relate to heat coming into the lake and negative fluxes to heat going out and given as a rate of heat change per unit area in W m^{-2} ,

$$Q_{\text{tot}} = Q_{\text{lin}} + Q_{\text{lout}} + Q_{\text{sin}} + Q_{\text{h}} + Q_{\text{e}} + Q_{\text{adv}} + Q_{\text{sed}}. \quad (2.3)$$

The surface heat fluxes dominate the heat budget, driving annual patterns of lake stratification, and are also subject to the impacts of climate change (Fink et al., 2014a; Schmid and Read, 2021; Wetzel, 2001b).

The radiative fluxes are the short and long-wave radiations. Incoming shortwave radiation is composed of the sum of all wavelengths between 300-3000 nm and expresses the energy from the sun, varying due to latitude, cloud cover, elevation, and shading. Some shortwave radiation will be reflected from the lake surface, based on the albedo, again varying by latitude, elevation, time of day, season, and wave or ice conditions (Kirk, 2010). Incoming longwave radiation is the largest heating term, and the out-going long-wave the largest loss term (Livingstone and Imboden, 1989). Incoming long-wave magnitude is determined by atmospheric temperature, humidity, and cloud cover, and approximately 97% of incident longwave is absorbed by a lake's surface (Schmid and Read, 2021). Out-going longwave radiation is a function of surface water temperature and often more than cancels out the incoming long-wave, giving a net cooling longwave (Livingstone and Imboden, 1989; Schmid and Read, 2021).

Non-radiative fluxes at the air-water interface are the sensible and latent heat fluxes. The sensible heat flux is a conductive flux between the lake surface and the atmosphere and can be a gain or loss term depending on meteorological conditions and lake surface temperature (Schmid and Read, 2021). The temperature gradient between the lake and atmosphere will determine the magnitude and direction of the heat flux, but is primarily a heat loss term (Fink et al., 2014a; Schmid and Read, 2021). Greater instability in the atmospheric boundary layer will also increase the heat loss from the lake, especially for smaller lakes (Woolway et al., 2017b). The latent heat flux of evaporation quantifies the energy that is lost or gained at the lake surface via a evaporation or condensation and varies according to the moisture and temperature gradients, which is based on the atmospheric conditions above the lake (Schmid and Read, 2021). Most latent heat exchange occurs as evaporation, giving a net cooling effect on the lake. The latent heat associated with melting ice also needs consideration in the heat budget of ice-covered lakes (Wetzel, 2001b).

The sediment heating term is determined by water depth and the adsorption of solar energy by the sediments. Generally, the sediment heat flux contributes a cooling flux during the warm season when heat is transported from the water column into the sediment and a warming flux during the cold season as the heat is released back into the water column (Fang and Stefan, 1998; Wetzel, 2001b). The sediment heat storage is most relevant for shallow lakes which receive direct solar heating to sediments and in the littoral zones of deeper lakes (De La Fuente, 2014; Wetzel, 2001b). Furthermore, the effects of heat exchange between the sediment and the water are most noticeable in ice-covered lakes where the heat fluxes across the lake surface are limited (Schmid and Read, 2021). However, even in these lakes the seasonal heat flux between the sediment and the overlying water typically does not exceed a few W m^{-2} (Schmid and Read, 2021), whereas surface heat fluxes are typically in the order of hundreds of W m^{-2} .

The final heat flux is the advective heat flux (Q_{adv}). The quantification of the Q_{adv} is given by Livingstone and Imboden (1989) as,

$$Q_{adv} = \frac{F_{inflow} \times C_{pw} \times \rho_w \times (T_{inflow} - T_{outflow})}{A_0}, \quad (2.4)$$

where F_{inflow} is the discharge into the lake ($\text{m}^3 \text{ s}^{-1}$), and $(T_{inflow} - T_{outflow})$ is the temperature difference between the inflow and the lake outflow ($^{\circ}\text{C}$), where the outflow temperature is assumed to be equal to the lake surface temperature. A_0 is the lake's surface area (m^2) and C_{pw} and ρ_w are the specific heat capacity and density of water, taken here to have the constant values of $4200 \text{ J kg}^{-1} \text{ }^{\circ}\text{C}$ and 1000 kg m^{-3} , respectively.

Few studies look at the importance of the advective flux. Previous work has shown that the advective heat flux can be a warming or a cooling flux at different times of the year, although in many studies it has found to be net cooling flux (Carmack et al., 1979; Fink et al., 2014a), with minor warming in the early spring (Fink et al., 2014a). However, the overall seasonal pattern of the advective heat flux is determined by the difference in temperature between inflowing and outflowing water, assuming a constant lake volume (Livingstone and Imboden, 1989; Schmid and Read, 2021). Groundwater and surface waters can both act as advective fluxes, with groundwater generally acting as a cooling flux (Kettle et al., 2012). The F_{inflow} and $T_{inflow}-T_{outflow}$ terms determine the temporal dynamics on seasonal and sub-seasonal timescales, with greater temperature differences and discharge increasing the magnitude of the heat flux. Additional parameters to consider in the quantification of the advective flux may come from the complex draw-off dynamics or water pumping in reservoirs (Xing et al., 2012) and anthropogenic heat pollution, from power plants for example (Kirillin et al., 2013; Råman Vinnå et al., 2017) or heat extraction (Gaudard et al., 2019).

Ultimately, the direction of the advective heat flux, warming or cooling is determined by whether the inflow is warmer or colder than the lake surface, and therefore the outflow water. Changes to residence time can change the magnitude of the flux (Fenocchi et al., 2017; Livingstone and Imboden, 1989; Smits et al., 2020), increasing at shorter WRTs. However, the impact of the advective flux is rarely considered in the heat budget, and the effect of WRT changes on thermal conditions is not well understood, especially in short-residence time lakes where the impact is likely to be larger.

Long-term seasonal cycles in the heat budget are caused by the Earth's orbit around the sun and the relative change in tilt of its axis towards (summer) or away from the sun (winter) and magnitude of the oscillation between the seasonal extremes is primarily driven by latitude, with higher latitude locations experiencing greater changes in solar radiation. For example, temperate lakes experience larger seasonal variations in incoming solar radiation, which drive temporal variability in the net heat balance, heating the lake in the summer and cooling it in the winter (Livingstone and Imboden, 1989; Schmid and Read, 2021), leading to predominantly monomictic or dimictic stratification patterns. Conversely, in tropical lakes, incoming solar radiation, and other heat fluxes are more consistent, resulting in small seasonal variation in the heat balance (Schmid and Read, 2021; Wetzel, 2001b). Inter-annual differences in heat budgets may be caused by large scale climate cycles such as the El Niño Southern Oscillation or the North Atlantic Oscillation causing anomalous precipitation, wind speeds, and air temperatures, particularly in North America and Europe, modifying heat budgets.

2.4.1 Impact of climate change on heat fluxes

Climate change impacts different terms of the heat budget, most directly through changes to air temperatures (Schmid and Read, 2021), leading to increased incoming longwave and changes the sensible heat flux between the lake and atmosphere (Schmid and Read, 2021). Solar brightening, increasing incoming short-wave radiation, has also been found to be contributing to warming of lakes beyond what would be expected with air temperature rise alone (Schmid and Köster, 2016), although increased humidity and cloud cover may be reducing short-wave incidence (Kirillin et al., 2017). As lake temperatures increase the heat losses through outgoing longwave and latent heat flux will also increase (Fink et al., 2014a). The timing and magnitude of river discharge (Arnell and Gosling, 2013; Gudmundsson et al., 2021; van Vliet et al., 2013), and the irregular heating of rivers relative to lakes (Fink et al., 2014a; Jonkers and Sharkey, 2016), is likely to have corresponding impacts on lake heat fluxes and water temperatures (Fenocchi et al., 2017; Fink et al., 2014a; Livingstone and Imboden, 1989; Smits et al., 2020). However, the changes to the advective heat flux are not regularly quantified in climate change impact studies on lakes.

2.4.2 Stratification

The different seasonal patterns of heating and cooling experienced by different lakes cause different patterns of vertical mixing and partitioning of the water column, termed *stratification*. Lake stratification describes the vertical partitioning of the water column into three layers with distinct characteristics (see Figure 2.4). The uppermost of these three layers is the *epilimnion* – the warmer, mixed, surface layer of the lake (Boehrer and Schultze, 2008; Kalff, 2002). This upper layer experiences turbulence, mainly in the form of wind shear and is in contact with the atmosphere (Kalff, 2002). The depth of this mixed layer primarily depends on wind speeds and the resistance to mixing forces from the density gradient (Kalff, 2002; Wetzel, 2001b). Wind speed is a function of lake surface area and fetch, with lakes with a larger surface area and fetch generally experiencing higher wind speeds and therefore tend to have deeper surface mixed layers (Gorham and Boyce, 1989; Winslow et al., 2015). The colder deep-water zone, the *hypolimnion*, is largely non-turbulent and separated from the atmosphere. These two zones are separated by a transitional zone, the *metalimnion*, characterised by a steep temperature gradient (*thermocline*) (Boehrer and Schultze, 2008).

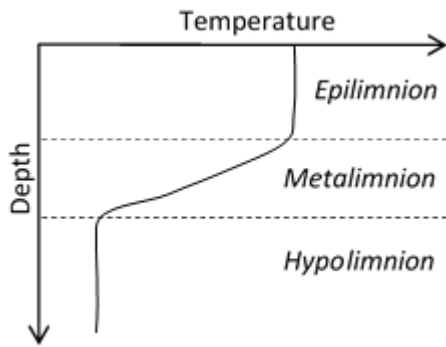


Figure 2.4 Conceptual temperature profile during a stratified period, comprised of an isothermal epilimnion (mixed layer), the cooler mixed hypolimnion, separated by a metalimnion, with a steep temperature gradient.

Stratification is brought about due to the density difference in waters of different temperatures, changing non-linearly with a maximum density at 3.94 °C. Therefore, differential warming of lake water can set up temperature and density gradients within the water column. Faster warming of the surface waters compared to the deeper waters means that this warmer, less dense water remains above the colder more dense water deeper down (Boehrer and Schultze, 2008; Kalff, 2002). A sustained period of stratification occurs when the turbulence and mixing energy from wind and mechanical processes are unable to mix solar energy, received at the lake surface, deeper in the lake (Boehrer and Schultze, 2008). The breakdown of stratification, *overturn*, occurs when cooling at the surface reduces the density difference sufficiently that the resistance to mixing is smaller than the mixing energies. This re-establishes an isothermal structure in the water column. If the water cools below 3.94 °C, the temperature of maximum density, a period of *inverse stratification* may occur, in which the surface water is cooler but less dense than deeper water.

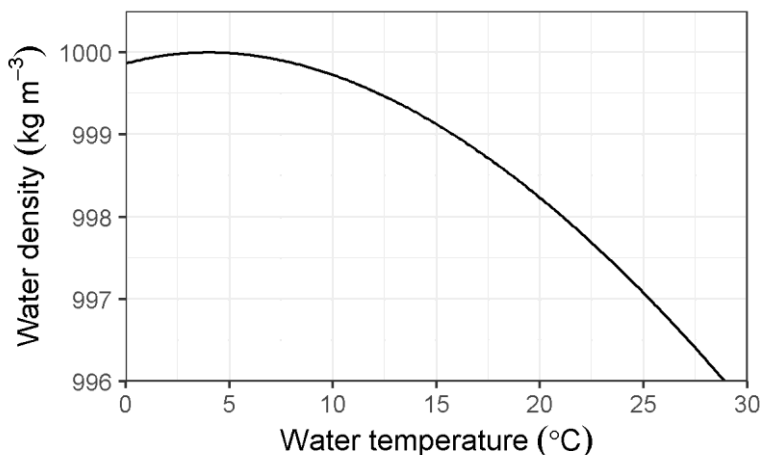


Figure 2.5 Relationship between water temperature and water density. Maximum density is at 3.94 °C. Water densities calculated using rLakeAnalyzer R package (version 1.11.4.1; Read et al., 2011).

Lake morphometry and climate determine the type of stratification that a lake experiences, originally classified by Hutchinson and Löffler (1956) and revised by Lewis (1983) into eight mixing regimes (Table 2.2): two monomictic regimes, dimictic, four polymictic regimes, and amictic. The meromictic classification include lakes in which the deep recirculation does not include the entire water body where a chemically different bottom layer, called monimolimnion, is continuously been present for at least one annual cycle (Boehrer and Schultze, 2008). Polymictic lakes tend to be shallow or very wind exposed (Kalff, 2002), with monomictic lakes dominating over dimictic systems at lower latitudes or altitudes where the mean annual temperature is higher than 10 °C (Kalff, 2002). Shallow, wind-protected temperate lakes stratify when maximum depth is greater than 3 m, with larger lakes (> 20 km²) requiring at least a maximum depth of 20 m.

Table 2.2 Lake mixing regime types (after Lewis 1983), plus the additional classification of meromictic.

Mixing regime	Frequency of full water	
	column mixing (per year)	Description
Cold monomictic	Once	Mostly ice-covered, becoming ice-free in summer, temperatures consistently < 4 °C.
Warm monomictic	Once	Have one period of continuous stable stratification followed by one mixing period. Are ice-free year round.
Dimictic	Twice	Ice cover for part of the year and stably stratified.
Discontinuous cold polymictic	Many times, irregularly	Ice covered for part of the year and ice free above 4 °C. Stratify during warmer periods.
Discontinuous warm polymictic	Many times, irregularly	Stratify during warmer periods, mixing regularly.
Continuous cold polymictic	Many times	Ice covered for part of the year and ice free above 4 °C. Stratify and mix daily.
Continuous warm polymictic	Many times	No ice cover. Stratify and mix daily.

Amictic	Never	Continuously ice-covered. Rare classification of lake confined to Antarctica.
Meromictic	Very rarely	A lake in which deeper water does not circulate during overturn due to its high density (usually the result of a high salt concentration).

Water transparency is also important in determining the heat transport and the development of stratification (Kirillin et al., 2017). Incident radiation is able to penetrate deeper in more transparent lakes, whereas in higher turbidity or high-colour lakes, more of the radiation is absorbed in the upper portion of the water column (Kalff, 2002). Thus, higher turbidity lakes often have shallower mixed depths compared to clearer lakes with equivalent meteorological forcing (Kirillin et al., 2017).

In warm monomictic lakes, the temperatures follow a typical annual cycle of stratification and mixing, following changes to the heat budget (Boehrer and Schultze, 2008; Kalff, 2002; Wetzel, 2001b). In spring, the surface waters of lakes are heated more rapidly than the heat is distributed by mixing energy. Increased temperature at the surface increases the resistance to mixing due to density differences and complete mixing is inhibited, creating a stratified water column – *stratification onset*. The water column is split into the three layers, with the upper layer being isothermal, the metalimnion exhibiting a steep temperature gradient, both above an isolated cooler hypolimnion. The depth of maximum temperature gradient is termed the *thermocline*. The depth of the mixed layer and thermocline changes depending on meteorological conditions that drive turbulence and convective cooling in the upper layers. Lakes begin to cool in the autumn, with losses of heat exceeding gains, as surface water temperatures begin to exceed average daily air temperatures (Kalff, 2002). Eventually the density difference between the epilimnion and the metalimnion reduces below the wind energy (Carmack et al., 1986), resulting in thermocline erosion and mixed layer deepening, as cooler metalimnetic water is incorporated into the mixed layer. Autumn *overturn* is complete once the lake has become isothermal until ice cover establishes (in dimictic lakes) or the following stratification onset in the spring. Overturn in winter may also be driven in part by the advective heat fluxes and turbulence from groundwater and/or surface flows (Kettle et al., 2012; Laval et al., 2012). If surface waters continue to cool below 3.94 °C, ice cover can form. Ice covered lakes exhibit a temperature gradient from 0 °C at the surface to a maximum

temperature in the water column from when ice cover was established (Kalff, 2002). Small convective currents may develop during this time, due to solar energy penetrating the ice or through the intrusion of inflows (Kalff, 2002; Palmer et al., 2021). Spring melt occurs due to increased solar energy, surface ice melt and addition of warm inflows, mixing with the $< 4\text{ }^{\circ}\text{C}$ water below the ice. This induces turbulence, which alongside increasing solar radiation causes water column mixing and ice-off. The degradation of winter ice cover can be rapid, often taking place in a few hours, especially if associated with a strong wind (Wetzel, 2001b). Following ice off, the water at all depths is near the temperature of maximum density and warming or cooling only elicits small changes in density difference per unit change in temperature. Therefore, the resistance to mixing is small and low wind energy is able to mix the water column, maintaining a fully mixed water column. This is the *spring overturn* or *spring mixing* event. In a monomictic system these conditions would persist from autumn overturn until the next stratification onset.

The stability of the stratification or stratification strength is quantified in numerous ways, but generally describes the resistance of the water column to full mixing or the energy required to fully mix the water column. A simplistic metric for understanding stratification strength is the difference between surface and bottom temperature. Due to the non-linear relationship between temperature and density, and the impact of salinity on density, a more useful metric is the density difference between top and bottom. Another metric, Schmidt stability is the amount of energy required to mix the water column to isothermal conditions and is given per unit area (W m^{-2}). Initially formulated by Schmidt (1915) and revised by Idso (1973), it quantifies the resistance of stratification to disruption and the extent to which the hypolimnion is isolated from the surface (Wetzel, 2001b).

2.4.2.1 Importance for lake functioning

Stratification dynamics are important for the functioning of lake ecosystems. During stratification, the density gradient inhibits mixing across the thermocline, governing the vertical distribution of nutrients, biota, and dissolved gases (Kalff, 2002). The mixing regime is important in determining the likely presence of an isolated hypolimnion, the light climate experienced by phytoplankton, and the availability of appropriate thermal and oxygen habitat for aerobic organisms, among other lake functions.

The stability of the stratification as well as the length of the seasonally stratified period is important for biota, especially phytoplankton. Kalff (2002) states that “the development of the metalimnion and the restrictions imposed on circulation as well as the modifications to

the light climate experienced by phytoplankton, makes stratification the single most important physical event for biota". The onset of stratification and the development of a surface mixed layer improves the light climate for phytoplankton, as mixing in the surface layer maintains cells in the euphotic zone. The relationship between surface mixing depth (Z_{mix}) and euphotic depth (Z_{eu}) is important for determining the vertical distributions of phytoplankton biomass (Figure 2.6; Kalff, 2002; Hamilton *et al.*, 2010). Where Z_{eu} is deeper than Z_{mix} a deep chlorophyll maxima (DCM) can form. Reductions in water clarity associated with eutrophication can prevent the formation of a DCM and the chlorophyll maximum occurs closer to the surface (Hamilton *et al.*, 2010).

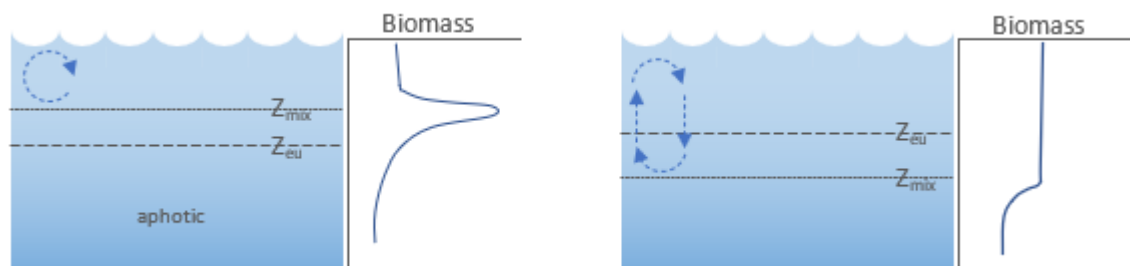


Figure 2.6 Influence of the euphotic depth (Z_{eu}) and mixed layer (Z_{mix}) on the vertical distribution of phytoplankton biomass (modified from Thornton *et al.*, 1990).

More stable stratification favours buoyant species and those able to control their position in the water column (Fadel *et al.*, 2015). Flagellated phytoplankton, and those with gas vesicles, are able to control their position within the water column and hence have a competitive advantage over other species in stratified systems. Increases to water column stability therefore increases the risk of cyanobacterial blooms (Paerl and Huisman, 2008; Winder and Sommer, 2012). Cyanobacteria form buoyant surface blooms that shade out other phytoplankton and suppresses their growth through competition for light (Jöhnk *et al.*, 2008). Earlier and longer stratification, alongside surface warming trends, have been associated with broad-scale increases of cyanobacteria abundances in US reservoirs (Smucker *et al.*, 2021).

Stable stratification, especially in productive lakes, drives oxygen depletion in the hypolimnion, leading to anoxia under high rates of depletion. The hypolimnion is isolated from the air-water interface, preventing oxygen being mixed downwards. Oxygen used up in water column respiration, the mineralization of organic matter, and the release of reduced substances from anoxic sediment (Bouffard *et al.*, 2013; Müller *et al.*, 2012) cannot be replenished, so oxygen concentrations reduce. Therefore, the length of stratification is important for determining how long the hypolimnion is isolated from the atmosphere and consequently the spatial and temporal extent of anoxia in a lake (Snortheim *et al.*, 2017; Zhang

et al., 2015). The relationship between stratification and oxygen dynamics is further explored in Section 2.6.2.

Changes to water column stability modify vertical mixing energy (Heinz et al., 1990; Imberger, 2013; Saber et al., 2018). Vertical diffusivities can vary by orders of magnitude throughout the year depending on water column stability: higher vertical diffusivity under low stability and lower vertical diffusivity under higher stability (Cornett and Rigler, 1987; Saber et al., 2018). The two chiefly cited sources of vertical mixing energy in lakes are wind and surface cooling (Imberger, 2013; Saber et al., 2018) but inflows into lakes also have the potential to affect vertical mixing. Additional cooling from the advective heat flux (Section 2.4) may also promote convective mixing and reductions in water column stability (Kimura et al., 2014; Liu et al., 2020) increasing vertical mixing (Brand et al., 2008; MacIntyre et al., 2002). These changes in stability, could therefore have consequences for the downwards mixing of oxygen into the hypolimnion, rarely investigated thus far.

2.5 Climate change impacts on lake thermal dynamics

Anthropogenic greenhouse gas emissions have increased global temperatures by an average of 0.85 °C (0.65-1.06 °C) between 1880-2012 (IPCC, 2014). Temperatures are expected to continue to rise and are likely to exceed +1.5 °C by the end of the century relative to baselines (1850-1900; IPCC, 2014). Given the coupling of lakes and climate (Adrian et al., 2009; Schindler, 2009), the impact of climate warming has the potential to impact lake physical functioning including water temperatures, stratification and mixing dynamics (Woolway et al., 2020).

2.5.1 Changes to water temperatures

Many lake are experiencing increases in surface water temperatures (O'Reilly et al., 2015). The mean rate of warming of lakes was found to be 0.34 °C decade⁻¹ (1985-2009), although the rate is variable and some lakes are exhibiting cooling trends (O'Reilly et al., 2015). Heat budget analysis suggests that around 80% of air temperature warming will be converted into surface water warming, due to increased rates of evaporation (Roderick et al., 2014; Wang et al., 2018). Some lakes are experiencing warming rates that exceed air temperature increases, attributed in some instances to earlier onset of stratification. In Laurentian Great Lakes, earlier onset of stratification has contributed to warming rates above those of air temperature (Austin and Colman, 2007; Piccolroaz et al., 2015; Woolway and Merchant, 2017). Earlier stratification reduces the volume of water affected by surface heating, increasing the rate of warming (Piccolroaz et al., 2015; Woolway and Merchant, 2017). Additional warming may also be

coming from increases in incoming solar radiation (*solar brightening*), linked to improved air quality (Schmid and Köster, 2016). Inconsistent trends with air temperature warming suggest that lake specific parameters are important, including lake morphometry (Kraemer et al., 2015; Winslow et al., 2015), climate region (Woolway and Merchant, 2017), and lake clarity (Pilla et al., 2018; Rose et al., 2017; Tanentzap et al., 2008).

Rates of warming also vary due to lake-specific characteristics. Smaller lakes in Wisconsin were found to have different warming trends to larger lakes in the same region (Winslow et al., 2015). In lakes with surface areas less than 0.5 km², the warming trend was confined to the upper-most layers and little change was found in the deeper waters, whereas in larger lakes warming trends were at a higher rate and more consistent throughout the water column (Winslow et al., 2015). This difference is thought to be due to lower wind driven turbulence over smaller lakes, due to smaller fetch, and therefore mixing of heat lower into the water column is reduced (Winslow et al., 2015). Lakes of different mixing regimes have shown different patterns of warming, with polymictic lakes showing greater rates of bottom water warming than stably stratifying lakes (Richardson et al., 2017) due to frequent mixing events during the summer that mix heat throughout the water column.

Temperature changes in lake temperatures are temporally variable (Toffolon et al., 2020; Winslow et al., 2017), differing between seasons (Winslow et al., 2017; Woolway et al., 2019b). Trends in summer warming have been the primary focus, but there is increasing evidence that to fully understand climate change impacts knowledge of impacts throughout the year is needed (Winslow et al., 2017). Annual minimum temperatures in Blelham Tarn, in the English Lake district, are increasing at twice the rate of summer temperatures and in Loch Feeagh, Ireland, the rate is four times faster (Woolway et al., 2019b). Analysis of monthly surface water temperature warming rates in lakes situated in Wisconsin, USA found that temperature warming rates in late summer and early autumn (0.062-0.081 °C year⁻¹) were more than twice the rates in spring and summer (0.031-0.013 °C year⁻¹) (Winslow et al., 2017). Understanding this month to month variability is important as it can exceed between-lake differences in surface water warming rates (Winslow et al., 2017).

2.5.2 Changes to lake stratification and mixing regimes

Warming has also caused changes to lake mixing regimes (Kirillin et al., 2017; Kraemer et al., 2015; Shatwell et al., 2019; Woolway and Merchant, 2019). Projections under future climate are for lengthening and strengthening of the summer stratified period in monomictic and dimictic lakes (Darko et al., 2019; Ladwig et al., 2021; Smucker et al., 2021; Woolway et al.,

2021b), due to preferential warming of the surface waters, and reduced warming or even cooling in some lakes at depth (Richardson et al., 2017). Already, evidence shows that stratification onset has become earlier (Foley et al., 2012; Winder and Schindler, 2004; Woolway et al., 2021b) due to warmer spring temperatures (Foley et al., 2012; Magee and Wu, 2017). Woolway *et al.* (2021) showed that in the Northern Hemisphere stratification onset is projected to be 22 ± 7 days earlier under a high emissions scenario, lengthening stratification by 33 ± 12 days overall.

Additionally, climate change warming is projected to change lakes from dimictic to monomictic (Råman Vinnå et al., 2021; Woolway and Merchant, 2019). Global analysis suggests 17% of lakes likely to experience this alteration by the last decade of the century (Woolway and Merchant, 2019), including the loss of ice cover and reductions in inverse stratification in winter (Sharma et al., 2019; Woolway et al., 2019b). Some lakes that are currently monomictic are projected to become meromictic (Fenocchi et al., 2018; Mesman et al., 2021), with stratification persisting from one summer to the next without complete mixing (Woolway et al., 2020). Deep lakes are already showing reductions in the occurrence of complete winter mixing (Rogora et al., 2018; Yankova et al., 2017), which has implications for the seasonal replenishment of oxygen in the hypolimnion (see Section 2.6.2). Future projections in Lake Geneva estimate that this deep lake will have 50% fewer complete mixing events by 2100 (Schwefel et al., 2016).

2.5.3 Non-air temperature changes

Despite the focus on air temperature changes in most climate change studies, other factors can contribute to surface water temperature change. Changes to wind speeds and water transparency have also been shown to be driving or modifying long-term trends in water temperatures (Butcher et al., 2015; Pilla et al., 2018; Stetler et al., 2020; Winslow et al., 2015). Wind stilling patterns in recent decades (McVicar et al., 2012) have been linked to increasingly stable stratification and higher surface temperatures (Stetler et al., 2020; Woolway et al., 2019a, 2017a). Using long-term records and hydrodynamic modelling, atmospheric stilling, has been attributed to 27% of the increase in water column stability in northern hemisphere lakes, and shallowing of surface mixed layer as wind speeds have declined (Stetler et al., 2020; Woolway et al., 2019a). Stilling has led to longer stratified periods in monomictic lakes and extended thermal stratification in polymictic lakes (Stetler et al., 2020; Woolway et al., 2019a, 2017a). Higher forest cover related to increased wind sheltering is also associated with cooling bottom waters despite regional climate warming (Tanentzap et al., 2008). As the tree line is

expected to advance under a warmer climate there is expected to be increases in the length of stratification in these regions (Klaus et al., 2021).

Water clarity is important for heat distribution and the vertical extent of warming (Butcher et al., 2015; Richardson et al., 2017). Lakes with higher water clarity exhibit greater rates of deep-water warming (Butcher et al., 2015), and reductions in clarity are linked to increased surface warming (Pilla et al., 2018; Richardson et al., 2017) as more heat is absorbed in the upper water column (Kalf, 2002). Brownification in Lake Giles, a previously transparent (Secchi depth = 7.2 m) deep lake (maximum depth = 24 m), from 1988 to 2017 was linked to a $1.04\text{ }^{\circ}\text{C decade}^{-1}$ increase in surface temperature and a $1.54\text{ }^{\circ}\text{C decade}^{-1}$ in deep-water temperature when there were no significant air temperature trends (Pilla et al., 2018).

Changes in precipitation and evaporation driven by climate warming (IPCC, 2014) are projected to induce change in river flow for large proportions of the world (Arnell and Gosling, 2013; Milly et al., 2005; van Vliet et al., 2013). Additionally, increased pressure on water resources from abstraction is also likely to modify river discharge (Döll et al., 2009; Rio et al., 2018). Already trends of river flows provide evidence for the role of anthropogenic climate change as a causal driver of recent trends in global river flows (Gudmundsson et al., 2021). Projected changes to discharge can be large, and, unlike air temperature warming, may be bi-directional, ranging from large increases (>50%) to large decreases (> 80%), depending on the climate projections, geographic region (Arnell et al., 2015; van Vliet et al., 2013) and even between catchments in the same region (Fowler and Kilsby, 2007; Garner et al., 2017a). In addition to annual changes, potential changes to river flow seasonality is projected, resulting in larger peak flows and lower low flows (Prudhomme et al., 2013; van Vliet et al., 2013).

River flow projections are generally more uncertain than air temperature warming and have been less often considered in climate impacts on lakes (Bayer et al., 2013; Christianson et al., 2020; Komatsu et al., 2007; Taner et al., 2011; Valerio et al., 2015). Modelling studies that have considered river flow changes have mostly used watershed modelling coupled with hydrodynamic or ecosystem models to look at specific projections of climate in an individual lakes (Bayer et al., 2013; Komatsu et al., 2007; Taner et al., 2011; Valerio et al., 2015), using down-scaled climate projections. The impact of future climate on lake temperatures is generally dominated by air temperature warming (Taner et al., 2011; Valerio et al., 2015). Some studies have considered flow and air temperature results separately and together to disentangle these co-occurring impacts, showing that river flow changes moderated warming effects to some extent (Bayer et al., 2013; Valerio et al., 2015). In Lake Iseo (annual average

WRT = 4.3 years), when flow changes were not included epilimnetic temperatures were up to 3 °C warmer than when they were (Valerio et al., 2015). All studies that have modelled future river flow impacts have looked at maximum of two scenarios. Given the uncertainty around projections of river flow assessing a larger range of river flow conditions would give greater insights into how a range of lakes might respond to climate induced flow changes. Modelling of smaller, short-residence time lakes has also been neglected, despite the likely importance of flow changes for these systems.

2.6 Deep water oxygen dynamics and internal loading

Hypolimnetic oxygen concentration during the stratified period is a key lake water quality indicator. Low oxygen concentrations ($< 2 \text{ mg O}_2 \text{ L}^{-1}$, *hypoxia*) or complete deficiency ($< 1 \text{ mg O}_2 \text{ L}^{-1}$, *anoxia*) during large periods of the year, due to increased metabolism of organic matter (Bouffard et al., 2013; Cooke et al., 2005), can be indicative of eutrophication. Hypolimnetic anoxia is of environmental importance as it limits habitat availability for aerobic organisms, causes reducing redox conditions under which nutrients, such as phosphorus, are released from the sediment into the water column.

2.6.1 Sources and sinks of hypolimnetic dissolved oxygen

Dissolved oxygen (DO) concentrations are determined by a complex interaction of production and consumption processes, including sediment and water column (areal and volumetric) oxygen demands, diffusion and turbulent mixing of oxygen from the air-water interface, as well as primary production (Bouffard et al., 2013; Cornett and Rigler, 1987; Müller et al., 2012). These processes vary seasonally due to changes in productivity, in response to external drivers such as the loading of organic matter and nutrients from the catchments (de Eyto et al., 2016; Marcé et al., 2008), and due to changes in the lake's thermal structure (Hanson et al., 2006).

Oxygen supply from the atmosphere occurs due to sub-saturation at the lake's surface. Molecular diffusion in calm waters is very weak and wind-induced turbulence is the major mechanism of DO changes (Kalff, 2002). In-lake sources of DO are dominated by primary production in the euphotic zone. Photosynthesis by phytoplankton, benthic algae, and macrophytes produce dissolved oxygen in the euphotic zone. Higher rates of primary production are therefore related to elevated concentrations of oxygen. In the hypolimnion, mixing of oxygen downwards, from these productive and surface-interacting zones is the primary source of oxygen during stratification (Bouffard et al., 2013).

Rivers and streams are often highly oxygenated, maintaining saturation above 85% and even become supersaturated, therefore providing oxygen to the lake (Neal et al., 2002; Wetzel, 2001c; Williams and Boorman, 2012). Inflows can also intrude into the water column at different heights depending on their water densities (Fink et al., 2016; MacIntyre et al., 2006; Rueda and MacIntyre, 2009) and so can act as a source of oxygen to deep water. The impact of rivers on hypolimnetic oxygen concentrations have previously been considered in deep lakes and reservoirs with cold plunging inflows (Andradóttir et al., 2012; Fink et al., 2016; Liu et al., 2020; Marcé et al., 2010) and under ice when the whole water column is isolated from atmospheric oxygen inputs (Palmer et al., 2021). However, in smaller, shallower, temperate systems the contribution of inflows to short-term deep-water oxygen dynamics has not been well quantified. As described in Section 2.4.2.1 inflows may also be contributing to oxygen dynamics in the hypolimnion due to their destabilising effect on the water column that enhances downward vertical mixing of oxygen.

Sink terms are dominated by respiration processes in plants, animals, and bacteria. Organic matter produced in the epilimnion sinks into the hypolimnion, mineralisation of which consumes oxygen (Bouffard et al., 2013; Müller et al., 2019). Therefore, higher productivity in the epilimnion can increase DO depletion in the hypolimnion. Allochthonous inputs of organic matter can also induce additional depletion (de Eyto et al., 2016; Marcé et al., 2008). In the hypolimnion, further oxygen consumption comes from the release of reduced substances from anoxic sediment (Bouffard et al., 2013; Müller et al., 2012).

2.6.2 Long term trends in hypolimnetic anoxia

As described above (section 2.4.2.1), the development of a thermocline restricts the resupply of oxygen from the lake surface to replace that which is consumed through depleting processes, such as water column respiration, the mineralization of organic matter, and the release of reduced substances from anoxic sediment (Bouffard et al., 2013; Müller et al., 2012). In sufficiently productive lakes hypolimnetic anoxia can develop due to the high rates of oxygen depletion (Foley et al., 2012; Jane et al., 2021; North et al., 2014). Therefore, the length of the stratified period is a key driver of the duration and extent of hypolimnetic anoxia (Crossman et al., 2018; Jane et al., 2021). Changes to oxygen depletion have been related to long-term increased stratification length and strength (Foley et al., 2012; Jane et al., 2021; North et al., 2014; Smucker et al., 2021). An analysis of long-term records in 393 temperate lakes showed widespread decline in deep-water oxygen concentrations, associated with longer thermal stratification. Average reductions of 0.42 mg L^{-1} since 1980, a loss of over 18% of oxygen, were observed during the summer period (Jane et al., 2021). In Lake Zurich, a large

deep lake, earlier stratification between 1972-2010 was associated with earlier development of hypoxic conditions (North et al., 2014) and between 1989 and 2020 in 20 US reservoirs hypoxia duration increased by two months (Smucker et al., 2021). Modelling suggests further increases in seasonal anoxia duration and extent as climate warming continues (Ladwig et al., 2021; Schwefel et al., 2016; Snorheim et al., 2017), expediting the onset of the anoxic period (Missaghi et al., 2017).

As well as changes to the length of stratification in monomictic lakes, there has been evidence of fewer complete mixing and full-replenishment of oxygen of hypolimnion in some deep lakes (Ito and Momii, 2015; Rogora et al., 2018; Schwefel et al., 2016). Abrupt climate warming since the late 1980s has been linked to the cessation of complete mixing, and long-term hypolimnetic anoxia (21 years) in a deep (max depth 233 m) lake in Japan (Ito and Momii, 2015). In another deep lake, Lake Geneva, events with complete mixing of temperature and oxygen in winter are projected to decrease by around 50% by 2100, reducing hypolimnetic oxygen concentrations in winter (Schwefel et al., 2016). Recent trends towards decreasing deep-water oxygen concentrations in Italy's deep alpine lakes are also related to fewer complete mixing events, none occurring between 2004-2016 in two of the five lakes studied (Rogora et al., 2018). In polymictic lakes, the development of stratification at increasing rates and durations, has been shown to increase occurrence of hypoxia and oxygen depletion (Cortés et al., 2021; Martinsen et al., 2019; Wilhelm and Adrian, 2008)

As well as stratification, other anthropogenic impacts may be contributing to long-term trends in deep-water anoxia. Some studies have suggested that eutrophication is also contributing to reduced oxygen concentrations in some lakes, potentially acting synergistically with stratification changes (Foley et al., 2012; Jane et al., 2021). Increased productivity in the epilimnion is an important source of organic matter to the hypolimnion and mineralisation contributes to greater DO depletion (Foley et al., 2012). However, modelling by Ladwig *et al.* (2021) suggested that the inter-annual dynamics in primary production were not influential in controlling duration of anoxia for Lake Mendota, a eutrophic, stratifying lake. Browning trends, caused by increased dissolved organic matter concentrations in a small oligotrophic lake, were also related to increased oxygen depletion, reducing minimum summer oxygen concentrations by more than 4 mg L⁻¹ over a 27 year period (Knoll et al., 2018).

Given the relationship between oxygen saturation and water temperature (Jane et al., 2021; Lee et al., 2018; Zhang et al., 2015), reduced concentrations may be expected in warmer lakes. However, trends suggest that in temperate lakes at least, hypolimnetic anoxia is not linked to

reductions in solubility (Zhang et al., 2015) as there has been little change in temperature ($-0.01\text{ }^{\circ}\text{C decade}^{-1}$; Jane *et al.*, 2021).

2.6.3 High-frequency deep-water oxygen dynamics

Compared to the study of long-term trends in hypolimnetic oxygen concentrations, the short-term dynamics are not well studied. High-frequency measurements of oxygen have mostly been used in studies of lake metabolism using surface measurements (e.g. Staehr *et al.*, 2010; Zwart *et al.*, 2017; Fernández Castro *et al.*, 2021). There is growing evidence, from high-frequency data, that the relationship between physical lake processes, stratification and water column stability, and hypolimnetic oxygen dynamics operates over these shorter timescales. Previous work has investigated short-term oxygen depletion during short-term (days to weeks) stratification in polymictic lakes (Martinsen *et al.*, 2019; Wilhelm and Adrian, 2008). Stratification events during summer in the polymictic Müggelsee, Germany lasting in the order of a few weeks were related to short-term depletion of oxygen, with anoxic conditions ($< 2\text{ mg L}^{-1}$), accounting for up to 25% of the lake volume (Wilhelm and Adrian, 2008). The short-term dynamics of oxygen under ice have also received some attention (e.g. Obertegger *et al.*, 2017; Smits *et al.*, 2021).

The impact of individual storm events has also shown perturbations to deep-water dissolved oxygen related to impacts on the lake's thermal structure (Huang *et al.*, 2014; Jennings *et al.*, 2012; Liu *et al.*, 2020; Weinke and Biddanda, 2019). Storms may influence short-term oxygen dynamics due to increased wind speeds and increased surface cooling, causing reduced water column stability (M. R. Andersen *et al.*, 2020; Kimura *et al.*, 2014; Woolway *et al.*, 2018). Changes to water column stability modify vertical mixing energy; under higher stability, the rates of vertical mixing, crucial for determining hypolimnetic oxygen concentrations, are reduced (Cornett and Rigler, 1987; Heinz *et al.*, 1990; Papst *et al.*, 1980). In Blelham Tarn, UK, a storm event that caused a sharp increase in turbulent wind energy flux and reduced surface heating, coincided with a 65% decrease in water column stability and increase in the deep-water dissolved oxygen concentration, suggesting entrainment of oxygenated water from the mixed layer (Jennings *et al.*, 2012). However, these extreme events do not fully represent typical conditions and studies have mostly been in large, deep lakes and reservoirs that are less globally numerous and may respond differently than smaller lakes to external drivers (wind, cooling, inflows).

Short-term oxygen dynamics have implications for our understanding of the processes affecting DO concentrations, but little is known about short-term dynamics and physical

controls on hypolimnetic oxygen concentrations in seasonally stratifying lakes. This is despite the fact that these dynamics are likely to have implications for biogeochemical cycling and habitat availability in lakes. Increasing deployment of sensors to collect high-frequency oxygen data is expanding the opportunities to investigate these types of dynamics.

2.6.4 Importance of deep-water oxygen dynamics

Many aerobic species have oxygen requirements for growth, including fish, zooplankton, and macroinvertebrate species (Kalf, 2002). Fish species vary in their requirements (Alabaster and Lloyd, 1982), with some more tolerant species able to persist at lower concentrations (2-5 mg L⁻¹), whereas more sensitive species, such as salmonids, require high oxygen concentrations (5-9 mg L⁻¹). Given the oxygen requirements for aerobic species, the occurrence of widespread anoxia in lakes can limit the habitat available to them as feeding grounds, for egg laying, and as daytime refugia in zooplankton.

In addition to oxygen requirements, the temperature constraints of some species can further limit their access to suitable habitat. Coldwater fish species such as trout, require cool oxygenated waters. With warmer water temperatures and increasing extent of anoxia in lakes under climate change, species such as these are subject to what is termed the *dissolved oxygen-temperature squeeze* (Coutant, 1985). Aerobic species having to inhabit shallower parts of the water column to find their oxygen requirements, but finding sub-optimal temperature conditions (Coutant, 1985; Matthews and Berg, 1997; Missaghi et al., 2017). Long-term records of temperate lakes suggest that 68% of lakes were experiencing declining habitat for these cold-water species (Jane et al., 2021), and in one lake there was an increase in lethal habitat for cold-water fish of 85% (Missaghi et al., 2017). One such species, is the vendace (*Coregonus albula*), which requires cool well oxygenated water. A modelling study by Elliott & Bell (2011), showed that under future climate, the habitat availability in Bassenthwaite Lake, UK would decline due to more than 2 °C of lake warming and a 10% reduction in oxygen concentration. Over a 20-year period the number of years with > 20 consecutive days of no viable habitat was 8 times higher under future climate than with current climate.

Internal loading of nutrients from nutrient-rich bed sediments is another important consequence of anoxic conditions in the hypolimnion. Seminal work by Mortimer (1942) showed that oxygenated sediments retain phosphorus by fixation to iron while reduced sediments release phosphorus by reduction of iron and subsequent dissolution of complexes of iron and phosphorus. Anoxic conditions cause the reduction of iron compounds but also

impact microbial metabolism, further releasing P into the water column (Boström et al., 1988). Internal P supply often occurs in highly bioavailable forms as soluble reactive phosphorus (Nurnberg, 1988), furthering the impact on lake systems.

Empirical evidence for the importance of oxygen concentrations for internal loading is widespread (North et al., 2014; Radbourne et al., 2019; Spears et al., 2007; Tammeorg et al., 2017), often indicated by peaks in SRP concentrations in the hypolimnion in late summer due to the high-magnitude internal release of redox-sensitive sediment P (Mackay et al., 2014a; Spears et al., 2007). With increasingly stable and longer stratification, longer anoxic periods, increased release of SRP from sediments would be expected. Evidence from Esthwaite Water, showed that during years of high stability and longer stratification, internal loading contributed 50% of the total SRP load, compared to only 34% under less stable conditions (Mackay et al., 2014a).

Despite the long-standing paradigm in limnology that dissolved oxygen concentrations in the hypolimnion control the release of P from sediments (Hupfer and Lewandowski, 2008), and evidence as shown above, it is likely that the controls on internal P loading are more complex (Boström et al., 1988; Hupfer and Lewandowski, 2008). Hupfer & Lewandowski (2008) argue that this simplistic relationship between DO and P is not always realistic, also presenting limitations for the use of hypolimnetic aeration/oxygenation in some lakes (Gächter and Wehrli, 1998; Tammeorg et al., 2017). Other parameters including temperature, nitrate concentration, and pH may also be similarly important (Boström et al., 1988; Jensen and Andersen, 1992; Pettersson, 1998; Spears et al., 2007) as well as bacteria-mediated P release (Hupfer and Lewandowski, 2008). Equally, the ability for sediments to retain P requires available binding materials, including iron or aluminium (Gächter and Müller, 2003; Kopáček et al., 2005) and is not simply a consequence of low DO concentrations.

2.7 Lake management

The value and importance of lakes and their ecosystem services is threatened by external stressors. These stressors are primarily climate, invasive species introduction, and pollution relating to anthropogenic sources, such as nutrient enrichment and eutrophication. These stressors are acting in combination as well as isolation, often compounding the individual impacts on lake systems (Birk et al., 2020; Moss et al., 2011; Spears et al., 2021). Climate warming, particularly, is compounding eutrophication impacts (Birk et al., 2020; Spears et al., 2021) and there is ever increasing need for adaptive management focusing on in-lake methods

to accelerate improvement in water quality to meet legislative targets (such as the EU WFD and US Clean Water Act) and maintain vital ecosystem services. Eutrophication has been identified as the primary cause of lakes failing to meet regulatory water quality targets (Birk et al., 2020). Caused by anthropogenic inputs of phosphorus (P) and nitrogen (N) from catchment sources, eutrophication results in excess phytoplankton growth, a loss of biodiversity, and low oxygen conditions. The economic cost of poor water quality is likely to be in the billions per year, globally. In the UK alone, eutrophication impacts, in particular algal blooms, were estimated to cost £173 million annually, with the potential to rise to £481 million under a 4 °C warmer climate change scenario (Jones et al., 2020). Therefore, methods to manage and restore lakes degraded by eutrophication have received significant research and economic focus.

External nutrient load reductions are the primary measure to improve in-lake conditions (Lürling and Mucci, 2020; Van Liere and Gulati, 1992). However, lakes can be slow to recover and problems can persist in lakes decades after reductions (McCrackin et al., 2017), often attributed to internal loading (Does et al., 1992; Søndergaard et al., 2003; Van Liere and Gulati, 1992). The release of nutrients accumulated in bed sediments maintains water column nutrient concentrations. In stratifying lakes, internal loading principally occurs in the summer period where the development of anoxia in the hypolimnion overlying lake bed sediments promotes redox conditions where Fe-P complexes are reduced and their dissolved components liberated across diffusive concentration gradients to the water column (see Section 2.6.4). In order to speed up the recovery of lakes degraded by internal nutrient loading, there is growing need for in-lake measures (Lürling and Mucci, 2020; Zamparas and Zacharias, 2014).

2.7.1 Methods to manage internal loading

A range of in-lake measures have been proposed to control internal loading (Lürling et al., 2020). Methods target hypolimnetic anoxia or sediment-P binding to decrease the intensity of internal loading. Measures that target hypolimnetic anoxia include hypolimnetic aeration and oxygenation (Preece et al., 2019; Toffolon et al., 2013), artificial mixing (Visser et al., 2016), and less frequently, hypolimnetic withdrawal (see Nürnberg, 2019). Of these, hypolimnetic aeration/oxygenation are the most common. Hypolimnetic aeration and oxygenation use direct injection of air/oxygen, via bubble plume diffusers and side-stream saturation (SSS), where water is withdrawn from the lake, injected with concentrated oxygen gas and returned to the hypolimnion (Cooke et al., 2005; Preece et al., 2019). Problems with these methods include hypolimnetic warming and destabilisation of the stratification and upwards mixing.

Such mixing could result in the entrainment of nutrients from the hypolimnion to the epilimnion, resulting in elevated nutrient concentrations in the photic zone and increased nutrient availability (Gerling et al., 2014). Hypolimnetic oxygenation deployed at Lake Serraia, a small, shallow, peri-alpine lake caused hypolimnetic warming of up to 9 °C, associated with enhanced rates of organic matter decomposition, increased water circulation, sediment remobilisation and increased turbidity (Toffolon et al., 2013).

The deployment of bubble plume mixers is restricted to deeper lakes (> 10 m), because using this method in shallower water bodies is more likely to disrupt thermal stratification (Cooke et al., 2005; Preece et al., 2019). Conversley, SSS is deployable in lakes with smaller hypolimnion as more oxygen can be added with low water flow rate, thereby causing less mixing (Gerling et al., 2014). Using pure oxygenation rather than aeration is likely to reduce the number of devices needed, minimising turbulence, and using air also increases the chances of high levels of nitrogen gas being present and potentially leading to gas bubble disease in fish (Beutel and Horne, 1999). A recent review of hypolimnetic oxygenation found that the method was mostly successful, improving aerobic conditions for fish a zooplankton, and reducing internal loading (Preece et al., 2019). However, the direct impacts could not be fully attributed to hypolimnetic oxygenation as it has been often applied in conjunction with other restoration efforts (e.g. nutrient load reductions, chemical capping). However, the technology remains expensive, incurring long-term operational and maintenance costs (Preece et al., 2019). These methods require long-term deployment to be effective, Preece *et al.* (2019) reporting at least a decade of deployment throughout the stratified season is needed. Shorter-term deployment has quickly resulted in improvements being lost once discontinued (Cooke et al., 2005; Preece et al., 2019). However, a long-term (10 year) deployment in two Swiss eutrophic lakes did not improve lake internal loading, as although the anoxia was reduced the sediment P retention capacity was insufficient to prevent loading (Gächter and Wehrli, 1998).

Further methods target sediment-P binding as a means to reduce internal loading, by increasing the retention capacity of the sediment (Mackay et al., 2014b; Spears et al., 2016). Termed geo-engineering, these methods intervene with biogeochemical cycles to control internal loading (Lürling et al., 2016). Common P-sorbents include aluminium (Kuster et al., 2020), lanthanum modified bentonite (Lang et al., 2016; Spears et al., 2016), and calcium (Mehner et al., 2008). Geo-engineering methods have had mixed success (Mackay et al., 2014b; Spears et al., 2014). A review of the longevity of water quality improvements following aluminium additions varied between no improvement and > 30 years (Huser et al., 2016a). Reduced longevity may be due to insufficient control of external loads, insufficient dosing of

sorbents, and resuspension of material especially in smaller lakes (Abell et al., 2020; Huser et al., 2016a; Kuster et al., 2020). In Loch Flemmington, UK, reductions in algal blooms were not sustained past two years following lanthanum application due to sediment remobilisation and high external P loads (Lang et al., 2016). The cost of application can also be prohibitive to widespread application in the field (Mackay et al., 2014b), limiting their application to smaller lakes (Abell et al., 2020). However, Douglas *et al.* (2016) suggest that in the context of whole catchment solutions, P-adsorptive treatments may be a low-cost solution if effective, but a systems level cost-benefit analysis is needed to fully understand whether methods should be considered (Douglas et al., 2016). Sediment removal or dredging could also remove high-nutrient sediments to limit internal loading, but can be expensive and ecologically destructive (Bormans et al., 2016; Cooke et al., 2005; Does et al., 1992).

Additional methods target the symptoms of the internal loading, specifically high algal biomass. These include biomanipulation, flocculant additions and herbicide application (see Cooke *et al.*, 2005; Abell *et al.*, 2020).

2.7.2 Use of WRT changes in management

Water residence time changes have been used in lake management as a means of diluting nutrient concentrations and to promote direct flushing of phytoplankton cells (León et al., 2016; Lewtas et al., 2015; Londe et al., 2016; Uttormark and Hutchins, 1980). The magnitude of direct flushing effects on algae is dependent on the growth rate of the species present (Kalff, 2002; Lucas et al., 2009) and therefore differentially impacts certain species (Padisák et al., 1999; Reynolds et al., 2012). Only where flushing rates exceed growth rates (loss > growth) will washout occur (Lucas et al., 2009; Reynolds et al., 2012). Addition of low nutrient water will also reduce the concentration of limiting nutrients via dilution (Jørgensen, 2002; Lewtas et al., 2015). This limits the potential growth of the phytoplankton (Jones and Elliott, 2007) and the maximum algal biomass (Cooke et al., 2005; Lewtas et al., 2015). Together dilution and flushing combine to improve water quality by reducing phytoplankton growth rate and carrying capacity of the system and/or increasing loss rate (Lewtas et al., 2015; Welch, 1981). The use of dilution/flushing methods have had mixed success. Intermittent flushing of Moses Lake, alongside external load reductions, reduced total P concentrations from 156 $\mu\text{g L}^{-1}$ to 70-90 $\mu\text{g L}^{-1}$ and chlorophyll *a* concentrations from 45 mg L^{-1} to 15 mg L^{-1} , although problems with internal nutrient loads persisted (Jones and Welch, 1990; Welch, 1981; Welch and Patmont, 1980). In Lake Veluwe, flushing reduced internal loading, and TP and chlorophyll *a* concentrations both reduced by more than 75% (Hosper and Meyer, 1986; Jagtman et al., 1992). However, changes occurred alongside the application of P-stripping to waste water

effluent and flushing water was high in calcium, increasing binding capacity in the lake (Hosper and Meyer, 1986; Jagtman et al., 1992). WRT changes have also been used to disrupt cyanobacteria blooms in impounded rivers (Bormans and Ford, 2002; Mitrovic et al., 2011, 2006; Webster et al., 2000) by reducing water column stability and increasing turbidity, which act to control algal blooms (Mitrovic et al., 2011; Webster et al., 2000). WRT manipulations are yet to be used broadly, especially to inhibit summer stratification and associated seasonal anoxia and internal loading.

2.7.3 Optimising management

It is likely that due to variation in morphology, hydrology and eutrophication history, systems will respond differently to restoration and management measures and therefore a study prior to implementation would inform on the likely implications at the system level (Van Liere and Gulati, 1992; Verspagen et al., 2006). Optimising the success of restorations is dependent on thorough diagnosis and evaluation of the processes causing poor lake quality, prior to initiating measures (Cooke et al., 2005; Klapper, 2007; Lürling et al., 2016; Stroom and Kardinaal, 2016). Pre-intervention analysis will aid in setting realistic goals and targets for restoration (Cooke et al., 2005; Klapper, 2007) and help prevent the implementation of costly inappropriate methods (Cooke et al., 2005), if important factors are overlooked. These factors include the relative importance of internal and external nutrient sources (Lürling et al., 2016).

While there has been some success using these existing in-lake methods, restoration outcomes have been inconsistent (Huser et al., 2016b), and can incur high capital and running costs (Mackay et al., 2014b; Visser et al., 2016). With the pressure to achieve water quality targets, the threat of climate change, and the mixed success of existing measures, there is a need for innovative methods to tackle internal loading.

2.8 Summary

This review has highlighted the importance of water residence time for chemical and ecological processes in lake systems. However, less is currently known about the impact of water residence time changes on lake thermal dynamics, also fundamental for lake functioning. The review shows that water residence time impacts on lake thermal structure are needed to inform management and to understand lake responses to climate change impacts more fully. WRT manipulation to control internal nutrient loading is a novel approach that requires robust assessment of its efficacy. A systematic approach to understanding WRT impact on lake thermal structure and a thorough assessment of a whole lake application will help inform future management practice. Furthermore, despite acknowledging the other

impacts of climate change on lake systems, few studies have quantified how water residence time changes will impact lake thermal structure. These changes are likely to be especially relevant for smaller, short-residence time lakes that are understudied in the literature generally but are globally abundant and important. Finally, this review has highlighted that the contribution of inflows to short-term deep-water oxygen dynamics has not been well quantified, especially in smaller, shallower, temperate systems. However, inflows have the potential to be important in these systems by destabilising stratification and enhancing downward vertical mixing of oxygen or as a direct intrusion of oxygenated inflow to below the thermocline.

Chapter 3 Methodology and site description

3.1 Study site

3.1.1 Location and morphometry

Elterwater is a small, shallow lake situated in the English Lake District in the northwest of England (54.4287 °N, 3.0350 °W). The lake comprises three distinct basins (inner, middle, and outer) separated by narrow channels or bars, with a total length of 0.9 km. The outer basin is the largest and deepest and the inner basin the smallest (Table 3.1). The primary inflow to the lake is the Great Langdale Beck (GLB), flowing from the northwest into the outer basin, and the Little Langdale Beck (LLB), which flows from the south into the middle basin. Historic maps and evidence of paleochannels around the lake suggest the original routing of GLB was into the middle basin. Similarly, LLB was also diverted into the outer basin, with more recent work to restore the channel into the middle basin (see Section 3.1.5). These two inflows account for approximately 98% of the total hydraulic load (Environment Agency, 2000). Smaller ephemeral tributaries and field drains discharge into the inner basin, accounting for the other 2% of inflow. Additional flow into the inner basin comes from the pipeline diversion implemented in 2016 (see Section 3.1.5). The outflow of the system is the River Brathay, which flows out of the outer basin to the southeast (Figure 3.1). The River Brathay ultimately discharges into the north basin of Windermere, 4 km downstream. The complex basin and throughflow configurations mean that the residence time varies significantly between the basins. Previous work estimated water residence times in the outer basin as the shortest (0.6 days) and the middle and inner basins as having longer residence times, 15, and 26 days, respectively (APEM, 2012). This thesis focuses on the inner basin, having undergone restoration measures, described in Section 3.1.5, to improve the poor water quality.

Table 3.1 Morphometric characteristics of the three basins of Elterwater (from Goldsmith et al., 2003; Maberly et al., 2016)

	Inner	Middle	Outer
Surface area (km²)	0.03	0.07	0.08
Mean depth	2.3	2.3	2.5
Maximum depth	6.5	6	7.5

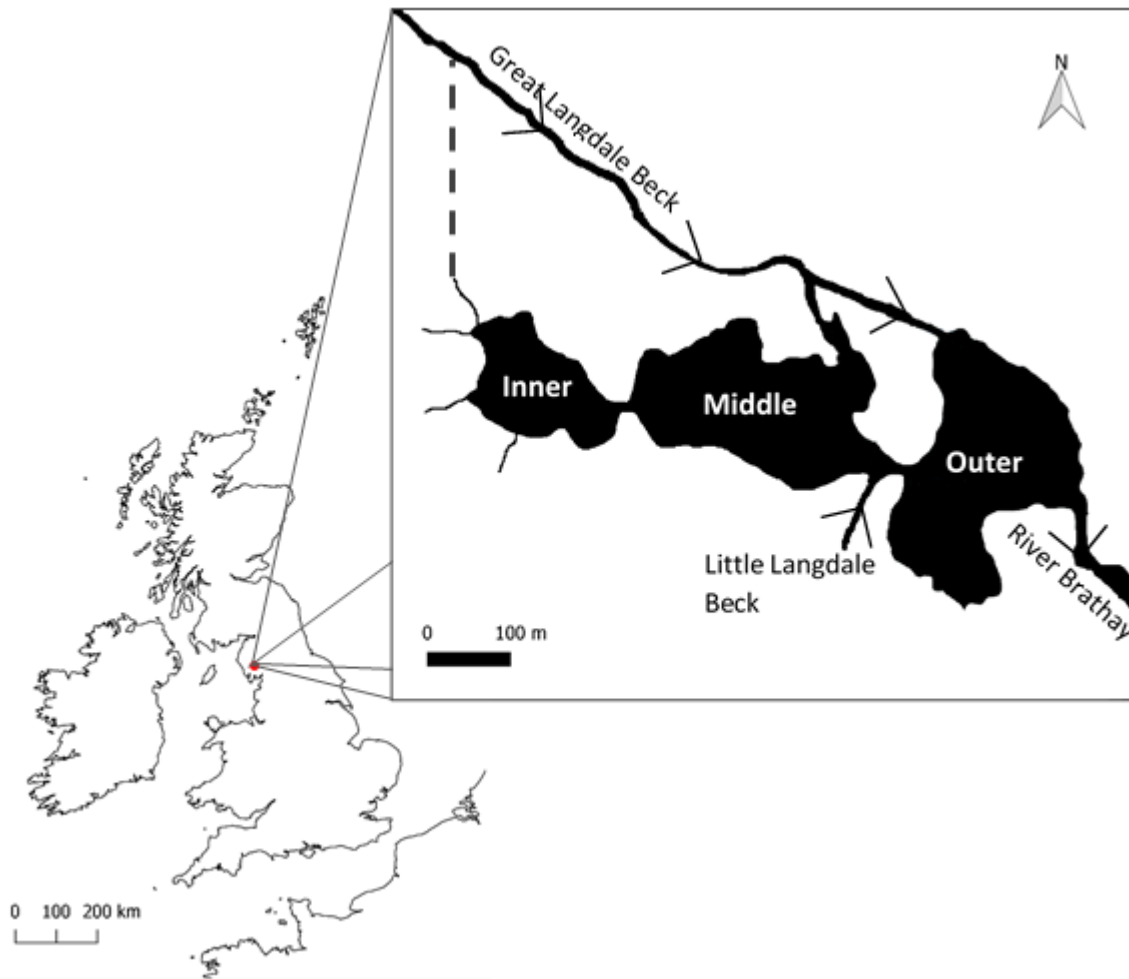


Figure 3.1 Map of Elterwater with its major inflow and outflows labelled. Approximate location of the flow diversion, implemented in 2016, is shown with a dashed line.

3.1.2 Catchment land-use

Elterwater is situated in the upper part of the larger catchment of Windermere, in the Langdale valley. It forms part of the River Brathay's catchment. Elterwater's catchment extends around the lake to the northwest and west, has an area of 51.3 km², a mean elevation of 309 m (a.o.d) and a slope of 17° (UK Lakes Portal, 2020). The landcover is predominantly acid grassland (41.4%), broadleaved woodland (13.5%), and rough grassland (10.7%). Grassland for grazing (improved grassland) makes up 7.5% of the catchment. Further areas of montane (7.7%), coniferous woodland (4.2%) heather and heather grassland (4.2% and 4.1%) are also found in the catchment (Morton et al., 2011). The immediate surroundings of the lake are grazed pasture, bog, and wet woodland. The catchment includes the small upland tarns of Blea Tarn, Little Langdale Tarn and Stickle Tarn. There are several small settlements within catchment, including Elterwater village (800 m to the north), through which the GLB flows.

3.1.3 Climate

The northwest of England and the Cumbrian Lake District specifically has a wet but mild climate (Figure 3.2), experiencing orographic rainfall by moisture-rich atmosphere driven in from the Atlantic to the west. Data from the nearby, Newton Rigg, weather station from 1960 – 2021 shows that the region experiences high annual rainfall, averaging 954 mm per year, highest in autumn and winter (> 100 mm of rainfall on average in December), and lowest in spring and summer (< 50 mm of rainfall in April). In summer, mean daily maximum temperatures is 18.5 °C and sunshine hours peak at > 180 per month in June. The temperate climate experienced at Elterwater is mild, with average minimum temperatures above 0 °C and therefore ice-cover is infrequent, with Elterwater inner basin generally stratifying from April to October (Figure 3.3). The lake is sheltered by the high elevation and tree cover in the immediate proximity.

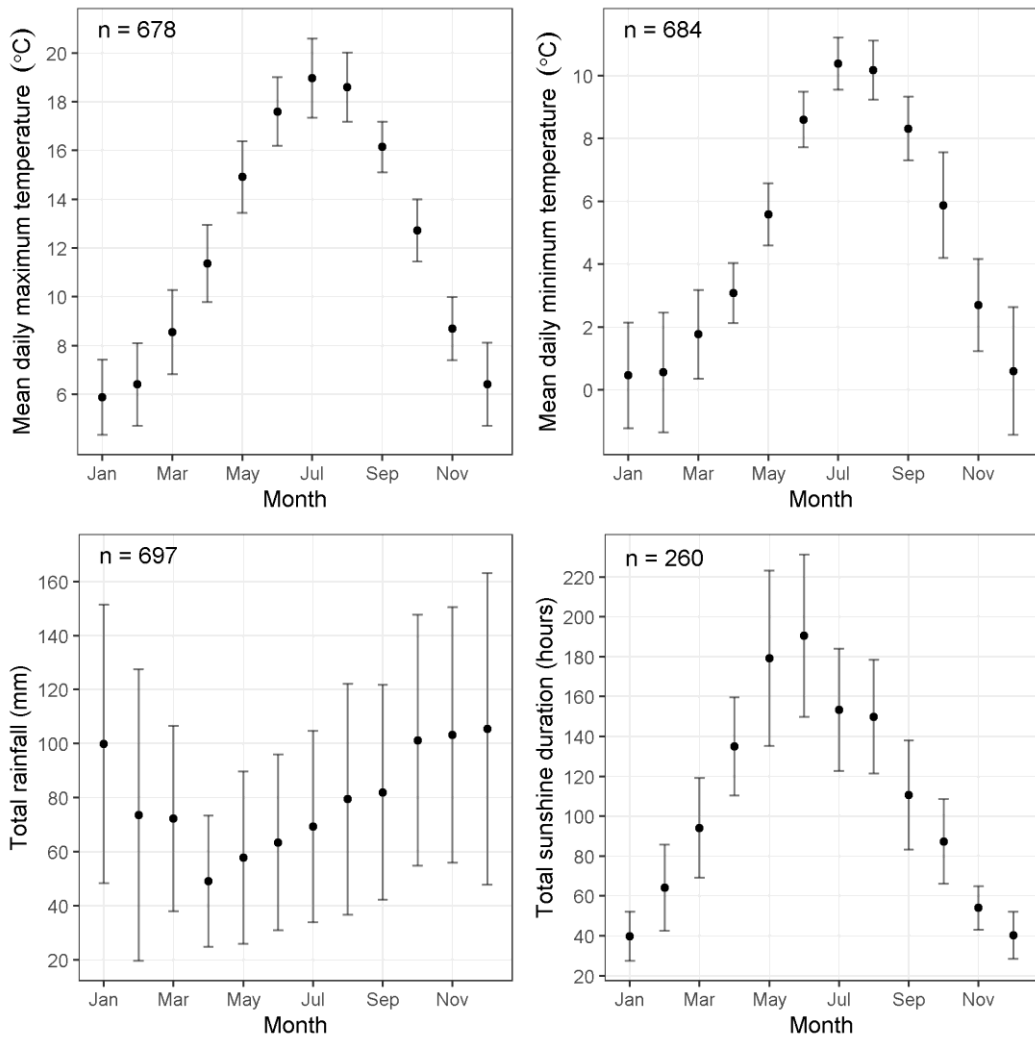


Figure 3.2 Average climate at Newton Rigg meteorological station. Points show mean values and error bars are ± 1 standard deviation of climate variable measured. N represents the number of monthly measurements from the period 1960 – 2021. Sunshine duration data were collected from 1960 – 1981 only.

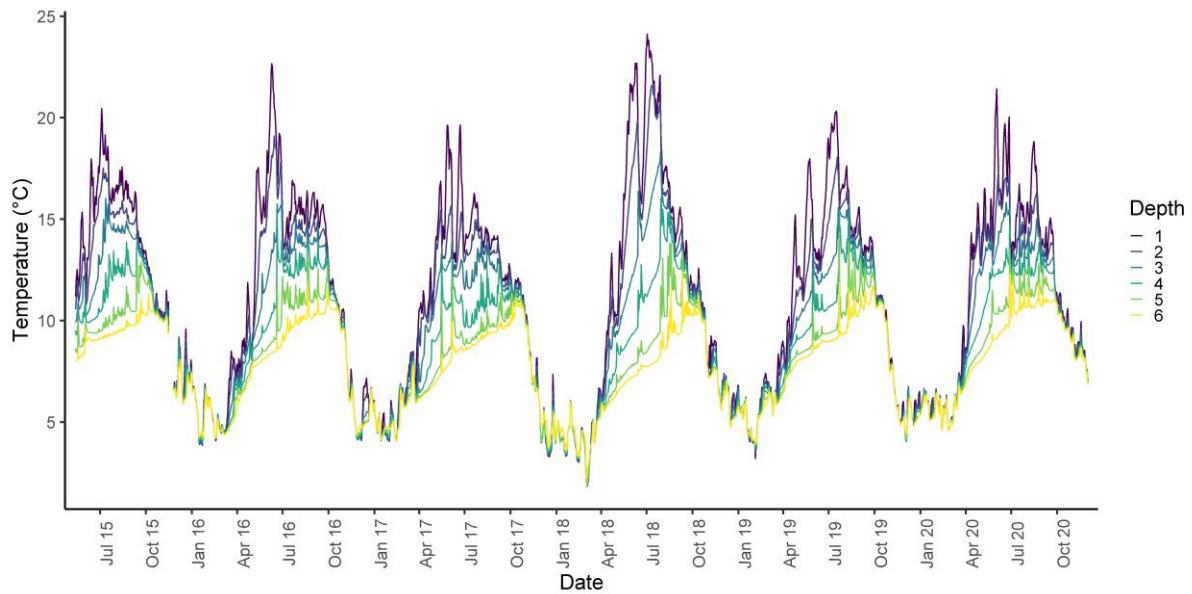


Figure 3.3 Daily average water temperatures measured in the inner basin of Elterwater from May 2015 to December 2020.

3.1.4 Water quality and nutrient loads

The water quality of Elterwater varies considerably between basins, from oligotrophic in the outer basin to mesotrophic in the middle basin and eutrophic in the inner basin, thought to be driven by the difference in water residence times (APEM, 2012; Environment Agency, 2000). The lake has been affected historically by nutrient enrichment due to the discharge from a nearby waste-water treatment works (WwTW) into the inner basin from 1973 until 1999 (Zinger-Gize et al., 1999). Other likely sources of nutrient inputs are livestock, particularly sheep that graze in the immediate fields, agricultural run-off, sewage discharges from septic tanks, erosion and natural leaching from the soil, and atmospheric nitrogen used by nitrogen-fixing phytoplankton. The inner basin is the most nutrient-enriched, with total phosphorus and chlorophyll a concentrations regularly exceeding eutrophic thresholds (Figure 3.4). Historically, both the inner and middle basins were dominated by macrophytes in a clear-water state, but switched to a turbid water state dominated by algal biomass, with management intervention likely required to force a change back to a clear water state (APEM, 2012).

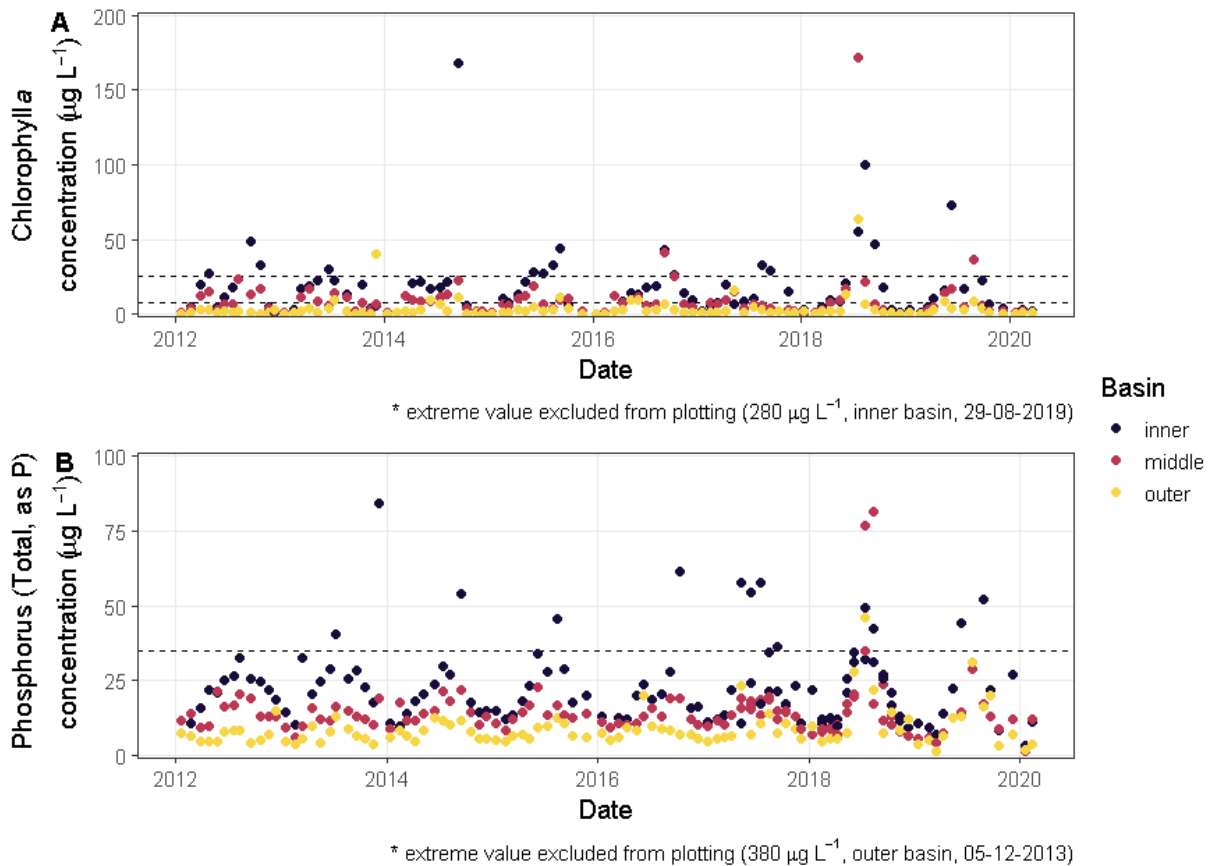


Figure 3.4 A) Chlorophyll *a* and B) total phosphorus concentrations in Elterwater's three basins (inner, middle and outer) for the period 2012-2019. Dashed lines show the mean (chlorophyll and TP) and maximum (chlorophyll only) concentrations for eutrophic class (OECD). Data available on the UK Lakes Portal (at <https://eip.ceh.ac.uk/apps/lakes/detail.html#wbid=29222>) which uses Environment Agency water quality data from the Water Quality Archive (Beta) published under an Open Government Licence.

The lake sits within the Elterwater Site of Special Scientific Interest (SSSI), designated due to the examples of lakeshore wetlands and transitional habitat as well as the occurrence of wetland and standing water floral species. All seven units of the SSSI are designated as unfavourable (last surveyed 2016), with 58% of the site assessed to be in declining condition. Poor water clarity, high algal cover, and fine sediment are cited as reasons for poor condition and restricted development of marginal macrophyte beds.

3.1.5 Management history

In an attempt to improve water quality following long-term nutrient enrichment, rerouting of the effluent discharge occurred in 1999, discharging into the River Brathay downstream of Elterwater. Prior to this rerouting, WWTW discharge was estimated to account for 45-60% of inflow into the inner basin (Stockdale, 1991; Zinger-Gize et al., 1999).

The legacy of past effluent input into the inner basin is present in the accumulation of nutrients in the lake sediments, which provides an internal source of nutrients. Sediment TP concentrations in the deep parts of the inner basin exceed $4500 \mu\text{g g}^{-1}$, suggesting there is a high potential for internal loading of nutrients from the sediments (Mackay et al., 2020). Evidence of deoxygenation below 4 m in the inner basin during the summer stratified period (Beattie et al., 1996; Zinger-Gize et al., 1999) has been observed regularly and coupled with high nutrient concentrations in lake sediments; it is supposed that internal loading is likely driving continued poor water quality (APEM, 2012).

A report commissioned in 2012, suggested that, given the likely dominance of internal loads during the summer stratified period, reconfiguration of inflows to reduce the water residence time of the inner basin presents a means of restoring the lake (APEM, 2012). A pipeline was constructed, diverting part of the GLB flow into the inner basin, the purpose of which was to impede thermal stratification in the summer, to inhibit the development of hypolimnetic anoxia and internal nutrient loading. Alongside this, Little Langdale Beck was also re-routed to its original channel into the middle basin.

In January 2016, the pipeline was installed running from the GLB into a field drain that discharges into the inner basin (Figure 3.1 and Figure 3.5) and continues to operate (as of September 2021). The offtake structure of the pipeline contains a hydro-brake system. The system restricts transfers through the pipe when flow in GLB drops below Q85 (flow percentile) and limits the maximum offtake to $0.122 \text{ m}^3 \text{ s}^{-1}$ based on Environment Agency abstraction limits. The discharge of this transfer is monitored by the South Cumbrian Rivers Trust (SCRT) using a pressure transducer housed in the offtake structure. These data were obtained for the pipeline from July 2017 to December 2019. Prior to these measurements, the flow through the pipeline was estimated based on Q85 values, abstraction limits, and the relationship developed between GLB flow measurements and pipeline discharge (see Section 3.3.3).



Figure 3.5 Photographs of the off-take structure (left) on the Great Langdale Beck and the discharge of the pipeline into a field drain which discharges into Elterwater inner basin (right).

3.2 Field monitoring – primary data

Data were collected in the inner basin, as the primary focus of this thesis, at the deepest point, using high-frequency and traditional lake sampling methods.

3.2.1 High-resolution monitoring

High-frequency temperature and dissolved oxygen profiles were collected at Elterwater, using sensors deployed on a buoy, moored at the basin's deepest point. A chain of RBRsolo temperature sensors recorded the water temperature every 4 minutes, at 0.5, 1, 2, 3, 4, 5, and 6 m from May 2015-Dec 2019. These sensors are accurate to ± 0.002 °C. Hourly averaged data were quality checked and sensor errors were identified. Errors and gaps in the data occurred due to sensor error and sensor maintenance. Gaps in temperature profiles were generally small (<1 day) and accounted for 1.6 % of data, and were resolved with linear interpolation. Hourly averaged profiles were used to calibrate and validate the hydrodynamic model, GOTM, used in experimental scenarios in Chapters 4, 5 and 7. These data were also used in Chapter 6, to look at short-term changes in water column stability.

PME miniDOT oxygen sensors (Precision Measurement Engineering, Vista, California, USA) recorded dissolved oxygen concentrations, via a fluorescence method, every 15 minutes at 1 m, 3 m, 5 m, and 6 m. The sensors are accurate to 0.3 mg L^{-1} and fitted with anti-fouling wipers to reduce the growth of biofilms on the optical sensor. Sensors were deployed in May 2018

until December 2019, although some gaps are present in the data due to sensor error and sensor maintenance. Quality checks of the data were carried out and potentially erroneous measurements removed based on visual inspection of plots, rates of change, and maximum and minimum possible values. Gaps in the data due to sensor maintenance or sensor errors, accounting for 1 % of the data, were linearly interpolated (gaps < 4 hours). The 1 m sensor failed in July 2019 and was not redeployed, giving just the 3 m, 5 m, and 6 m values for the period July – Dec 2019. Oxygen measurements were hourly and daily averaged. These data are used in Chapter 6 to look at short-term dissolved oxygen replenishment events in the deep-water.

3.2.2 Field data collection

Lower frequency water sampling was carried out at Elterwater between May 2018 and December 2019. During the stratified period and the weeks running up to the onset, weekly sampling was carried out, with sampling frequency reduced to monthly during the winter. This was done as the summer period was of greater interest in this study, with the focus of the work on the effect of WRT on stratification, anoxia, and internal loading in the summer. On each sampling visit, water samples were taken at the deepest point of the basin to create a vertical profile. Water samples were collected using a van Dorn sampler at discrete depths from the surface to 6 m. Dip samples were also taken from the main basin inflow (inflow), and the outflow from the inner basin to the middle basin (outflow). Samples for chlorophyll *a* analysis were collected in 0.5 L bottles, a sub-sample of this was used for Total Phosphorus analysis and stored in Falcon tubes. Samples for Soluble Reactive Phosphorus (SRP) analysis were filtered in the field using Sartorius cellulose acetate filters (pore size = 0.45 μm). All water samples were stored in a cool dark environment until analysis.

As well as water samples, vertical profiles of dissolved oxygen, pH, and conductivity were collected using a Yellow Springs Instruments-EXO2 multi-parameter sonde (Xylem, OH, USA). Profiles were taken by lowering the sonde, taking measurements every 10 seconds, through the water column and keeping it at each depth for 5 minutes to allow the sonde to stabilise. Measurements were taken at each half-meter interval from 0.5 to 6 m. Data were downloaded prior to the next sampling visit, the first and last minute of measurements taken at each depth was discarded. Sensors were calibrated monthly according to manufacturers' specifications.

A LI-COR underwater sensor was used to measure photosynthetically active radiation (PAR) at half meter intervals from 0.5 to 6 m. Secchi disk extinction depth (m) was measured on each sampling day and used to estimate the light extinction coefficient (k) according to Kalff (2002),

$$k = \frac{1.7}{Z_{SD}}$$

where Z_{SD} is the extinction depth.

3.2.3 Laboratory analysis

A known amount of water was filtered using a 47 mm Whatman GF/C microfiber filter (pore size = 1.2 μm), on the day of collection. Filters, retaining the chlorophyll sample, were frozen and analysis completed within six months. Analysis was completed according to a spectrophotometry method, using a heated methanol extraction, according to Talling (1974), measuring absorbance at 665 nm with chlorophyll *a* concentration, in $\mu\text{g L}^{-1}$, calculated as,

$$\text{chlorophyll } a = (13.9 \times A_{\text{corr } 665} \times \frac{1}{d}) \times \frac{v}{V} \times 1000$$

where V = known volume of filtered sample (ml), v = volume of methanol, d = path length of cuvette, $A_{\text{corr } 665}$ = corrected absorbance at 665 nm ($A_{665} - A_{750}$). 13.9 approximates the reciprocal of the specific absorption coefficient at 665 nm for chlorophyll *a* in methanol.

To determine the amount of phosphorus dissolved in the water, analysis for soluble reactive phosphorus was carried out on filtered samples that filter out particulate phosphorus. Samples were analysed on the day of collection using a molybdenum blue colourmetric method based on the reaction between ammonium molybdate and antimony potassium tartrate in sulphuric acid, which forms an antimony-phospho-molybdate complex. Using ascorbic acid, the complex is reduced and read colourmetrically at 880 nm using a spectrophotometer and concentrations of SRP, in $\mu\text{g L}^{-1}$, calculated as,

$$SRP = A_{\text{corr}} \times \frac{40}{V} \times F$$

where A_{corr} = sample absorbance – (blank absorbance + sample colour blank absorbance); V = volume of sample, F = 172.0 (concentration of phosphorus ($\mu\text{g L}^{-1}$) per unit of absorbance). On each sampling date a new calibration curve was created using prepared standard (50 $\mu\text{g L}^{-1}$) diluted to samples containing 10, 20, 30, 40, and 50 $\mu\text{g L}^{-1}$, as well as a quality check completed using an additional 50 $\mu\text{g L}^{-1}$ stock diluted to 10 $\mu\text{g L}^{-1}$ and compared against the 10 $\mu\text{g L}^{-1}$ calibration sample.

Raw water samples were analysed for total phosphorus concentrations based on the same standard molybdenum blue colourmetric method, with an additional potassium persulfate digestion step (Murphy and Riley, 1962; Standing Committee of Analysts, 1980). Alongside the water samples, standard solutions were prepared and analysed to create a calibration curve and values blank corrected.

3.3 Field monitoring – secondary data

3.3.1 Elterwater water quality data

Regular monitoring is conducted by the Environment Agency, on all three basins at Elterwater, in accordance with requirements for the Water Framework Directive. For the inner basin, monthly integrated samples of the top 5 m of the water column are collected at the basin's deepest point. Laboratory analysis of samples is carried out for Total Phosphorus, soluble reactive phosphorus and chlorophyll *a* according to standard methods. Chlorophyll *a* analysis used by the EA is a cold acetone extraction, unlike the heated methanol method used in UKCEH, including for Elterwater and Blelham samples. Although not directly comparable initial analysis suggested no difference in the mean values and methods were consistent throughout the time period allowing consistent differences between lakes, important for the statistical analysis methods in Chapter 4. Data obtained from the EA for the period 2012-2019 was quality checked for errors gaps. These data were used primarily in the Before-After-Control-Impact analysis (Chapter 4) as a long-term record of water quality in the inner basin of Elterwater. To ensure matched samples between Elterwater and Blelham, monthly average values were calculated by linearly interpolating between samples (using a maximum gap between samples of 45 days) to a daily time step then calculating the monthly average.

3.3.2 Blelham Tarn water quality data

Data from the long-term monitoring of Blelham Tarn were used in the BACI analysis as a "control". Data were provided by the UKCEH Lake Ecology long-term monitoring project. Integrated water samples of the top 5 m of the water column were collected fortnightly from 2012-2019. Laboratory analysis methods for TP, SRP, and chlorophyll *a* follow those described for primary data collected samples in Section 3.2.2. Data obtained from the UKCEH long-term monitoring for the period 2012-2019 was quality checked for errors gaps. To ensure matched monthly values between Elterwater and Blelham Tarn the raw fortnightly values were linearly interpolating (maximum gap between samples 45 days) to a daily time step then a monthly average calculated.

3.3.3 Lake inflow

3.3.3.1 Inflow discharge

Flow into Elterwater, used in Chapters 4-7, was calculated for the study period 2012-2019 by differentiating two parts of the flow; 1) flow from ungauged tributaries, 2) flow from the pipeline installed during the restoration work in 2016. Flow from ungauged tributaries was estimated as 2% of the gauged outflow of Elterwater on the River Brathay at Jeffy Knotts

station (54.4219 °N, Long: 2.9864 °W), based on previous work by the Environment Agency (2000). Hourly gauged flow for the River Brathay was obtained from the Environment Agency for the period 2012-2019, with missing data, due to faulty sensors, filled in using linear interpolation (gaps ≤ 3 hours) or the relationship between the neighbouring Rothay discharge measured at Miller Bridge House (54.4284 °N, 2.9711 °W). The relationship between measurements was calculated as

$$Q_{Brathay} = Q_{Rothay}^{1.01}$$

Flow from the pipeline was obtained from the South Cumbrian Rivers Trust, measured at the offtake at the Great Langdale Beck, since its construction in 2016. Daily values were obtained from 2016-July 2017 and hourly data from July 2017-2019. There were gaps in the data due to sensor error and maintenance. Small gaps (< 24 hours) were filled using linear interpolation and larger gaps based on a statistical relationship between the measurements of flow in the pipeline and the River Brathay gauged flow (< 1 % of values). This relationship is bounded by legal abstraction limits and a minimum flow requirement in the GLB set by the Environment Agency. The low flow limit in the GLB, when abstraction is permitted, is $0.383 \text{ m}^3 \text{ s}^{-1}$. When GLB flow dropped below this the pipeline flow was set to 0. The maximum discharge through the pipe, based on abstraction limits is $0.122 \text{ m}^3 \text{ s}^{-1}$. The 95th percentile of measured GLB discharge that produced the maximum (capped) pipeline discharge ($0.122 \text{ m}^3 \text{ s}^{-1}$) was calculated to be $2.0 \text{ m}^3 \text{ s}^{-1}$. Where this discharge was exceeded in the source it was assumed that the pipeline discharge would be maximised ($0.122 \text{ m}^3 \text{ s}^{-1}$). If outflow discharge was between $0.383 \text{ m}^3 \text{ s}^{-1}$ and $2.0 \text{ m}^3 \text{ s}^{-1}$ a general additive model was fitted between Brathay outflow discharge and pipeline (Figure 3.6). The smooth term was significant at $p < 0.01$ and the model had an R-squared of 0.528. This model was used to estimate the missing diversion discharge values. From 2016-2019, the ungauged tributary flow and pipeline flow summed to give the overall flow.

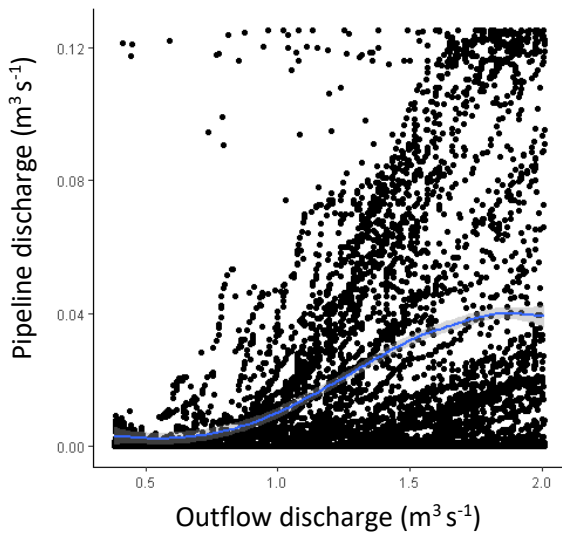


Figure 3.6 Observations of the relationship between gauged outflow (River Brathay) and pipeline discharge. Blue line represents the fitted GAM model.

3.3.3.2 Inflow temperature

Inflow water temperatures were measured at the offtake for the pipeline on the GLB, with data provided by the South Cumbrian Rivers Trust for the period July 2017-December 2019. To estimate inflow temperature before these measurements a relationship between the mean of the previous 12 hours air temperature and water temperature was developed. A linear regression with an intercept of 3.2 and a slope of 0.67 produced an R-squared of 0.88 and a RMSE of 1.30 °C (see Figure 3.7).

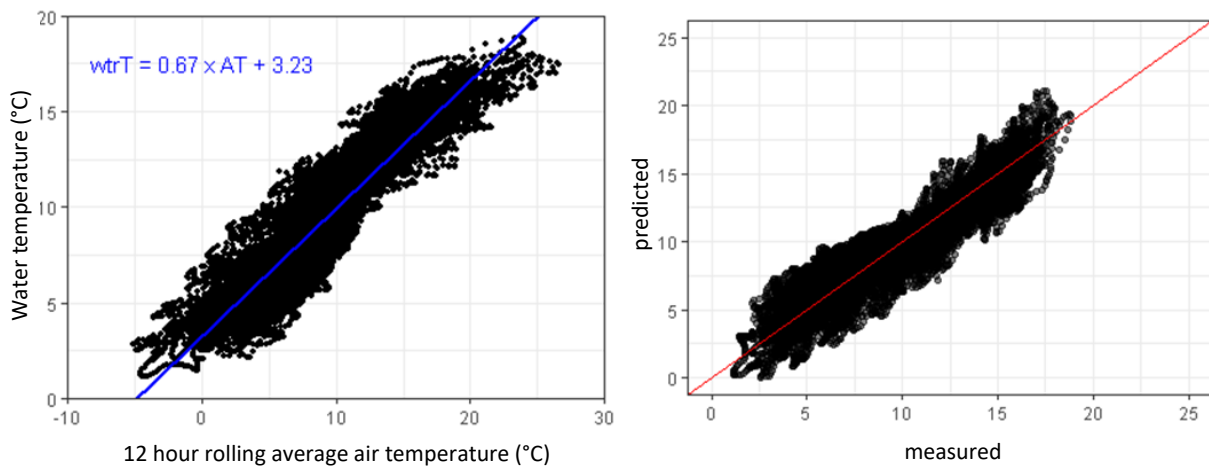


Figure 3.7 A) Prediction of water temperature based on the 12-hour rolling average air temperature. Points show observations and blue line the fitted linear model. B) Predicted vs observed inflow water temperatures using the linear model fit. Red line shows the 1-1 line.

3.3.4 Meteorological data

Meteorological data are not measured at Elterwater, so these data were taken from the automatic water quality monitoring (AWQM) buoy deployed on Belham Tarn. The AWQM

buoy at Blelham measures air temperature, wind speed, relative humidity, and short-wave radiation at 2.5 m above the lake surface. Blelham Tarn is in close proximity to the study site (< 5 km), with similar elevation and fetch, thus meteorological conditions will be similar to those experience at Elterwater. Air pressure was given as a constant value of mean air pressure at sea level and cloud cover calculated based on the difference between observed short-wave radiation and maximum clear-sky short-wave radiation using the *suncalc* (Thieurmel and Elmarhraoui, 2019) and *insol* (Corripio, 2019) R packages. Night-time short-wave radiation was set to 0, and the maximum short-wave radiation was calculated, depending on the day of year and time of day. Cloud cover (as a fraction was) was estimated as:

$$cloud\ cover = 1 - \frac{observed}{maximum\ possible}$$

The mean cloud cover for the previous day was used as an estimate for nighttime cloud cover.

Gaps were present in the observations due to sensor errors and maintenance. Gaps in the data less than 24 hours (air temperature, relative humidity, and wind speed) or 6 hours (short-wave radiation) were infilled using a linear interpolation (Table 3.2). For gaps exceeding these limits, infilling was done using relationships between the data recorded at Blelham Tarn and data recorded by the nearby buoy located on the south basin of Windermere.

Table 3.2 Percentage (%) missing in the 2012-2019 meteorological data and the linear regression between Blelham and Windermere buoy data variables (2012-2019)

Variable	% missing before	% missing after	Intercept	Slope	<i>p</i>	Adjusted r- squared
Air temperature	6.8	0	-0.978	1.056	< 0.001	0.957
Wind speed	4.4	0.3	0.090	0.548	< 0.001	0.572
Solar radiation	1.9	0	3.913	0.931	< 0.001	0.895
Relative humidity	4.2	1.3	-1.809	1.024	< 0.001	0.863

Final gaps in the wind speed were filled by average values within a seven day window around the missing value and for relative humidity based on a linear regression between Blelham Tarn and Esthwaite Water buoy weather station values (intercept = -5.917, slope = 1.07, *p* < 0.001, adjusted R-squared = 0.915).

This continuous time series of meteorological data were used to drive the hydrodynamic model GOTM, used in Chapter 4, 5, and 7. The data were also used to calculated lake surface heat fluxes and wind power using Lake Heatflux Analyzer (Woolway et al., 2015b), for Chapter 5 and 6.

3.3.5 Bathymetry

Bathymetric data for the inner basin of Elterwater (the focus of this thesis), was derived from a bathymetric map (Haworth et al., 2003), and gave a hypsographic curve used in Chapters 4, 5 and 7 to run GOTM as well as in all Chapters to calculate WRTs.

3.4 Modelling methods

3.4.1 GOTM description

The General Ocean Turbulence Model (GOTM) is a one-dimensional process-based hydrodynamic model. Originally developed for investigating turbulent flows in oceans, it has since been modified for use in lakes, and has been applied to many in-land systems, both as a stand-alone hydrodynamic model and also coupled to water chemistry and lake ecosystem models (e.g. GOTM-FABM-PCLake). The model was developed to model the hydrodynamic and thermodynamic processes that control vertical mixing, by solving transport equations of momentum, salt, and heat (Umlauf et al., 2005). GOTM simulates water temperatures of vertical layers, of fixed depth, using meteorological, inflow data and specified bathymetry to study dynamics of air-sea fluxes, mixing dynamics and stratification processes (Burchard et al., 1999). Detailed descriptions of the model equations can be found in Umlauf and Burchard (2005) and Burchard *et al.* (1999).

In this thesis, GOTM v4.1.0 was applied using a $k-\epsilon$ style model for calculating vertical mixing, Fairall *et al.* (1996a, 1996b) formulation of heat and momentum fluxes and Clark *et al.* (1974) for long-wave back radiation. A second order turbulence closure, k-epsilon dynamic model was used, ignoring internal wave mixing and implementation of the surface flows method.

GOTM was selected to model lake hydrodynamics in this is thesis due to its application and success at reproducing thermal conditions in lake systems. The model implements widely accepted physical equations to resolve turbulence and thermodynamic processes in natural waters. Previous research has applied GOTM to a range of scientific and management research questions including the impact of climate change on lake thermal conditions (Ayala et al., 2020; Darko et al., 2019; Moras et al., 2019) and extreme events (Chen et al., 2020; Mesman et al., 2020). GOTM can also be run at a sub-daily time step, an appropriate temporal scale for investigating WRT questions.

3.4.2 Driving data and boundary conditions

GOTM uses meteorological, inflow data and a lake hypsographic curve (depth-volume relationship) in order to estimate water temperatures and mixing. In this thesis, driving data

was derived from various observations at Elterwater, nearby meteorological stations, and river flow gauging stations (as described in Sections 3.3.3 and 3.3.4).

3.4.3 Model calibration

The purpose of model calibration is to minimise the difference between modelled and observed outcomes, by fine-tuning model parameters based on lake specific conditions. The parameters used in the calibration can differ between systems, due to lake-specific characteristics that determine their sensitivity. A calibration run was conducted comparing modelled and observed water temperature profiles for 2018. An auto-calibration tool, ACPy (Bolding and Bruggeman, 2017), was used for calibration following initial manual tweaking of parameters to identify sensitive parameters. ACPy performs automatic optimisation, based on maximum-likelihood approach, of model parameter sets using a differential evolution method (Storn and Price, 1997) based on user-defined parameter ranges (Table 4.2). ACPy searches the parameter space for optimal parameter values. Model fit was assessed based on three metrics: root mean square error (RMSE), Nash-Sutcliffe efficiency (NSE) and mean absolute error (MAE),

$$RMSE = \sqrt{\frac{\sum_{i=1}^n (mod-obs)^2}{n}}$$

$$NSE = 1 - \frac{\sum (obs-mod)^2}{\sum (obs-obs)^2}$$

$$MAE = \frac{\sum |mod-obs|}{n},$$

where *mod* and *obs* are the modelled and observed water temperatures. The optimisation was run three times to ensure results were similar to prevent equifinality issues, and the “best” parameter set used.

Elterwater inner basin was calibrated using six parameters (Table 3.3): three non-dimensional scaling factors relating to wind speed (*wsf*), short-wave radiation (*swr*) and outgoing surface heat flux (*shf*) plus the physical parameters minimum kinetic turbulence (*k-min*) and non-visible (*g1*) and visible light attenuation (*g2*). Modifying these parameters allows to minimise error in the input data due to the difference in conditions between Elterwater and the location of the weather station. The fourth parameter was k_{min} , the minimum allowable kinetic turbulence allowed. This was bounded at the lower end by the value of molecular diffusion, $1.4 \times 10^{-7} \text{m}^2 \text{s}^{-1}$. The calibration also used parameters for visible (*g2*) and non-visible light attenuation (*g1*). Non-visible light attenuation was fixed at the median value given in Woolway *et al.* (2015), 0.45. The visible light attenuation value was allowed to vary in the range of *g2* calculated as,

$$g_2 = \frac{1}{k},$$

where k the light extinction coefficient, derived from secchi disk extinction depths (Z_{SD}).

Table 3.3 The maximum, minimum and final parameters values, optimised during the auto-calibration route. Model performance statistics for the calibration (2018) and validation (2019) periods reported as root mean squared error, Nash-Sutcliffe efficiency and mean absolute error.

Calibration factor	Max allowable value	Min allowable value	Final parameter value
swr	1.1	0.85	0.95
shf	1.2	0.8	0.80
wsf	1.1	0.9	1.08
k-min	1.0×10^{-5}	1.4×10^{-7}	1.4×10^{-7}
g2	0.5	2	0.61

	RMSE (°C)	NSE	MAE (°C)
Calibration	0.93	0.97	0.72
Validation	0.97	0.92	0.75

Due to the availability of observations the model calibration was conducted on the data collected in 2018 and model fit assessed against water temperature profile observations.

3.4.4 Model validation

The model validation uses the parameter set selected during calibration in a separate simulation to test the model's success on another time period to see if it can accurately replicate observed conditions. A validation run was conducted comparing modelled and observed water temperature profiles for 2019. Again, the simulation was assessed based on RMSE, NSE, and MAE, replicating conditions well in the lake (Table 4.2). The calibrated and validated model was used in experimental scenarios in Chapters 4, 5 and 7, to understand how WRT changes impact Elterwater's thermal structure. The specific methods used in each of these experiments are described within the data chapters.

Chapter 4 Can reductions in water residence time be used to disrupt seasonal stratification and control internal loading in a eutrophic monomictic lake?

(Olsson, F., Mackay, E.B., Barker, P., Davies, S., Hall, R., Spears, B., Exley, G., Thackeray, S.J., Jones, I.D., 2022. Can reductions in water residence time be used to disrupt seasonal stratification and control internal loading in a eutrophic monomictic lake? *J. Environ. Manage.* 304. doi:10.1016/j.jenvman.2021.114169)

4.1 Abstract

Anthropogenic eutrophication caused by excess loading of nutrients, especially phosphorus (P), from catchments is a major cause of lake water quality degradation. The release of P from bed sediments to the water column, termed *internal loading*, can exceed catchment P load in eutrophic lakes, especially those that stratify during warm summer periods. Managing internal P loading is challenging, and although a range of approaches have been implemented, but long-term success is often limited, requiring lake-specific solutions. Here, we assess the manipulation of lake residence time to inhibit internal loading in Elterwater, a shallow stratifying lake in the English Lake District, UK. Since 2016, additional inflowing water has been diverted into the inner basin of Elterwater to reduce its water residence time, with the intention of limiting the length of the stratified period and reducing internal loading. Combining eight years of field data in a Before-After-Control-Impact study with process-based hydrodynamic modelling enabled the quantification of the residence time intervention effects on stratification length, water column stability, and concentrations of chlorophyll *a* and phosphorus. Annual water residence time was reduced during the study period by around 40% (4.9 days). Despite this change, the lake continued to stratify and developed hypolimnetic anoxia. As a result, there was little significant change in phosphorus (as total or soluble reactive phosphorus) or chlorophyll *a* concentrations. Summer stratification length was 2 days shorter and 7% less stable with the intervention. Our results suggest that the change to water residence time in Elterwater was insufficient to induce large enough physical changes to improve water quality. However, the minor physical changes suggest the management measure had some impact and that larger changes in water residence time may have the potential to induce reductions in internal loading. Future assessments of internal loading management requirements should combine multi-year observations and physical lake modelling to provide improved understanding of the intervention effect size required to alter

the physical structure of the lake, leading to increased hypolimnetic oxygen and reduced potential for internal loading.

Keywords: Lake restoration, lake management, water quality, lake modelling, hypolimnetic anoxia, destratification

4.2 Introduction

The degradation of fresh waters is a pervasive and persistent problem (Smith, 2003). In Europe alone, 60 % of surface waters failed ecological quality targets set by the European Water Framework Directive in 2018, with little to no improvement in the ecological quality of lakes being reported in over a decade (EEA, 2018). The principal cause of degradation for lakes remains eutrophication (Birk et al., 2020), caused by anthropogenic inputs of phosphorus (P) and nitrogen (N) from catchment sources that result in excess phytoplankton growth, a loss of biodiversity, and low oxygen conditions (Jeppesen et al., 2007; Søndergaard et al., 2005). In 2018, eutrophication impacts in the UK, in particular algal blooms, were estimated to cost £173 million annually, with the potential to rise to £481 million under a 4 °C warmer climate change scenario (Jones et al., 2020).

External nutrient load reductions are the primary measure to improve in-lake conditions (Lürling and Mucci, 2020; Van Liere and Gulati, 1992). However, problems can persist in lakes decades after reductions (McCrackin et al., 2017). Slow recovery can often be attributed to the release of nutrients accumulated in bed sediments, maintaining water column nutrient concentrations, a process known as *internal loading* (Does et al., 1992; Søndergaard et al., 2003; Van Liere and Gulati, 1992). In temperate zone stratifying lakes, internal loading principally occurs in the summer period. High biological oxygen demand in the isolated hypolimnion depletes oxygen that cannot be replenished as the water column density inhibits mixing. Anoxia in the hypolimnion overlying lake bed sediments promotes redox conditions where Fe-P complexes are reduced and their dissolved components liberated across diffusive concentration gradients to the water column (Mortimer, 1942; Nürnberg, 1984). In order to meet legislative water quality targets (e.g. the European Water Framework Directive and the US Clean Water Act), there is a growing need for in-lake measures to control of internal loading (Lürling and Mucci, 2020; Zamparas and Zacharias, 2014).

A range of in-lake measures have been proposed to control internal loading (Lürling et al., 2020). These include sediment dredging (Bormans et al., 2016; Does et al., 1992), chemical inactivation (Mackay et al., 2014; Spears et al., 2016), hypolimnetic aeration and oxygenation (Preece et al., 2019; Toffolon et al., 2013), artificial mixing (Visser et al., 2016), and less

frequently, hypolimnetic withdrawal (Nürnberg, 2019). These in-lake measures vary in their approach but generally target the manipulation of hypolimnetic anoxia or sediment-P binding to decrease the intensity of internal loading (Figure 4.1). Increasing inflow discharge has also been used to promote direct flushing of phytoplankton cells and/or to dilute nutrient concentrations, with moderate short-lived effects (Jagtman et al., 1992; Verspagen et al., 2006; Welch and Patmont, 1980; Zhang et al., 2016). While there has been some success using these existing in-lake methods, restoration outcomes have been inconsistent (Huser et al., 2016), and can incur high capital and running costs (Mackay et al., 2014; Visser et al., 2016). With the pressure to achieve water quality targets, the threat of climate change, and the mixed success of existing measures, there is a need for innovative methods to tackle internal loading.

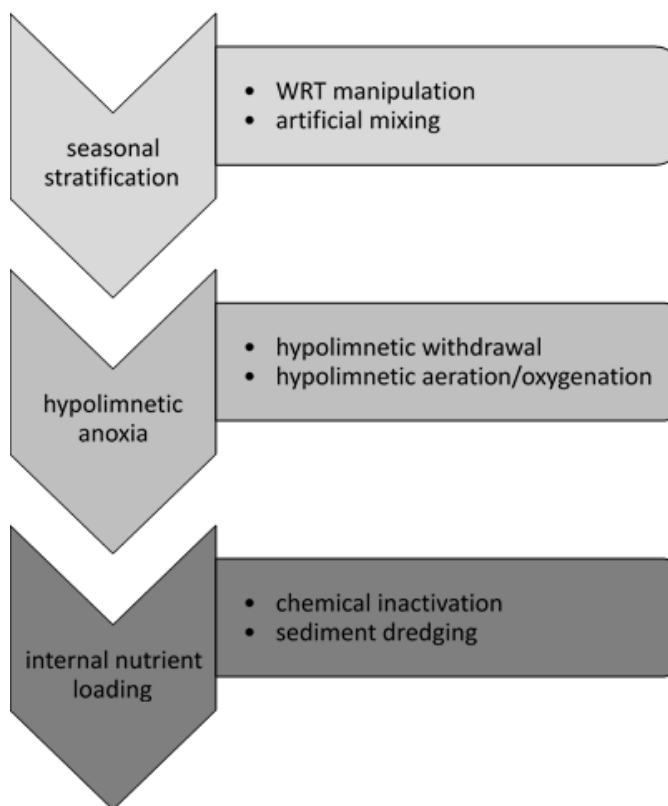


Figure 4.1 Different aspects of the stratification → anoxia → internal P loading sequence are targeted by different in-lake restoration methods.

In some cases, water residence time (WRT) reductions may present an effective method to inhibit stratification, suppressing internal loading and algal blooms in stratifying lakes. Lake inflows can impact the thermal structure of lakes, influencing lake water temperatures (Carmack et al., 1979; Fenocchi et al., 2017). Previous reservoir modelling suggests that maintaining flow levels to reduce WRT can modify stratification (Li et al., 2018; Straškraba and Hocking, 2002). In addition, lakes with shorter WRTs or periods of reduced water residence time can experience a shorter stratified period and periods of increased mixing (M. R.

Andersen et al., 2020; León et al., 2016; Li et al., 2018; Straškraba and Hocking, 2002). Thus, artificial manipulations of water residence time may present another technique to suppress anoxia and internal loading through increased cooling of in-lake temperatures and reduction to stratification length and strength.

It is important to assess efficacy of novel management measures using whole-lake case studies alongside robust statistical and process modelling approaches. The Before-After-Control-Impact (BACI) statistical approach, in which a control system is used alongside an impacted system, has been shown to detect changes not possible using impact lake data only (Christie et al., 2019; Smokorowski and Randall, 2017). Multiple years of pre- and post- intervention data is also needed to allow inter-annual variability to be separated from intervention impacts (Smokorowski and Randall, 2017; Underwood, 1994). Furthermore, high-resolution data can provide valuable insights and increased statistical power in the detection of responses to management (Kerr et al., 2019). Moreover, lake modelling can be used to provide process understanding with which to better understand restoration impacts and refine future applications (Janssen et al., 2015). Despite their synergistic potential, this combination of methods is uncommon in restoration assessments. We combine these approaches, here, to assess the efficacy of WRT management to control stratification and internal loading, in a small eutrophic lake, Elterwater, in the English Lake District, UK.

Using eight years of pre- and post-intervention monitoring data (2012-2019), water quality profiles, and hydrodynamic modelling, we investigated the impact of decreasing the WRT, by means of a diversion of flow from a river through the lake initiated in 2016, using the BACI approach to assess responses in (1) WRT, (2) the intensity and duration of stratification, (3) development of hypolimnetic anoxia, and (4) nutrient and chlorophyll *a* concentrations in the water column. We discuss indicators of effectiveness and outline approaches that may be used to refine the intervention in Elterwater, and potentially in other lakes.

4.3 Methods and materials

4.3.1 Impact site

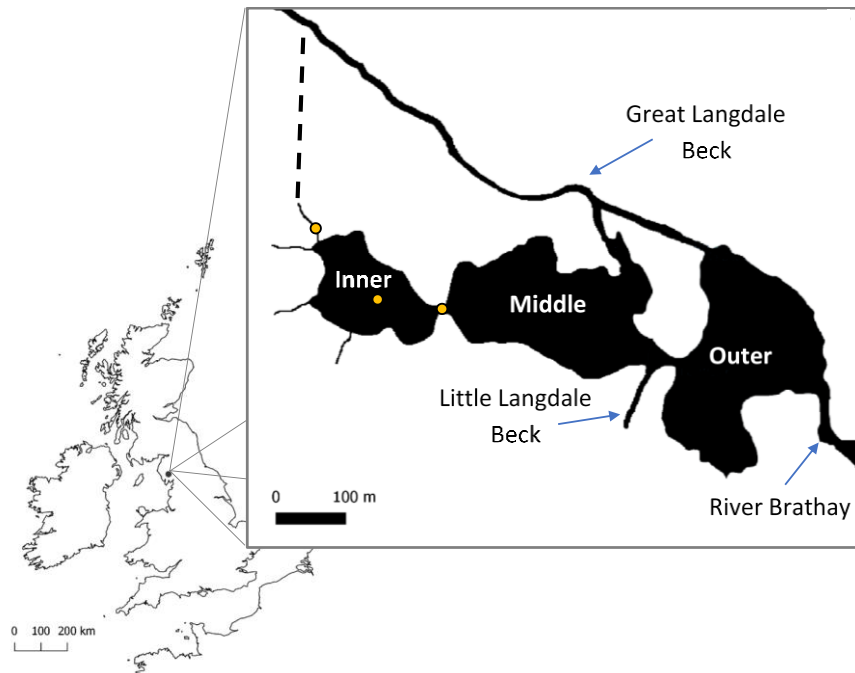


Figure 4.2 Map of Elterwater with its major inflow and outflows labelled. Approximate location of the flow diversion, implemented in 2016, is shown with a dashed line and sampling locations with yellow circles.

Elterwater is a small lake located in the English Lake District, UK. It has three distinct basins, inner, middle, and outer (Figure 4.2), with the main inflow, the Great Langdale Beck (GLB), and outflow, River Brathay, flowing into and out of the outer basin, respectively. Smaller inflows discharge into the inner and middle basins. Due to the system's hydrology, the WRT varies significantly between the basins, with previous studies estimating around 15-20 days in the inner and middle basins and as little as 0.5 days in the outer basin (APEM, 2012; Beattie et al., 1996). The inner basin of Elterwater (Elterwater-IB) was the main target of the restoration efforts and is the focus of this study. The inner basin is the smallest of the three basins and the most nutrient-enriched (Section 4.7). Elterwater-IB was, historically, the primary discharge point for wastewater treatment effluent (Zinger-Gize et al., 1999) and in-lake concentrations of total phosphorus (as TP) and chlorophyll *a* regularly exceed eutrophic status (see Section 4.7; Nürnberg, 1996). Sediment TP concentrations in the deep parts of the inner basin exceed $4500 \mu\text{g g}^{-1}$, suggesting there is a high potential for internal loading of nutrients from the sediments (Mackay et al., 2020). Internal loading of nutrients under anoxic conditions, during the annual summer stratification period, is suspected to be the source of the persistent water

quality problems (APEM, 2012) and we present evidence of persistent summer spikes in TP and chlorophyll *a* (Figure S 4.7.1-1) to support this (Søndergaard et al., 2002).

Table 4.1 Hydromorphometric and physiochemical comparison of Impact and Control sites. Data from 2015 Lakes Tour (Maberly et al., 2016) and Haworth et al. (2003).

Attribute	Elterwater inner basin (Impact)	Blelham (Control)
Location	Lat: 54.4287 Long: -3.0350	Lat: 54.3959 Long: -2.9780
Elevation (m above ordinance datum)	53	47
Surface area (km ²)	0.031	0.1
Mean depth (m)	3.3	6.8
Maximum depth (m)	6.5	14.5
Annual mean WRT (days)	20	50
Catchment area (km ²)	1.0	4.3
Annual mean total phosphorus concentration (µg L ⁻¹)	18.3	24.5
Annual mean chlorophyll <i>a</i> (µg L ⁻¹)	16	23
Annual mean alkalinity (m equiv m ⁻³)	285 (low)	450 (medium)

4.3.2 Control site

Blelham Tarn (control site) is a small monomictic lake located approximately 5 km to the southeast of Elterwater (impact site) and is morphometrically and trophically similar to the impact site (Table 4.1). Blelham Tarn was selected as the “control” site for the BACI analysis as the sites are close together, share similar physio-chemical characteristics pre-restoration (Table 4.1), thermally stratify, develop hypolimnetic anoxia (Foley et al., 2012), and exhibit internal loading (Gray, 2019). While all lakes are unique, the similarities shared between Elterwater and Blelham Tarn allow comparison over the experimental period. The site is part of the UKCEH Cumbrian Lakes Monitoring Platform (see <https://ukscape.ceh.ac.uk/our-science/projects/cumbrian-lakes-monitoring-platform>), with both a fortnightly long-term monitoring programme and a monitoring buoy providing water quality and meteorological data for the study period (2012-2019).

4.3.3 Data collection

4.3.3.1 Flow and water residence times

Inflow to Elterwater-IB, before the restoration, had been estimated as 2% of lake outflow discharge (Environment Agency, 2000), measured at the River Brathay gauging station. Since the intervention in 2016, additional water flow has increased the discharge into the basin via

a diversion from GLB. This diversion forms an underground pipeline (approximately 0.7 m diameter) running 350 m from the GLB river channel to one of the small field drains that discharges into the inner basin (Figure S 4.7.2-1). Flow through the pipe is not maintained at a consistent discharge but acts passively diverting a small proportion of the GLB flow. The pipeline is monitored and maintained by the South Cumbria Rivers Trust, and they provided daily (January 2016-July 2017) and hourly (July 2017-2019) discharge data for the pipeline. There were gaps in the data due to sensor error and maintenance. Small gaps (< 24 hours) were filled using linear interpolation. Larger gaps were filled based on a statistical relationship between flow measurements in the pipeline and the River Brathay gauged flow. This relationship is bounded by legal abstraction limits ($0.122 \text{ m}^3 \text{ s}^{-1}$) and a minimum flow requirement in the source river (Q85, $0.383 \text{ m}^3 \text{ s}^{-1}$) (Section 4.7.3.1). A hydro-brake system operates to shut off the pipeline when the flow is outside of these limits. The total flow into Elterwater-IB is the gauged pipeline discharge plus the 2% of the gauged outflow.

Water residence time (WRT) was calculated as,

$$WRT = \frac{V}{Q} \quad \text{Equation 4.1}$$

Where V is the basin volume and Q is the outflow discharge. By assuming outflow is equal to inflow discharge and constant basin volume (from Haworth et al., 2003), inflow discharge, as determined above, can be used to calculate water residence times at each hourly time step. When calculating monthly, seasonal, or annual WRTs the mean inflow discharge for that period was calculated and used in Equation 4.1. WRTs were calculated for the post-intervention period, both with and without the additional intervention flow, to isolate the exact change in WRT caused by the intervention.

4.3.3.2 Biological and chemical data

Water sampling

In Elterwater-IB, monthly water samples were collected for water chemistry analysis at the deepest point in the basin from 2012-2019 using a 5 m integrated sampling tube. Additionally, in 2018-2019 water samples were collected in Elterwater-IB at 0.5 m and 6 m from the surface, using a Ruttner sampler, and from the basin inflow and outflow (Figure 4.2). Dissolved oxygen profiles were taken using a Yellow Springs Instruments-Exo2 multi-parameter sonde (Xylem, OH, USA) weekly during stratification and monthly during isothermal conditions between May 2018 and December 2019. Measurements were taken at 0.5 m intervals from 0.5 m to 6.5 m. Oxygen sensors were calibrated monthly according to the manufacturer's specifications. In

Blelham Tarn, integrated water chemistry samples of the top 5 m of the water column were taken at the deepest point of the lake, fortnightly from 2012 to 2019.

Laboratory methods

Chlorophyll *a* was measured as a proxy for phytoplankton biomass. A measured volume of the water was filtered onto a Whatman GF/C filter paper from the integrated sample. Filter papers were frozen, and analysis completed within six months. Samples from Elterwater-IB were extracted using a cold acetone extraction. At Blelham, samples were extracted using heated methanol, according to Talling (1974). Although the extraction method differs between sites, consistent methods were used across the entire period, so any difference in values due to the extraction method will be maintained. Total phosphorus (TP) concentrations, from both Elterwater-IB and Blelham, were determined using a potassium persulphate ($K_2S_2O_8$) digestion and colourimetric analysis using the molybdenum blue method from 2014 -2019. A different method was used prior to 2014. Therefore only 2014-2019 samples were used for TP data analysis to avoid methodological issues affecting the results. We determined gross summer internal load estimates using a mass balance approach (Nürnberg, 2009, 1984). Soluble reactive phosphorus (SRP) concentrations were determined from a 50 ml sub-sample filtered using a Sartorius cellulose acetate 0.45 μ m filter into an acid-washed polypropylene tube. All SRP concentrations were determined using a colorimetric method according to Stephens (1963) and carried out on the day of collection. Bioavailable phosphorus (BAP), that is, phosphorus which readily assimilates or is already assimilated by biomass, was calculated as the concentration of SRP plus chlorophyll *a* concentration, following Reynolds & Davies (2001).

Preparing data for analysis

Data were linearly interpolated to a daily timestep and then a monthly average calculated to give paired monthly values from 2012 to 2019. TP covered 2014 to 2019. Larger gaps (> 1 month) were not interpolated and left as missing values.

4.3.4 Statistical modelling and impact assessment

To assess the effects of the intervention on in-lake water chemistry (TP, SRP, chlorophyll *a*) we used Before-After (BA) and BACI analysis for the period before intervention (2012-2015) and after (2016-2019). All statistical analyses on field data were carried out on monthly observations, using R (R Core Team, 2020), with the mgcv (version 1.8; Wood, 2017) and emmeans (version 1.5.0; Lenth, 2020) packages.

4.3.4.1 Before-After-Control-Impact (BACI)

This statistical design considers the relative change in the “impact” site compared to the “control” site. There were no known changes in land-use or catchment management during the study period at Blelham or Elterwater, except for the Elterwater flow diversion work, described above. It is assumed that any variation in the control site (Blelham) will be driven by interannual and seasonal variation in weather that would also drive similar variation within the nearby treatment site (Elterwater). Short-lived differences are likely to be masked by the noise contributed by other errors in the data and are unlikely to result in a long-term shift in conditions at the site (Lang et al., 2016).

The difference between lakes was calculated as Elterwater-IB minus Blelham. In the case of chlorophyll *a* and SRP, data were log-transformed before the differences were calculated, to account for positive skew and non-additivity in the data. To account for autocorrelation in the time series data, monthly data were used (Stewart-Oaten et al., 1986), and a temporal component (Season) was included in the models. The BACI analysis used two-way ANOVAs, fitted with an interaction between Intervention, before or after, and Season (winter - Dec, Jan, Feb; spring - Mar, Apr, May; summer - Jun, Jul, Aug; or autumn - Sep, Oct, Nov) to account for expected differences in responses between seasons and to minimise non-additivity issues (Stewart-Oaten et al., 1986). The assumptions of the models were checked visually using diagnostic plots of residuals and lag plots of autocorrelation (see Section 4.7.4).

Statistical coherence of the control and impact sites before the intervention (2012-15) was confirmed using regression analysis of lake differences against date to ensure that the slope did not deviate significantly from zero ($p > 0.05$) (as per McGowan et al., 2005) (see Section 4.7.5).

4.3.4.2 Before-After (BA)

Before-after analysis of Elterwater-IB data was used as a confirmatory method to strengthen results seen in the BACI analysis. BA models were fitted using generalised linear models (GLMs) with a gamma distribution and log-link function. The assumptions of the model were checked visually using diagnostic plots of residuals and lag plots of autocorrelation.

4.3.4.3 Seasonality changes

Changes in the seasonal pattern of TP, SRP, and chlorophyll *a* following the intervention were assessed by fitting General Additive Models (GAM) using a Gamma distribution, with a log-link function and a lag-1 auto-correlation structure. The GAM included intervention (Before or

After) as an ordered factor parametric term, plus an overall smoother for month, and a smoother for the difference between the periods as predictors of concentration.

4.3.5 Hydrodynamic modelling

4.3.5.1 Model description

Water temperature profiles were not taken in Elterwater-IB before May 2015, so before-after timeseries were not available. Therefore, a process-based physical lake model was used to derive hourly water temperatures at Elterwater-IB with and without the intervention. The lake version of the General Ocean Turbulence Model (GOTM), a one-dimension hydrodynamic model, uses measured meteorological data, specified bathymetry and inflow discharge and temperature to estimate in-lake water temperature profiles (Umlauf et al., 2005). GOTM uses a fixed layer structure and resolves turbulent kinetic energy production and diffusion between these layers to estimate vertical water temperature profiles. GOTM was run at an hourly timestep with 50 vertical layers from 2016-2019. Previous studies have successfully applied GOTM to a range of lake systems (Darko et al., 2019; Mesman et al., 2020; Moras et al., 2019).

The nearby automatic water quality monitoring buoy at Blelham Tarn measures the required input meteorology (air temperature, wind speed, relative humidity, and short-wave radiation). Gap filling of meteorological data was done using linear interpolation for small gaps (< 24 hours or 6 hours for short-wave radiation) and relationships with other local meteorological stations when there were larger gaps (see Section 4.7.6). Alongside inflow discharge, as per section 4.3.3.1, inflow temperature was measured on the diversion pipeline since July 2017. Before July 2017, hourly water temperature estimates were made based on a relationship derived between observations of inflow temperature and the previous 12 hours' average air temperature (Section 4.7.3.2).

4.3.5.2 Model calibration and validation

GOTM was calibrated for Elterwater-IB using observed water temperature profiles from 2018 and validated using 2019 profiles. GOTM was calibrated using an auto-calibration tool, ACPy (Bolding & Bruggeman, 2017), which uses a differential evolution method to estimate the best parameter set, based on a maximum-likelihood measure. The parameters estimated were three non-dimensional scaling factors relating to wind speed (*wsf*), short-wave radiation (*swr*) and outgoing surface heat flux (*shf*) plus minimum kinetic turbulence (*k-min*) and non-visible (*g1*) and visible light extinction (*g2*). Model fit was assessed against observations for water column temperatures using the metrics root mean square error (RMSE), Nash-Sutcliffe efficiency (NSE), and mean absolute error (MAE), giving a good fit between the modelled and

observed water temperatures in both the calibration and validation periods (Table 2). For a full description of the model parameters, ranges used in calibration, and the validation process, see Section 4.7.7.

Table 4.2 The maximum, minimum and final parameters values, optimised during the auto-calibration route. Model performance statistics for the calibration (2018) and validation (2019) periods reported as root mean squared error, Nash-Sutcliffe efficiency and mean absolute error.

Calibration factor	Max allowable value	Min allowable value	Final parameter value
swr	1.1	0.85	0.95
shf	1.2	0.8	0.80
wsf	1.1	0.9	1.08
k-min	1.0×10^{-5}	1.4×10^{-7}	1.4×10^{-7}
g2	2.0	0.5	0.61

	RMSE (°C)	NSE	MAE (°C)
Calibration	0.93	0.97	0.72
Validation	0.97	0.92	0.75

The resulting model was used in two scenarios: 1) a ‘with intervention scenario’ using observed input data to predict the actual water temperatures in Elterwater-IB from 2016-2019; 2) a ‘no intervention scenario’ using inflow discharge without the additional inflow from the intervention, to estimate water temperatures if no intervention had occurred (2016-2019), thus isolating the impact of the intervention on the lake’s thermal structure. The water temperature profiles were averaged on to a daily time step.

4.3.5.3 Stratification and stability metrics

Metrics of stratification length and water column stability were calculated. A minimum density difference between the top and bottom of the water column of 0.1 kg m^{-3} was used to define stratification occurrence (Wilson et al., 2020), equivalent to a temperature difference of 0.5-1 °C depending on the water temperature. Based on this 0.1 kg m^{-3} threshold, the following stratification metrics were calculated:

- Total number of stratified hours (as day equivalents)
- Length of the longest continuously stratified period

- Onset and overturn dates of the longest stratified period

Water column stability during the stratified period, measured as Schmidt stability (Idso, 1973), was calculated using the rLakeAnalyzer R package (version 1.11.4.1; Read et al., 2011). Mixed depth was calculated using a modified version of the rLakeAnalyzer meta.depths function, using a density difference threshold (0.1 kg m^{-3}) between the top and bottom water layers and a minimum density gradient of $0.1 \text{ kg m}^{-3} \text{ m}^{-1}$ to define the mixed depth.

4.4 Results

4.4.1 Changes to WRT

Using measurements of the intervention flow and estimates of the natural flow, we compared WRTs with and without the additional piped water for the period after intervention (2016-2019). Summer average WRT was reduced by 8 ± 5 days (mean \pm standard deviation) with the intervention in place. Spring and summer had larger reductions in WRT than winter and autumn. Overall, the mean annual WRT was around 5 ± 1 days shorter with the intervention than without. Within season variability was also large; daily WRTs varied by orders of magnitude within seasons, in summer ranging from almost 700 days to < 2 days without the intervention. With the intervention the variability reduces as the longest WRTs were suppressed, reducing the maximum daily WRTs from 700 to 462 days.

4.4.2 Changes to stratification and lake water temperatures

Comparing the two modelled temperature scenarios for 2016-2019, one with the intervention and the other without, shows there have been changes caused by additional flow from the diversion pipe. These changes depend on the season. Overall, with the intervention, average water column temperature was cooler in summer (difference in average temperature -0.7 ± 0.2 °C) and in winter the lake was warmer (change in average $+0.5 \pm 0.1$ °C) (Figure 4.3a). Spring and autumn changes in average temperatures were smaller than summer and winter. The change in water temperatures with the intervention varied by depth, with surface water temperatures (SWT) generally showing larger differences than deeper water except in autumn when deeper water cooled more than surface water (Figure 4.3b).

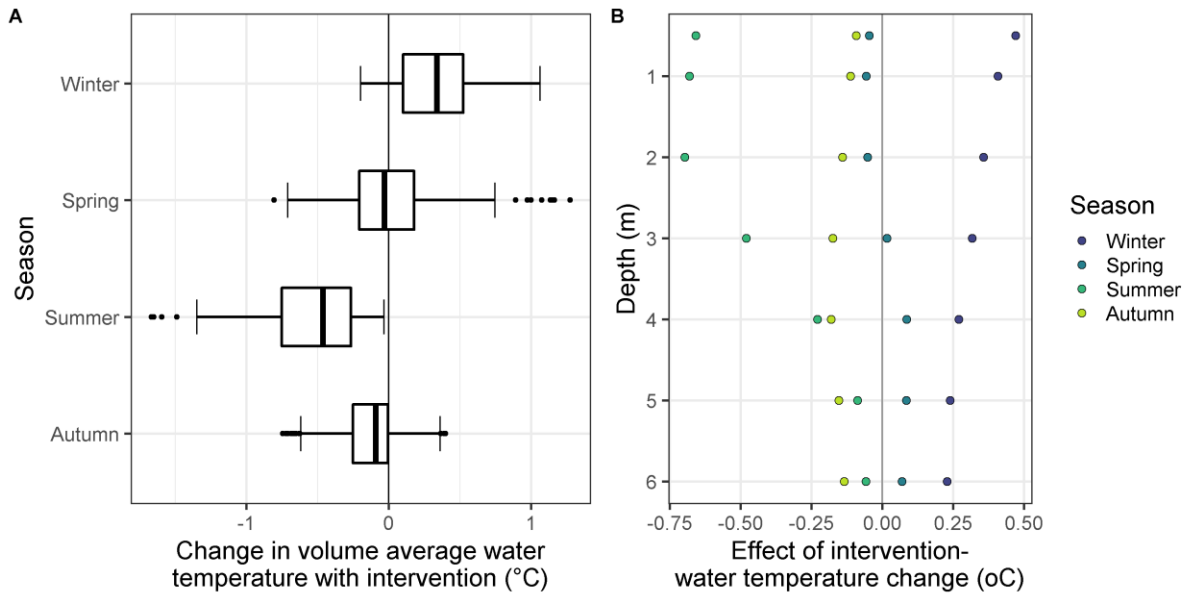


Figure 4.3 a) change in volume averaged water column temperature in each season, b) water temperature changes at different depths with the intervention. Positive values indicate warming and negative values cooling, compared to water temperatures without the intervention.

Overall, increased flow tended to increase stratification in the winter and reduce stratification in the summer. The modelling results show that stratification occurrence increased following the intervention, due to increases in transient stratification during the winter. Without the intervention the average number of stratified days per year would have been 177 days (min = 168, max = 183), compared to 179 days per year with the intervention (min = 171, max = 185). However, the intervention, on average, shortened the longest continuous period of stratification in the summer by 2 days, from 156 (min = 145, max = 165) days to 154 (min = 145, max = 163). With the intervention, Elterwater-IB's average stratification onset remained the 14th April (earliest = 28th March, latest = 1st May) but overturn was expedited by 2 days from 16th to 14th September (earliest = 7th September, latest = 29th September).

Average Schmidt stability for the stratified period ranged from 11.1 J m⁻² to 20.6 J m⁻² without the intervention and 9.8 J m⁻² to 20.0 J m⁻² with the intervention. The mean value decreased from 15.4 to 14.4 J m⁻², a reduction of 7%.

4.4.3 Natural inter-annual variability

The "natural" inter-annual variability of annual and summer WRTs in Elterwater-IB for the 8 years of the study (4 years before plus 4 years after without intervention) was assessed (Table 4.3). Summer WRT varied by 23 days (maximum = 31 days, minimum = 8 days) and annual WRT by 6 days, across the 8 years. This inter-annual variability in summer WRTs was almost three times the reduction estimated to have been caused by the intervention (i.e. 8 days).

Modelled mean summer SWTs across the 8 years varied by 5 °C between years and maximum summer SWTs varied by 7 °C. This variability in mean summer SWT was an order of magnitude larger than the 0.7 °C cooling estimated to have been caused by the intervention. Inter-annual variability in mean winter SWTs was 1.6 °C and minimum winter SWTs was 1.9 °C, three to four times the estimated effect of the intervention (0.5 °C). The change in dates of stratification onset and overturn were minor compared to the variation in onset and overturn dates that were estimated to occur naturally in Elterwater-IB. The onset date varied by 49 days and overturn by 25 days.

Table 4.3 Summary of the water residence time, water temperatures and stratification metrics for the two modelled scenarios (2016-2019 with and with intervention) compared with the natural variability in parameters (2012-2019 without intervention). Values show the mean and the range (minimum – maximum).

	With (2016-2019)		Without (2016-2019)		Natural variability (2012-2019)	
	Mean	Range	Mean	Range	Mean	range
Annual WRT (days)	8	7 - 9	13	11-15	12	9 - 15
Summer WRT (days)	10	7-15	18	13-31	19	8 - 31
Mean summer SWT (°C)	17.9	16.2 - 20.2	18.5	17.0 - 20.7	16.1	14.1 - 19.2
Max summer SWT (°C)	23.8	22.5 - 26.6	24.5	23.4 - 26.7	24.0	20.0 - 27.0
Mean winter SWT (°C)	5.1	4.7-5.4	4.6	4.0 - 5.1	4.9	4.2 - 5.8
Minimum winter SWT (°C)	2.5	2.4 - 2.7	2.4	2.1 - 2.7	2.4	1.5 - 3.4
Days stratified	179	171 - 185	177	168 - 183	177	166 - 192
Longest period of stratification (days)	154	145 - 163	156	145 - 165	155	121 - 186
Day of onset	14 th Apr	29 th Mar - 1 st May	14 th Apr	29 th Mar - 1 st May	17 th Apr	29 th Mar - 17 th May
Day of overturn	14 th Sep	7 th Sep - 29 th Sep	16 th Sep	7 th Sep - 29 th Sep	18 th Sep	7 th Sep - 2 nd Oct
Stratification stability (J m ⁻²)	14.4	9.8-20.0	15.4	11.1-20.6	14.2	10.0 - 20.6

4.4.4 Changes in lake water quality

Annual mean TP concentrations in Elterwater-IB showed a slight change in the “After” period compared to the “Before”, relative to the control site, although this was not significant ($p = 0.538$). There was a significant interaction of season and period ($p = 0.025$) in the BACI ANOVA, which indicates the response of TP concentration in each period differed depending on the season. In winter and autumn, the TP concentration increased relative to control, but in spring and summer there was a relative decrease (Figure 4.4a). However, post-hoc analysis indicated that only the spring intervention effect was significant ($p = 0.017$) with an average reduction in Elterwater-IB relative to the control (Table 4.4). The B-A analysis confirmed these responses (Section 4.7.8), with no significant overall effect of the intervention or an effect in individual seasons ($p > 0.05$). There was also no significant change in the seasonality of TP concentrations (Figure S 4.7.8-1), confirmed by the fitted GAM curve for After being no different to Before ($p = 0.721$).

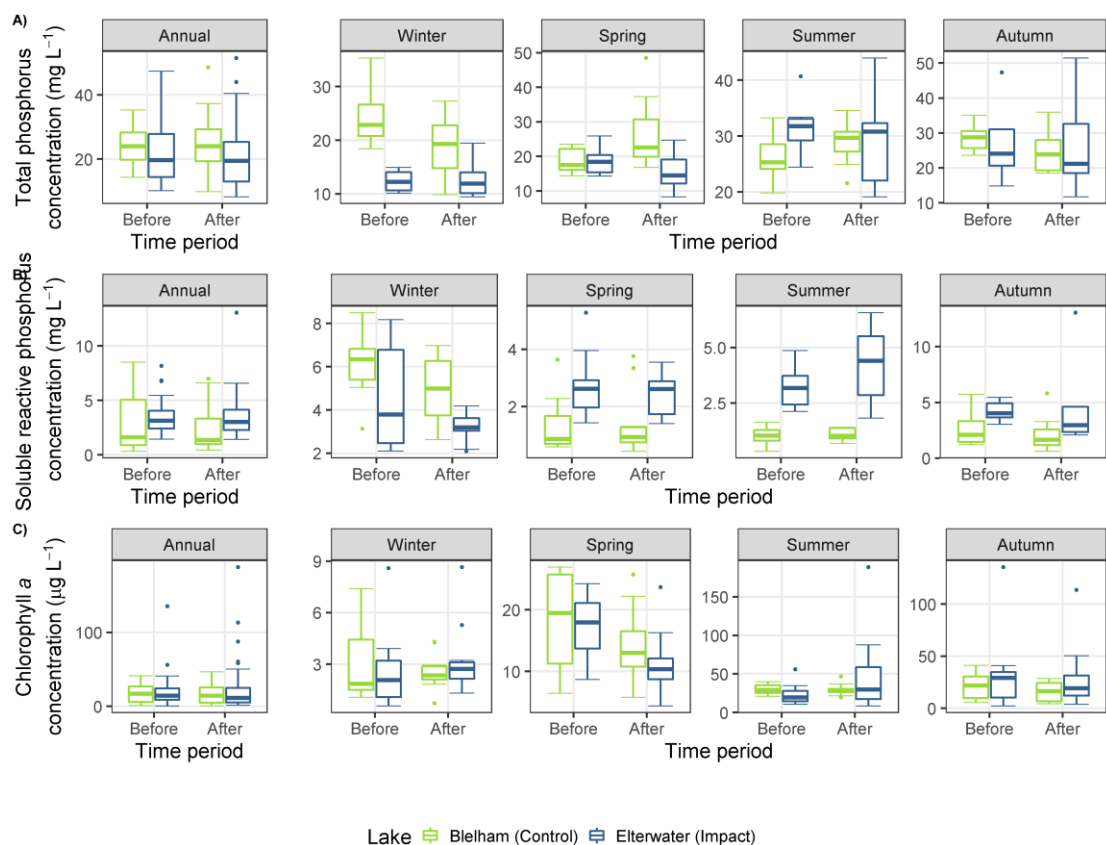


Figure 4.4 a) Total phosphorus, b) soluble reactive phosphorus and c) chlorophyll a concentrations in Elterwater-IB (impact) and Blelham (control) sites before and after intervention, annually and grouped by season.

BACI analysis indicated that the annual mean SRP concentration at Elterwater-IB was unchanged following the onset of the intervention (Table 4.4) and no significant difference in the response between seasons (Figure 4.4b). The B-A analysis confirmed these responses (Section 4.7.8). There was also no significant change in the seasonality of SRP concentration (Figure S 4.7.8-1), confirmed by the fitted GAM curve for After being no different to Before ($p = 0.164$).

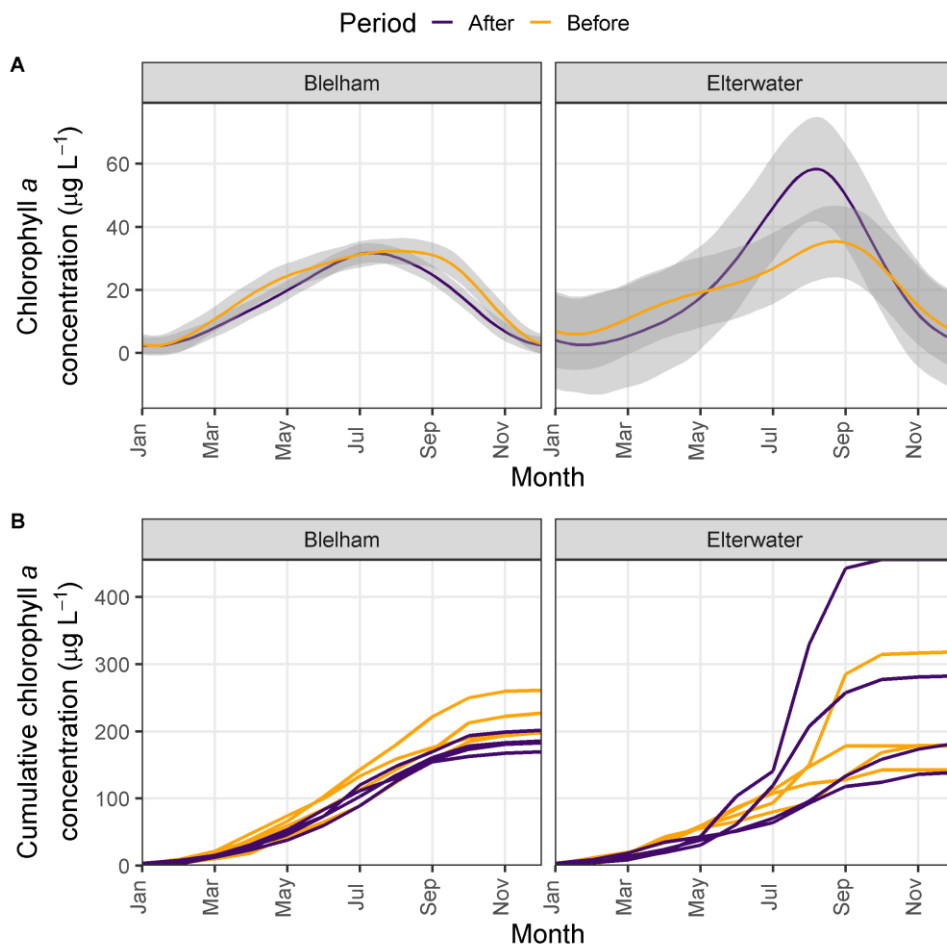


Figure 4.5 a) average annual chlorophyll *a* dynamics (shading shows ± 1 SE) and b) cumulative chlorophyll accumulation for each year before and after restoration at the control (Blelham) and impact (Elterwater-inner basin) lakes.

Annual mean chlorophyll *a* concentration in Elterwater-IB increased slightly following the intervention, relative to the control (Table 4.4). However, this increase was not significant ($p = 0.702$) and there was no significant interaction between season and period ($p = 0.093$). Post-hoc analysis indicated no significant change in any individual seasons (Figure 4.5c; $p > 0.05$). There was also no significant change in the seasonality of the chlorophyll *a* concentration (Figure 4.5), confirmed by the GAM modelling approach ($p = 0.364$). However, there was large

inter-annual variability in the seasonality of chlorophyll dynamics (Figure 4.5), including elevated summer chlorophyll concentrations in both the before and after periods.

Table 4.4 Before-After-Control-Impact (BACI) analysis results using a two-way Analysis of Variance including the effect of the interaction of Period (Before and After) and season on mean difference between lakes (Elterwater – Blelham). Where a significant interaction was found, post-hoc analysis of contrasts was done to look at Period effect in individual seasons. Bold face and asterisks denote significant results at the 0.05 () level.*

	Mean difference ± SD		P-value	
	Before	After	Period × Season	Period
TP (annual)	-2.5 ± 11.0	-3.9 ± 9.3	0.025 *	0.538
Winter	-12.9 ± 5.4	-5.9 ± 4.2		0.117
Spring	0.0 ± 5.5	-10.4 ± 12.1		0.017 *
Summer	5.6 ± 7.6	-0.1 ± 7.36		0.191
Autumn	-2.7 ± 16.9	0.8 ± 7.0		0.484
SRP (annual)	1.1 ± 2.0	1.3 ± 2.8	0.748	0.588
Winter	-1.5 ± 2.2	-1.8 ± 1.5		-
Spring	1.4 ± 1.5	1.1 ± 1.1		-
Summer	2.2 ± 1.0	3.2 ± 1.8		-
Autumn	1.8 ± 1.0	2.7 ± 3.8		-
Chlorophyll <i>a</i> (non-transformed data)	-0.1 ± 19.5	7.3 ± 30.7	0.093	0.702
Winter	-0.3 ± 2.3	0.7 ± 2.4		-
Spring	-0.8 ± 6.9	-2.9 ± 5.0		-
Summer	-6.7 ± 10.7	18.3 ± 52.9		-
Autumn	9.7 ± 38.7	12.6 ± 26.2		-

Profiles from 2018-2019 showed that following the intervention anoxia occurred in up to 20% of the lake volume during the summer (Figure 4.6). In addition, accumulation of BAP persisted in the deepest part of the lake, indicating internal loading (Figure 4.6). Concentrations of BAP at 6 m were > 5 times that at 0.5 m during the summer stratified period (Figure 4.6). Furthermore, the mass-balance results suggest that internal loading continues contributes

three times more to the TP budget than external loads during summer following the intervention (Section 4.7.9).

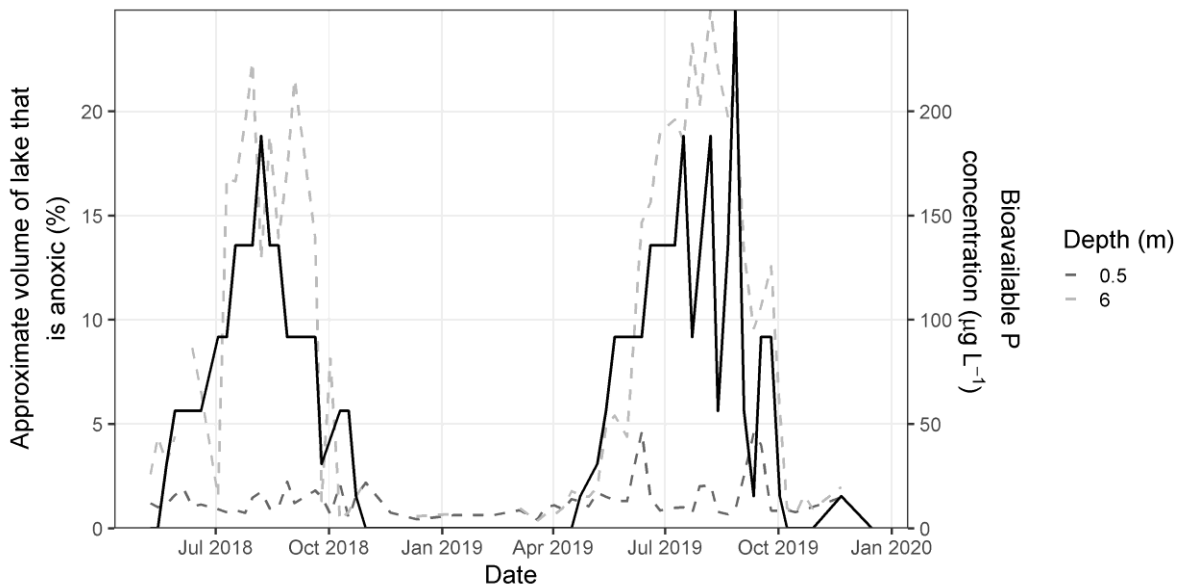


Figure 4.6 Approximate volume of Elterwater-IB that is anoxic ($< 2 \text{ mg L}^{-1}$, solid line) and concentration of biological available phosphorus (dashed lines) in the surface (0.5 m) and hypolimnion (6 m) based on profiles collected from May 2018 - December 2019.

4.5 Discussion

4.5.1 Changes to Elterwater-IB WRT

This study aimed to assess the success of the WRT manipulations in affecting the physical structure and water quality, based on four elements of the restoration: 1) WRTs, 2) thermal structure, 3) development of hypolimnetic anoxia, and 4) nutrient and chlorophyll *a* concentrations. Although there was some change in WRTs, it was not sufficient to have a large effect on the thermal structure, with anoxia persisting and no evidence for significant reductions to internal loading or water column nutrient and chlorophyll *a* concentrations. The intervention reduced annual WRT by 40% and seasonal WRTs by 29 – 45%. The change in summer WRT induced by the piped inflow was equivalent to approximately 8 days shorter WRT, a smaller change than the natural variability in WRT between years. Compared to other flushing and dilution case studies, this percentage change in WRT was lower. Dilution efforts at Moses Lake, Lake Veluwe and Lake Taihu, reduced annual WRTs by 63% (Welch et al., 1992), 75% (Cooke et al., 2005; Hopper and Meyer, 1986) and 51% (Hu et al., 2010), respectively. In the years when flushing and dilution occurred in Moses and Veluwe Lakes, both non-stratifying lakes, more than 50% reductions in TP concentrations were reported and chlorophyll concentrations reduced (Cooke et al., 2005; Hopper and Meyer, 1986; Welch et al., 1992). Reasons why these schemes appear more successful could relate to the larger overall

reductions in WRT, the initial WRT, and the rate of flushing being maintained through pumping rather than via the passive flow diversion in Elterwater and that water quality conditions prior to intervention were worse than at Elterwater, leaving the potential for greater improvements.

4.5.2 Changes to thermal structure and stratification

The change in WRT had a small but quantifiable impact on Elterwater-IB's physical structure, partially satisfying element 2 of the assessment. The summer stratified period was shortened by 2 days and was 7% less stable, and average summer surface water temperatures were 0.7 °C cooler with the intervention, demonstrating the cooling effect of the inflow in summer (Carmack et al., 1979; Richards et al., 2012). However, the cooling effect was not sufficient to break down stratification and considerably larger changes in WRT would be required to modify the heat budget sufficiently to induce the desired changes to thermal structure.

In the summer, lake surface heat fluxes are likely to be considerably larger than the heat flux exerted by the inflows (Livingstone and Imboden, 1989) and are therefore difficult to overcome, despite a 45% decrease in WRT. Previous modelling studies in two reservoirs, considering a range of WRTs, suggest that flow can affect stratification (Li et al., 2018; Straškraba and Hocking, 2002). Halving reservoir WRT, using a constant inflow rate, resulted in a 30 day shorter stratified period, with both later onset and earlier overturn (Li et al., 2018). However, Straškraba & Hocking (2002) suggest that below a WRT of 200 days, WRT changes have an effect on stratification stability, but not on stratification length. Both reservoir modelling studies use a constant flow into the reservoir, maintaining the cooling effect. Field evidence linking shorter WRTs with shorter stratified periods is often gathered at times of concurrent meteorological change, such as storm-related increases in wind speed and reductions in solar radiation (M. R. Andersen et al., 2020; Woolway et al., 2018). Such evidence both highlights the importance of these transient weather effects for stratification, but also partially confounds our ability to discern the specific effects of WRT change, and sustained impacts on a seasonal time scale. The importance of each of these parameters varies among lakes due to lake-specific morphology, heat budgets, and climate. The minor changes in stratification length, following the intervention, suggests larger WRT reductions or more targeted changes in WRTs may be needed in Elterwater-IB to effect a larger change in the thermal structure of the lake.

4.5.3 Prevention of hypolimnetic anoxia and internal loading as a means to reduce nutrient and phytoplankton concentrations

Our results showed evidence of continued hypolimnetic anoxia, and the accumulation of BAP in deep water, suggesting that internal loading continued in Elterwater-IB following the intervention. Previous water diversion interventions provide limited evidence of their effect on internal loading, as the target action was dilution and flushing of nutrients and phytoplankton biomass. However, evidence from Moses Lake suggests internal loading may have increased following increased flushing rate due to greater sediment resuspension (Welch and Patmont, 1980). Our results also show that internal loading remains a dominant source of nutrients to the water column. The water source of the intervention is lower in nutrients than the lake (APEM, 2012) and, where internal loads exceed external loads, the additional flow may act to dilute nutrient concentration (Elliott et al., 2009; Jones et al., 2011). As we saw no significant change in P concentration with the intervention, it suggests that there is either no dilution effect or the effect is being compensated for by additional internal loading.

WRT changes can affect phytoplankton concentrations in several ways, including through changes to thermal structure, nutrient loading, and direct flushing. In our study, in-lake chlorophyll *a* concentrations did not change after the intervention, suggesting the change in WRT was insufficient to reduce phytoplankton growth by reducing internal loading or by increasing losses through increased flushing. Reducing WRT has been shown to reduce phytoplankton biomass through flushing in other studies (Hosper and Meyer, 1986; Welch et al., 1992), although drawing direct conclusions on cause-effect in case studies reporting on this effect is often complicated as a result of multiple restoration measures including external load reduction. A modelling study showed a 50% increase in discharge only reduced chlorophyll *a* by 12% (Zhang et al., 2016), failing to reduce nutrient concentrations or impact growth rate sufficiently. Although not assessed here, decreases in WRT can also impact losses of zooplankton to a greater extent than phytoplankton where the flushing rates exceeds the growth of the former but not the latter (Obertegger et al., 2007; Rennella and Quirós, 2006). In our study, the lack of response in chlorophyll *a* concentration is not surprising given that nutrient concentrations also did not change, a result that is commonly reported in similar hydrological interventions across other case studies (Hu et al., 2010; McGowan et al., 2005; Zhang et al., 2016). No significant change in chlorophyll *a* concentration with the intervention indicates that either none of the flow-related mechanisms had much obvious effect or were cancelling each other out. The lack of changes could also suggest an element of resilience to WRT changes, especially as the rate of inflowing water is not maintained consistently and was

within hydrological and physical conditions naturally occurring in Elterwater. The modest change in WRT might alter species composition, by selecting for taxa with different growth rates (Reynolds et al., 2012) potentially occurring before any noticeable change in total biomass. Indeed, species turnover might actually have a compensatory effect on total biomass, maintaining biomass with more well adapted species.

4.5.4 Implications for future restoration in Elterwater and other lakes

The success of lake restoration measures, particularly over the long term, is often limited (Jilbert et al., 2020; Søndergaard et al., 2007). One common reason for failure is insufficient understanding of site-specific aspects of lake functioning and nutrient sources before restoration measures are implemented (Hamilton et al., 2018; Lürling et al., 2016). Insufficient understanding of pre-restoration functioning within a system means that interventions can commonly fail, especially if the source of the nutrient loading (Lürling et al., 2016) or water residence times is poorly understood.

Using a hydrodynamic model, we demonstrated that the intervention to decrease WRT in Elterwater-IB had a measurable but minor effect on stratification and water temperature compared to the natural variability of these physical variables. Other research has shown that the inter-annual variability can far exceed restoration or management anthropogenic impacts (e.g. Fink et al., 2014), a consequence being that longer time series are needed to identify treatment effects statistically. For example, in this study the large inter-annual variability in chlorophyll concentrations may have masked smaller but genuine impacts that could only be identified statistically with a much longer timeseries of data. Therefore, understanding the inter-annual variability over significant time periods is crucial to design effective schemes and detect “real” and relevant changes. This highlights the need for multi-year studies to fully determine intervention effects (Smokorowski and Randall, 2017), also allowing for adaptive management of protected sites (Tanner-McAllister et al., 2017), crucial for long-term success.

In addition, single site Before-After studies can fail to capture changes caused by external factors, co-occurring with management (Stewart-Oaten et al., 1986), and including a “control” site in BACI analysis, partially alleviates this (Smokorowski and Randall, 2017; Stewart-Oaten et al., 1986) by accounting, for example, for the effects of local weather (Schwartz, 2015). Had we not employed the BACI approach, utilising long-term data, we may, for example, have incorrectly concluded that the apparent decrease in spring TP and chlorophyll *a* concentrations in Elterwater (Figure 4.4) were direct effects of the intervention, whereas, similar changes were observed in our control lake. However, “control” systems are not perfect

controls (Kerr et al., 2019), despite providing some level of comparison to be able to identify local climate effects (Schwartz, 2015).

For the hydrological interventions at Elterwater, a simple 1-D hydrodynamic model has allowed us to further isolate the intervention impact, however small, of modifying inflow rates on lake stratification. This modelling approach is transferable to other sites and could be applied to conduct site-specific assessments to inform the suitability of this approach given specific lake characteristics, heat budgets, and climate. A similar study, prior to intervention, could have highlighted the scale and timing of WRT manipulation required to impact stratification.

4.6 Conclusions

Water residence time was reduced in all seasons in Elterwater-IB and this had quantifiable, if small, effects on lake temperatures. The extent of the change in the lake's thermal structure was insufficient to induce significant changes in water quality, with summer stratification, seasonal anoxia, and internal loading persisting after the intervention. Greater changes, or more targeted WRT manipulations, would be needed to modify lake physical structure sufficiently to inhibit stratification in this lake, whilst also considering undesirable effects on ecosystem function. Hydrodynamic modelling and a systems approach to lake restoration, including knowledge of nutrient sources and inter-annual variability, would be crucial to determine the magnitude of change required to produce a measurable effect on lake water quality.

4.7 Supplementary information for Chapter 4

4.7.1 Trophic status of Elterwater

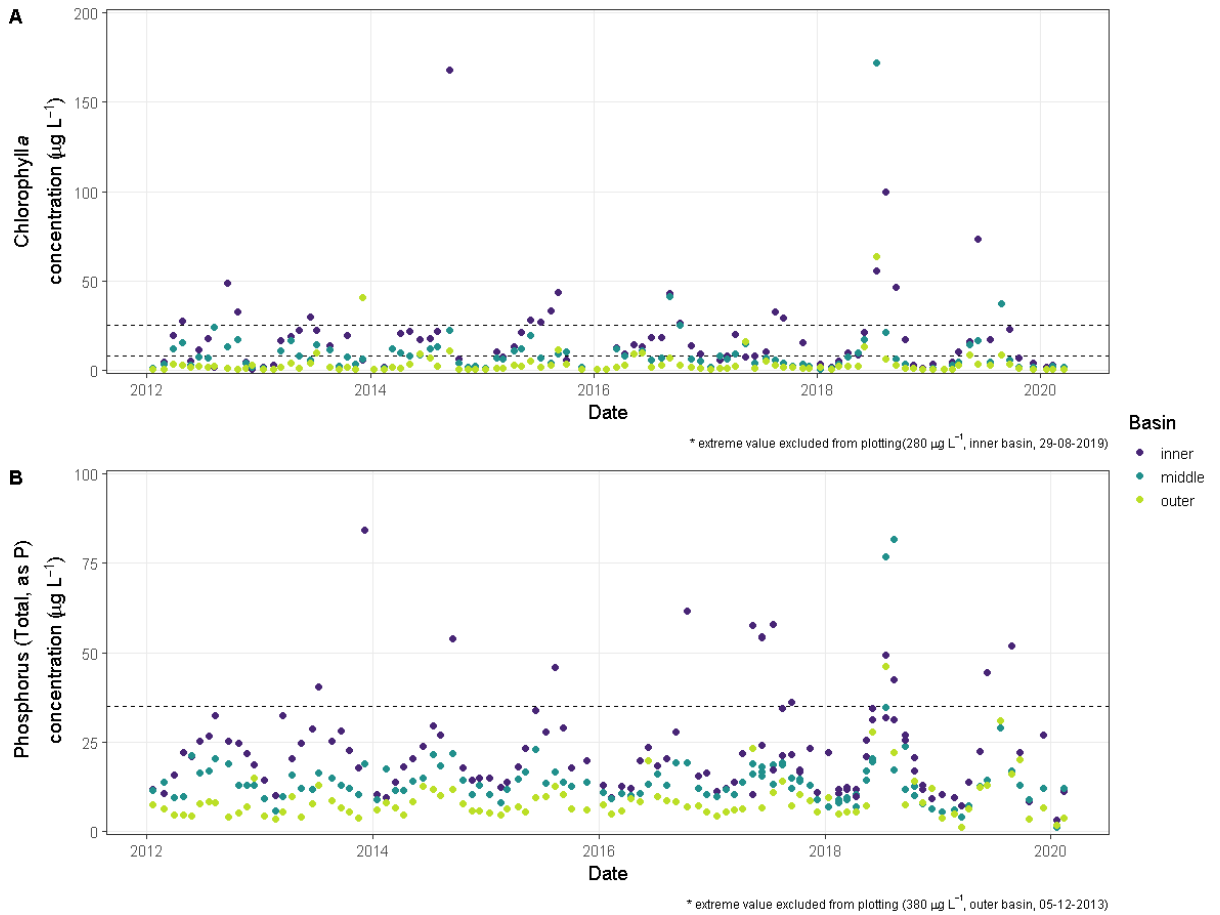


Figure S 4.7.1-1 A) Chlorophyll a and B) total phosphorus concentrations in Elterwater's three basins (inner, middle and outer). Dashed lines show the mean (chlorophyll and TP) and maximum (chlorophyll only) concentrations for eutrophic class (OECD)

Data available on the [UK Lakes Portal](#) that uses Environment Agency water quality data from the Water Quality Archive (Beta) published under an Open Government Licence.

4.7.2 Photographs of the intervention pipeline



Figure S 4.7.2-1 Photographs of the off-take structure on the Great Langdale Beck and the discharge of the pipeline into a field drain which discharges into Elterwater-IB

4.7.3 Estimating inflow discharge and temperature during unmeasured periods

4.7.3.1 Inflow discharge estimates

Using the measurements from the diversion (Jan 2016 to Dec 2019) a workflow was developed to estimate the missing values in the inflow discharge measurements (274 missing values, < 1% of data), based on the gauged discharge in the River Brathay (lake outflow). The maximum discharge through the pipeline, based on Environment Agency defined abstraction limits is $0.122 \text{ m}^3 \text{ s}^{-1}$. The minimum discharge in the source river when abstraction is permitted is $0.383 \text{ m}^3 \text{ s}^{-1}$. The 95th percentile of measured source discharge that produced the maximum (capped) diversion discharge ($0.122 \text{ m}^3 \text{ s}^{-1}$) was calculated. When this discharge was exceeded in the source it was assumed the diversion discharge would be maximised ($0.122 \text{ m}^3 \text{ s}^{-1}$). Where the source discharge dropped below $0.383 \text{ m}^3 \text{ s}^{-1}$ the diversion would be $0 \text{ m}^3 \text{ s}^{-1}$. Between these flows, a general additive model was fitted between the measured lake outflow and diversion discharges. The smooth was significant at $p < 0.01$ and the model had an R-squared of 0.53. The gam.check function was used to visually check model fit.

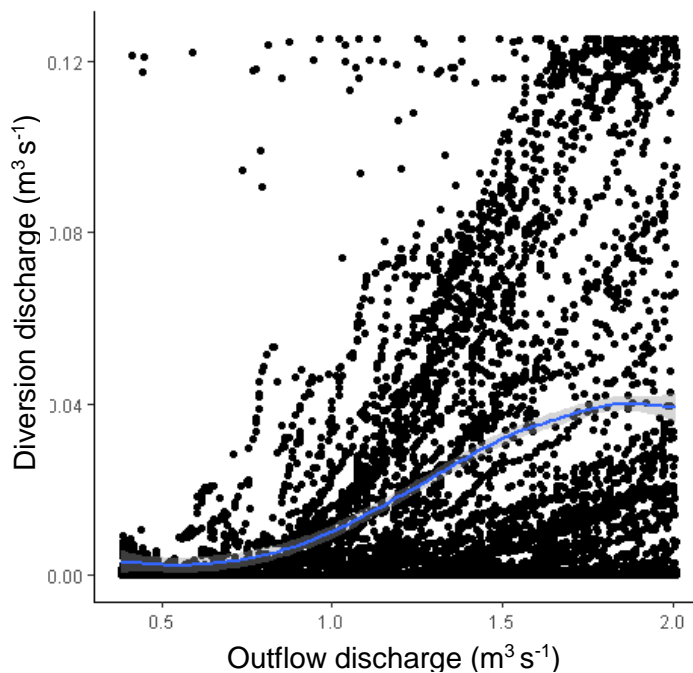


Figure S 4.7.3-1 observations (points) and model fit between outflow and piped discharge

```
> summary(mod)
Family: gaussian
Link function: identity

Formula:
Q_m3_s.t ~ s(Q_m3_s.JK, k = 20)

Parametric coefficients:
              Estimate Std. Error t value Pr(>|t|)
(Intercept) 0.0576170  0.0002488   231.6  <2e-16 ***
---
Signif. codes:  0 '***' 0.001 '**' 0.01 '*' 0.05 '.' 0.1 ' ' 1

Approximate significance of smooth terms:
              edf Ref.df   F p-value
s(Q_m3_s.JK) 16.68  18.26 1314  <2e-16 ***
---
Signif. codes:  0 '***' 0.001 '**' 0.01 '*' 0.05 '.' 0.1 ' ' 1

R-sq.(adj) = 0.534  Deviance explained = 53.5%
GCV = 0.0012972  Scale est. = 0.0012961  n = 20937
```

Diagnostic plots:

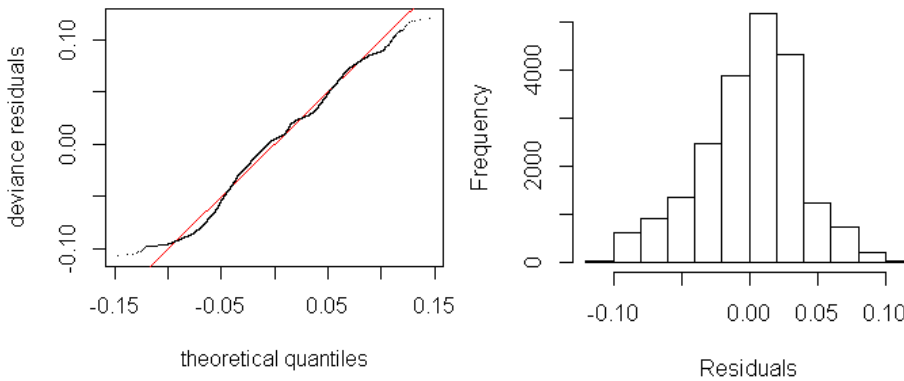


Figure S4.7.3-2 diagnostic plots of the gam model fitted between the outflow and piped discharge

4.7.3.2 Inflow temperature estimates

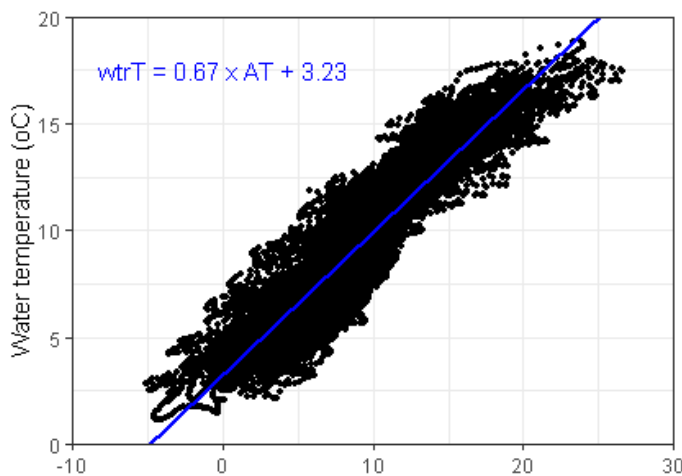


Figure S4.7.3-4 Prediction of water temperature based on the 12 hour rolling average air temperature. Points show observations and blue line the fitted linear model

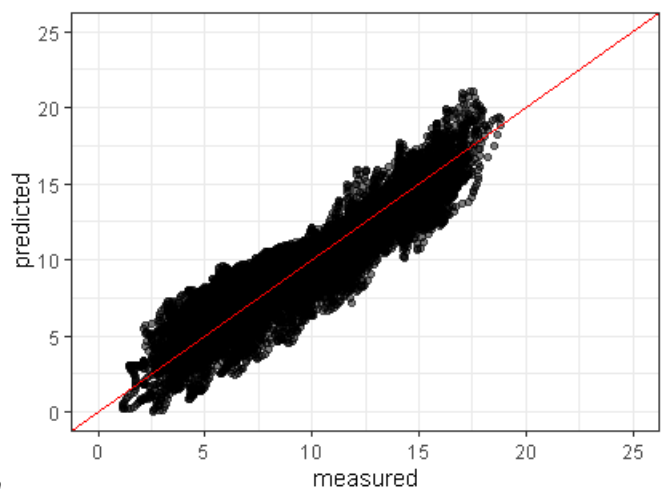


Figure S 4.7.3-3 Predicted vs observed water temperatures. red line shows the 1-1 line

```
Call:
lm(formula = merge$pipe_T ~ merge$AT_ma)

Residuals:
    Min       1Q   Median       3Q      Max
-4.0825 -0.8289  0.0215  0.8135  4.7420

Coefficients:
              Estimate Std. Error t value Pr(>|t|)
(Intercept)  3.227604   0.019197   168.1  <2e-16 ***
merge$AT_ma  0.671351   0.001718   390.9  <2e-16 ***
---
Signif. codes:  0 '***' 0.001 '**' 0.01 '*' 0.05 '.' 0.1 ' ' 1

Residual standard error: 1.297 on 20911 degrees of freedom
(11 observations deleted due to missingness)
Multiple R-squared:  0.8796,    Adjusted R-squared:  0.8796
F-statistic: 1.528e+05 on 1 and 20911 DF,  p-value: < 2.2e-16
```

A relationship between the mean of the previous 12 hours' air temperature and inflow water temperature was developed using the measurements taken of air temperature and inflow temperature between July 2017 and Dec 2019. This relationship was used to estimate inflow temperature prior to these measurements (January 2012-June 2017). A linear regression with an intercept of 3.2 and a slope of 0.67 produced an R-squared of 0.880 and a RMSE of 1.30 °C. Assumptions of the model were checked and confirmed visually.

4.7.4 Diagnostic plots for BACI analysis (two-way ANOVA on between lake differences).

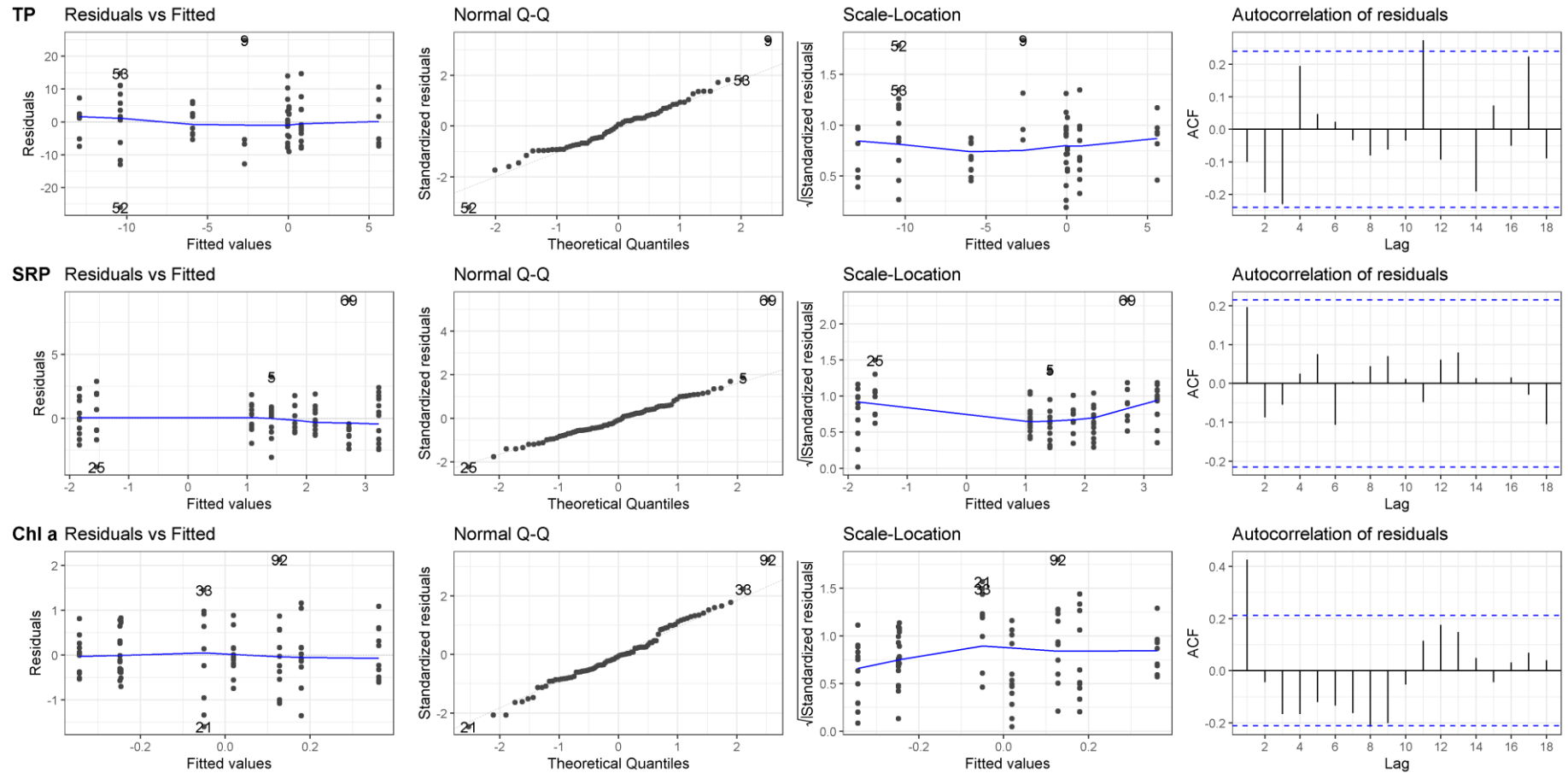


Figure S 4.7.4-1 Diagnostic plots for BACI analysis (two-way ANOVA on between lake differences). Plots were generated using ggfortify R package's autoplot function and the base R acf function. The plots of residuals were visually inspected for normality, equal variance, and auto correlation.

4.7.5 Pre-intervention statistical coherence

Linear model of the difference between Blelham and Elterwater (or difference of logged values for SRP and chlorophyll) as a function of date. All models showed non-significant slopes, suggesting the slope is not significantly different from zero and thus no change in the difference between sites over the time period.

Table S 4.7.5-1 P-values of the slopes for the linear models fitted between date and the difference in TP values or log(values) SRP and chlorophyll.

	Slope	Std error	p-value
TP	-4.15	4.81	0.399
SRP	0.19	0.11	0.087
Chlorophyll <i>a</i>	-0.044	0.097	0.652

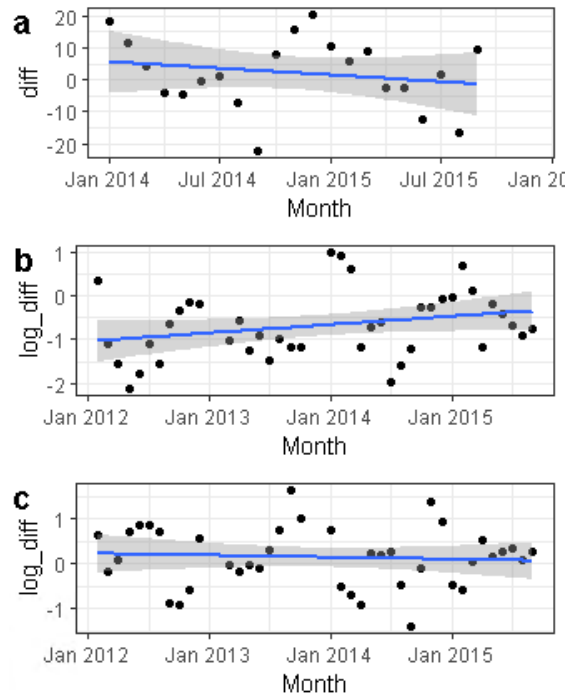


Figure S 4.7.5-1 Plots of water chemistry data fitted with a linear model for the period before intervention. Plots show a) TP, b) SRP, and c) chlorophyll a)

4.7.6 Protocol for processing Blelham meteorological data

4.7.6.1 Gap filling protocol for meteorological data (2012-2019)

- Gaps of less than 24 hours were filled using linear interpolation, for solar radiation the maximum gap was 6 hours, to avoid interpolating between day and night.
- Where gaps remained a linear model was fitted between Blelham and Windermere buoy (see <https://ukscape.ceh.ac.uk/our-science/projects/cumbrian-lakes-monitoring-platform>) meteorological data, using data from 2012-2019.

Table S 4.7.6-1 Linear regression between Blelham and Windermere buoy data variables.

Variable	% missing before	% missing after	Intercept	Slope	p	Adjusted r-squared
Air temperature	6.8	0	-0.978	1.056	< 0.001	0.957
Wind speed	4.4	0.3	0.090	0.548	< 0.001	0.572
Solar radiation	1.9	0	3.913	0.931	< 0.001	0.895
Relative humidity	4.2	1.3	-1.809	1.024	< 0.001	0.863
Surface water temperature	4.3	0.04	-0.639	1.047	< 0.001	0.924

For the remaining missing values the following protocol was used:

1. Wind speed – average wind speed for 24 hours previous and 1 week after the missing value.
2. Relative humidity – linear regression between Blelham Tarn and Esthwaite Water buoy weather station values (intercept = -5.917, slope =1.07, $p < 0.001$, adjusted R-squared = 0.915).
3. Surface water temperature – linear interpolation.

4.7.6.2 Solar radiation and cloud cover calculations

This method used the *suncalc* (Thieurmel & Elmarhraoui, 2019) and *insol* (Corripio, 2019) R packages.

1. Night-time values (between sunset and sunrise) were set to 0.
2. Calculate clear sky solar radiation, dependent on the time of day and the day of the year
3. The cloud cover (between 0 and 1) was estimated by comparing observed solar radiation and clear sky solar radiation

$$cloud\ cover = 1 - \frac{observed}{maximum\ possible}$$

Mean cloud cover for the previous day was estimated as the night-time cloud cover.

Thieurmel, B. & Elmarhraoui, A. (2019). suncalc: Compute Sun Position, Sunlight Phases, Moon Position and Lunar Phase. R package version 0.5.0. <https://CRAN.R-project.org/package=suncalc>

Corripio, J. G. (2019). insol: Solar Radiation. R package version 1.2.1. <https://CRAN.R-project.org/package=insol>

4.7.7 Calibration and validation of the hydrodynamic model

The General Ocean Turbulence Model was calibrated and validated for use on Elterwater-IB. The model parameters used in the calibration included three non-dimension scaling factors; short-wave radiation factor (*swr*), surface heat factor (*shf*) and wind speed factor (*wsf*). Modifying these parameters allows to minimise error in the input data due to the difference in conditions between Elterwater and the location of the weather station. The fourth parameter was *kmin*, the minimum allowable kinetic turbulence allowed. The factors were allowed to vary between 0.85-1.1 for *swr*, 1.2-0.8 for *shf*, and 0.9-1.1 for *wsf*. This was bounded at the lower end by the value of molecular diffusion, $1.4 \text{ e}^{-7} \text{m}^{-2} \text{ s}^{-1}$. The calibration also used parameters for visible (*g2*) and non-visible light attenuation (*g1*). Non-visible light attenuation was fixed at the median value given in Woolway *et al.* (2015), 0.45. The visible light attenuation value was allowed to vary in the range of *g2* calculated as,

$$g_2 = \frac{1}{k'}$$

where *k* the light extinction coefficient, derived from measurements of secchi disk extinction depths (*Z_{SD}*) taken in 2018 and 2019, calculated according to Kalff (2002):

$$k = \frac{1.7}{Z_{SD}}$$

The calibration minimised the difference between simulated and measured water temperatures. The calibration routine was run three times, and the parameters giving the best model fit were used. Model fit evaluation used three metrics; root mean square error (RMSE), Nash-Sutcliffe efficiency (NSE), and mean absolute error (MAE),

$$RMSE = \sqrt{\frac{\sum_{i=1}^n (mod-obs)^2}{n}}$$

$$NSE = 1 - \frac{\sum (obs-mod)^2}{\sum (obs-obs)^2}$$

$$MAE = \frac{\sum |mod-obs|}{n}$$

where *mod* and *obs* are the modelled and observed water temperatures. Parameters were calibrated to produce modelled output that minimised RMSE and MAE and gave NSE values closest to 1. The best parameter values gave a model fit with a RMSE of 0.93 °C, a MAE of 0.72 °C, and a NSE of 0.94. Using the parameters estimated in the calibration routine for 2018 (Table 4.2), a validation run was completed using 2019 driving data and observations. The model fit for the validation period was a RMSE of 0.97 °C, a MAE of 0.75 °C, and a NSE of 0.92, suggesting the model replicates observed water temperatures within a reasonable margin of error.

4.7.8 Before-After analysis of water chemistry variables

Output for the GLM models fitted for the Before-After analysis using a gamma distribution and log-link function. Estimated marginal means were also analysed, using a 0.95 confidence interval. Results for the analysis of Elterwater water chemistry data (Total Phosphorus, Soluble Reactive Phosphorus, chlorophyll *a*) are shown. Before period (2012-2015), After (2016-2019).

4.7.8.1 Total Phosphorus

Table S 4.7.8-1 Result of GLM for total phosphorus comparing the Before and After periods. The effect of the intervention was not significant

Response	ChiSq	DF	P
Period	1.885	1	0.1697
Season	97.860	3	<0.001
Period:Season	2.765	3	0.4294

Table S 4.7.8-2 Result of the estimated marginal means tests of Before-After contrasts for each season. The results given on the log scale. The test shows a significant difference between TP values in Spring in the Before and After period.

Season	estimate	SE	z.ratio	p.value
Winter	0.030	0.139	0.213	0.831
Spring	0.264	0.120	2.196	0.028
Summer	0.052	0.120	0.433	0.665
Autumn	0.007	0.132	0.049	0.961

4.7.8.2 Soluble Reactive Phosphorus

Table S 4.7.8-3 Result of GLM for total phosphorus comparing the Before and After periods. The effect of the intervention was not significant.

Response	ChiSq	DF	P
Period	0.071	1	0.537
Season	17.683	3	<0.001
Period:Season	6.561	3	0.230

Table S 4.7.8-4 Result of the estimated marginal means tests of Before-After contrasts for each season. The results given on the log scale.

Season	estimate	SE	z.ratio	p.value
Winter	0.185	0.158	1.175	0.240
Spring	0.104	0.136	0.766	0.444
Summer	-0.200	0.136	-1.477	0.140
Autumn	0.094	0.161	0.583	0.560

4.7.8.3 Chlorophyll *a*

Table S 4.7.8-5 Result of GLM for total phosphorus comparing the Before and After periods. The effect of the intervention was not significant.

Response	ChiSq	DF	P
Period	0.146	1	0.702
Season	77.385	3	<0.001
Period:Season	6.420	3	0.093

*Table S 4.7.8-6 Result of the estimated marginal means tests of Before-After contrasts for each season. The results given on the log scale. The test shows a significant difference between chlorophyll *a* values in Summer in the Before and After period.*

Season	estimate	SE	z.ratio	p.value
Winter	-0.166	0.386	-0.431	0.666
Spring	0.449	0.332	1.352	0.176
Summer	-0.703	0.332	-2.118	0.034
Autumn	0.150	0.366	0.409	0.682

4.7.8.4 Seasonal dynamics of total phosphorus and soluble reactive phosphorus concentrations before and after intervention

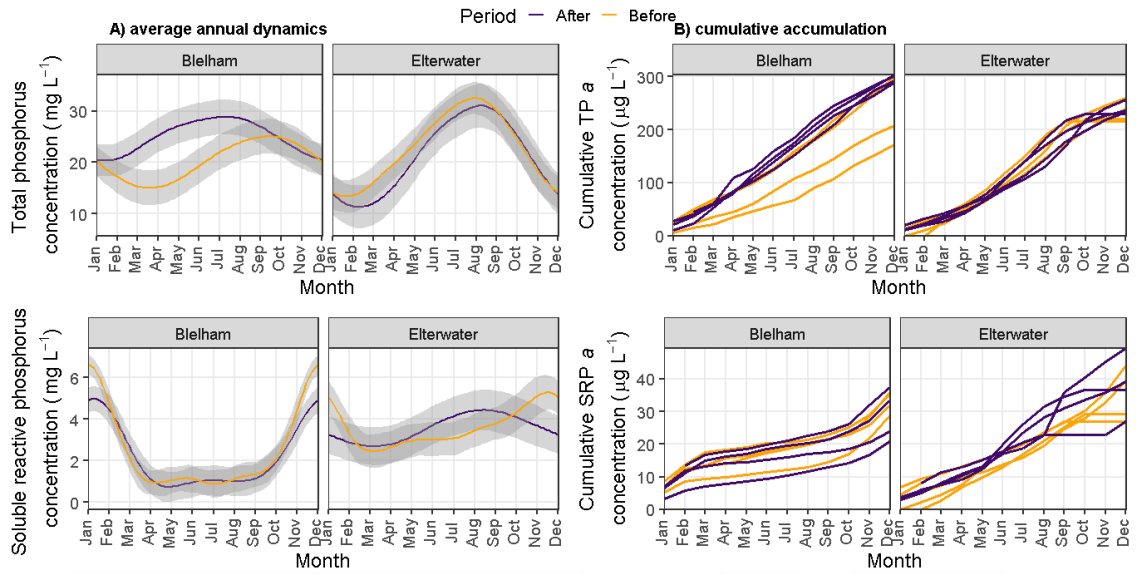


Figure S 4.7.8-1 a) average annual dynamics of total phosphorus (TP) and soluble reactive phosphorus (SRP) (shading shows ± 1 SE) and b) cumulative TP and SRP accumulation for each year before and after restoration at the control (Blelham) and impact (Elterwater-inner basin) lakes

4.7.9 Predicted vs measured TP retention

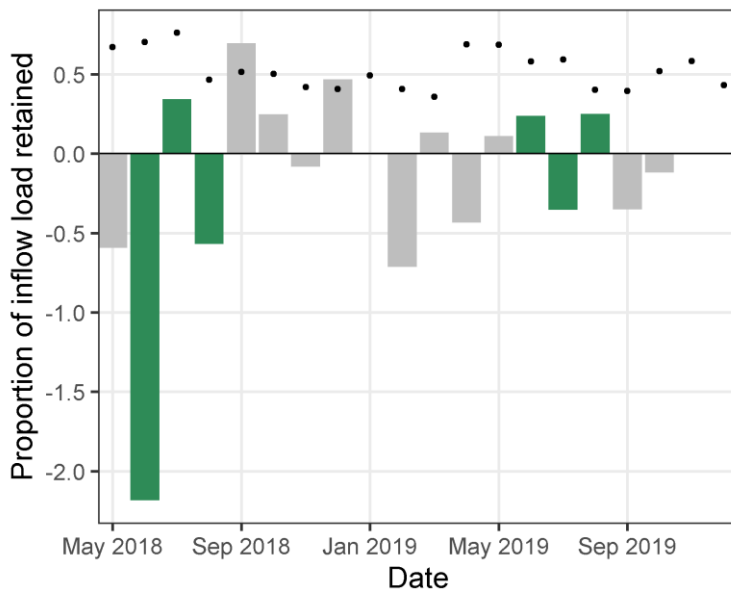


Figure S 4.7.9-1 Proportion of monthly inflow TP load retained in the basin (columns) and predicted TP retention according to water load (points), estimated according to Nurnberg (2009). Summer values highlighted in green.

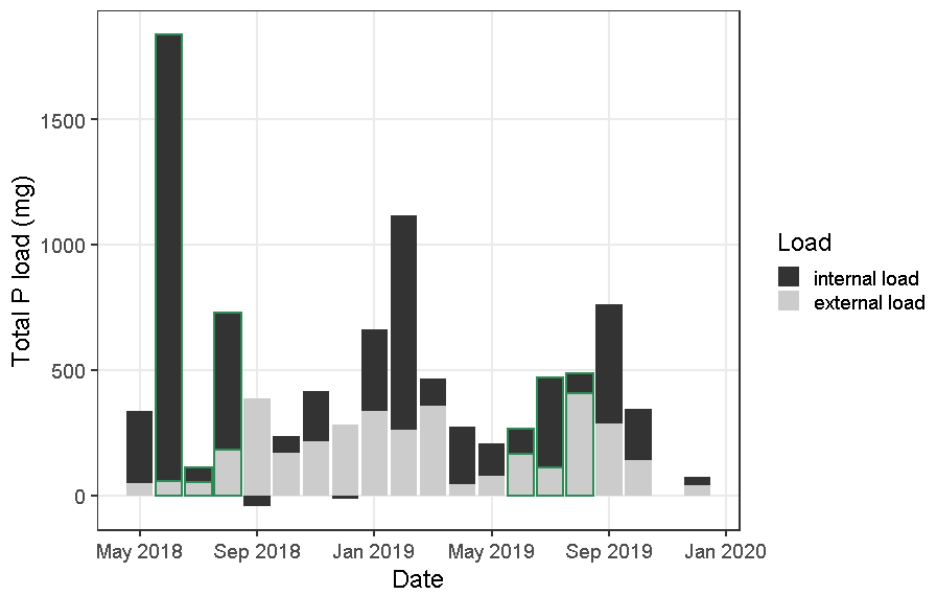


Figure S 4.7.9-2 Gross internal and external loads per month estimated via mass balance method (Nürnberg 2009). Summer loads are highlighted in green.

Table S 4.7.9-1 Total summer load contributed by internal and external sources from 2018-2019

Load	Total (mg)
Gross external	977
Gross internal	2926

Based on the mass-balance method of Nürnberg (2009), the predicted retention of P was estimated. Where the predicted retention estimate is less than observed retention, this indicated internal loading (Figure S 4.7.9-2). Gross internal loading was also estimated and compared with gross external load (Figure S 4.7.9-2), and contributes more to the total loading, especially during the summer months (shown highlighted in green).

Chapter 5 Annual water residence time effects on thermal structure: a potential lake restoration measure?

(**Freya Olsson**, Eleanor B. Mackay, Tadhg Moore, Phil Barker, Sian Davies, Ruth Hall, Bryan Spears, Ian D. Jones (2021). Annual water residence time effects on thermal structure: a potential lake restoration measure? In review at Journal of Environmental Management)

5.1 Abstract

Innovative methods to combat internal loading issues in eutrophic lakes are urgently needed to speed recovery and restore systems within legislative deadlines. In stratifying lakes, internal phosphorus loading is particularly problematic during the summer stratified period when anoxia persists in the hypolimnion, promoting phosphorus release from the sediment. A novel method to inhibit stratification by reducing residence times is proposed as a way of controlling the length of the hypolimnetic anoxic period, thus reducing the loading of nutrients from the sediments into the water column. However, residence time effects on stratification length in natural lakes are not well understood. We used a systematic modelling approach to investigate the viability of changes to annual water residence time in affecting lake stratification and thermal dynamics in Elterwater, a small stratifying lake in the northwest of England. We found that reducing annual water residence times shortened and weakened summer stratification. Based on finer-scale dynamics of lake heat fluxes and water column stability we propose seasonal or sub-seasonal management of water residence time is needed for the method to be most effective at reducing stratification as a means of controlling internal nutrient loading.

Keywords: Lake management, heat fluxes, hypolimnetic anoxia, GOTM, flushing

5.2 Introduction

Anthropogenic eutrophication is a problem in lakes worldwide (Smith and Schindler, 2009), characterised by excess algal growth, low oxygen and high turbidity. The scale of the problem has motivated extensive research and management action to reverse degradation. Primarily, action has focused on controlling the external loading of nutrients, mainly phosphorus (P), to improve water quality. However, internal sources of P, accumulated in the sediments, can continue to cause water quality problems and prolong recovery from eutrophication, despite external load reductions (Schindler, 2006; Søndergaard et al., 2003).

In stratifying lakes, internal P loading predominantly occurs during the summer stratified period. During summer stratification, high biological oxygen demand in the hypolimnion

depletes oxygen and, as oxygen cannot easily be mixed downwards from the surface, results in persistent anoxia (Foley et al., 2012; Spears et al., 2007). Anoxia leads to reducing redox conditions which promote increased fluxes of highly-bioavailable soluble P to the overlying water, a key driver of P accumulation in the hypolimnion (Mortimer, 1942; Nürnberg, 1984). Longer stratification can prolong the period of anoxia (Foley et al., 2012; Jane et al., 2021; Snorheim et al., 2017), by suppressing downwards mixing.

Lake thermal structure is primarily controlled by the interaction of surface heat fluxes (short-wave and long-wave radiation and sensible and latent heat fluxes) but throughflows also contribute to the heat budget, quantified by the advective heat flux (Fenocchi et al., 2017; Livingstone and Imboden, 1989). Previous research suggests that, in some lakes, throughflows can be a dominant heat loss term, annually (Richards et al., 2012), particularly acting to cool the lake in the summer (Carmack et al., 1979; Colomer et al., 1996; Richards et al., 2012). By increasing inflow discharge, and thus reducing the lake's water residence time (WRT), the effect is increased (Smits et al., 2020).

There has not been extensive research on WRT effects on the advective heat flux and its control of stratification; however, what has been done suggests that shortening WRTs may present a viable method to manage stratification and internal loading. Field observations suggest that large episodic inflow events (e.g. storms) temporarily increase the inflow cooling (M. R. Andersen et al., 2020) and, generally, shorter WRT systems have shorter periods of summer stratification (León et al., 2016). Reservoir modelling studies looking at short vs long WRT scenarios found that shorter WRTs are associated with weaker and shorter periods of summer stratification (Li et al., 2018; Straškraba and Hocking, 2002; Yang et al., 2020), although these studies did not investigate WRT changes systematically and maintained constant flow rates, unrealistic in natural lakes. Larger advective heat fluxes at shorter WRTs and the dominant cooling effect in the temperate summer, suggests that reducing WRT may be expected to weaken stratification and shorten the stratified period. WRT manipulation to control stratification is likely to be most applicable in small lakes where hydrological control is most achievable (Paerl et al., 2016) and residence times markedly changed. It is also likely that only at short residence times, will the change induced by an increased advective flux be sufficient to overcome surface heat flux effects during peak summer. Small lakes (0.1 – 1 km²) are numerically dominant globally, representing 87% of the global total and 26% of lakes have a short residence time (<100 days; Messenger et al., 2016). Given this, if the technique is effective, it has the potential to be viable in numerous lakes globally.

Water residence time manipulation has been used in past restorations as a flushing or dilution method for algal control, to some effect (Dai et al., 2020; Jagtman et al., 1992; Welch et al., 1992). Other in-lake methods have been used to target internal P load reduction (Lüring and Mucci, 2020; Søndergaard et al., 2007), including dredging (Bormans et al., 2016), the addition of chemical binding agents to sediments (Mackay et al., 2014a; Spears et al., 2016), as well as aeration and withdrawals of the hypolimnion to reduce hypolimnetic anoxia (Bormans et al., 2016; Preece et al., 2019). Artificial mixing, as a means of destratification, using bubblers and axial flow pumps, is also used in some lakes (Cooke et al., 2005; Visser et al., 2016). While these physical and chemical techniques have had some success in controlling internal loading, success has not been consistently long-term (Cooke et al., 2005; Huser et al., 2016a), some methods can be ecologically destructive (Goldyn et al., 2014), and capital and running cost high (Mackay et al., 2014a). Therefore, further novel methods, if practicable and effective, may be valuable in managing internal loading.

Despite the potential for WRT changes to influence stratification suggested, a whole-lake application of the method failed to induce the desired changes. In 2016, a restoration effort in a small stratifying UK lake used WRT manipulation to target stratification in an attempt to limit the length of the anoxic period and control the internal loading of nutrients (Olsson et al., 2022). Annual WRT (AWRT) was reduced by approximately 38% (5 days) through the rerouting of water from a nearby stream into the basin via a diversion pipeline. The restoration aimed to reduce the length of the summer stratified period to maintain oxic conditions in the hypolimnion and limit summer internal nutrient loading. Results showed that there was little improvement in the water quality (assessed by phosphorus or chlorophyll *a* concentrations) and stratification and hypolimnetic anoxia persisted, despite some reductions in summer water temperatures and water column stability (Olsson et al., 2022). The failure to reduce stratification length significantly suggests that the change to WRT was insufficient to induce large changes in the thermal structure (Olsson et al., 2022). The investigation highlighted the need for a more systematic assessment of the interaction of WRTs, lake heat fluxes, and stratification dynamics in short residence time lakes to understand how much impact changing flow could have on stratification.

In this paper, we aim to understand how lake management, targeting physical controls on internal nutrient loading, may better utilise WRT manipulations to modify the advective heat flux and control stratification. We use a systematic modelling approach that maintains natural flow variability, to look at the effect of modifying AWRT on annual thermal dynamics, with a particular focus on the summer stratified period. A modelling approach allows for the

examination of the impacts of incremental changes in flow rates across many scenarios. We hypothesise that,

- a) Increasing discharge will increase the summer cooling effect of the stream and therefore reduce summer water temperatures and increase mixed depth,
- b) Stratification length and strength will be modified by changes to WRT, with shorter WRTs weakening and shortening periods of summer stratification,
- c) Management strategies can be optimised to control stratification, and the consequent anoxia and internal loading, by considering the seasonality of discharge and flow impacts on in-lake water temperatures.

5.3 Methods

5.3.1 Site description

Elterwater is a small monomictic lake in the northwest of England, UK (Lat: 54.4287, Long: -3.0350). The lake has three distinct basins: inner, middle, and outer (Figure 5.1). Elterwater's main inflow, Great Langdale Beck, discharges into the outer basin, with the outflow, the River Brathay, also flowing out of the outer basin. Smaller inflows discharge into the inner and middle basins. Due to the hydrology of the system, average annual WRTs vary between the basins, previously estimated to be around 15-20 days in the inner and middle basins to as little as 0.5 days in the outer basin (Beattie et al., 1996; APEM, 2012) with high seasonal variability.

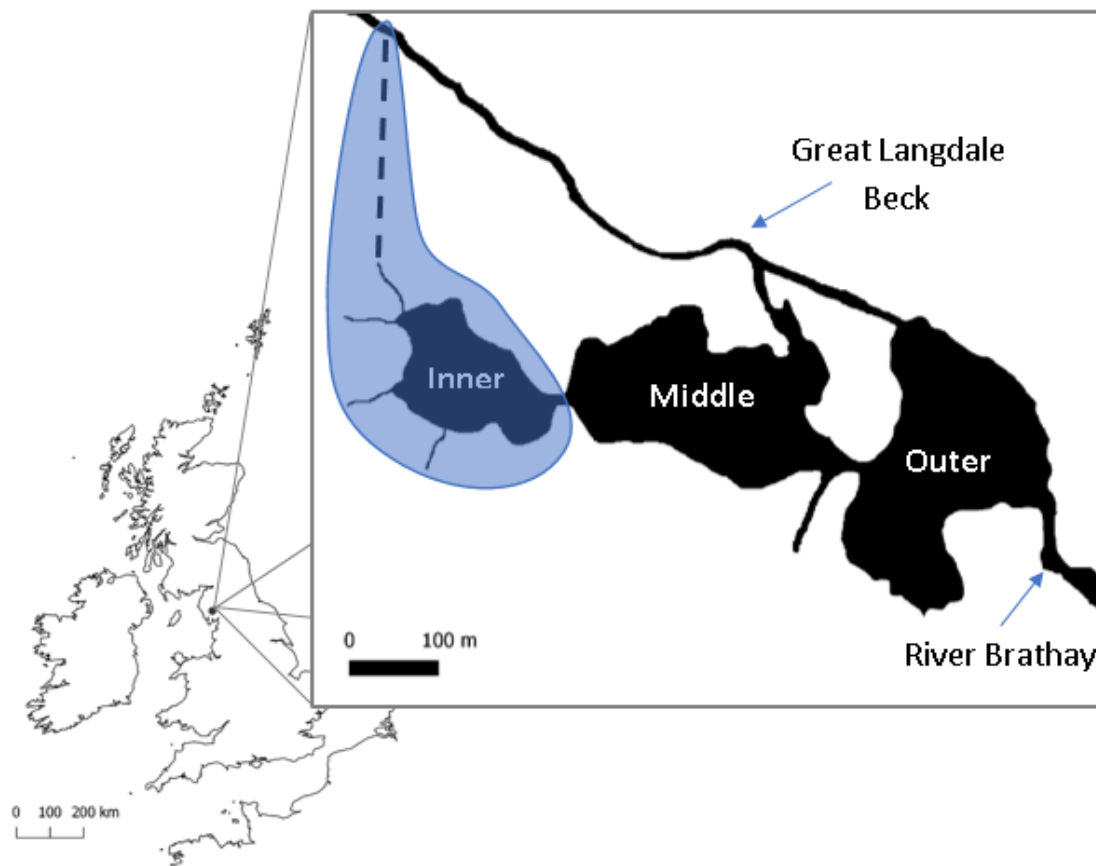


Figure 5.1 Map of Elterwater. The main inflow (Great Langdale Beck) and outflow (River Brathay) are shown alongside the restoration diversion (dashed line). Elterwater inner basin, the modelled system, is highlighted.

The inner basin (Elterwater-IB; max depth = 6.5 m, mean depth = 3.3 m, area = 0.03 km², catchment area = 1.0 km²), the smallest and most enriched of the basins, was historically the location of waste-water effluent discharge (Zinger-Gize et al., 1999) and the target of the unsuccessful water residence time management to control stratification and anoxia. A full description of the basin's condition and management action can be found in Olsson et al. (2022 & Chapter 4). Elterwater-IB is the focus of the modelling study reported here.

5.3.2 Model description

The General Ocean Turbulence Model (GOTM), a 1-D process-based water column model, was used to model the impacts of changing WRTs on the lake's thermal stratification. GOTM uses measured meteorological data, specified bathymetry and inflow data to model vertical mixing dynamics, lake surface heat fluxes and temperatures in natural waters (Burchard et al., 2006; Umlauf and Burchard, 2005). The model has been applied to several lakes since its development (e.g. Darko et al., 2019; Kerimoglu et al., 2017; Moras et al., 2019) and is able to

replicate accurately in-lake thermal conditions. GOTM was run at an hourly time-step with a spatial resolution of 0.12 m (50 layers) over the top 6 m of the water column.

5.3.2.1 Input and validation data

Meteorological data (air temperature, wind speed, relative humidity, and short-wave radiation) was obtained from the automatic water monitoring buoy at Blelham Tarn (surface area 0.1 km², see <https://www.ceh.ac.uk/our-science/monitoring-site/lake-observatories>), which is close to the study site (< 5 km). Data were collected January 2018 – December 2019 at 4-minute intervals, 2.5 m above the lake surface (see Table 5.1) and hourly averaged.

Table 5.1 Data collected at Elterwater and Blelham Tarn for model boundary conditions

Driving data	Sensor type	Accuracy	Source
Wind speed	Vector Instruments A100LK anemometer	1% ± 0.1 ms ⁻¹	Blelham tarn in situ meteorological monitoring buoy (hourly data) see UKLEON website
Air Temperature	Onset HOBO U23_001 logger	± 0.21 °C	(https://ukleon- data.ceh.ac.uk/)
Relative Humidity	Onset HOBO U23_001 logger	± 2.5%	
Short-wave Radiation	Kipp & Zonen CMP6 pyranometer	Expected daily uncertainty <5%	
In-lake temperature profiles	RBR Solo T	± 0.002 °C	Thermistor chain at deepest point in Elterwater-IB
Hypsograph			Haworth <i>et al.</i> (2003)

GOTM requires a continuous time series of forcing data. Gap filling of meteorological data was done using linear interpolation for small gaps (<24 hours) and relationships with other meteorological stations for larger gaps (Section 5.7.2). As meteorological variables can alter significantly with height, the 2.5 m observed data were corrected to the required 2 m for temperature and relative humidity and 10 m for wind speed, using modified equations from Lake Heat Flux Analyzer (Woolway *et al.*, 2015b). Cloud cover was estimated by comparing observed short-wave radiation and the maximum clear-sky radiation on any given day (see

Section 5.7.2.2). The average for the previous day was used as an estimate for night-time cloud cover and where observations of short-wave radiation were missing.

Inflow into Elterwater-IB from small ungauged tributaries and ephemeral streams, is estimated as 2% of the outflow measured on the River Brathay gauging (Environment Agency, 2000). Since the restoration, additional discharge from the diversion pipeline has increased the flow into the basin. The full Elterwater-IB inflow discharge was the sum of these two inflow measurements. Discharge and inflow water temperature data from the pipeline was obtained from the South Cumbrian Rivers Trust. Outflow temperature was assumed to be equal to the lake surface temperature and discharge equal to inflow, thus maintaining water level.

Water temperature was recorded every 4 minutes using a chain of temperature loggers every metre from 1 – 6 m depth, at the deepest point in the inner basin. These data were hourly averaged and used as initial conditions and for model calibration and validation.

5.3.2.2 Model calibration/validation

Model fit was assessed against observations of water column temperature at an hourly time-step. The calibration period was 01/01/2018 to 31/12/2018. The auto-calibration tool, ACPy (Bolding and Bruggeman, 2017; Storn and Price, 1997), was used for the model calibration. ACPy uses a differential evolution method to estimate the best parameter set based on a maximum-likelihood measure. Each calibration routine had 2000 model runs, each with different parameter values, trending towards a best fit. GOTM was calibrated using six parameters (Table 5.2): three non-dimensional scaling factors relating to wind speed (wsf), short-wave radiation (swr) and outgoing surface heat flux (shf) plus the physical parameters minimum kinetic turbulence (k-min) and visible (g_2) and non-visible light attenuation (g_1). The non-visible light extinction (g_1) was estimated as 0.45, based on the median from Woolway *et al.* (2015). The range of visible light extinction (g_2) used in the calibration was calculated as the maximum and minimum of,

$$g_2 = \frac{1}{k},$$

where k , the light extinction coefficient, is derived from measurements of secchi disk extinction depths (Z_{SD}) taken in 2018 and 2019, calculated according to Kalff (2002):

$$k = \frac{1.7}{Z_{SD}}$$

The calibration minimised the difference between modelled and measured water temperatures and was assessed based on three metrics: root mean square error (RMSE), Nash-Sutcliffe efficiency (NSE) and mean absolute error (MAE), calculated as,

$$RMSE = \sqrt{\frac{\sum_{i=1}^n (mod-obs)^2}{n}},$$

$$NSE = 1 - \frac{\sum (obs - mod)^2}{\sum (obs - \overline{obs})^2},$$

$$MAE = \frac{\sum |mod - obs|}{n},$$

where *mod* and *obs* are the modelled and observed water temperatures. Parameters were calibrated to produce modelled output that minimised RMSE and MAE and gave NSE values closest to 1. The calibration was run three times and the optimum set of parameters (Table 5.2) gave a model fit with an RMSE of 0.90 °C, a NSE of 0.94 and a MAE of 0.71 °C and show a good visual fit between observed and modelled temperatures (Figure 5.2).

Table 5.2 Parameters optimised during the calibration route. The maximum, minimum and final parameter values are shown.

Calibration factor	Min allowable value	Max allowable value	Final parameter value
swr	0.85	1.1	0.954
shf	0.8	1.2	0.800
wsf	0.9	1.1	1.082
k-min	1.4 e ⁻⁴	1.0 e ⁻⁵	1.4 e ⁻⁷
g2	0.5	2	0.611

Using the parameters estimated in the calibration (Table 5.2), a validation run was completed using 2019 driving data and observations. The model fit for the validation period resulted in a good fit (RMSE = 0.98 °C, NSE = 0.92, MAE = 0.74 °C).

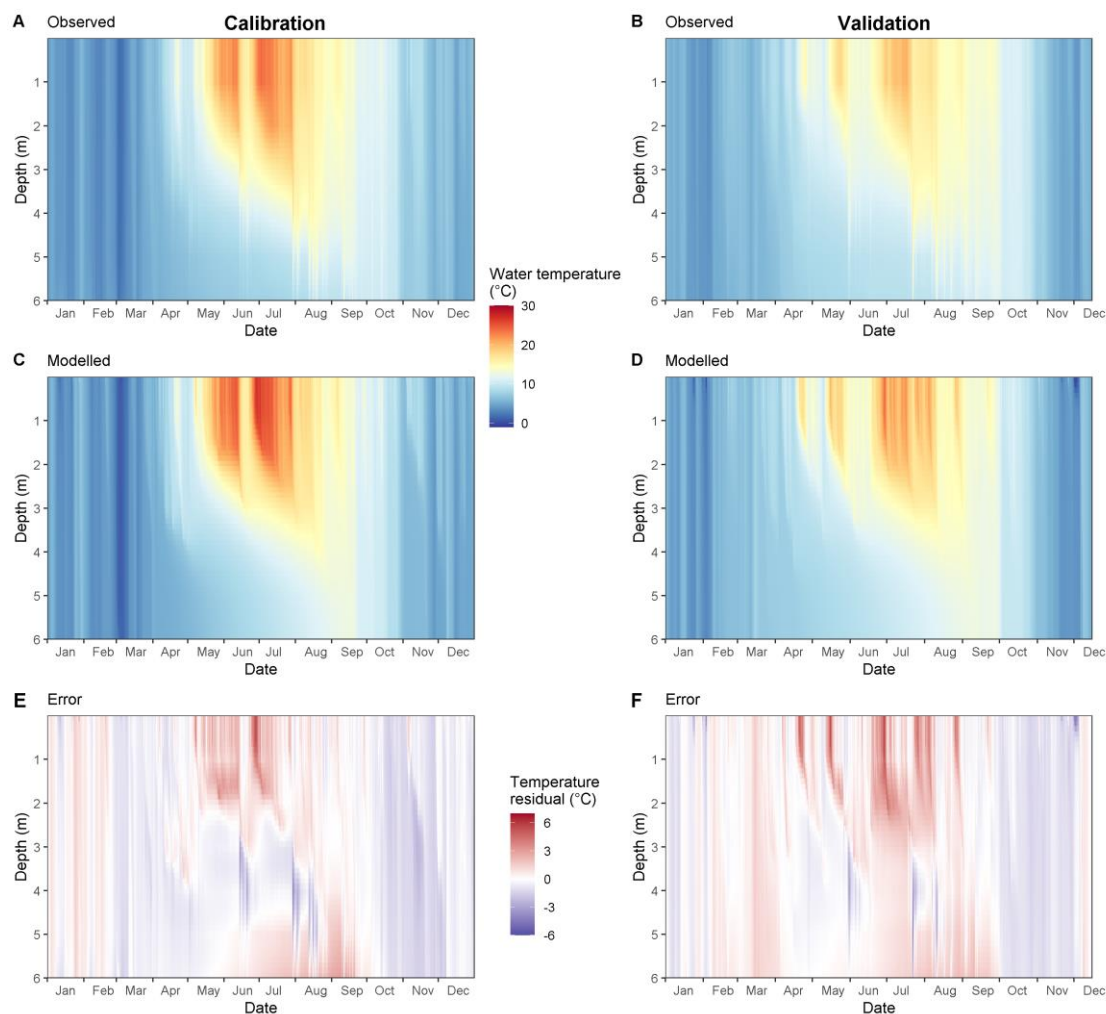


Figure 5.2 A-D: Modelled and observed water temperatures for the calibration and validation periods. E-F model error, as the residual between observed and modelled water temperature.

5.3.3 Model experiments

Using this calibrated and validated model, scenarios were run with modified annual WRT (AWRT). AWRT was calculated as,

$$AWRT = \frac{\text{lake volume}}{\text{annual mean discharge}}$$

AWRTs were modified by multiplying the inflow discharge by values from 0.1 to 10 in steps of 0.1, giving 100 scenarios with AWRTs for Elterwater-IB ranging from < 1 day to 88.6 days. Additionally, the instantaneous WRT was calculated for each hourly time step, using the hourly measured discharge.

5.3.4 Measuring WRT impacts

5.3.4.1 Heat fluxes

GOTM calculates the following lake surface heat fluxes at each timestep: incoming short-wave radiation (Q_{sin}), the net long-wave (Q_{net}), sensible heat flux (Q_h) and latent heat flux (Q_e). These heat fluxes were summed to give the total lake surface heat flux (Q_{surf_tot}).

Modifying WRTs changes the heat exchange by throughflows, termed the advective heat flux, Q_{adv} ($W\ m^{-2}$), diagnosed following Livingstone & Imboden (1989) as,

$$Q_{adv} = \frac{F_{inflow} \times C_{pw} \times \rho_w \times (T_{stream} - T_{lake})}{A_0},$$

where F_{inflow} is the inflow discharge ($m^3\ s^{-1}$) and $(T_{stream} - T_{lake})$ is the temperature difference between the inflow and the lake outflow ($^{\circ}C$), where the outflow temperature is assumed to be equal to the lake surface temperature. A_0 is the lake's surface area (m^2) and C_{pw} and ρ_w are the specific heat capacity and density of water, given as the constants $4200\ J\ kg^{-1}\ ^{\circ}C$ and $1000\ kg\ m^{-3}$, respectively. For each AWRT scenario, Q_{adv} and Q_{surf_tot} were calculated at each time step.

A Generalized Additive Model (GAM) curve was fitted through a three-day moving average of each of the heat fluxes, using the `mgcv` R package (Wood, 2011). The GAM used a REML method with a smoothing parameter for date.

Additionally, Q_{adv} was evaluated based on absolute direction (heating or cooling) and its direction relative to Q_{surf_tot} (additive or counter), giving four possible effects: counter cooling, counter heating, additive cooling, and additive heating.

5.3.4.2 Stratification metrics

A minimum density difference of $0.1\ kg\ m^{-3}$ between the top and bottom of the water column was used to define when stratification occurred. Occurrence of stratification can vary depending on the density difference threshold used (Gray et al., 2020) so we repeated the calculation with other thresholds, but there was no difference in the patterns observed in the data (see Section 5.7.3). Using the $0.1\ kg\ m^{-3}$ difference, the following stratification metrics were calculated:

1. total frequency of "normal" stratification (number of hourly time steps for which $T_{top} > T_{bottom}$ and the density difference threshold is exceeded),
2. frequency of inverse stratification (number of time steps for which $T_{bottom} > T_{top}$ and the density difference threshold is exceeded),

3. length of the longest continuously stratified period (the length of the longest continuous period for which the density difference threshold is exceeded)
4. start and end dates of the longest stratified periods (the date bounds for the longest continuously stratified period, as defined above)

Water column stability, measured using Schmidt stability (Idso, 1973), S_T , was calculated using the LakeAnalyzer R package (Read et al., 2011). Mixed depth was calculated using a modified version of the LakeAnalyzer meta.depths function, using a density difference threshold (0.1 kg m^{-3}) between the top and bottom water layers and a gradient threshold of $0.1 \text{ kg m}^{-3} \text{ m}^{-1}$. All metrics were compared across AWRTs scenarios on a monthly and seasonal scale to assess seasonally different responses. Seasons were defined as: spring = March, April, and May; summer = June, July, and August; autumn = September, October, and November; winter = December, January, and February.

5.4 Results

5.4.1 Changes to the advective heat flux

The inflow-lake temperature difference and the inflow discharge control the magnitude and direction of Q_{adv} and are both highly seasonal. Discharge was considerably larger in the winter than the summer (Table 5.3 and Figure 5.3a). In the summer, the unmodified discharge into the inner basin was estimated to be as little $0.002 \text{ m}^3 \text{ s}^{-1}$ compared to an estimated maximum flow of $2.17 \text{ m}^3 \text{ s}^{-1}$ during a storm event. This was reflected in the instantaneous water residence times which varied from >500 days to <1 day (Figure 5.3a). Similarly, the difference between inflow and lake temperature varied with season (Figure 5.3b). In the winter, the inflow water was slightly warmer than the lake temperature, whereas in the summer the inflow was substantially cooler than the lake water. Due to the seasonality of inflow-lake temperature differences and inflow discharge, Q_{adv} also showed a distinct seasonal cycle (Figure 5.4); a positive, warming flux in the winter and a negative, cooling flux in the summer (Table 5.3).

Table 5.3 Seasonal mean discharge, water residence time (WRT), inflow-lake temperature differences, extreme low (Q95) and high (Q5) flow percentiles and advective (Q_{adv}) and total surface heat (Q_{surf_tot}) fluxes in Elterwater inner basin under unchanged conditions. Values in brackets show the median values of flow parameters.

Season	Average discharge (median), m^3s^{-1}	WRT (median), days	Temperature difference (inflow-lake), $^{\circ}C$	Q95, m^3s^{-1}	Q5, m^3s^{-1}	Q_{adv} (median), $W m^{-2}$	Q_{surf_tot} $W m^{-2}$
Winter (n = 2160)	0.21 (0.21)	6 (5)	1.3	0.04	0.42	43.6 (36.1)	-47.4
Spring (n = 2208)	0.09 (0.08)	13 (15)	-1.3	0.01	0.22	0.172 (-4.0)	14.9
Summer (n = 2208)	0.07 (0.01)	15 (83)	-6.2	0.002	0.24	-33.5 (-13.1)	14.1
Autumn (n = 2184)	0.16 (0.06)	7 (19)	-0.3	0.02	0.60	3.19 (-0.2)	-18

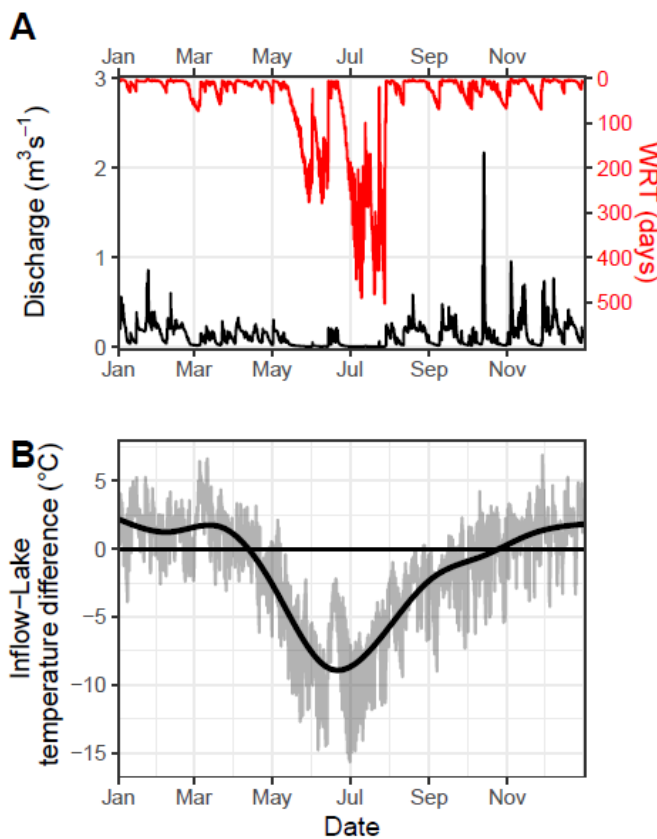


Figure 5.3 Controls on the advective heat flux during the baseline scenario (2018) A) discharge and WRT and B) inflow-lake temperature difference.

Changing AWRT modified Q_{adv} dynamics, primarily affecting the magnitude of Q_{adv} , rather than the direction (Figure 5.4a), as the discharge is multiplicative in the advective heat flux calculation (Equation 7). The magnitude of Q_{adv} was smaller at longer AWRTs and larger at shorter AWRTs (Figure 5.4a). At shorter AWRTs, there were greater increases in Q_{adv} in winter than summer, as the discharge is already large. The general pattern for Elterwater-IB is that winter has a small temperature difference and a large discharge and summer a large temperature difference but a small discharge.

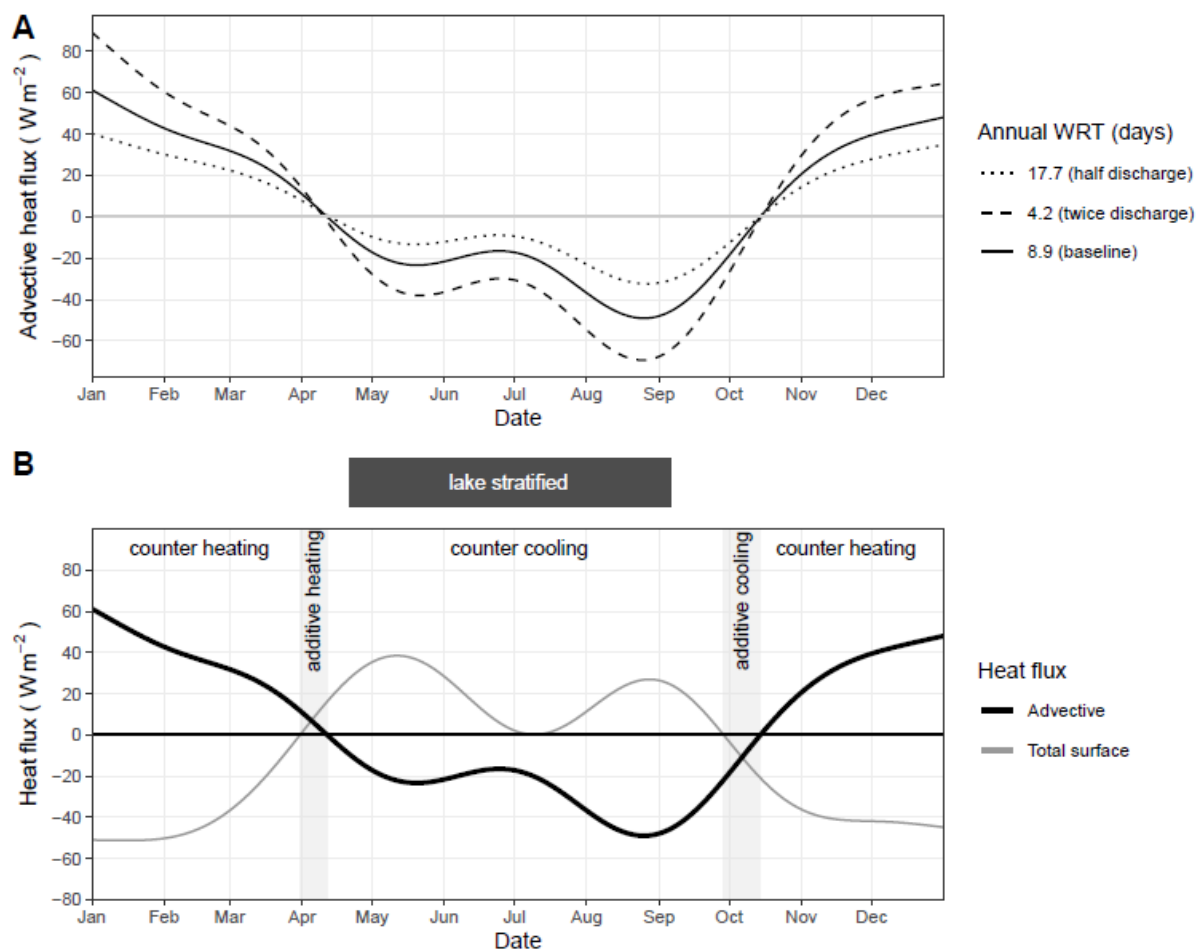


Figure 5.4 A) General Additive Model fit to three-day average values comparing the advective heat flux (Q_{adv}) for 2018 at different annual water residence times and B) a General Additive Model fit to three-day average values of the baseline advective flux (Q_{adv}) and the total lake surface heat flux (Q_{surf_tot}), including labels of the impact of the advective flux on the total lake surface heat flux. The duration of the longest continuous stratified period under unmodified conditions is also shown.

5.4.2 Contribution of the inflow heat flux to the overall heat budget

Q_{adv} and Q_{surf_tot} showed differing seasonal dynamics (Figure 5.4b). Therefore, at different times of the year the contribution of Q_{adv} to the overall heat budget of the lake differed. The seasonal patterns for the two heat fluxes generally showed an opposite pattern (Figure 5.4b).

On average, Q_{surf_tot} acted to cool the lake in the winter and warm the lake in the summer, in contrast to the Q_{adv} dynamics. Q_{surf_tot} and Q_{adv} switched between warming or cooling around the same time, during the early spring and autumn (Figure 5.4b). During this transition from warming to cooling and vice versa, both the advective and lake surface heat fluxes both became small.

5.4.3 Changes to temperature dynamics

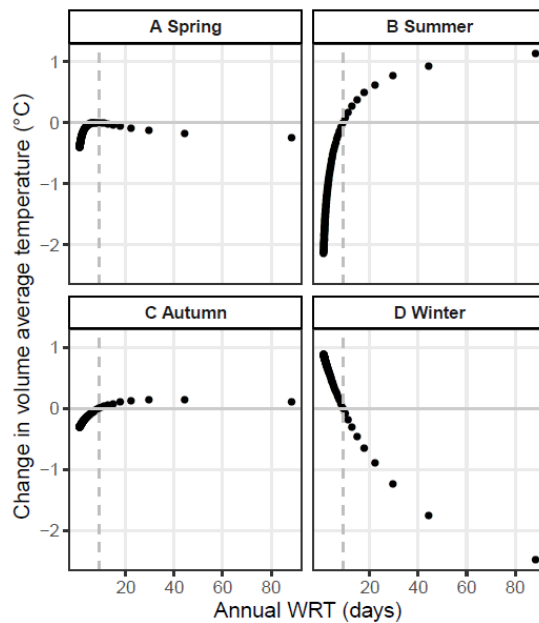


Figure 5.5 Change in volume averaged lake temperature across different seasons. Dotted lines represent unchanged AWRT.

AWRT-driven changes to Q_{adv} modified temperature dynamics and the thermal structure within the lake. An average water column temperature, accounting for layer volume, was calculated along with surface water temperature. Both lake volume-average and surface temperatures changed with AWRT, but the direction of the change was seasonal (Figure 5.5 and Figure S 5.7.4-1). In the summer, shortening AWRTs caused decreases in water temperatures. However, in the winter, shorter AWRTs slightly increase water temperatures. Conversely, longer AWRTs caused warming in the summer and cooling in the winter. The largest

temperature changes were seen in the summer, when AWRT is < 1 day, resulting in a > 2 °C decrease in average water column temperature in June and August (Figure S 5.7.4-1). The largest increase is only around 1 °C, in January, at shorter AWRTs. The effect diminishes with lengthening residence time, especially in the summer (Figure 5.5).

5.4.4 Changes to stratification

AWRT was positively related to the length of the summer stratified period. Shortening AWRTs caused a decrease in the length of summer stratification, with longer continuously stratified periods at longer AWRTs (Figure 5.6a). The shortening of summer stratification at shorter AWRTs was driven by later spring onset (up to 16 days later) and an earlier autumn overturn

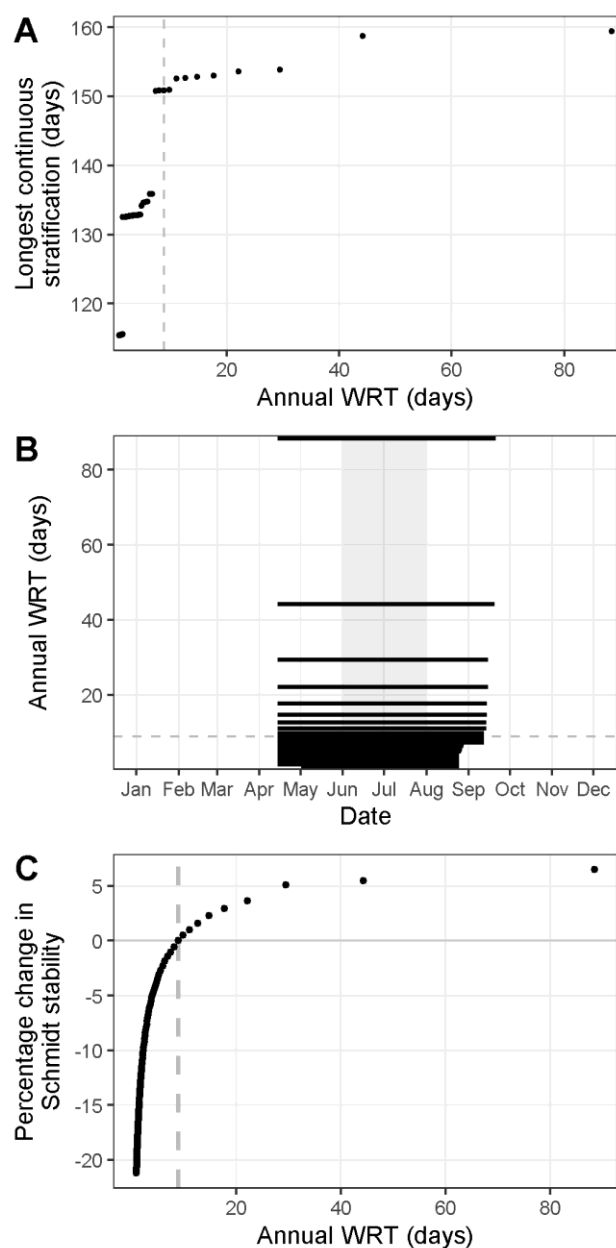


Figure 5.6 A) Change to the length of the longest continuous stratified period. B) Dates of onset and overturn at different AWRT. The solid black lines indicate the period of continuous stratification. The grey shading covers June and July, which are stratified under all AWRTs tested. C) Percentage change to stratification strength (as Schmidt stability) during June and July. Dotted lines represent unchanged AWRT.

(up to 19 days earlier) (Figure 5.6b). However, the main change was in the timing of overturn, except at the two shortest AWRTs. There was no change in stratification onset when AWRT was increased above unchanged values.

The changes in AWRT also modified the strength of the stratification. June and July remain stratified in all AWRT scenarios, so we used these months to look at changes to stratification strength that are not affected by changes to stratification length. Lengthening the AWRT resulted in increased water column stability during June and July, by around 8% (Figure 5.6c). Conversely, when the AWRT was shortened, there was up to a 20% decrease in water column stability (Figure 5.6c). Despite the decrease in stability at shorter AWRTs, there was no AWRT scenario that completely inhibited stratification forming during the summer months, with June and July being consistently stratified across all AWRTs. The mixed depth in June and July was unchanged by variations in discharge, remaining around 1.5 m for all scenarios.

Changes to the AWRT also have an effect outside the summer stratified period. At longer AWRTs, there was an increase in the frequency of winter inverse stratification, with no inverse stratification occurring below an AWRT of 14 days (Figure 5.7a). Overall, at shorter AWRTs, there was an increase in the frequency of normal stratification throughout the year (Figure 5.7b), despite a decrease in longest period of continuous stratification (Figure 5.6a). This is

driven by increases in transient stratification throughout the autumn and winter that exceeded the reduction in stratified days in the summer.

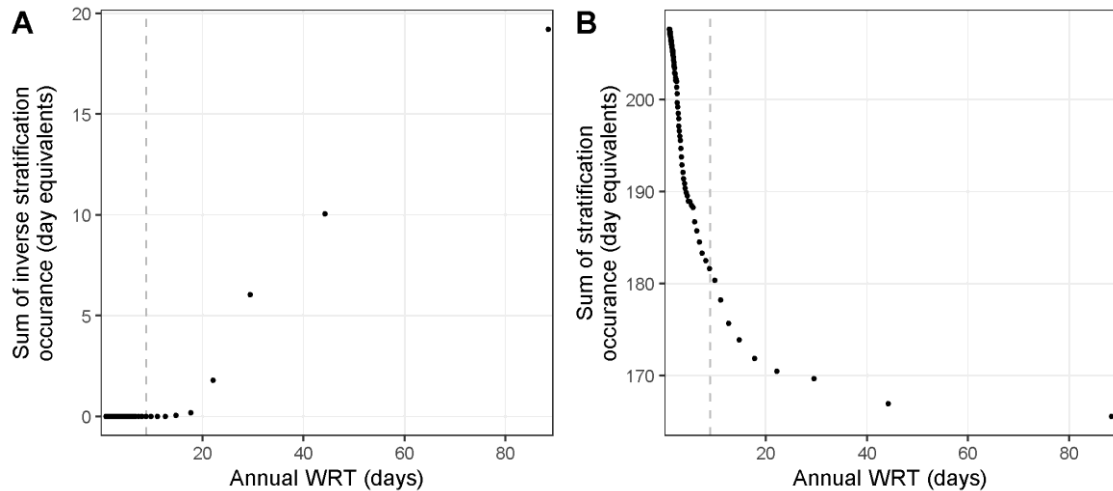


Figure 5.7 A) Occurrence of inverse stratification, converted into days, at each AWRT; B) total occurrence of normal stratification, converted to days. Dashed lines indicate the unmodified AWRT.

5.5 Discussion

The aim of this study was to establish how manipulations of WRTs affect the summer stratified period, with a view to controlling internal nutrient loading, which can be problematic for lake recovery. Understanding the effects of WRT changes on thermal dynamics will inform how management may be able to utilise manipulations of WRT to reduce internal loading. We also wanted to understand WRT effects on the year-round thermal dynamics of a lake.

Our results show that the heat flux exerted by the throughflow affects the lake water temperature and has a different effect depending on the season, causing warming in the winter and cooling in the summer. Furthermore, the AWRT determined the magnitude of Q_{adv} , either warming or cooling, magnifying the natural seasonality at shorter WRTs (M. R. Andersen et al., 2020; Smits et al., 2020). This supports hypothesis 1 that increasing discharge increases the summer cooling effect, reducing in-lake summer temperatures. Other studies have also shown the seasonality of advective heat fluxes (Carmack, 1979; Fink et al., 2014a), generally finding an overall cooling effect of throughflows with the exception of warming in the early spring (Carmack, 1979; Carmack et al., 1979; Fenocchi et al., 2018). Seasonal- and climatological-specific relationships between lake and inflow temperature are important to determine the seasonality of Q_{adv} (Fenocchi et al., 2018; Laval et al., 2012). For example, in higher altitude/latitude settings, a much larger cooling flux is likely in the early spring from snowmelt entering the lake (Flaim et al., 2019; Smits et al., 2020), compared to this temperate

system. As well as the direction of Q_{adv} , the magnitude was also seasonal, generally being larger in the winter than the summer. Coupled with reduced surface fluxes in winter, Q_{adv} has a larger effect on the overall heat budget in winter than during the summer when surface heating is large and Q_{adv} smaller due to lower inflow discharge (Table 5.3).

At shorter AWRTs, increased advective cooling shortened and weakened the period of continuous summer stratification, results supporting previous modelling (Li et al., 2018; Straškraba and Hocking, 2002) and the second hypothesis outlined. Our results show the changes to AWRT had the most effect on the overturn of stratification. Overturn was earlier with shorter AWRTs, with changes to stratification onset only occurring at the shortest AWRTs. Earlier overturn has been identified previously when WRT is shorter (Huang et al., 2014; Li et al., 2018; Wang et al., 2012) and supports previous work also suggesting that changes to stratification length are more pronounced by expediting overturn than preventing onset (Li et al., 2018). Controlling WRT at the end of the stratified period, when the inflow is cooling faster than the lake (Laval et al., 2012), increases the effect of advective cooling on weakening stratification, resulting in the potential for an earlier overturn and shorter stratified period. Although shortening stratification, which is the aim of the management, there is a risk that earlier overturn may bring internally loaded nutrients into the photic zone (Radbourne et al., 2019) in larger quantities and earlier in the growing season (Kalff, 2002), promoting algal growth. This may be detrimental for water quality in the short term but, if the biomass is flushed out quickly, could improve water quality in the longer term by increasing nutrient export from the system (Radbourne et al., 2019).

However, no scenario of shorter AWRT completely inhibited stratification and mixed depth remained unchanged. Mixed depth did not show deepening as expected, remaining at 1.5 m for all scenarios, and perhaps demonstrates the importance of atmospheric forcing (wind speed and solar radiation) in determining mixed depth (Straškraba and Hocking, 2002). Consequently, deepening of the mixed depth is more likely to occur during storms where increased flow is coupled with higher wind speeds and reductions in solar radiation (M. R. Andersen et al., 2020; Woolway et al., 2018).

Shortening AWRT to weaken stratification, although not inhibiting, may still be useful for management as it makes the lake more likely to undergo a mixing event from a storm, for example, replenishing deep water oxygen levels that become depleted during stratification (Huang et al., 2014). A storm is more likely to cause complete mixing if a lake is less strongly stratified before the event (Stockwell et al., 2020). Oxygen depletion has also been found to

be lower under weaker stratification (Foley et al., 2012), maintaining oxic conditions longer despite continued stratification, which would reduce the potential for the accumulation of nutrients in the hypolimnion.

As well as the summer effects, our results have shown that the seasonality of responses to changes in AWRT will cause year-round effects in lake systems. Shortening AWRTs acts to increase warming in the winter, promoting transient periods of stratification and warmer water temperatures. There has been little previous research on AWRT changes effecting winter water temperatures, although there is evidence for inflow warming of lakes during the winter months (Colomer et al., 1996). Increased warming may be detrimental to water quality during the winter, encouraging winter algal growth (Weyhenmeyer, 2001). Winter lake warming may also advance onset of stratification and spring blooms the following year (Rodgers, 1987; Yang et al., 2016) and modify the phytoplankton assemblage of spring bloom (Yang et al., 2016).

5.5.1 Applicability to other sites

The residence time of Elterwater-IB is very short (annual WRT approximately 9 days). Recent modelling, however, revealed that, even at an annual WRT of 100 days, simulations of lake temperatures that ignored inflow and outflow effects exhibited statistically significant deviations from observations, emphasising the importance of inflow-outflow dynamics at WRTs of this magnitude (Almeida et al., 2022). Lakes with an annual WRT of ≤ 100 days account for 1 in 4 lakes worldwide (Messenger et al., 2016) and therefore the results within this study would be applicable for a large number of lakes. Furthermore, small lakes, like Elterwater-IB (surface area = 0.03 km², are likely to be most impacted by WRT changes as the advective heat flux scales with discharge and inversely with lake size (Schmidt and Read, 2021). Small lakes represent the majority of lake globally (Downing et al., 2006; Messenger et al., 2016; Verpoorter et al., 2014). Verpoorter et al. (2014) estimated that lakes with a surface area of 0.002 – 0.01 km² make up 77% of lakes globally (90 million). Besides these small, short residence time systems, larger longer residence time lakes have also shown the importance of inflows on lake thermal dynamics. For example, Lake Iseo, Italy, has a WRT of 4.3 years and modelling showed that epilimnetic temperature was 3 °C warmer when inflow cooling effects were not included (Valerio et al., 2015).

5.5.2 Future management

Modifying WRT on an annual scale did not change the summer WRT sufficiently to overcome summer stratification. By considering the year-round effects and the seasonality of both the

direction and magnitude of Q_{adv} and Q_{surf_tot} , and water column stability a more appropriate management strategy is considered. Specifically, targeting the period around overturn may be more conducive to manipulation as a means of shortening the stratified period and implementing different management approaches at other times of year.

The inflow-lake temperature difference controls when Q_{adv} switches from winter warming to summer cooling in the spring. The timing of this switch from a heating flux in the winter to a cooling flux in the summer, relative to the lake surface heat fluxes and water column stability, will determine when WRT interventions might be most useful (hypothesis 3). Based on the smoothed dynamics of the advective and surface heat fluxes and water column stability, we have identified four periods within the annual cycle for which different management strategies will be appropriate, in the context of this temperate system (Figure 5.8).

1. *Spring and early summer, prior to stratification*

Both the advective and lake surface fluxes are warming. Therefore, decreases in WRT at this time of year would have the effect of bringing forward stratification onset, rather than delaying it.

2. *Peak summer*

Stratification is at its strongest. At these times, temperature differences between the lake and inflow are such that the throughflows acts to cool the lake. However, at these times discharge is low, so shortening WRT will only be able to weaken stratification.

3. *Run-up to overturn*

The inflow-lake temperature differences and inflow discharge are sufficient that changes in WRT will be able to expedite overturn. Q_{surf_tot} is positive but small, and stability decreasing, therefore increased Q_{adv} cooling, at shorter WRTs, promotes overturn of stratification.

4. *Post overturn and winter*

Q_{adv} is a warming flux and no artificial decreases in WRT are recommended, to prevent increased warming and transient stratification impacts.

This finer-scale approach to management of seasonal WRTs may be more appropriate than a coarser scale change to AWRT.

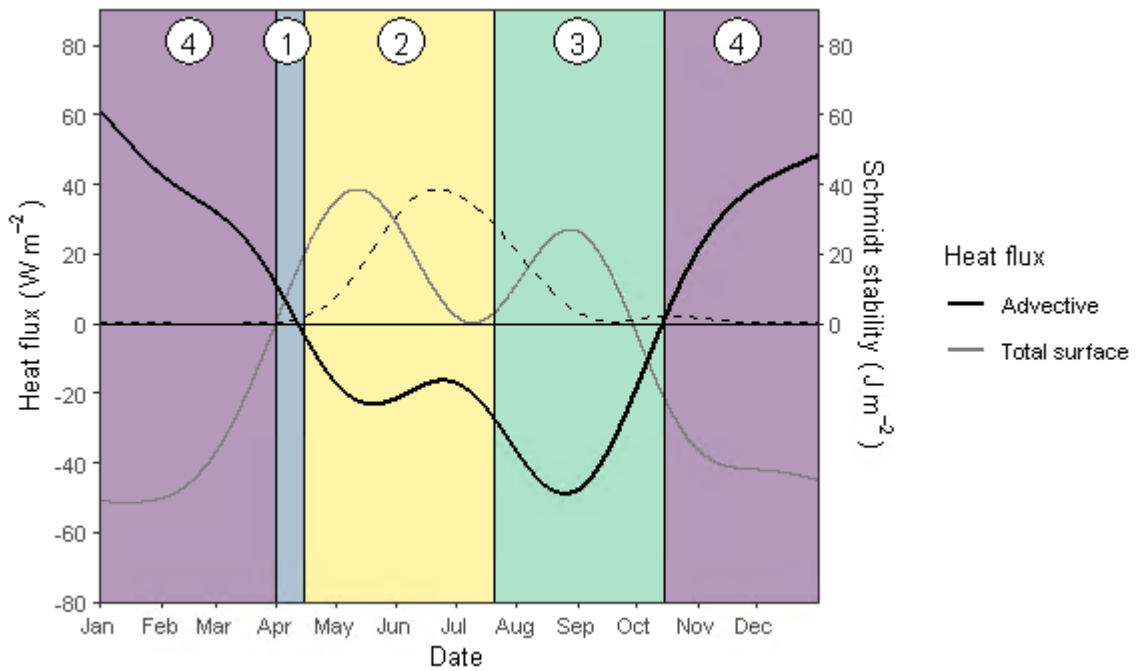


Figure 5.8 Conceptualisation of the timings of different management strategies proposed for Elterwater. Labelled numbers relate to the periods discussed in the text. Dashed line shows a smooth of the Schmidt stability under unmodified conditions.

1. Prior to stratification (both the stream and lake surface fluxes are warming): no change in WRT recommended; 2. Peak summer (stratification is at its strongest): decreases in WRT will only weaken stratification; 3. Run-up to overturn (Q_{surf_tot} is positive but small, Q_{adv} cooling): changes in WRT will expedite overturn; 4. Post-overturn and winter (Q_{adv} is warming): no artificial increases in discharge, prevent increased warming.

5.6 Conclusions

Our results demonstrate the seasonality of responses to changes in AWRT. No AWRT scenario inhibited stratification completely, suggesting that finer scale management may be needed if WRT manipulations are to be used to control internal loading via stratification inhibition. Greater understanding of warming and cooling effects of throughflows and their contribution to a lake's heat budget throughout the year will help to target periods when the manipulation of WRT will be most effective in specific systems. Modelling, as we have done here, is useful pre-intervention to understand the effects of management strategies before costly engineering work is carried out and should consider lake-specific heat flux and stability dynamics.

5.7 Supplementary information for Chapter 5

5.7.1 Elterwater trophic status

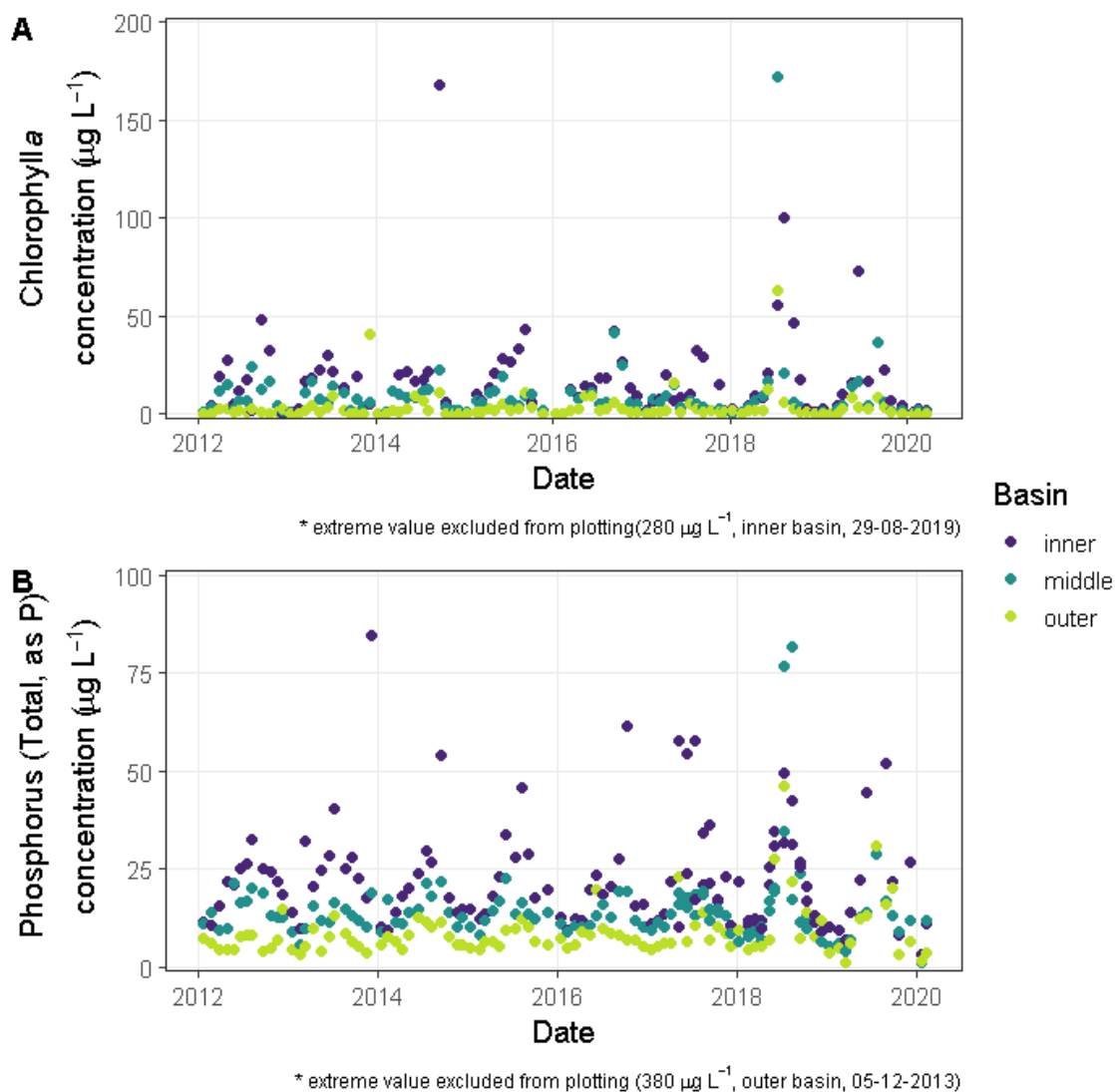


Figure S 5.7.1-1 A) Chlorophyll a and B) total phosphorus concentrations in Elterwater's inner, middle and outer basins.

5.7.2 Protocol for processing Blelham meteorological data

5.7.2.1 Gap filling protocol for meteorological data (2012-2019)

- Gaps of less than 24 hours were filled using linear interpolation, for solar radiation maximum gap was 6 hours
- Where gaps remained a linear model was fitted between Blelham and Windermere buoy meteorological data, using data from 2012-2019.

Table S 5.7.2-1 Percentage (%) missing in the 2018-2019 meteorological data and the linear regression between Blelham and Windermere buoy data variables (2012-2019).

Variable	% missing before	% missing after	Intercept	Slope	p	Adjusted r-squared
Air temperature	10.2	0	-0.978	1.056	< 0.001	0.957
Wind speed	10.2	0	0.090	0.548	< 0.001	0.572
Solar radiation	4.8	0	3.913	0.931	< 0.001	0.895
Relative humidity	3.7	0	-1.809	1.024	< 0.001	0.863

5.7.2.2 Solar radiation and cloud cover calculations

R packages `suncalc` (Thieurmel & Elmarhraoui, 2019) and `insol` (Corripio, 2019)

1. Night-time values (between sunset and sunrise) were set to 0
2. Clear sky solar radiation, dependent on the time of day and the day of the year, was calculated
3. Observed solar radiation and clear sky solar radiation were compared to estimate the cloud cover (between 0 and 1):

$$cloud\ cover = 1 - \frac{observed}{maximum\ possible}$$

4. Mean cloud cover for the previous day was estimated as the night-time cloud cover

Thieurmel, B. & Elmarhraoui, A. (2019). `suncalc`: Compute Sun Position, Sunlight Phases, Moon Position and Lunar Phase. R package version 0.5.0. <https://CRAN.R-project.org/package=suncalc>

Corripio, J. G. (2019). `insol`: Solar Radiation. R package version 1.2.1. <https://CRAN.R-project.org/package=insol>

5.7.3 Thresholds for defining stratification

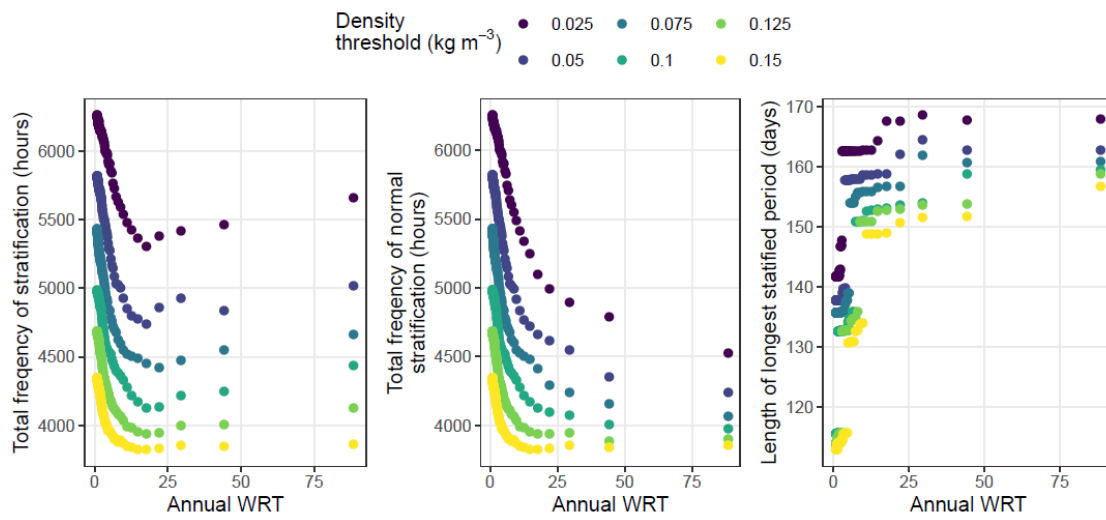


Figure S 5.7.3-1 Testing the density difference threshold for defining stratification on the pattern of changes in stratification metrics with AWRT.

5.7.4 Change to seasonal surface water temperature

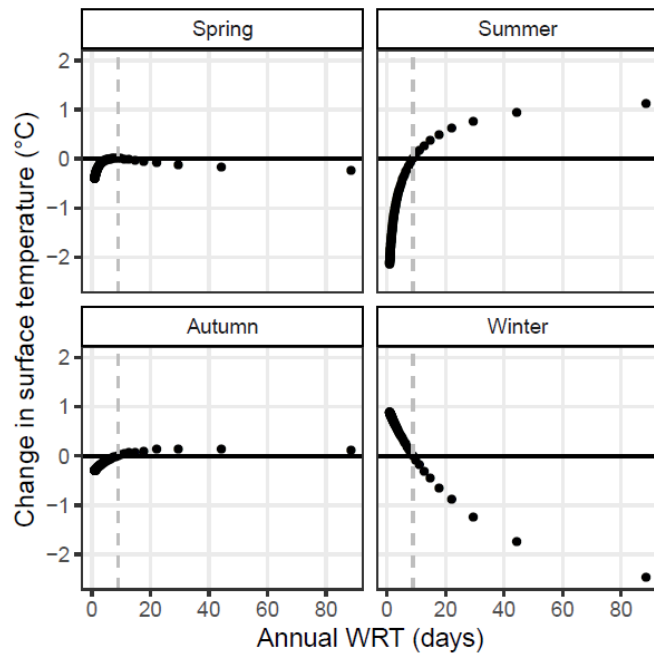


Figure S 5.7.4-1 Change in lake surface temperature for each season

5.7.5 Changes to stratification and water temperatures on a monthly scale

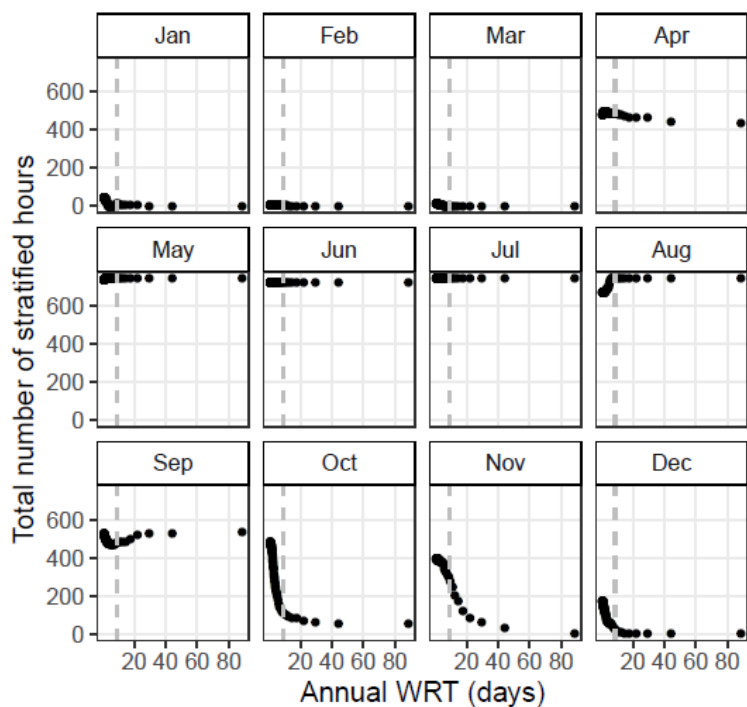


Figure S 5.7.5-1 Total frequency of normal stratification, per month, for each AWRT tested in Elterwater.

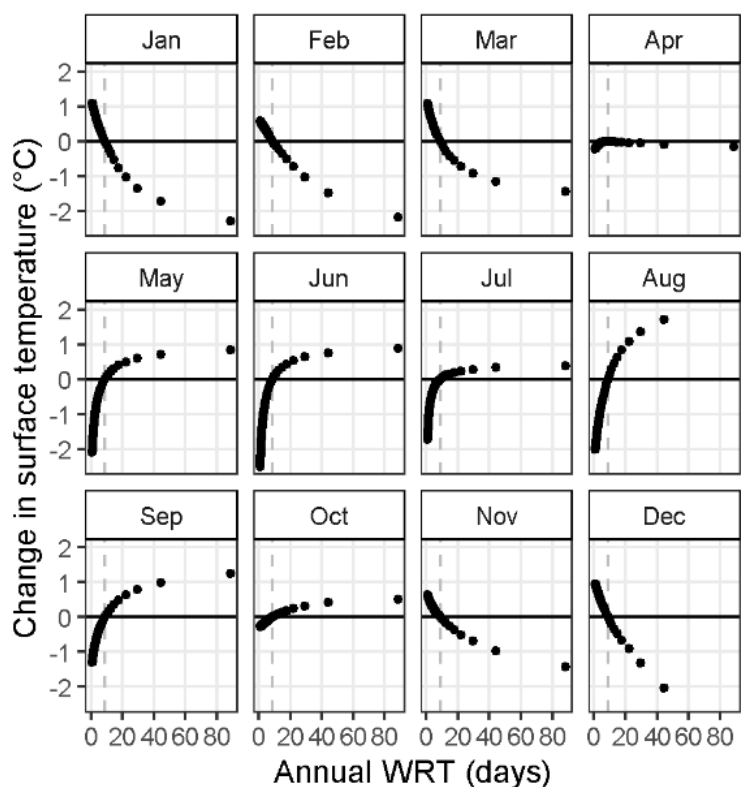


Figure S 5.7.5-2 Change in surface temperature in each month.

Chapter 6 Hypolimnetic reoxygenation during seasonal anoxia is related to inflow events in a small temperate lake

(**Freya Olsson**, Eleanor B. Mackay, Phil Barker, Sian Davies, Ruth Hall, Bryan Spears, Ian D. Jones (2021). In preparation for submission to *Freshwater Biology*)

6.1 Abstract

Hypolimnetic oxygen concentration is a key lake water quality indicator and complete depletion of oxygen, *anoxia*, affects biogeochemical cycling of nutrients and habitat availability for aerobic organisms. During the stratified period, the formation of a thermocline restricts the resupply of oxygen from the lake surface to replace that which is consumed through depleting processes. In stratifying lakes, the length and strength of the stratified period are often cited as key drivers of hypolimnetic anoxia, with changes to oxygen depletion related to long-term changes in stratification duration. However, there is little understanding of oxygen dynamics on a sub-seasonal scale, or the role of inflows in oxygen replenishment events in deep waters. Here, high-frequency data from a small stratifying lake are used to understand the sub-seasonal dynamics of deep-water oxygen during the stratified season and understand how high discharge inflow events can influence deep-water oxygen concentrations during the stratified period. Our results have shown that inflows can act as an important source of oxygen to the deep waters of a small temperate lake. High inflow events were associated with reduced water column stability and increased vertical mixing of oxygen from the surface, while inflows could also be contributing oxygen into the metalimnion through direct intrusion of oxygenated influent water. Increasing use of high-frequency oxygen data provides greater opportunities to understand the physical processes that drive reoxygenation, which has implications for understanding a lake's oxygen budget, biogeochemical cycling of nutrients, and improving the modelling of oxygen dynamics in lakes.

6.2 Introduction

Hypolimnetic oxygen concentration during the stratified period is a key lake water quality indicator. Low oxygen concentrations ($< 2 \text{ mg O}_2 \text{ L}^{-1}$, *hypoxia*) or complete deficiency ($< 1 \text{ mg O}_2 \text{ L}^{-1}$, *anoxia*) during large periods of the year, due to increased metabolism of organic matter (Bouffard et al., 2013; Cooke et al., 2005), can be indicative of eutrophication. Anoxia in the hypolimnion is of environmental importance as it limits habitat availability for aerobic organisms such as macroinvertebrates and fish (Alabaster and Lloyd, 1982; Kalff, 2002) and causes reducing redox conditions under which nutrients, such as phosphorus, as well as toxic

metals, are released from the sediment into the water column (Mortimer, 1942; Nürnberg, 1984).

Oxygen concentrations in deep-waters are determined by a complex interaction of production and consumption processes, including sediment and water column (areal and volumetric) oxygen demands, diffusion and turbulent mixing of oxygen from the air-water interface, as well as primary production (Bouffard et al., 2013; Cornett and Rigler, 1987; Müller et al., 2012). These processes vary seasonally due to changes in productivity, in response to external drivers such as the loading of organic matter and nutrients from the catchments (de Eyto et al., 2016; Marcé et al., 2008), and due to changes in the lake's thermal structure (Hanson et al., 2006).

In seasonally stratifying lakes, water temperatures and water column stratification are particularly important in determining deep-water dissolved oxygen (DO) concentrations (Crossman et al., 2018; Jane et al., 2021) due to the physical isolation of the bottom water layer during the stratified period. Stable stratification and the formation of a thermocline restricts the resupply of oxygen from the lake surface to replace that which is consumed by water column respiration, the mineralization of organic matter, and the release of reduced substances from anoxic sediment (Bouffard et al., 2013; Müller et al., 2012), causing oxygen depletion and hypolimnetic anoxia, in sufficiently productive lakes (Foley et al., 2012; Jane et al., 2021; North et al., 2014). Long-term changes to the length and strength of the stratified period have been associated with changes in hypolimnetic oxygen concentrations and depletion rates in lakes (Foley et al., 2012; Jane et al., 2021; Marcé et al., 2010). Long-term records show that as the climate warms, the length and the strength of the stratified period during summer is increasing (e.g. Woolway *et al.*, 2020; O'Reilly *et al.*, 2015), leading to a greater duration and spatial extent of seasonal anoxia (Foley et al., 2012; Jane et al., 2021; North et al., 2014; Smucker et al., 2021). Modelling predicts further increases in seasonal anoxia duration and extent as the climate warming continues (Ladwig et al., 2021; Schwefel et al., 2016; Snortheim et al., 2017).

There is growing evidence, from high-frequency data, that the relationship between physical lake processes, stratification and water column stability, and oxygen dynamics also operates over shorter timescales. High-frequency oxygen measurements have previously been used primarily to investigate surface oxygen concentrations relating to estimates of lake metabolism (e.g. Staehr et al., 2010; Fernández Castro et al., 2021). Evidence of hypolimnetic changes are less well studied, with previous work focussing on DO depletion during short-term or diurnal stratification in polymictic lakes (Martinsen et al., 2019; Wilhelm and Adrian, 2008),

the impact of storm events on oxygen concentrations through heat loss induced convective mixing (Kimura et al., 2014; Liu et al., 2020), and processes under ice (Obertegger et al., 2017; Smits et al., 2021). Short-term oxygen dynamics have implications for our understanding of lake processes but little is known about short-term dynamics and physical controls on hypolimnetic oxygen concentrations in seasonally stratifying lakes. This is despite the fact that these dynamics are likely to have implications for biogeochemical cycling and habitat availability in lakes.

Changes to water column stability modify vertical mixing energy; under higher stability, the rates of vertical mixing, crucial for determining hypolimnetic oxygen concentrations, are reduced (Heinz et al., 1990). Wind and surface heat flux are the two primarily cited sources of vertical mixing energy in lakes (Imberger, 2013; Saber et al., 2018) but inflows into lakes also have the potential to affect vertical mixing, thus impacting deep-water oxygen concentration. Inflows act as an advective heat flux (Livingstone and Imboden, 1989; Schmid and Read, 2021), modifying the heat content of the lake by bringing in water of different temperature than is exported by outflows (Fenocchi et al., 2017; Livingstone and Imboden, 1989). In summer, this heat flux can induce cooling (Carmack et al., 1979; Richards et al., 2012), which promotes convective mixing and reductions in water column stability (Kimura et al., 2014; Liu et al., 2020), potentially moving oxygenated surface water to the hypolimnion (Brand et al., 2008; MacIntyre et al., 2002). Furthermore, rivers and streams are often highly oxygenated (Neal et al., 2002; Williams and Boorman, 2012), bringing in oxygen directly to the lake, either to the surface or within the water column depending on inflow and lake water densities (Fink et al., 2016; MacIntyre et al., 2006; Rueda and MacIntyre, 2009).

These processes have primarily been considered in deep lakes and reservoirs with cold plunging inflows (Fink et al., 2016; Liu et al., 2020; Marcé et al., 2010) and under ice when the whole water column is isolated from atmospheric oxygen inputs (Palmer et al., 2021). In smaller, shallower, temperate systems the contribution of inflows to short-term deep-water oxygen dynamics has not been well quantified, and has often been disregarded in modelling studies (e.g. Ladwig *et al.*, 2021; Cortés *et al.*, 2021; Darko *et al.*, 2019). Inflow effects could be important in these systems by destabilising stratification and enhancing downward vertical mixing of oxygen or as a direct intrusion of oxygenated inflow below the thermocline.

Here, high-frequency oxygen, inflow discharge, and temperature data from a small stratifying lake in the English Lake District, UK, are used to understand the sub-seasonal dynamics of deep-water oxygen during the stratified season in a small, temperate lake. The overall aim is

to elucidate how high discharge inflow events can influence deep-water oxygen concentrations during the stratified period by,

- 1) examining how oxygen replenishment during the summer stratified period is related to inflow discharge and other potential drivers of replenishment (wind power and surface cooling),
- 2) considering how these drivers, especially inflow discharge, relate to in-lake stability and vertical mixing of oxygen,
- 3) and discussing the importance of inflows to the reoxygenation of deep-water in small, stratifying lakes given future climate change and the potential use in lake management.

6.3 Methods

6.3.1 Site description

Elterwater is a small eutrophic lake situated in the English Lake District, UK. The lake is formed of three basins, inner, middle, and outer, which are connected by narrow channels (Figure 6.1). The main inflow, the Great Langdale Beck (GLB), flows into the middle and outer basin, and the outflow, the River Brathay, flows out of the outer basin. The inner and middle basins are fed by small tributaries in addition to a pipeline, which diverts a portion of the GLB flow into the inner basin (Figure 6.1). Water residence times vary significantly between the basins, from an annual average of around 15-20 days in the inner and middle basins to as little as 0.5 days in the outer basin (APEM, 2012; Beattie et al., 1996). The inner basin, the focus of this study, is the smallest of the three basins and is relatively shallow (maximum depth = 6.5 m, mean depth = 3.3 m, volume = 101,022 m³) and is monomictic.

During the stratified period, typically April to October, the sinks of oxygen in the isolated hypolimnion outweigh sources, resulting in depletion of oxygen and anoxic conditions developing in the hypolimnion. Oxygen concentrations at depth quickly deplete following the onset of stratification in the early spring. Weekly monitoring of the full water column shows anoxia reaches depths as shallow as 4 m in the summer period and prevails in some parts of the lake until stratification overturn in autumn (Olsson et al., 2022; Chapter 4). Evidence of internal loading, due to reducing redox conditions, shows that the internal sources of phosphorus contribute considerably to the nutrient budget of the basin (Olsson et al., 2022; Chapter 4), with nutrient concentrations in the bed sediments exceeding 4500 µg total phosphorus g⁻¹ (Mackay et al., 2020).

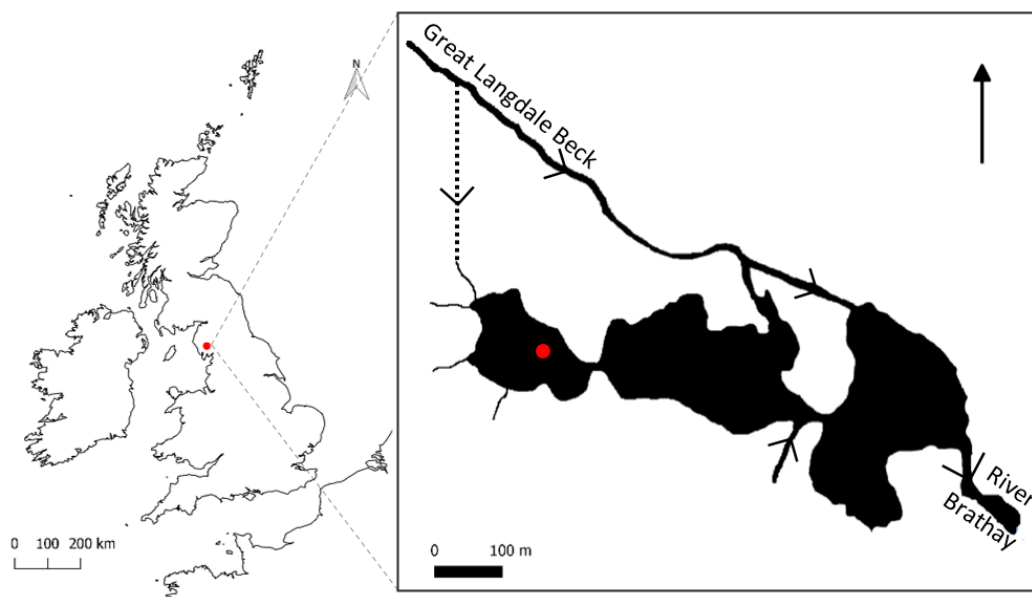


Figure 6.1 Study site – Elterwater inner basin in the northwest of England, UK, with the location of the monitoring buoy indicated by the red circle. The dashed line shows the approximate location of the pipeline installed in 2016 to divert part of the main inflow into the inner basin from the Great Langdale Beck into the inner basin.

6.3.2 Data collection

6.3.2.1 Dissolved oxygen

Dissolved oxygen measurements were taken at the deepest point of the inner basin (Figure 6.1), using PME miniDOT sensors (Precision Measurement Engineering, Vista, California, USA), accurate to 0.3 mg L^{-1} and fitted with wipers to prevent biofouling. Sensors were placed at 3 m and 5 m depths and recorded dissolved oxygen concentrations at 15 minutely intervals from May 2018 to December 2019. Quality checks of the data were carried out and potentially erroneous measurements removed based on visual inspection of plots, rates of change, and maximum and minimum possible values. Gaps in the data due to sensor maintenance or sensor errors, accounted for $<1 \%$ of the data. Daily average concentrations were taken for each depth measurement. Weekly measurements with higher vertical resolution were taken at the deepest point of the lake, every 1 m within the water column using a Yellow Springs Instruments-Exo2 multi-parameter sonde (Xylem, OH, USA). Oxygen sensors were calibrated monthly according to the manufacturer's specifications. In the absence of dissolved oxygen measurement of the inflow, the concentration was assumed to be at 100% saturation (Neal et al., 2002; Williams and Boorman, 2012) and oxygen concentration estimated based on water temperature using the R package Lake Metabolizer (Winslow et al., 2016).

6.3.2.2 Water temperatures profiles

Water temperature profiles were taken at 4-minutely intervals at the deepest point of the inner basin at 0.5, 1, 2, 3, 4, 5, and 6 m below the surface. Measurements were taken using RBRsolo temperature sensors (RBR, Ottawa, Canada), accurate to ± 0.002 °C. Daily average temperatures were calculated at each depth.

6.3.2.3 River flow and temperature

The main inflows into the inner basin are from ungauged tributaries and the pipeline, constructed in 2016 as a restoration measure, which diverts some flow from the Great Langdale Beck into the inner basin. Flow from the ungauged tributaries has been estimated as 2% of the lake outflow measured at Jeffy Knotts gauging station on the River Brathay (Environment Agency, 2000). Hourly data of the River Brathay flow was obtained from the Environment Agency for England. Values for missing or unreliable data (<1 % data) were obtained by linearly interpolating over small gaps (<3 hours) or estimated based on a relationship with the adjacent River Rothay gauged data. Additional discharge from the pipeline was obtained from the South Cumbrian Rivers Trust, with missing values (2 %) interpolated (<24 hours) or estimated based on the relationship with the other inflows (see Section 6.7.1.2). The combined flow from the ungauged tributaries and the pipeline was used as the total flow into the basin and outflow was assumed to equal total inflow. Daily average discharge were used in analysis.

15-minutely inflow temperature was obtained from the South Cumbrian Rivers Trust, measured at the pipeline off-take using a HOBO U20L-01 data logger (Onset, Bourne, MA, USA), accurate to ± 0.44 °C, and averaged to get daily inflow temperature. Using in-lake water temperature profiles, the depth of neutral buoyancy was calculated for the inflowing water as the depth at which inflow temperature and lake water temperature were the same, giving an estimate of intrusion depth (Imberger, 1985; Imberger and Patterson, 1989).

6.3.2.4 Meteorology and heat fluxes

Hourly average meteorological data were obtained from the automatic water quality monitoring (AWQM) buoy on Blelham Tarn, 5 km to the southeast of Elterwater. Blelham Tarn is in close proximity to Elterwater and is of similar size and elevation. Meteorological data from Blelham Tarn are therefore assumed to provide a good estimate for the meteorological conditions experienced over Elterwater. Observations of air temperature (°C), relative humidity (%), wind speed (m s^{-1}), and incoming short-wave radiation (W m^{-2}) were collected at 15-minute intervals at the buoy, and hourly averaged. Where gaps were present in the data due to sensor error or maintenance, smaller gaps (< 24 hours or 6 hours for short-wave

radiation), were filled by linear interpolation or estimated based on relationships between Blelham Tarn buoy data and data collected at two other local lake-buoy meteorological stations (Section 6.7.2). Daily averaged meteorological data were used in analysis.

Lake surface heat fluxes were calculated using Lake Heat Flux Analyzer (LHFA; Woolway *et al.*, 2015), a MATLAB code package that calculates surface energy fluxes in lakes, using the observed meteorological and lake surface temperature data. The total surface heat flux (Q_{tot}) was calculated as the sum of the calculated surface heat fluxes ($W\ m^{-2}$):

$$Q_{tot} = Q_{sin} + Q_{lin} + Q_{sr} + Q_e + Q_h + Q_{lout} ,$$

the incoming short-wave radiation (Q_{sin}), reflected short-wave radiation (Q_{sr}), the sensible (Q_h) and latent (Q_e) heat fluxes, the incoming long-wave (Q_{lin}) and the outgoing long-wave radiation (Q_{lout}).

Wind power, a measure of the physical wind forcing over the lake ($W\ m^{-2}$), was calculated from Wüest *et al.*, (2000);

$$P_{10} = \rho_{air} C_{10} W_{10}^3 ,$$

where ρ_{air} is the density of air ($1.2\ kg\ m^{-3}$), C_{10} is the transfer coefficient of momentum at 10 m, and W_{10}^3 is the cube of the wind speed at 10 m, calculated from the buoy measurements taken at 2.5 m. C_{10} and W_{10}^3 were calculated using LHFA (Woolway *et al.*, 2015b), using daily meteorological and lake surface temperature data.

6.3.2.5 Light and chlorophyll a

Water samples were collected weekly at 0.5, 1, 2, 3, 4, 5, and 6 m at the deepest point of the lake. A measured volume of the water was filtered onto a Whatman GF/C filter paper and chlorophyll extracted using a cold acetone extraction and analysed via a spectrophotometer according to Talling (1974). A LI-COR underwater sensor was used to measure photosynthetically active radiation (PAR) at half-meter intervals from 0.5 to 6 m weekly, during the seasonal anoxic period.

6.3.3 Data analysis

6.3.3.1 Identifying events

To identify oxygen replenishment events during the stratified period the data were truncated. The “seasonal anoxic period” was defined as the period when the water at 5 m was not continuously oxygenated greater than $1\ mg\ L^{-1}$. This gave two summer periods, from 2018 and 2019, lasting 96 days and 133 days, respectively. DO replenishment events at 5 m (DO_{5_events}) were identified as days with the following criteria: an oxygen concentration greater than

1 mg L⁻¹ and a change in oxygen concentration from the previous day greater than 0.5 mg L⁻¹. During an extended oxygenation event, the overall timing was taken as the local maximum.

6.3.3.2 Vertical mixing and stability

Using daily water temperature profiles, the LakeAnalyzer R package (Read et al., 2011) was used to calculate water density profiles and Schmidt stability, following the method of Idso (1973). The vertical diffusivity (K_z) into the 5 m layer was estimated at 4.5 m by applying the gradient-flux method using measured daily water temperature profiles (Heinz et al., 1990) and basin bathymetry from Haworth *et al.* (2003). The method is applicable in the deep-water, below both the mixed layer and the photic depth, and uses the following equation:

$$K_{4.5} = \frac{\sum_{4.5}^{6.5} a \times V}{G \times A},$$

where $a = \frac{\partial T}{\partial t}$, the temporal change in the temperature of each 1 m box (4.5-5.5 m, 5.5-6.5 m), V is the volume of each 1 m box, $G = \frac{\Delta T_{4-5}}{\Delta z}$, the vertical temperature gradient from 4 to 5 m, and A is the area at 4.5 m.

The vertical diffusive flux of oxygen at 4.5 m was estimated based as the product of K_z , the oxygen concentration gradient between 4 m and 5 m, and the area of the lake at 4.5 m depth. Oxygen concentration was not measured at high frequency at 4 m. The 4 m concentration was therefore estimated by linear interpolation between the 3 and 5 m sensors. Lower frequency measurements (weekly) were taken using a sonde and compared to the daily-interpolated 4 m estimate to approximate the error in the 4 m estimation by this method. The estimation was reasonably good, with an error between the estimated and measured values of 0.815 ± 2.377 mg L⁻¹ (mean \pm standard deviation). The systematic bias (0.815 mg L⁻¹) was used to correct the estimate of daily DO at 4 m. The vertical flux of oxygen from the 4 m layer to the 5 m layer ($VF_{DO_{4.5}}$) was then calculated as:

$$VF_{DO_{4.5}} = K_{4.5} \times \frac{(DO_4 - DO_5)}{D_{4.5}} \times A_{4.5},$$

where DO is the dissolved oxygen concentration at 4 and 5 m, $A_{4.5}$ is the area at 4.5 m, $D_{4.5}$ is the height difference between layers (here 1 m) and $K_{4.5}$, the vertical diffusivity at 4.5 m.

6.3.3.3 Identifying potential drivers of DO_{5_events}

The potential drivers of DO_{5_events} were examined by, initially, visually comparing time series of potential drivers and in-lake conditions with the occurrence of the DO_{5_events}. A logistic regression model was used to look at the effect of potential drivers on the likelihood of a DO_{5_events} occurring. The deviance residuals were checked for autocorrelation, using a Durbin-

Watson test and visual inspection of autocorrelation lag plots (Section 6.7.3). Additionally, logistic regression requires linear relationships between the predictors and the logit of the outcome (see Section 6.7.3), and removal of highly correlated predictor variables (checked via correlation calculations – see below).

We also calculated the correlation between potential drivers of oxygenation events to ascertain whether drivers may be acting in combination or as a proxy for some larger event (e.g. storm). Due to the temporal autocorrelation present in the data (Section 6.7.4), the variables were differenced to remove this dependence. The data were also non-normally distributed and so the non-parametric Spearman's Rank correlation was calculated, which requires a monotonic relationship only.

Finally, high inflow discharge events (Q_{events}) were also identified, as days where discharge exceeded $0.1 \text{ m}^3 \text{ s}^{-1}$ and the timing as the local maximum in an extended high discharge event. We identified co-occurring DO and Q events based on the occurrence of both criteria in any 3-day window, allowing for the events to occur on the same day or on adjacent days.

6.4 Results

6.4.1 Oxygen replenishment “events”

The seasonal anoxic periods ran from 7th June 2018 to 10th September 2018 and 17th May 2019 to 26th September 2019, lasting 96 days and 133 days, respectively. Across the two seasonal anoxic periods, eighteen $\text{DO}_{5_}\text{events}$ were identified (Figure 6.2). The oxygen concentration during a single $\text{DO}_{5_}\text{event}$ reached a maximum concentration of 10.4 mg L^{-1} , and overall, during the $\text{DO}_{5_}\text{events}$ the mean concentration was 3.6 mg L^{-1} . Across both periods, there are no DO events during late-June and early July, but otherwise events take place throughout the period.

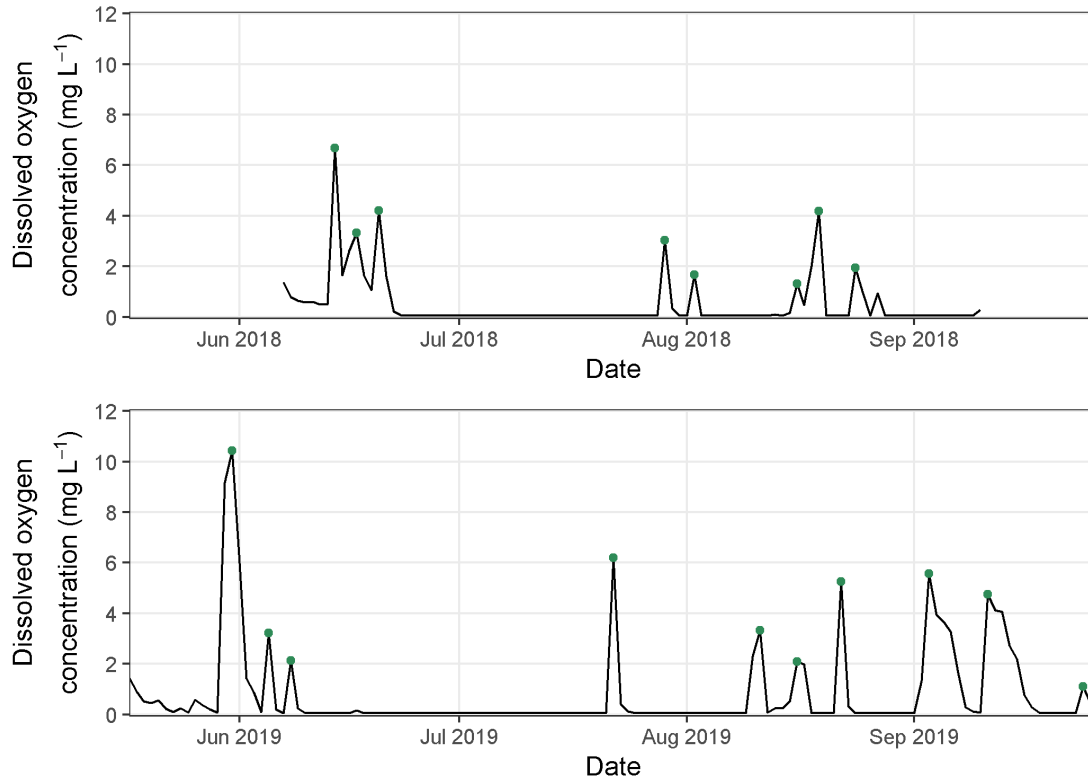


Figure 6.2 Identified dissolved oxygen replenishment events (green points) during the seasonal anoxic periods in 2018 and 2019 (DO no longer continuously $> 1 \text{ mg L}^{-1}$).

6.4.2 Potential drivers of re-oxygenation

Across the two periods, inflow discharge varies between a minimum of $0.003 \text{ m}^3 \text{ s}^{-1}$ and a maximum of $0.88 \text{ m}^3 \text{ s}^{-1}$. In both years, there are sustained periods of low flow in late-June and July. Generally, 2019 was wetter, with a mean discharge of $0.15 \text{ m}^3 \text{ s}^{-1}$ ($n = 133$) compared to $0.08 \text{ m}^3 \text{ s}^{-1}$ in 2018 ($n = 96$). DO_{5_events} are associated with times of elevated discharge (Figure 6.3). The discharge associated with DO_{5_events} ranged from 0.12 to $0.88 \text{ m}^3 \text{ s}^{-1}$ and had a median of $0.33 \text{ m}^3 \text{ s}^{-1}$. This compares to a median discharge throughout the two seasonal anoxic periods of $0.05 \text{ m}^3 \text{ s}^{-1}$ ($n = 229$).

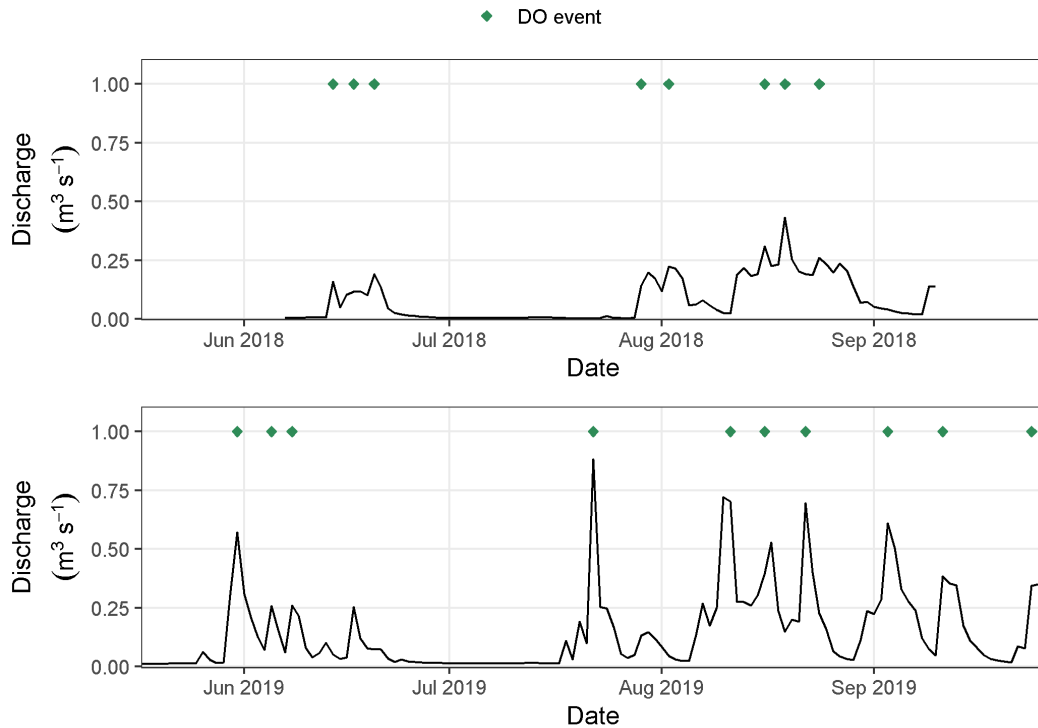


Figure 6.3 Inflow discharge during the two periods alongside the identified dissolved oxygen replenishment events at 5 m (points).

Generally, during the summertime, Q_{tot} is a heating (positive) flux, acting to increase water temperatures (Figure 6.4). Q_{tot} fluctuates between days of heating and cooling, with smaller cooling than heating fluxes, trending towards increased cooling (more negative values) later in the summer. The DO_{5_events} take place slightly more often when there is surface cooling rather than heating (61 % of events), as indicated by negative total surface heat fluxes (Figure 6.4), although 39% of events occur on days of surface heating. The mean surface heat flux during the DO_{5_events} was -18 W m^{-2} compared to a mean of 43 W m^{-2} during the seasonal anoxic periods. Several occasions of peak cooling did not coincide with a DO_{5_events} (Figure 6.4).

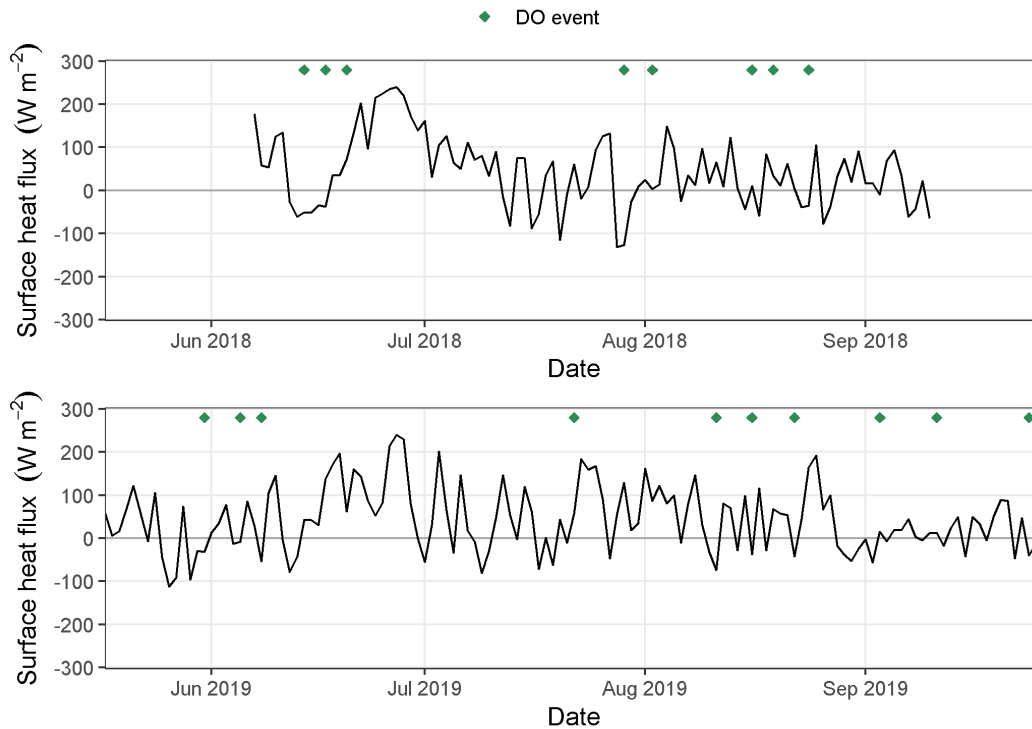


Figure 6.4 Total surface heat flux during the two periods alongside the identified dissolved oxygen replenishment events at 5 m (points). Negative surface heat flux represents surface cooling and positive heat flux surface warming.

Generally, wind power is low with peaks exceeding 0.1 W m^{-2} occurring periodically throughout the two summer periods (Figure 6.5). The mean wind power during the DO_{5_events} was 0.08 W m^{-2} , three times the mean wind power of the whole period of 0.03 W m^{-2} . Some DO_{5_events} occur during periods of increased wind power (Figure 6.5), seven events had wind power above average. However, not all DO_{5_events} were associated with increased wind power. 40% of the DO_{5_events} had wind power less than the mean during the seasonal anoxic period (0.03 W m^{-2}) such as the final event of 2019 and events in mid-August of 2018 (Figure 6.5).

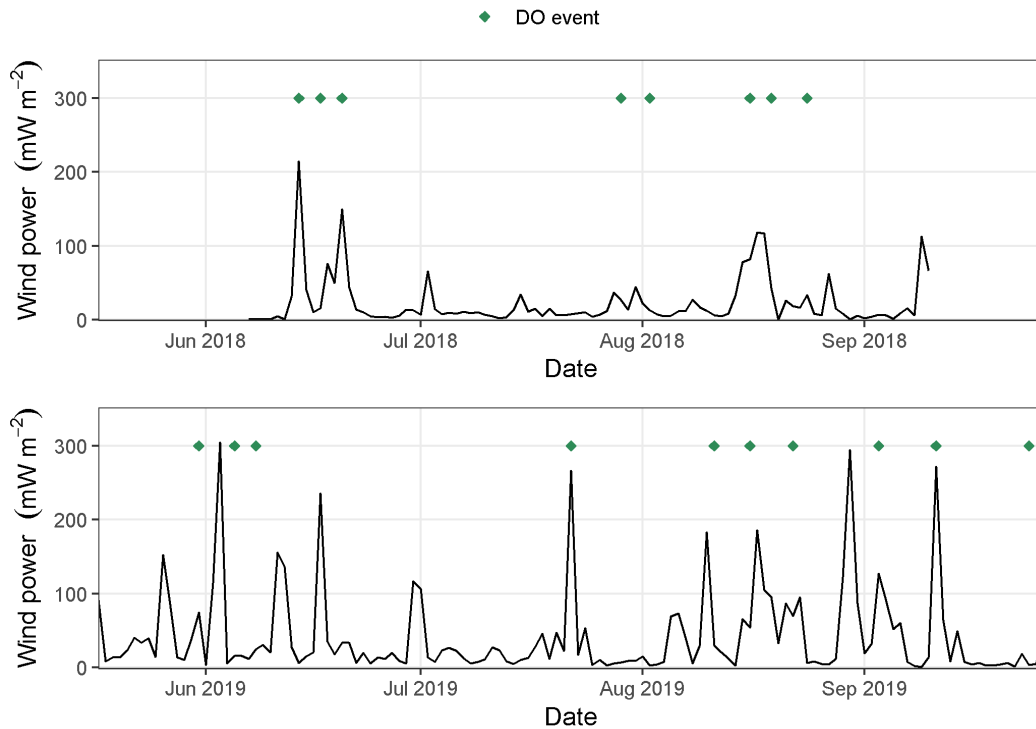


Figure 6.5 Wind power during the two periods alongside the identified dissolved oxygen replenishment events at 5 m (points).

6.4.3 Water column structure changes and DO events

Throughout both seasonal anoxic periods, the water column remains stratified until complete overturn in the autumn. The DO_{5_events} were typically synchronous with periods of lower stability or occasionally when there was a large drop in stability following a period of high stability (Figure 6.6). Mean Schmidt stability for the DO_{5_events} was 7 W m^{-2} , compared to a mean stability of 13 W m^{-2} during the whole period.

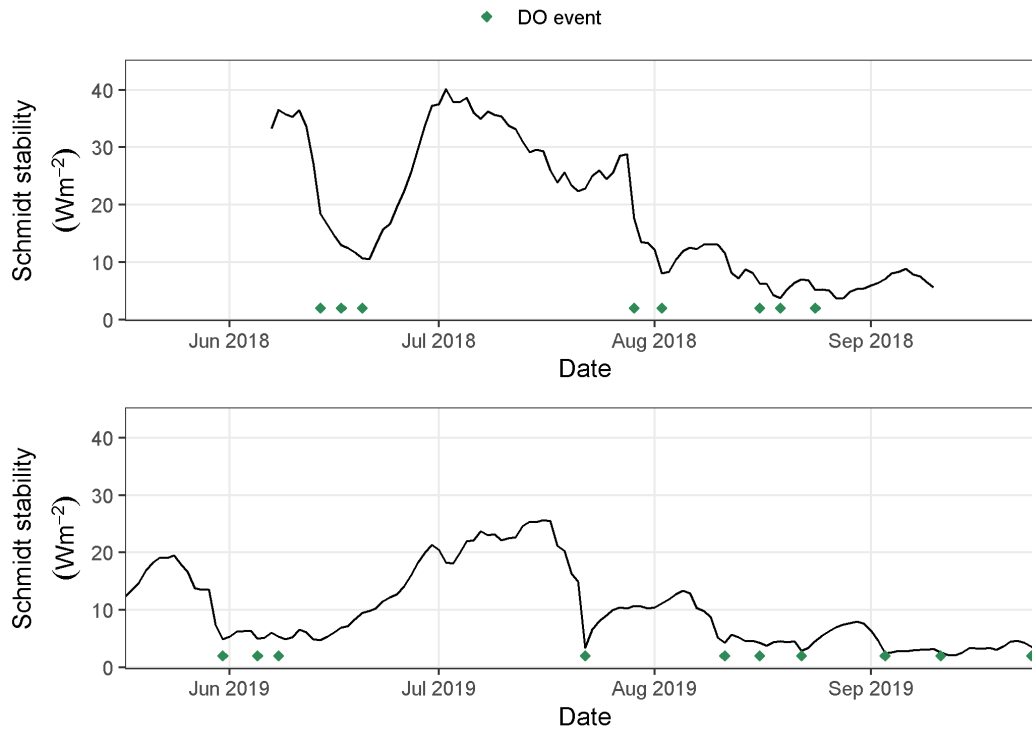


Figure 6.6 Schmidt stability during the two periods alongside the identified dissolved oxygen replenishment events at 5 m (points).

$K_{4.5}$ was on average 10 times higher, in the order of magnitude of $10^{-5} \text{ m}^2\text{s}^{-1}$, during the DO_{5_events} compared to $10^{-6} \text{ m}^2\text{s}^{-1}$ or lower throughout the seasonal anoxic period. $K_{4.5}$ exceeded $10^{-5} \text{ m}^2\text{s}^{-1}$ in both summers (5 and 6 occasions) and is generally larger in the later part of the summer than in the earlier part of the summer (Figure 6.7). 94% of DO_{5_events} took place at times when there was an increase of an order of magnitude or more of K_z above molecular diffusivity ($1.4 \times 10^{-7} \text{ m}^2\text{s}^{-1}$) at 4.5 m (Figure 6.7).

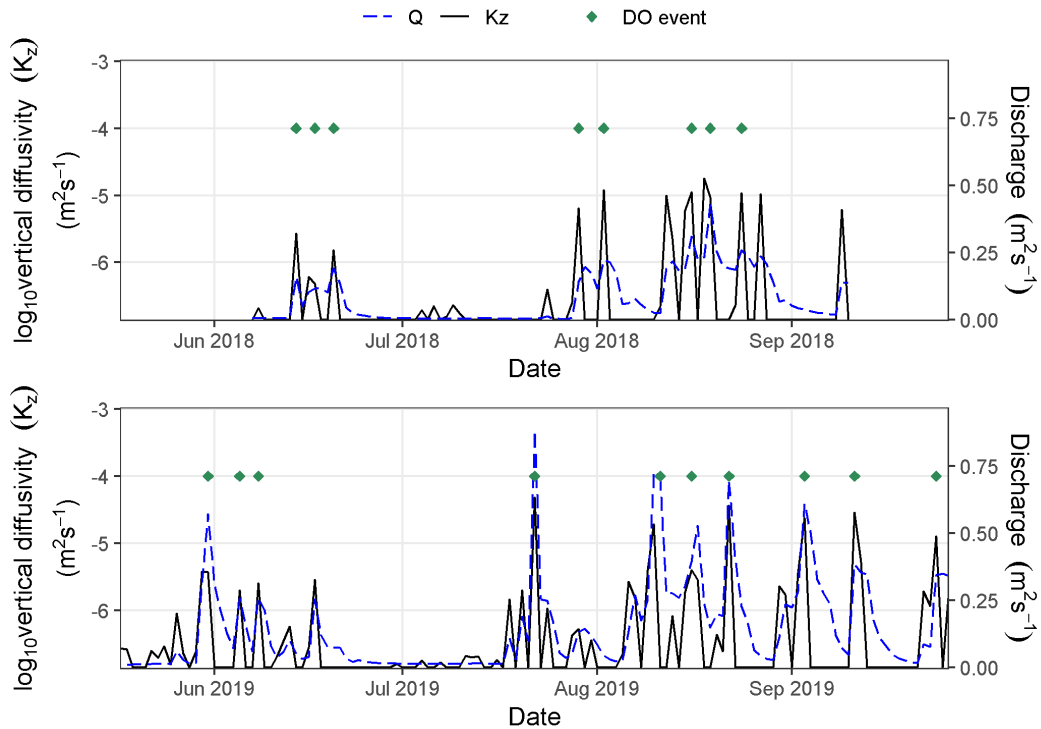


Figure 6.7 Vertical turbulent diffusivity (K_z) and inflow discharge during the two periods alongside the identified dissolved oxygen replenishment events at 5 m (points).

6.4.4 Relationship between drivers and DO events

There is a relationship between the inflow discharge and the proportion of days with DO events (Figure 6.8a); as the flow increases the proportion of days with DO events increases. 75% of all days with discharge above $0.5 \text{ m}^3 \text{ s}^{-1}$ were associated to DO replenishment events, whereas only 5% of days with a discharge below $0.5 \text{ m}^3 \text{ s}^{-1}$ were associated with DO replenishment (Figure 6.8a). Wind power and the proportion of days with DO_{5_events} do not show any relationship (Figure 6.8b). Surface heat flux during the events ranged from -127 to 72 W m^{-2} , with 39% of DO events occurring during periods of surface warming (Figure 6.8c). There was a negative relationship between Q_{tot} and the occurrence of DO events (Figure 6.8). As the cooling heat flux got bigger (more negative), there was a higher proportion of days with DO events. > 20% of dates with a surface cooling flux greater than (more negative) -135 W m^{-2} had associated DO events. There was a slight negative relationship between water column stability and the occurrence of DO_{5_events} , with the proportion of days having a DO_{5_event} increasing at lower water column stabilities. No DO_{5_events} occurred when Schmidt stability was greater than 20 W m^{-2} , conditions prevalent for 25% of the time periods.

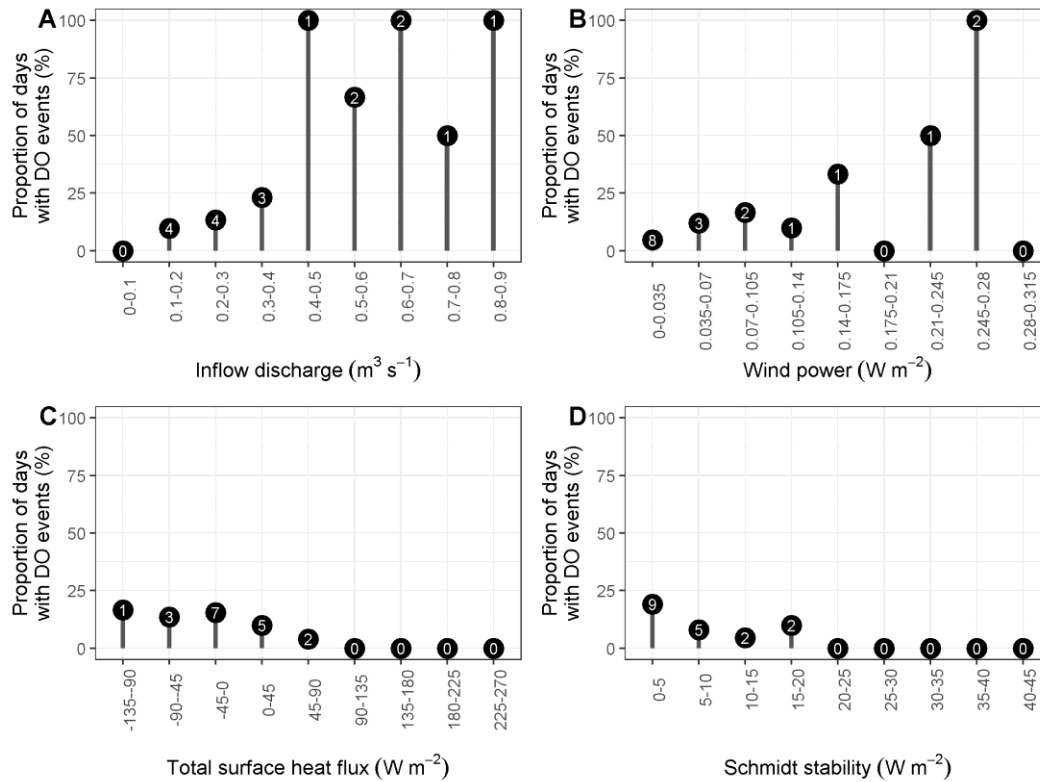


Figure 6.8 Proportion of days during the two identified periods in which there is a dissolved oxygen replenishment event at 5 m (as identified above) associated with different levels of A) inflow discharge, B) wind power, C) total surface heat flux, and D) Schmidt stability. Number of events are shown in the circles.

Throughout the seasonal anoxic periods, the Schmidt stability was negatively correlated to inflow discharge (Figure 6.9a; $n = 229$, $r = -0.39$, $p < 0.05$). Inflow discharge was also positively correlated to increased K_z (Figure 6.9b; $n = 229$, $r = 0.51$, $p < 0.05$). However, there was a single DO_{5_event} where the inflow discharge was high (2nd percentile), but K_z remained at the rate of molecular diffusion ($1.4 \times 10^{-7} \text{ m}^2 \text{ s}^{-1}$). If discharge were acting as a proxy for some other event (such as a storm), we may expect there to be a strong relationship between discharge and wind speeds and surface cooling, which are also associated to storms. However, the relationship between inflow discharge and Q_{tot} showed no correlation ($n = 229$, $r = -0.04$, $p = 0.59$) and there was a weak positive correlation between inflow and wind power ($n = 229$, $r = 0.32$, $p < 0.05$) throughout the periods (Figure 6.9d), with DO_{5_events} occurring at almost all wind intensities.

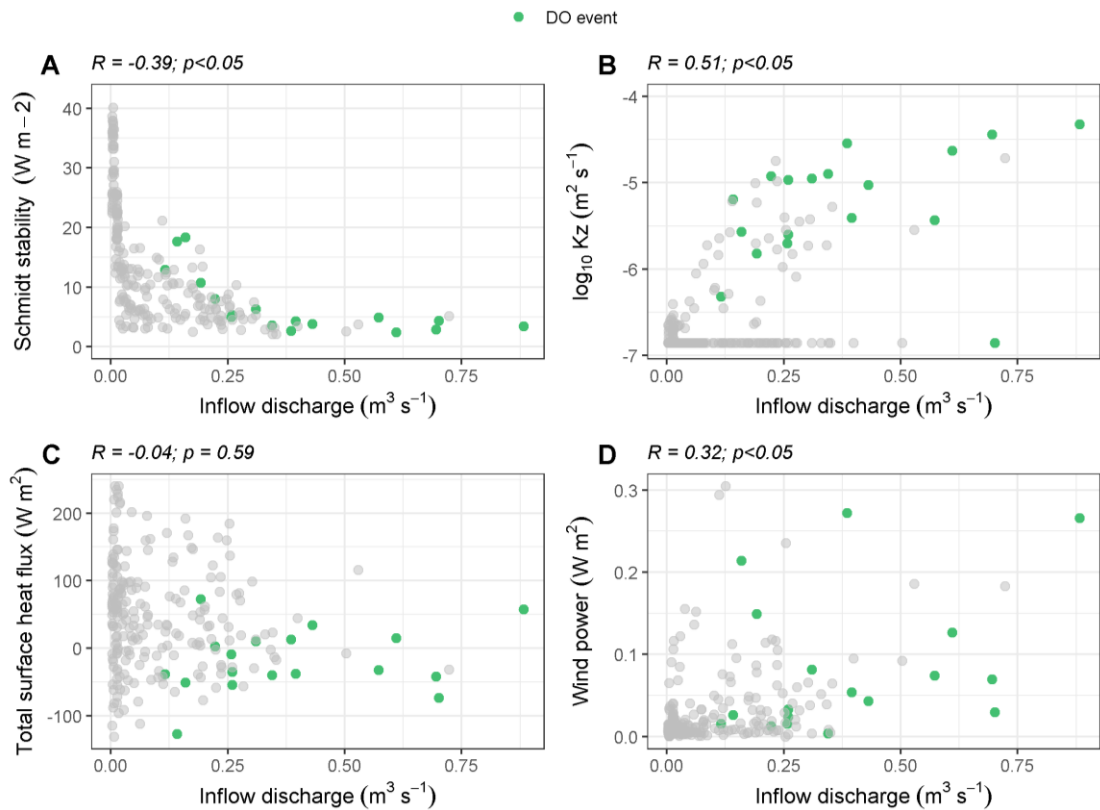


Figure 6.9 Relationship between inflow discharge and A) Schmidt stability flux, B) K_z , C) total surface heat flux, and D) wind power during the stratified periods. Green highlighted points indicate the dissolved oxygen replenishment events identified at 5 m. The results (R value, a significance) of the Spearman's Rank Correlation on differenced data are also shown above.

In total 28 Q_{events} were identified across the two periods. All DO_{5_events} took place on days when there were Q_{events} (Figure 6.10) although some high flow events occurred on days with no DO_{5_events} . Thirteen DO_{5_events} occurred on the same day as a Q_{event} , in four cases the DO_{5_event} preceded the Q_{event} by one day and in one case the Q_{event} preceded the DO_{5_events} by one day. In addition to these, 10 Q_{events} were not associated with a DO_{5_events} . All Q_{events} exceeding $0.3 \text{ m}^3 \text{ s}^{-1}$ coincided with a DO_{5_event} .

A logistic regression was run using the independent variables discharge and total surface heat flux (Q_{tot}). The other potential explanatory variables (wind power, Schmidt stability, and vertical diffusivity) were omitted from the model to avoid collinearity with discharge (as indicated in the Spearman's rank correlation results). The results of the logistic regression ($n = 229$), indicated that both discharge ($p < 0.001$) and Q_{tot} ($p = 0.004$) were significant predictors of DO_{5_events} . The coefficients of the logistic model suggest that for each $0.01 \text{ m}^3 \text{ s}^{-1}$ increase in discharge the odds of a DO_{5_events} increase by approximately 10 % and for each 1 W m^{-2} increase in Q_{tot} the odds of a DO_{5_events} decreases by 2 % (see Supplementary Information 6.7.5). A pseudo- R^2 value of 0.42 indicated a good level of model fit (McFadden, 1974) with Q explaining

a much larger proportion of the residual deviance than Q_{tot} (Section 6.7.5), compared to the null model.

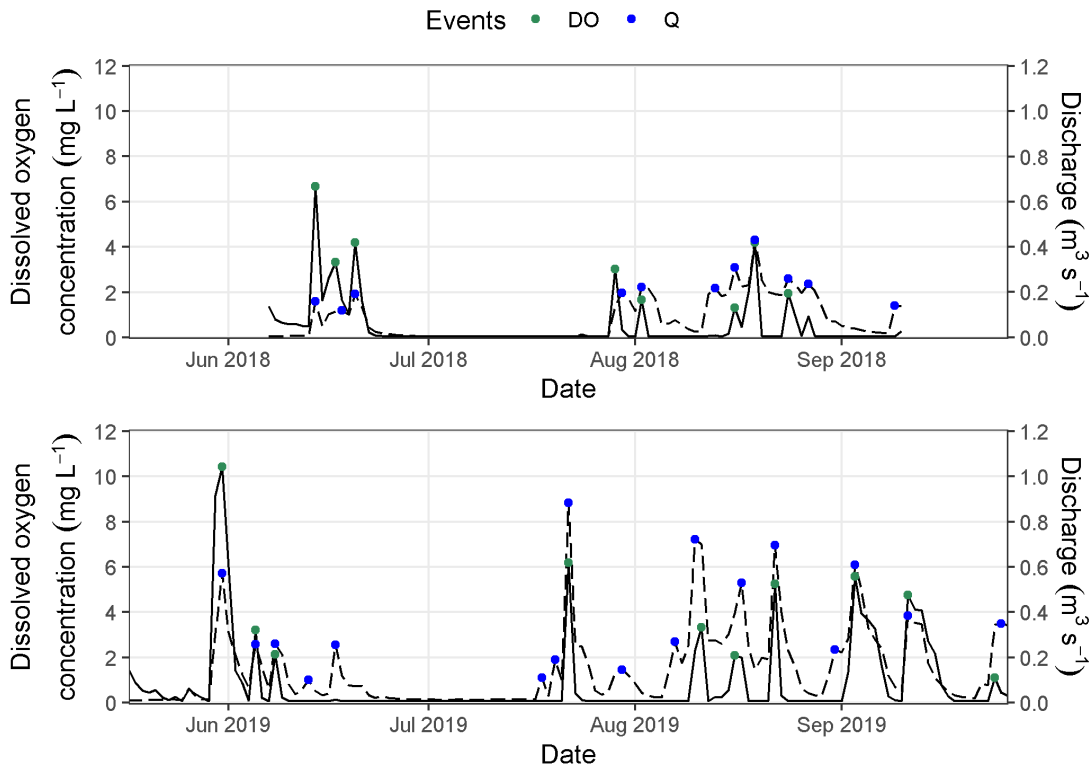


Figure 6.10 Identified high-discharge inflow events (blue) and dissolved oxygen replenishment events (green) during the seasonal anoxic periods in 2018 and 2019 (DO no longer continuously $> 1 \text{ mg L}^{-1}$).

6.4.5 Sources of oxygenation

The estimation of the downward vertical oxygen flux between the 4 and 5 m layers ($VF_{DO_{4.5}}$) shows that $VF_{DO_{4.5}}$ is generally sufficient to induce the change in oxygen concentration at 5 m. On average (median) the flux is $70.4 \text{ mg O}_2 \text{ s}^{-1}$, more than the change at 5 m (Figure 6.11). However, there are notably five events in which the estimate of $VF_{DO_{4.5}}$ is lower than the change in oxygen concentration at 5 m (Figure 6.11). Four of these events occur early in the seasonal anoxic periods.

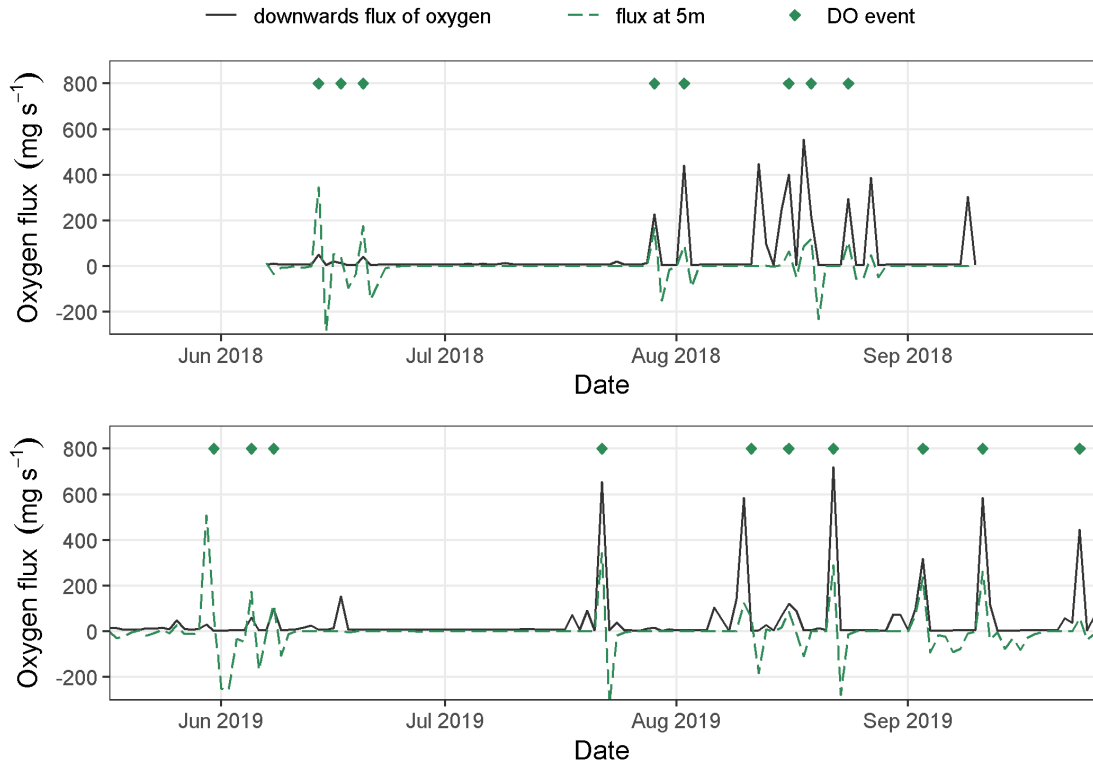


Figure 6.11 Downwards flux of oxygen (black line) from 4 to 5 m during the seasonal anoxic period. The change in oxygen at 5 m is also shown (green dashed) and the identified oxygen events at 5 m (points).

During the seasonal anoxic period, the inflow is cooler and denser than the surface waters ($3.6 \pm 2.4^\circ\text{C}$) but generally warmer than the deepest lake water and so may intrude into the water column as an interflow (Figure 6.12). The depth of neutral buoyancy of the inflow, as an estimate of intrusion depth, for each DO_{5_event} varies between 2.3 and 5.5 m, with a mean depth of 4.1 m (Figure 6.12). Generally, the intrusion depth deepens throughout the period as the difference between the inflow and 5 m water temperatures reduces (Figure 6.12), especially in 2019. During the events in which the estimated $VF_{\text{Do}_{4.5}}$ was insufficient to cause the DO_{5_event} , the inflow is estimated to be intruding to approximately 4 m or deeper (Figure 6.12).

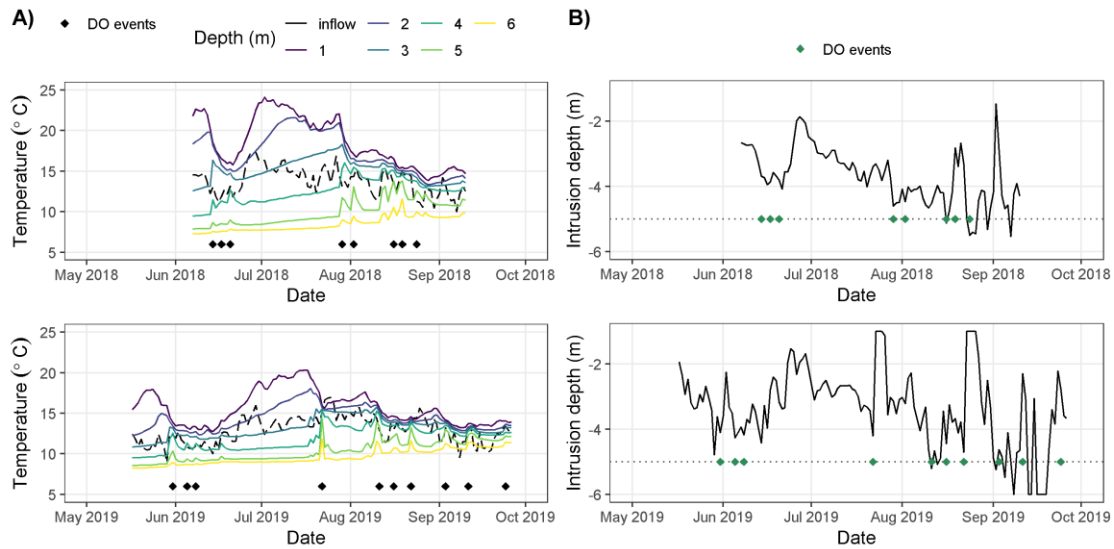


Figure 6.12 A) Water column and inflow (dashed) temperatures and B) Inflow intrusion depth estimated as the depth of the water column of equal density to the inflow during the two periods alongside the identified dissolved oxygen replenishment events at 5 m (points).

Weekly chlorophyll *a* profiles showed that a sub-surface maxima is present throughout the summer period in both years. Across the 29 spot sampling dates in which chlorophyll *a* profiles were measured, more than three quarters had a chlorophyll *a* maxima at 4 m or deeper and the remaining sampling dates had maxima at 2 or 3 m. Concentrations at 5 m consistently exceeded $50 \mu\text{g L}^{-1}$ throughout the summer (Figure 6.13a). The mean concentration at 5 m was $124 \pm 70 \mu\text{g L}^{-1}$ throughout the two periods, and during the DO_{5_events} was $112 \pm 76 \mu\text{g L}^{-1}$. The sub-surface chlorophyll maxima occurred despite the photic depth being typically above 5 m (<1% surface light, Figure 6.13b), except briefly in June 2018, when chlorophyll *a* concentrations at 5 m were low. Mean photic depth was slightly deeper during DO_{5_events} (3.9 ± 0.7 m) than the mean photic depth during the two summer periods (3.7 ± 0.6 m). No obvious relationship is evident between the chlorophyll *a* concentration at 5 m and the proportion of day with DO_{5_events} (Figure 6.13c).

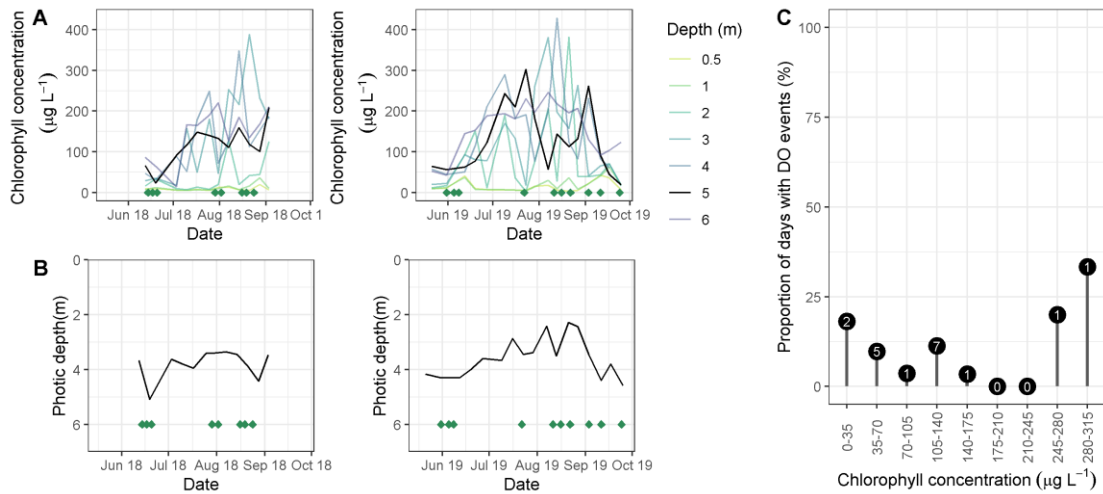


Figure 6.13 Chlorophyll *a* concentration at different depths in the water column. Concentrations at 5 m are shown with the black line. B) estimated photic depth (1% of surface light), and C) proportion of days during the two identified periods in which there is a dissolved oxygen replenishment event at 5 m. Green points on panels A and B show the dates of DO replenishment events at 5 m.

6.5 Discussion

Using high-frequency oxygen, discharge, and temperature data, we conducted analysis of the temporal dynamics of deep-water oxygen during the seasonal anoxic period and its relationship with high-discharge inflow events in a small, temperate lake. We showed that, during the stratified period, deep water oxygen replenishment events are highly correlated to inflow discharge events, with large inflow events more likely to be associated to DO_{5_events} than peaks in other potential drivers such as surface cooling and wind power. Discharge events themselves had no or low correlation with cooling and wind events. The inflow events were also correlated with reductions in water column stability, increased K_z and the vertical flux of oxygen at 4.5 m, to a greater extent than to cooling or wind events. This highlights the destabilising impact of the inflows and the subsequent impacts on vertical mixing of dissolved oxygen into the deeper water (Brand et al., 2008; Fink et al., 2016; Kimura et al., 2014). Increased K_z will mix more oxygenated water from shallower layers into the hypolimnion, an important flux of oxygen through the thermocline and driver of DO concentration at depth (Bouffard et al., 2013; Cortés et al., 2021). Prior evidence shows reduced seasonal hypolimnetic anoxia under less stable stratification, as depletion rates are lower and vertical mixing higher (Foley et al., 2012; Rogora et al., 2018).

While the majority of the DO_{5_events} were associated with downward vertical fluxes of oxygen sufficient to induce the changes seen, five of the 18 were not. This discrepancy suggests that additional oxygen from another source is providing oxygen to the 5 m layer at these times.

One potential source is the well-oxygenated inflow itself. River systems are generally well saturated with oxygen, usually above 85% but can become supersaturated (Neal et al., 2002; Williams and Boorman, 2012). Assuming that on average that water is fully saturated, this gives concentrations of between 10-12 mg L⁻¹ likely in the inflow to Elterwater, depending on the temperature range during this period. Our results show that this well oxygenated inflow is likely intruding as an interflow (Liu et al., 2020; MacIntyre et al., 2006) between 3 and 5 m below the lake surface, bringing oxygenated water below or into the thermocline, due to the negative buoyancy of the inflow (Fink et al., 2016; Marcé et al., 2010, 2008). Intrusion of the inflow could be providing the additional oxygen required for the changes in oxygen seen at 5 m, either through oxygen being injected directly at 5 m or into the layer above 5 m and mixed downwards. The five events where $VF_{Do_{4.5}}$ was insufficient to induce the DO concentration observed, the intrusion depth was at or below 4 m. This would mean our estimation of the oxygen concentration at 4 m would be an underestimate, resulting in higher downward vertical fluxes of oxygen. The intrusion of well-oxygenated inflow water has been shown to contribute significantly to the hypolimnetic oxygen concentration in deep alpine lakes and reservoirs (Fink et al., 2016; Liu et al., 2020) and to maintaining oxic conditions during the ice-covered period when the whole water column is isolated from the atmosphere (Palmer et al., 2021). Our results provide evidence for deep-water re-oxygenation in small temperate lakes during the seasonal anoxic period that has been overlooked outside of deep reservoir systems (e.g. Huang *et al.*, 2014; Liu *et al.*, 2020).

Here we have shown that during the seasonal anoxic period, the majority of replenishment events can be accounted for by the contribution of oxygen to 5 m from increased vertical mixing associated with high discharge events and that additional oxygen may be coming from direct injection by the oxygenated river. Despite the evidence presented for the two replenishment processes it remains difficult to disentangle directly the contribution of increased vertical mixing and direct intrusion to the oxygen flux at 5 m with the resolution of data available. In any case, our results demonstrate the importance of inflow events to the replenishment of deep-water oxygen during the stratified period in small, shallow lakes and present two viable and potentially complementary processes. The mass of oxygen being brought in by the inflow is likely to be relevant for the whole budget of oxygen in the lake, especially if it is intruding below the thermocline and into water with high oxygen demand.

Other processes potentially involved in the oxygen replenishment at depth may include primary production of oxygen through photosynthesis by phytoplankton and/or other autotrophic organisms. Inflows may also modify oxygen production and depletion processes

by introducing allochthonous nutrients and dissolved organic matter (Liu et al., 2020; Marcé et al., 2008), which promote photosynthesis and/or respiration (Liu et al., 2020; Zhang et al., 2015). The sub-surface maxima in chlorophyll *a* and the occurrence of phytoplankton at depth are likely to a source of oxygen to the deeper water in Elterwater, especially during the stratified period when the deep water is no longer in contact with the atmosphere. However, it is unlikely that autotrophic production is the primary driver of the DO replenishment events at 5m that we consider here. Despite high chlorophyll *a* concentrations, principally from phytoplankton, at this depth, we found no relationship between the DO_{5_events} and the chlorophyll *a* concentration and concentrations during the events were lower during the DO_{5_events} than during the period as a whole. However, accurate measurements of primary production in the anoxic zone are difficult, as oxygen consumption depletes oxygen as soon as its produced (Brand et al., 2016) since production rates can be 10-20 times lower than consumption rates (Brand et al., 2016). Oxygenic primary production can occur in the anoxic zones (Brand et al., 2016) and light flux requirements for some species are very low ($< 0.1 \mu E m^{-2} s^{-1}$; Raven *et al.*, 2000) so it is possible that primary production is contributing to DO replenishment. However, the timescales for this are likely to differ to those considered in the DO_{5_events} studied here, and there is no evidence in these results that this mechanism is a major contributor to the oxygen replenishment.

6.5.1 Implications of DO replenishment

The replenishment during the seasonal anoxic period at 5 m has important implications for understanding the habitat availability for aerobic organisms. Fish are able to persist in sub-optimal conditions for short periods at reduced growth rates and metabolism (Davis, 1975; Kalff, 2002). However, the replenishment of oxygen to deeper parts of the lake may provide respite from oxygen stress, especially for cold water fishes that require specific oxygen-temperature niches, allowing species to persist in what otherwise might be considered uninhabitable space (Alabaster and Lloyd, 1982; Kalff, 2002). Without the high-frequency data, prior to the advent of automated O_2 sensors, the extent and duration of anoxia may have been over-estimated, with important implications for processes such as internal loading (Mortimer, 1942; Nürnberg, 1984). There is a need for further investigation of the short-term impacts of DO replenishment in the hypolimnion to understand the importance of inflow related oxygen replenishment on ecological habitats and biogeochemical cycling.

The relationship between DO replenishment events and high inflow events is evident from the high-frequency data, which would not have been possible with traditional weekly, fortnightly, or monthly sampling, as the event duration is in the order of a couple of days. Using this high-

frequency data, we are able to show that dissolved oxygen in the hypolimnion is not just related to the stratification onset and overturn timing but does show sub-seasonal dynamics relating to short-term changes in physical parameters of water column stability, vertical mixing, and inflow discharge. Use of high-frequency data is crucial to understand these sub-seasonal dynamics. The implications of high discharge events for biogeochemical cycling, habitat availability, and the oxygen budget of lakes need to be better understood to better quantify these parameters. The understanding of sub-seasonal dynamics of hypolimnetic oxygen will also contribute to better model parameterisation of the processes. The results have also shown that the inflow impacts should not be discounted especially in smaller, short-residence time lakes, where the inflow could be contributing a large oxygen load.

The demonstration of the impact of inflows on sub-seasonal deep-water oxygen in short-residence time lakes also has implications when considering global climate change impacts in lakes (e.g. Fink *et al.*, 2016). Projections of lake impacts have shown seasonal responses to warming through longer and stronger periods of stratifications, resulting in greater extent and duration of seasonal hypolimnetic anoxia (Ladwig *et al.*, 2021; Rogora *et al.*, 2018; Woolway *et al.*, 2021b). Under more stable water column conditions, inflows may become increasingly important sources of dissolved oxygen to deep waters, through direct intrusion or increased vertical mixing, as demonstrated here. Reductions in summer river flow are projected for a large proportion of the global landmass under future climate (Arnell and Gosling, 2013; van Vliet *et al.*, 2013), reducing the load of highly oxygenated water into lakes during the summer period. Furthermore, river warming will have implications for the DO concentrations, as warmer water can hold less dissolved oxygen (Lee *et al.*, 2018; Taner *et al.*, 2011). There is evidence of faster warming in rivers than lakes in some regions (Jonkers and Sharkey, 2016). As a result of the reduced density difference between the inflow and the lake surface, the inflow will have a shallower depth of neutral buoyancy and intrusion depth into the water column, resulting in fewer intrusions into or below the thermocline. Some research shows that hypolimnetic warming is substantially less than epilimnetic warming (Pilla *et al.*, 2020), therefore exacerbating this impact.

In a lake management context, increasing the inflow discharge could induce DO replenishment without complete mixing of the water column, which would be potentially useful in limiting internal loading from anaerobic lake sediment. Methods to increase deep-water oxygen to suppress internal loading of nutrients are widespread (Lüring *et al.*, 2020; Preece *et al.*, 2019) and this could potentially add another alternative. Furthermore, if management is able to ensure inflows are sufficiently cool relative to lake temperatures, by shading (Garner *et al.*,

2017b; van Vliet et al., 2013) or heat extraction via heat pumps (Fink et al., 2014b; Gaudard et al., 2019) for example, this would induce interflows that would intrude deeper and would be more likely to replenish oxygen in the hypolimnion.

6.6 Conclusions

Our results have shown that inflows can act as an important source of oxygen to the deep waters of lakes, by inducing reduced water column stability and increased vertical mixing. Inflows could also be contributing oxygen through direct intrusion. This study showed that short-term DO replenishment events were associated to high discharge inflow, a relationship not previously considered in hypolimnetic oxygen dynamics of small, short-residence time lakes, with implications for lakes given the expected changes in river flow under future climate. As well as implications for changes to natural flows, these results suggest a potential management method to maintain oxygen concentrations in the hypolimnion, without destratifying a lake. Increasing use of high-frequency oxygen data provides greater opportunities to understand the sub-seasonal dynamics of deep-water dissolved oxygen and its relationship to lakes' inflows and physical structure, disentangling the processes acting to replenish oxygen at depth. This may have implications for understanding a lakes oxygen budget and understanding biogeochemical cycling of nutrients, as well as improving the modelling of oxygen dynamics in lakes.

6.7 Supplementary information for Chapter 6

6.7.1 Gap filling discharge data

6.7.1.1 Brathay flow data

Missing data, due to faulty sensors, were filled in using linear interpolation where the gaps \leq 3 hours. For gaps exceeding this the relationship between the neighbouring Rothay discharge, measured at Miller Bridge House (54.4284 °N, 2.9711 °W), was used. The relationship between measurements was calculated as:

$$Q_{Brathay} = Q_{Rothay}^{1.01}$$

6.7.1.2 Pipeline flow data

Using the measurements from the diversion (Jan 2016 to Dec 2019) the missing values in the inflow discharge measurements (274 missing values, < 1% of data) were estimated based on the gauged discharge in the River Brathay (lake outflow). The maximum discharge through the pipeline, based on Environment Agency defined abstraction limits is $0.122 \text{ m}^3 \text{ s}^{-1}$ and the minimum discharge in the source river for abstraction is $0.383 \text{ m}^3 \text{ s}^{-1}$. The 95th percentile of measured source discharge that produced the maximum (capped) diversion discharge ($0.122 \text{ m}^3 \text{ s}^{-1}$) was calculated. Values exceeding this value were assumed to give the maximum diversion discharge ($0.122 \text{ m}^3 \text{ s}^{-1}$). Where the source discharge dropped below $0.383 \text{ m}^3 \text{ s}^{-1}$ no diversion is permitted (flow = $0 \text{ m}^3 \text{ s}^{-1}$). Between these flows, a general additive model was fitted between the measured lake outflow and diversion discharges giving a significant smooth ($p < 0.01$). The model had an R-squared of 0.53. The gam.check function was used to check, visually, model fit.

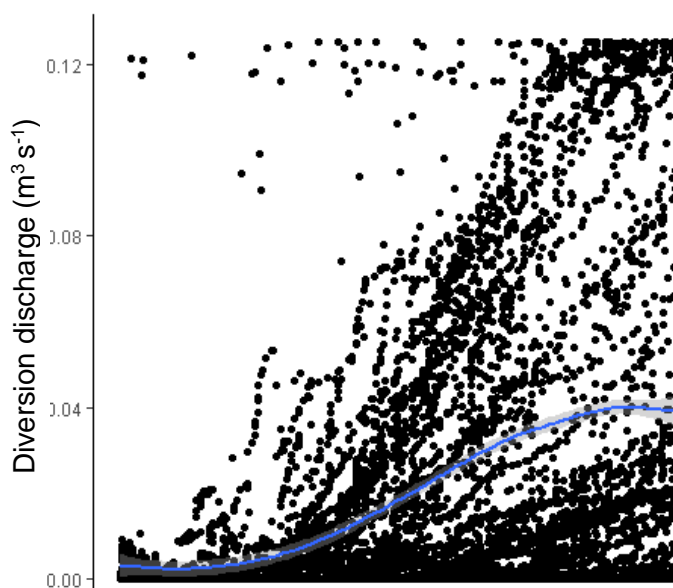


Figure S 6.7.1-1 Observations (points) and model fit between outflow and piped discharge.

```
> summary(mod)
Family: gaussian
Link function: identity

Formula:
Q_m3_s.t ~ s(Q_m3_s.JK, k = 20)

Parametric coefficients:
              Estimate Std. Error t value Pr(>|t|)
(Intercept) 0.0576170  0.0002488  231.6   <2e-16 ***
---
signif. codes:  0 '***' 0.001 '**' 0.01 '*' 0.05 '.' 0.1 ' ' 1

Approximate significance of smooth terms:
              edf Ref.df    F p-value
s(Q_m3_s.JK) 16.68  18.26 1314 <2e-16 ***
---
signif. codes:  0 '***' 0.001 '**' 0.01 '*' 0.05 '.' 0.1 ' ' 1

R-sq.(adj) = 0.534  Deviance explained = 53.5%
GCV = 0.0012972  Scale est. = 0.0012961  n = 20937
```

Diagnostic plots

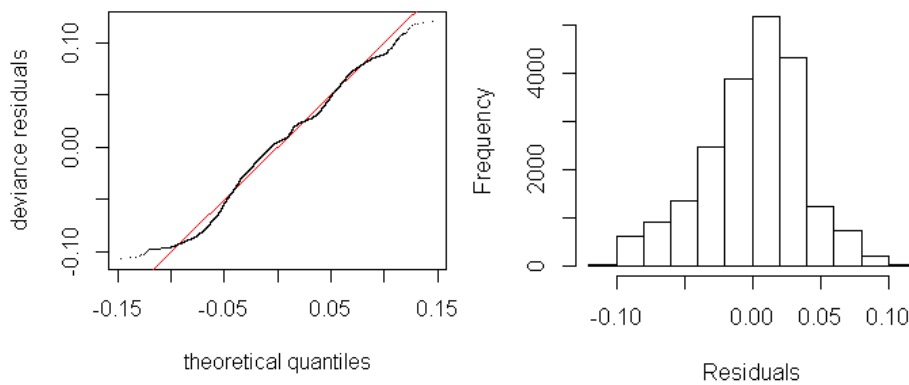


Figure S 6.7.1-2 diagnostic plots of the gam model fitted between the outflow and piped discharge.

6.7.2 Gap filling missing meteorological data

- From May 2018 – December 2019 < 1% of data were missing for all meteorological variables
- Gaps of less than 24 hours were filled using linear interpolation, for solar radiation the maximum gap was 6 hours, to avoid interpolating between day and night.
- Where gaps remained a linear model was fitted between Blelham, and Windermere or Esthwaite Water buoys (see <https://ukscape.ceh.ac.uk/our-science/projects/cumbrian-lakes-monitoring-platform>) meteorological data, using data from 2012-2019.
- Any remaining missing values the following protocol was used:
 - o Wind speed – average wind speed for 24 hours previous and 1 week after the missing value.
 - o Relative humidity – linear regression between Blelham Tarn and Esthwaite Water buoy weather station values (intercept = -5.917, slope =1.07, p < 0.001, adjusted R-squared = 0.915).
 - o Surface water temperature – linear interpolation.
- Solar radiation observations were checked using the `suncalc` R package (Thieurmel & Elmarhraoui, 2019). With hours between sunrise and sunset set to 0.
- Cloud cover is required to calculate the net surface heat flux and was estimated based on the difference between the observed solar radiation and the maximum clear sky radiation using the `insol` R package (Corripio, 2019).

$$cloud\ cover = 1 - \frac{observed}{maximum\ possible}$$

- Night-time cloud cover was estimated as the mean cloud cover for the previous day

Thieurmel, B. & Elmarhraoui, A. (2019). `suncalc`: Compute Sun Position, Sunlight Phases, Moon Position and Lunar Phase. R package version 0.5.0. <https://CRAN.R-project.org/package=suncalc>

Corripio, J. G. (2019). `insol`: Solar Radiation. R package version 1.2.1. <https://CRAN.R-project.org/package=insol>

6.7.3 Checking of assumptions for the logistic regression model

Assumption 1: Linearity

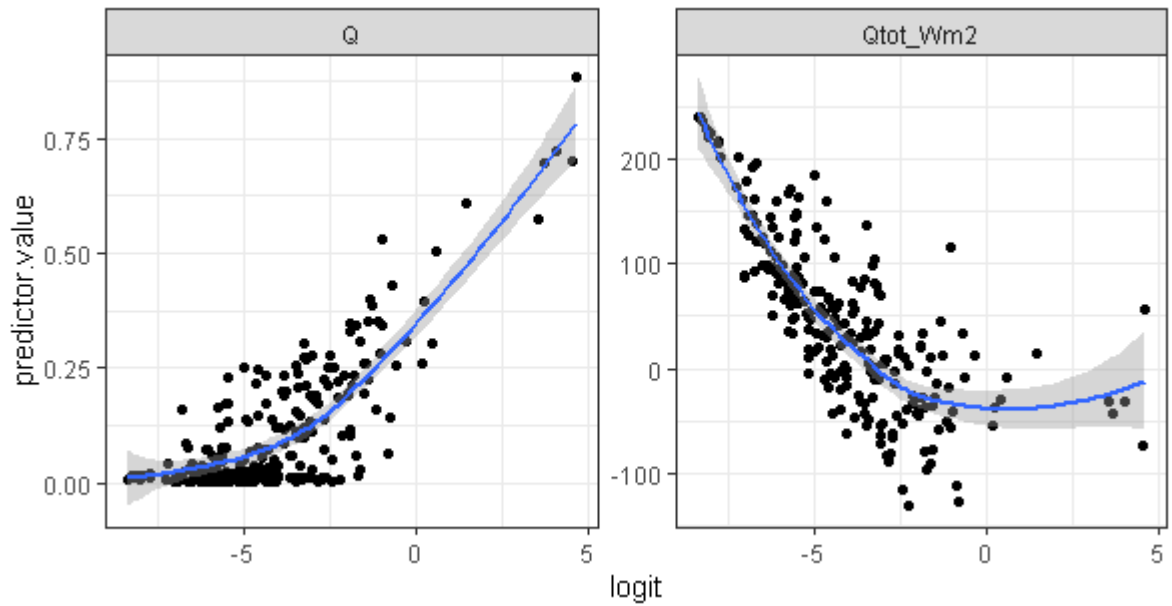


Figure S 6.7.3-1 Scatter plots of predictors and the logit of the outcome. Smoothed line is a loess smoother.

The predictor variables (discharge – Q and surface heat flux – Q_{tot}) demonstrate a linear relationship with the logit of the outcome.

Assumption 2: Independence – no auto correlation

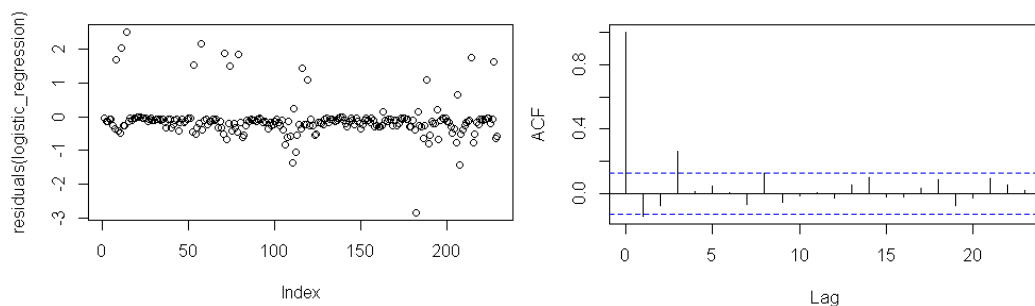


Figure S 6.7.3-2 Plots of the model residuals used to check for autocorrelation.

Table S 6.7.3-1 Output of the Durbin Watson Test run on the logistic regression.

Autocorrelation	D-W statistic	p-value
-0.08	2.16	0.17

Both the inspection of residual plots (Figure S 6.7.3-2) and output from the Durbin Watson test suggest there residuals are independent.

6.7.4 Checking assumptions of Spearman's Rank correlation

Autocorrelation:

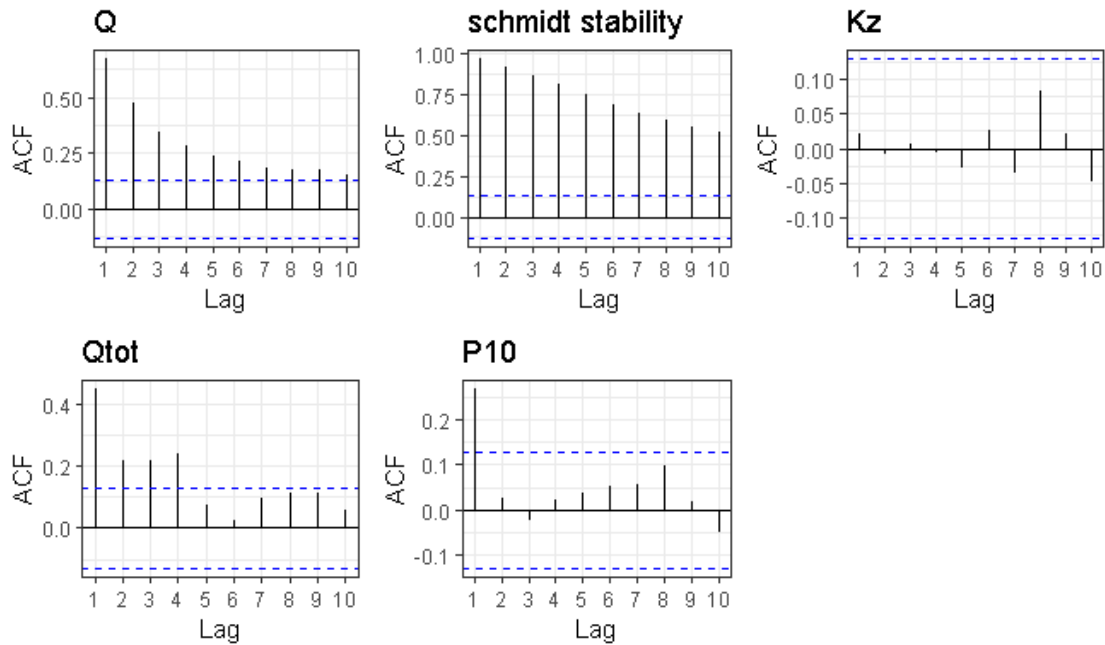


Figure S 6.7.4-1 Autocorrelation plots of raw data for the variables used in the spearman's correlation: discharge (Q), Schmidt stability, vertical diffusivity at 4.5 m (K_z), total surface heat flux (Qtot) and wind power (P10).

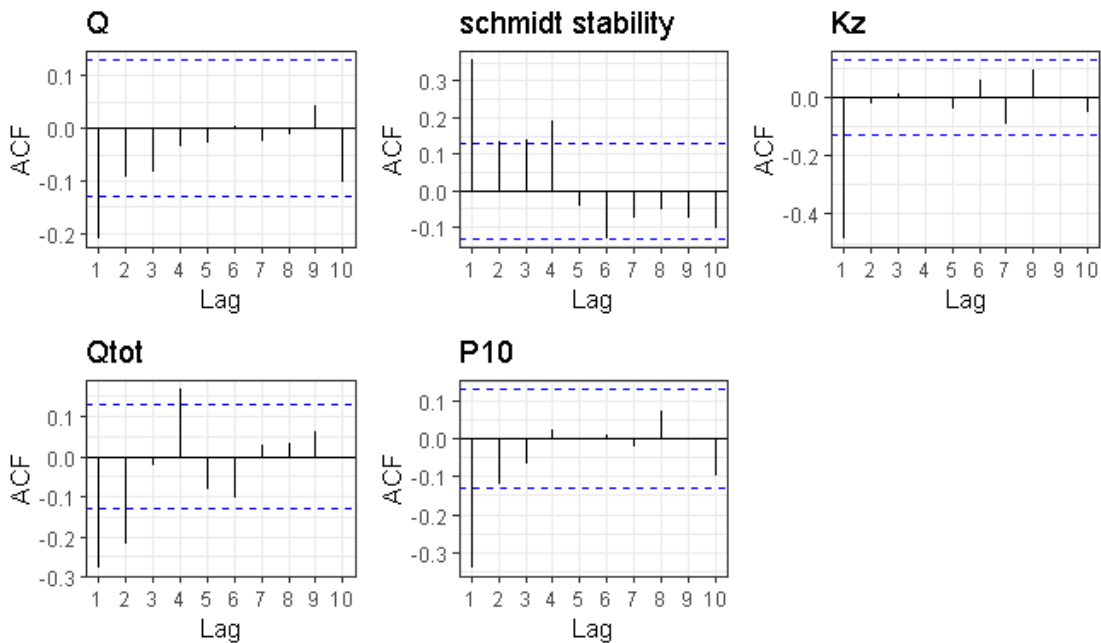


Figure S 6.7.4-2 Autocorrelation plots of differenced data for the variables used in the spearman's correlation: discharge (Q), Schmidt stability, vertical diffusivity at 4.5 m (K_z), total surface heat flux (Qtot) and wind power (P10).

6.7.5 Results of logistic regression

Table S 6.7.5-1 Output from the logistic regression using discharge (Q) and total surface heat flux (Q_{tot})

	Estimate	Std Error	Z value	Pr	Deviance resid.
Q	9.8	2.12	4.61	<0.001	42.95
Q_{tot}	-0.01	0.006	-2.85	0.004	10.78

Null deviance: 126.11, residual deviance: 72.38

Chapter 7 Dual climate threats of air temperature and inflow change impact the thermal structure of small temperate lakes

(Freya Olsson, Ellie B. Mackay, Phil Barker, Sian Davies, Ruth Hall, Bryan Spears, Ian D. Jones (2021). In preparation for submission to *Limnology & Oceanography*)

7.1 Abstract

In addition to air temperature rises, future climate change is predicted to change river flow. Throughflows contribute to the heat budget of lakes, as an advective heat flux, affecting their thermal structure. Despite the role of lake inflows on the lake heat budget, few studies have considered the sensitivity of lake temperatures to long-term shifts in river flow. Furthermore, the climate change impacts of air temperature warming and river flow changes will not act in isolation and are likely to interact in determining the in-lake thermal impacts. In this paper, we use a one-dimensional hydrodynamic model to test the sensitivity of lake thermal conditions to changes in air temperature and inflow discharge. We assess the independent and interacting effects of changes in air temperature and discharge for a small, short-residence time lake basin in the northwest of England, highlighting the potential impact of climate change on this lake type. Discharge changes had seasonal impacts on lake thermal structure due to the lake-inflow temperature difference, meaning that discharge reductions caused warming in the summer and cooling in the winter, whereas discharge increases caused cooling in the summer and warming in the winter. Summer surface water temperatures were 0.6 ± 0.1 °C warmer when discharge was reduced by 50%. We show how changes to inflow discharge may compound air temperature warming in lakes producing in-lake responses equivalent to an additional 0.7-0.8 °C of air temperature rise. Overall, the impact of discharge changes on lake temperatures has the potential to exacerbate or buffer the impacts of air temperature rises, depending on the direction of change and the relationship between inflow and in-lake temperatures.

Keywords: Climate change; lake modelling; river flow; lake temperatures; stratification

7.2 Introduction

Global climate change projections forecast an overall warming climate, with global mean surface temperature warming between 2.6 °C to 4.8 °C by 2100, relative to 1986-2005, if greenhouse gas emissions are not reduced (IPCC, 2014). The effects of climate warming are projected to warm lakes (Woolway et al., 2020) and impacts are already evident in lake thermal records (Kraemer et al., 2015; O'Reilly et al., 2015) as higher water temperatures,

longer and earlier periods of stratification, and loss of winter ice cover (Piccolroaz et al., 2020; Woolway et al., 2020). Lake modelling of climate change effects, using global and regional climate projections, predict further changes in thermal structure, and have considered the impact on single systems (e.g. Fenocchi et al., 2018; Komatsu et al., 2007) and at the global scale (Dokulil et al., 2021; Piccolroaz et al., 2020; Woolway et al., 2021b; Woolway and Merchant, 2019). Understanding climate change impacts on thermal conditions is important as the thermal structure of a lake can play a key role in its functioning (Woolway et al., 2020), including on oxygen dynamics (Foley et al., 2012; Rogora et al., 2018; Snortheim et al., 2017) and primary production (Paerl and Huisman, 2008; Smucker et al., 2021; Winder and Sommer, 2012).

In addition to warming, future climate change is predicted to change river flow (Arnell and Gosling, 2013; Gudmundsson et al., 2021), in some cases resulting in increased seasonality (van Vliet et al., 2013). Changes to river flow are driven by changes in precipitation, evapotranspiration, and abstraction pressures (Döll et al., 2009; IPCC, 2014). Changes to discharge can be large, and, unlike air temperature warming, may be bi-directional. Projected changes to river flow range from large increases (>50%) to large decreases (>80%), depending on the climate projections, geographic region (Arnell et al., 2015; van Vliet et al., 2013) and even between catchments in the same region (Fowler and Kilsby, 2007; Garner et al., 2017a). Super-imposed on to annual changes, are potential changes to seasonality of river flows resulting in larger peak flows and lower low flows (Prudhomme et al., 2013; van Vliet et al., 2013). Projections of regional and local river flow changes, even when just considering precipitation and evaporation changes, are generally much more uncertain than those for air temperature (IPCC, 2014). By investigating a range of discharge changes, it is possible to gain some understanding of the sensitivity of in-lake responses and on the processes impacted in different regions, given the uncertainty around future discharge changes.

The water temperatures in lakes are controlled by the heat budget, the culmination of heat fluxes acting on the lake. The primary heat fluxes are at the air-water interface and are short-wave radiation, long-wave radiation, sensible and latent heat fluxes (Schmid and Read, 2021). Throughflows also contribute to the heat budget of lakes, as an advective heat flux, affecting their thermal structure (Carmack et al., 1979; Livingstone and Imboden, 1989; Smits et al., 2020). The contribution of the advective heat flux from throughflows can be an important cooling source in the summer, counteracting surface heating (Carmack et al., 1979; Colomer et al., 1996; Fink et al., 2014a), as generally inflows bring in cooler water than that which is exported by the outflow. Therefore, changes to inflow discharge may modify the contribution

of the advective heat flux to the overall lake heat budget, altering in-lake thermal conditions (Fenocchi et al., 2017; Livingstone and Imboden, 1989; Smits et al., 2020).

Despite the role of lake throughflows in the lake heat budget, few studies have considered the sensitivity of in-lake temperatures to long-term shifts in river flow on lakes (Barontini et al., 2009; Bayer et al., 2013; Komatsu et al., 2007; Taner et al., 2011). As the advective heat flux scales with discharge and inversely with lake size (Schmidt and Read, 2021), the effects of the advective heat flux are likely to be at their largest in small, short-residence time lakes. There are many of these lakes globally; lakes under 1 km² with a residence time of < 100 days make up more than one in five of lakes globally (Messenger et al., 2016). Furthermore, smaller lakes have a disproportionate influence on global biogeochemical cycles (Downing, 2010; Holgerson and Raymond, 2016), and their mixing energy is more influenced by heating/cooling fluxes than by wind (Read et al., 2012), so changes to net heat fluxes could have larger impacts on these lakes than on larger lakes. Therefore, global changes to discharge could affect the heat budget and thermal structure of many lakes worldwide and have consequent global impacts on biogeochemical cycling.

The climate change impacts of air temperature warming and river flow changes will not act in isolation, and are likely to interact (Woolway et al., 2020). Therefore, there is a need to study the two in combination to understand fully the multivariate effects of climate change on lakes. By assessing air temperature and flow impacts on lake temperatures and thermal structure in combination, there is also an opportunity to compare the magnitudes of changes driven by each, to understand their importance to future thermal conditions. Furthermore, climate warming will also affect river temperatures (van Vliet et al., 2013), indirectly affecting lakes, by modifying the advective heat flux (Fink et al., 2014b; Råman Vinnå et al., 2018). Quantifying the contribution of these interacting, direct and indirect effects will provide a more complete analysis of lake ecosystems sensitivity to climate change.

In this paper, we use a one-dimensional hydrodynamic model to test the sensitivity of lake thermal conditions to incremental changes in air temperature and inflow discharge. We assess the independent and interacting effects of realistic changes in air temperature and discharge for a small, short-residence time lake in the northwest of England, highlighting the potential impact of climate change on this lake type. Using ranges of future conditions predicted for this temperate region:

- 1) We assess how changes to inflow discharge may compound air temperature warming in lakes, further increasing water temperatures, stratification duration, and water column stability.
- 2) We show the seasonality of discharge effects on lake temperatures and demonstrate the importance of considering discharge changes, especially in small lakes, when determining climate change impacts on lake thermal conditions.
- 3) We demonstrate the indirect effects of inflow warming as another important consideration for future climate impacts.

7.3 Materials and methods

7.3.1 Study site

Elterwater, the study site for this experiment, is a small, short-residence time lake in the northwest of England, UK (54.4287 °N, 3.0350 °W). The modelling was conducted on the inner basin (Figure 7.1 and Table 7.1) of the lake, the smallest of the lake's three basins, hereafter referred to as Elterwater-IB, as an example of a small, short-residence time system in a temperate region. Elterwater-IB is fed by several small, ungauged tributaries and, since 2016, by pipeline from the lake's main inflow the Great Langdale Beck (Figure 7.1). The basin has a history of anthropogenic nutrient additions that has produced nutrient-enriched sediments and high rates of internal loading during the summer stratified period (see Olsson et al., 2022; Chapter 4).

Table 7.1 Hydromorphometric characteristics of the inner basin of Elterwater (Elterwater-IB). Data from 2015 Lakes Tour (Maberly et al., 2016) and Haworth et al. (2003).

Characteristic	Elterwater-IB
Mean depth (m)	3.3
Maximum depth (m)	6.5
Elevation (m a.o.d)	53
Surface area (km²)	0.03
Annual WRT (days)	20

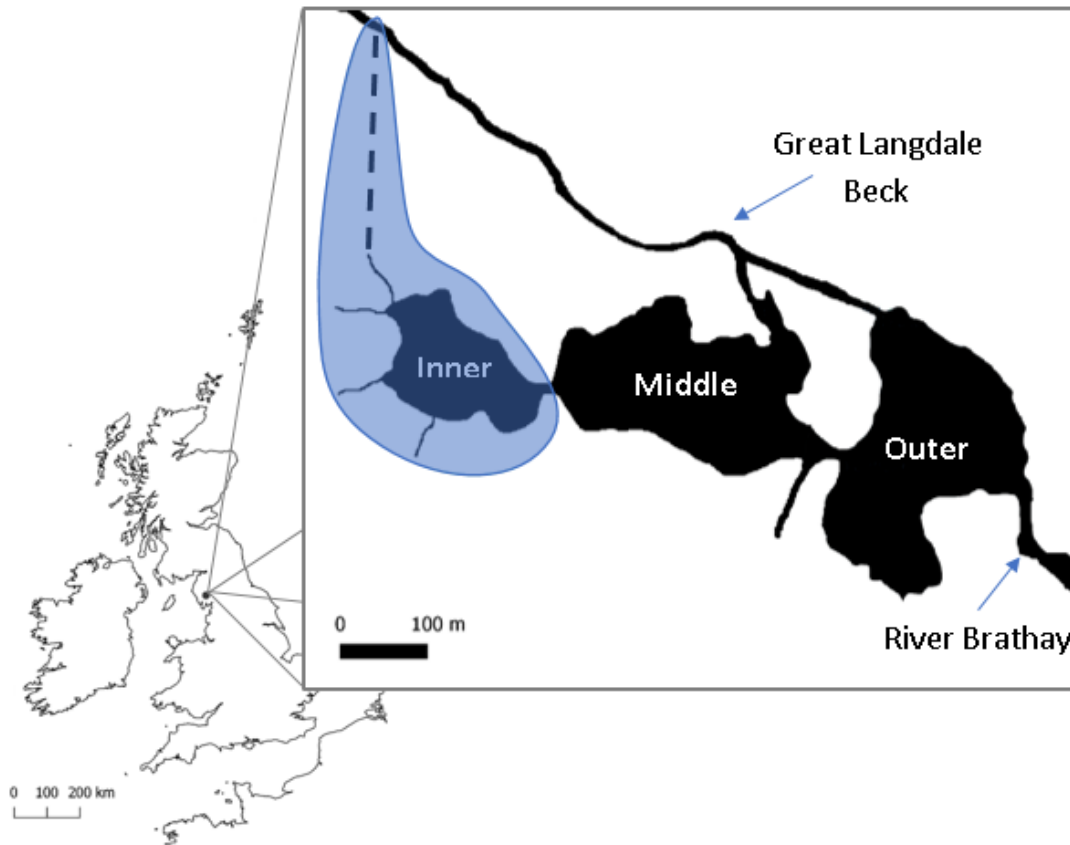


Figure 7.1 Map of Elterwater. The main inflow (Great Langdale Beck) and outflow (River Brathay) are shown alongside the pipeline diversion constructed in 2016 (dashed line). Elterwater inner basin, the modelled system, is highlighted.

7.3.2 The General Ocean Turbulence Model

In this study, the General Ocean Turbulence Model (GOTM), a 1-D process-based water column model, is used to model lake temperatures. GOTM uses measured meteorological data, inflow data, and bathymetry to model vertical mixing dynamics, lake surface heat fluxes, and temperatures in natural waters (Burchard et al., 1999; Umlauf and Burchard, 2005). Since its development, GOTM has been applied to a number of lakes (Darko et al., 2019; Kerimoglu et al., 2017; Moras et al., 2019) successfully replicating in-lake thermal conditions and mixing dynamics. In this study, GOTM was driven using hourly meteorological data using a vertical spatial resolution of 0.12 m (50 layers) across the top 6 m of the water column for eight years (2012-2019).

7.3.3 Boundary and initial conditions

The required meteorological driving data (air temperature, wind speed, relative humidity, and short-wave radiation) are not measured at Elterwater, so observations from an automated water monitoring buoy at Blelham Tarn were used. Blelham Tarn is close to the study site (< 5 km), is a similar size (0.1 km²), and has a similar elevation and fetch. The automated monitoring

buoy records meteorological and lake variables at 4-minute intervals, 2.5 m above the lake surface. Hourly averaged data was used to drive the model. GOTM requires a continuous time series of meteorological data and so gap filling of meteorological data was done using linear interpolation for small gaps (< 24 hours or 6 hours for short-wave radiation). For larger gaps, relationships with other meteorological stations were used to fill in the time series (see Section 7.7.1).

Before the pipeline construction in 2016, the flow through the inner basin was estimated to be 2 % of the measured outflow of the whole lake (EA, 2000). The flow used for 2012 to 2015 is therefore 2 % of the lake outflow and from 2016-2019 2 % of the lake outflow plus the gauged pipeline flow. The pipeline's discharge for 2016-2019, was provided by South Cumbrian Rivers' Trust. To get a continuous time series of flow data, required for GOTM, gaps were filled using a statistical relationship between the diversion flow measurements and the gauged outflow, taking into account abstraction limits and minimum river flow requirement in the water source set by regulating authorities (see Section 7.7.2.1). Inflow temperature was measured at the pipeline from July 2017 and a relationship developed between inflow temperature and a rolling average of the previous 12 hours air temperature (R-squared = 0.880, RMSE =1.30 °C, see Section 7.7.2.2), to estimate temperatures prior to this.

In-lake temperature profiles were measured at the deepest point in the inner basin, using RBRsolo temperature sensors (accurate to ± 0.002 °C), every 4 minutes at 0.5, 1, 2, 3, 4, 5, and 6 m. Hourly averaged profiles were used in the calibration and validation of the model. No initial profile was available for January 2012, so a 5 °C isothermal profile was specified, typical for January conditions in the lake. Different initial conditions were also tested but were not found to affect the responses.

7.3.4 Calibration and validation

GOTM was calibrated for Elterwater-IB using observations from 2018. Model fit was assessed against water temperature profile observations. An auto-calibration tool, ACPy (Bolding and Bruggeman, 2017), was used for calibration. ACPy estimates the best parameter set using a differential evolution method based on a maximum-likelihood measure. Each calibration routine had 2000 model runs, each with different parameter values, trending towards a best fit. GOTM was calibrated using six parameters (Table 7.2): three non-dimensional scaling factors relating to wind speed (wsf), short-wave radiation (swr), and outgoing surface heat flux (shf) plus the physical parameters minimum kinetic turbulence (k-min), non-visible (g1) and visible light attenuation (g2). g1 was estimated as 0.45, based on the median from Woolway

et al. (2015) prior to the auto-calibration routine. Observations of Secchi disk extinction depth from 2018-2019 were used to give the range of visible light extinction (g_2) used in the calibration routine.

$$g_2 = \frac{1}{k},$$

where k the light extinction coefficient, derived from Secchi disk extinction depths (Z_{SD}), calculated according to Kalff (2002):

$$k = \frac{1.7}{Z_{SD}}.$$

The calibration estimated model parameters that gave good agreement between the modelled and observed water temperatures, based on three metrics: root mean square error (RMSE), Nash-Sutcliffe efficiency (NSE), and mean absolute error (MAE),

$$RMSE = \sqrt{\frac{\sum_{i=1}^n (mod-obs)^2}{n}},$$

$$NSE = 1 - \frac{\sum (obs-mod)^2}{\sum (obs-\bar{obs})^2},$$

$$MAE = \frac{\sum |mod-obs|}{n},$$

where *mod* and *obs* are the modelled and observed water temperatures. A model validation was carried out using water temperature observations from 2019. The model validation demonstrated a good fit between observed and modelled water temperatures (Table 7.2).

Table 7.2 The maximum, minimum and final parameters values, optimised during the auto-calibration route. Model performance statistics for the calibration (2018) and validation (2019) periods reported as root mean squared error, Nash-Sutcliffe efficiency and mean absolute error.

Calibration factor	Max allowable value	Min allowable value	Final parameter value
swr	1.1	0.85	0.95
shf	1.2	0.8	0.80
wsf	1.1	0.9	1.08
k-min	1.0 e ⁻⁵	1.4 e ⁻⁷	1.4 e⁻⁷
g2	0.5	2	0.61

	RMSE (°C)	NSE	MAE (°C)
Calibration	0.93	0.97	0.72
Validation	0.97	0.92	0.75

This calibration and validation routine, in which an independent year of sub-daily water temperature profiles are used in each, is consistent with many lake hydrodynamic modelling studies, including for large model inter-comparison project (Golub *et al.*, in review).

7.3.5 Experimental scenarios

In order to understand the lake's sensitivity to changes in air temperature and flow conditions, we have chosen to utilise an incremental approach in which plausible but arbitrary modifications to climatic variables are made (Abdo et al., 2009). These synthetic incremental scenarios can be used to investigate a wide range of boundary conditions and test a system's sensitivity to climate changes (Abdo et al., 2009). The incremental method also allows us to disentangle responses to particular drivers that may co-occur (Soares and Calijuri, 2021), in this case, flow and air temperature changes, and investigate the underlying mechanisms and processes influenced by these climate variables (Snortheim et al., 2017). The use of bias-corrected climate model projections that apply future meteorological changes simultaneously, make inferring how individual changes impact processes problematic. Incremental methods have been used to investigate a wide range of climate change scenarios in lakes. For example, to explore how modified meteorology and/or flow affect lake thermal structure, anoxia, and/or phytoplankton assemblages (e.g. Christianson et al., 2020; Darko et al., 2019; Elliott and Defew, 2012; Snortheim et al., 2017), to investigate the combined impacts of nutrient loads and water temperature on lake ecology (e.g. Elliott et al., 2006; Rolighed et al., 2016), and to disentangle the response of phytoplankton communities to changes in mixed depth and temperature (Gray et al., 2019).

Using the validated model, two experiments were run, investigating the effect changing discharge (Q) on in-lake thermal conditions and its interaction with air temperature warming, the primary impact of climate change (IPCC, 2014) and the primary focus of many climate impact studies. Across the two experiments, we used nine temperature increments ranging from +0.5 to +4 °C of warming and seven discharge increments ranging from a 50% reduction to a 50% increase. The extremes in discharge and temperature changes were based on likely scenarios for the northwest of England, under future climate, by the end of the century. Previous catchment and hydrological modelling of the river flow in the region have predicted minor annual average decreases in river flow (<5%; Fowler and Kilsby, 2007; Prudhomme et al., 2012). However, seasonal changes in discharge can be more than an order of magnitude higher: 10-80% reductions in summer and 0-40% increases in winter, depending on the catchment and emissions scenario (Fowler and Kilsby, 2007; Ockenden et al., 2017; Prudhomme et al., 2012). Future projections for the Brathay catchment flow, in which Elterwater sits, from Prudhomme et al. (2012) estimate a reduction in summer of up to 70% and an increase of up to 30% in winter under a medium emissions scenario (see Section 7.7.3).

In the first experiment, GOTM was run for each combination of air temperature and inflow discharge changes (63 scenarios), looking at the combined and individual effects of air temperature and inflow changes on the thermal structure. Included in the air temperature scenario was the impact of warming on the inflow temperature, using the relationship developed from observations of air temperature and inflow temperature (see section 7.7.2.2) as per Valerio et al. (2015). In the second experiment, the same scenarios were run, but the air temperature changes were not applied to the inflow temperature, allowing us to quantify the how changes to inflow temperature impact in-lake thermal conditions, independent from discharge effects. River flow warming (van Vliet et al., 2013) has not been investigated previously as a potential driver of in-lake warming relating to climate change and may be indirectly affecting lakes, by modifying the advective heat flux (Fink et al., 2014b; Råman Vinnå et al., 2018).

Each scenario was run for an eight-year period (2012-2019) with the modified air temperature and/or inflow conditions. By running a multi-year scenario, and estimating the mean effects and the standard deviation, an understanding of the uncertainty derived from inter-annual variability in climate forcing can be gained.

7.3.6 Post-modelling analysis

Modelled water temperature profiles were used to calculate physical metrics. Schmidt stability, a measure of water column stability (Idso, 1973), was calculated using the LakeAnalyzer R package (Read et al., 2011). Mixed depth was estimated using two methods, as the mixed depth estimation can depend on the method used (Gray et al., 2020; Wilson et al., 2020). Method 1 used a modified version of rLakeAnalyzer, based on a maximum density gradient to define the thermocline and minimum density difference of 0.1 kg m^{-3} between top and bottom. Method 2 estimated mixed depth as the first depth with a density difference of 0.1 kg m^{-3} from the surface. These metrics, plus water temperatures, were averaged at a seasonal timescale for each of the eight years. The seasons were defined as follows: spring = March, April, May; summer = June, July, August; autumn = September, October, November; winter = December, January, February.

A minimum density difference between the top and bottom of the water column of 0.1 kg m^{-3} was used to define when stratification occurred and from this, the following stratification metrics were calculated for each year of the model run:

1. the longest continuously normally-stratified period (the length of the longest continuous period for which the density difference threshold, 0.1 kg m^{-3} , is exceeded and the surface temperature exceeds bottom temperature),
2. onset and overturn dates of the longest normally-stratified period (the date bounds for the longest continuously stratified period, as defined above),
3. cumulative number of hours per year of inverse stratification (number of hourly time steps that the density difference threshold is exceeded, and bottom temperature exceeds surface temperature),

Using the eight years of data, we calculate the change to mean conditions, as a percentage and an absolute change, and calculated the standard deviation of the changes, as a measure of variability between years. The air temperature-equivalent effect was also estimated for each discharge scenario (i.e. the air temperature change required to produce the equivalent change in response variable to that induced by the discharge change), by linear interpolation.

7.4 Results

7.4.1 Surface water temperature

Firstly, the scenarios with air temperature and discharge changes in isolation are presented. As expected, surface water temperatures (SWTs) increased with air temperature increases, with the effect relatively consistent between seasons (Figure 7.2a). Mean SWTs increased linearly by approximately $0.4 \text{ }^{\circ}\text{C}$ for each $0.5 \text{ }^{\circ}\text{C}$ of air temperature warming. The effect of changing discharge on SWT, both on the direction and magnitude of the impact, was dependent on season (Figure 7.2b). Discharge increases cooled SWTs in summer but warmed SWTs in winter, with smaller changes to SWT ($<0.2 \text{ }^{\circ}\text{C}$) in spring and autumn. Conversely, discharge decreases caused warming of SWTs in the summer but cooling in the winter. SWTs were also more affected by discharge decreases than increases, in both summer and winter. A 50% discharge reduction modified summer SWT by $+0.6 \pm 0.1 \text{ }^{\circ}\text{C}$ and winter SWT by $-0.7 \pm 0.1 \text{ }^{\circ}\text{C}$, compared to only $-0.4 \pm 0.07 \text{ }^{\circ}\text{C}$ in summer and $+0.3 \pm 0.05 \text{ }^{\circ}\text{C}$ in winter with 50% increased discharge.

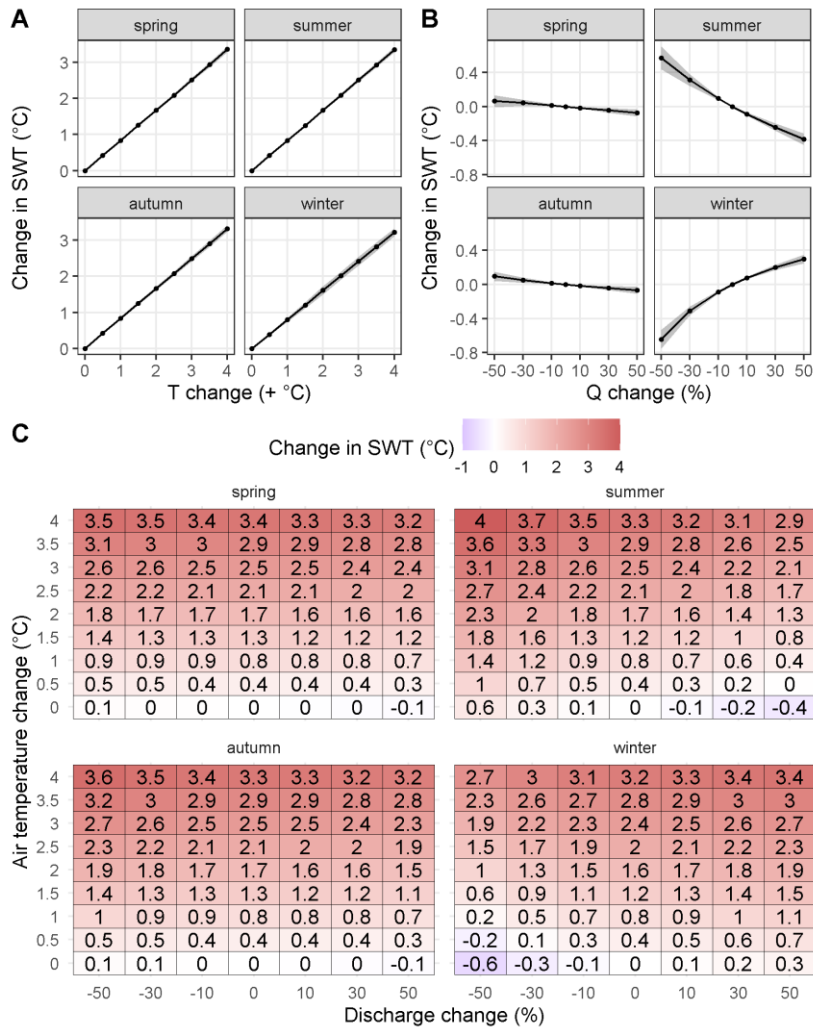


Figure 7.2 Change in surface water temperature (SWT) for A) air temperature (T) change, individually, B) discharge (Q) change, individually and C) the combined effect of change in air temperature and discharge. Values represent the difference from unmodified air temperature and flow conditions. Grey shading on A) and B) shows ± 1 standard deviation around the mean.

The results for the combined discharge and air temperature experiment showed that the change in summer SWT with discharge was relatively consistent across all air temperature scenarios tested (-0.4 °C with 50% increase and approximately $+0.7$ °C with 50% decrease: Figure 7.2c). The cooling of summer SWT caused by 50% discharge increase is greater than the 0.5 °C air temperature warming effect. The difference in SWT between a 50% increase and 50% decrease in discharge was between 0.7 ± 0.2 °C to 1.1 ± 0.2 °C in summer and 1.0 ± 0.2 °C to 0.7 ± 0.3 °C in winter (Figure 7.2c). The cooling effect of a 50% discharge reduction on winter SWT, reduced at higher rates of air temperature warming, from -0.6 ± 0.1 °C at 0 °C air temperature warming to -0.5 ± 0.1 °C at 4 °C air temperature warming. The cooling of winter SWT caused by a 50% discharge decrease negated a 0.5 °C air temperature increase. Conversely, increasing discharge by 50% compounded the air temperature warming effect.

The warming effects of discharge changes can be interpreted as the equivalent air temperature change required to produce the response induced by discharge changes – here referred to as the *air temperature equivalent*. In summer, the air temperature equivalent of a 50% discharge reduction was between 0.7 and 0.8 °C, increasing marginally at higher rates of air temperature warming (Figure 7.3a). Increasing discharge in winter produced an air temperature equivalent effect up to 0.4 °C when discharge increased by 50%, with the effect diminishing at higher rates of air temperature warming (Figure 7.3b).

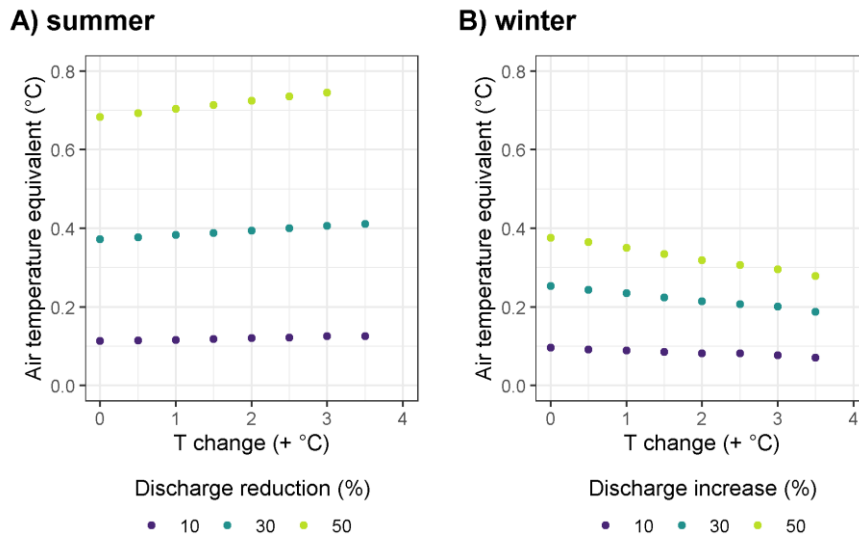


Figure 7.3 The air-temperature equivalent change in surface water temperature (SWT) caused by discharge reductions in summer (A) and discharge increases in winter (B) for each air temperature scenario. Only discharge scenarios that induced lake warming are included (reductions in summer and increases in winter). The effect of discharge changes alongside a 4 °C air temperature warming (and 3.5 °C & -50% Q in summer) were beyond the temperature-only effect at 4 °C so cannot be interpolated.

7.4.2 Bottom water temperature

The scenarios with air temperature and discharge changes in isolation are presented (Figure 7.4a and Figure 7.4b). The change in bottom water temperatures (BWTs) showed a seasonal response to air temperature warming, however, changes were smaller, and variability was higher, than for SWTs (Figure 7.4a). The rate of warming of BWTs was slightly higher in the winter than summer, increasing by $1.7\text{ °C} \pm 0.6\text{ °C}$ with 4 °C warming compared to $1.3\text{ °C} \pm 1\text{ °C}$ in summer. The greatest BWT increases were seen in autumn, warming by 0.3 to 0.4 °C per 0.5 °C of air temperature change, reaching a maximum of $2.8 \pm 0.9\text{ °C}$ of warming under a 4 °C warming air temperature.

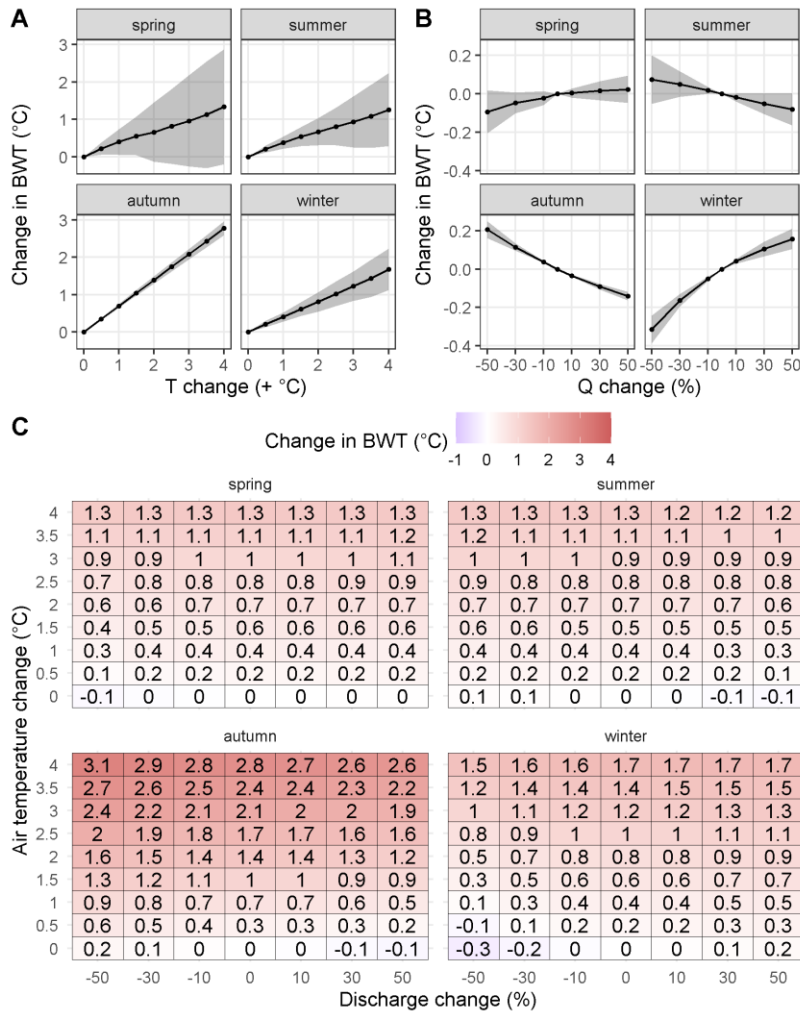


Figure 7.4 Change in bottom water temperature (BWT) for A) air temperature (T) change, individually, B) discharge (Q) change, individually and C) the combined effect of changes in air temperature and discharge. Values represent the difference from unmodified air temperature and flow conditions. Grey shading on A) and B) show ± 1 standard deviation around the mean.

There was a minor (<0.1 °C) effect of Q change on BWT in spring and summer (Figure 7.4b). Discharge changes had more of an effect in winter and autumn, changing bottom temperatures by -0.3 °C \pm 0.1 °C and $+0.2$ °C \pm 0.0 °C with a 50% reduction and by $+0.2$ °C \pm 0.1 °C and -0.1 °C \pm 0.0 °C at 50% increase (Figure 7.4c).

7.4.3 Stability and stratification

Under warming air temperature, the water column became more stable. Summer Schmidt stability increased by $6-8 \pm 1-16$ % and density difference between top and bottom by $5-7 \pm 1-16$ %, per 0.5 °C of air temperature warming (Figure 7.5a). Increases in discharge reduced the stability of the water column in summer due to the increased cooling effect of the throughflow. Stability was reduced by approximately $6\% \pm 2\%$ (Figure 7.5b) under a 50% increase in flow. Conversely, the cooling effect of the discharge in summer was reduced when

discharge was decreased. This caused higher water column stability; $9 \pm 4\%$ more stable with a 50% reduction in discharge (Figure 7.5b). This response is equivalent to the stability change caused a 0.7-0.8 °C air temperature rise. The effect of the interaction between discharge and air temperature changes on stability is synergistic. Discharge reductions compounded the increases in stability caused by air temperature warming to a greater extent than the two factors individually, especially at the highest rates of air temperature warming (Figure 7.5c).

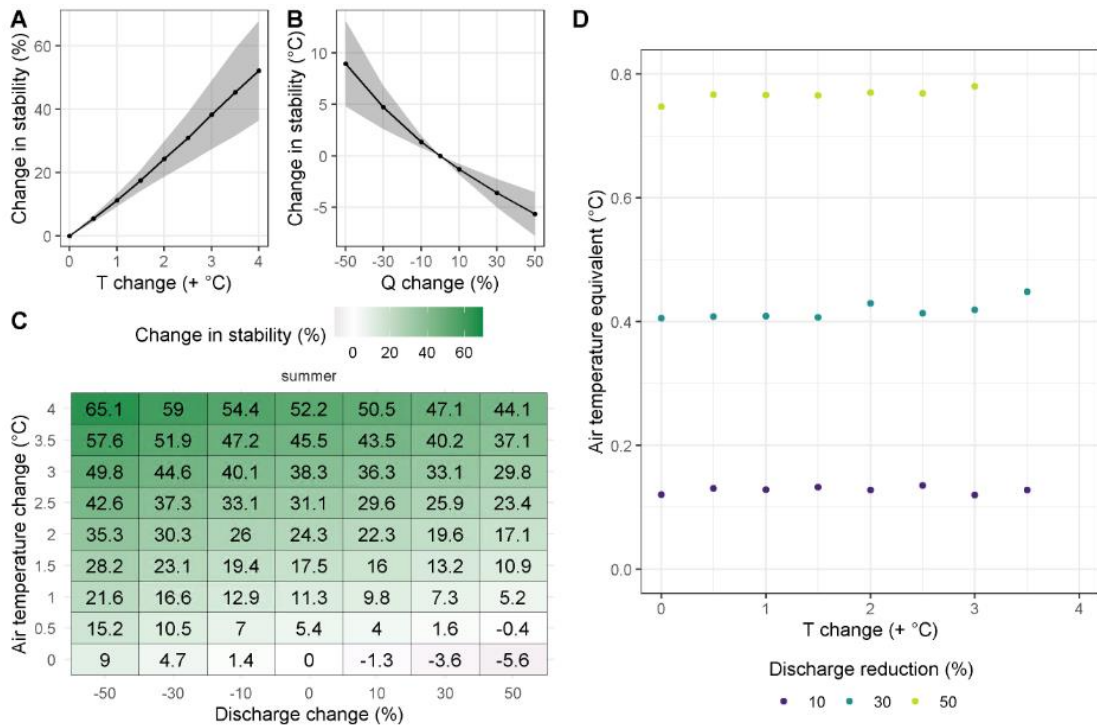


Figure 7.5 Change in summer Schmidt stability for each A) air temperature (T) change, individually, B) discharge (Q) change, individually and C) the combined effects of changes in air temperature and discharge. Values represent the difference from unmodified air temperature and flow conditions. Grey shading on A) and B) show ± 1 standard deviation around the mean. D) Air-temperature equivalent change in summer water column stability caused by discharge reductions for each air temperature scenario. The effect of discharge changes alongside a 4 °C air temperature warming (and 3.5 °C & -50% Q in summer) were beyond the temperature-only effect at 4 °C so could not be interpolated.

When air temperature was increased, greater stability also resulted in a longer summer stratified period. The mean length of the stratified period increased non-linearly with air temperature, and was up to 33 ± 23 days longer under a 4 °C warmer climate, with the impact of additional warming generally diminishing at higher levels of warming (Figure 7.6a). Longer stratification was caused by both an earlier stratification onset (27 ± 22 days; Figure 7.7a) and a later overturn (6 ± 3 days; Figure 7.7a). Under increased rates of flow, the longest period of stratification during the summer was up to 5 ± 11 days shorter (Figure 7.6b). The change in stratification length came from a later onset (2.5 ± 7.0 days, Figure 7.7b) and an earlier

overturn (2.5 ± 4.6 days; Figure 7.7b). Conversely, lower flow, and resultant reduced cooling, promoted a longer stratified period (2 ± 1 days) although no change in onset timing occurred. Reduced flow exacerbated the impacts of air temperature warming, further increasing the length of the stratified period, although the effect was non-linear. On the other hand, a 50% increase in discharge buffered the effect of an additional 0.5°C warming on summer stability and stratification length.

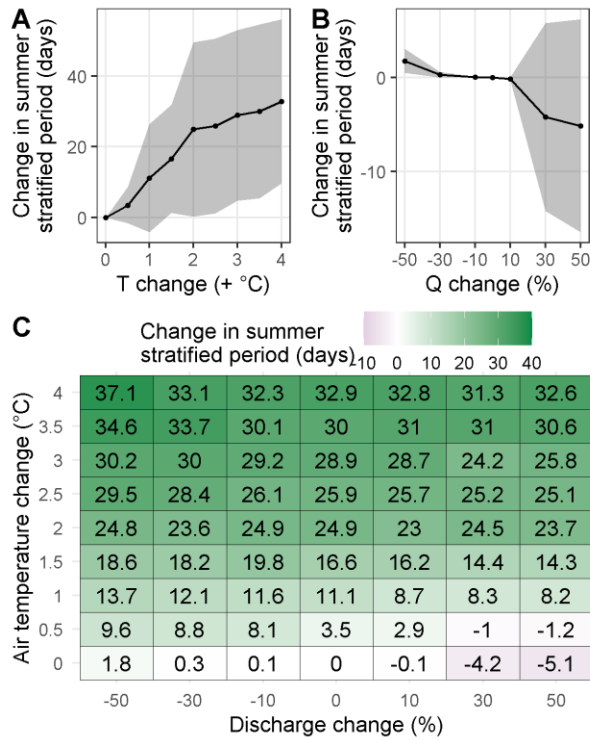


Figure 7.6 Change in length of the summer stratified period for each A) air temperature (T) changes, individually, B) discharge (Q) change, individually and C) the combined effect of air temperature and discharge changes. Values represent the difference from unmodified air temperature and flow conditions. Grey shading on A) and B) show ± 1 standard deviation around the mean.

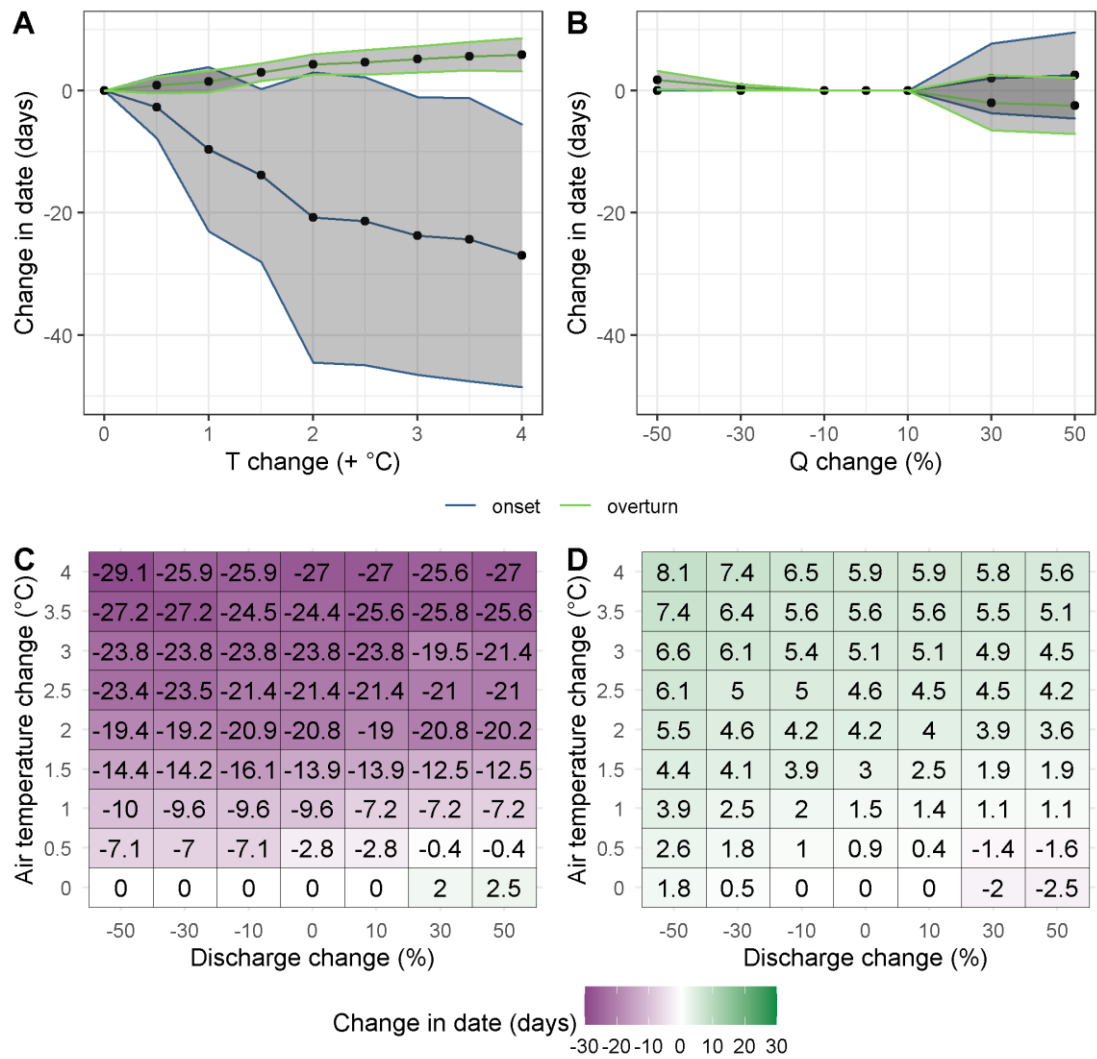


Figure 7.7 Change in the dates of onset and overturn of the summer-stratified period for A) air temperature (T) change and B) discharge (Q) changes. Panels C) and D) shows the combined effects of air temperature and discharge changes on stratification onset (C) and overturn dates (D). Values represent the difference from unmodified air temperature and flow conditions. Grey shading on A) and B) show ± 1 standard deviation around the mean.

Inverse stratification became less frequent under a warmer climate, decreasing non-linearly with air temperature warming (Figure 7.8a), with up to 112 ± 111 fewer hours of inverse stratification under a $+4$ °C warmer climate. Inverse stratification was more common under reduced discharge conditions (Figure 7.8b). There were 27 ± 24 fewer hours of inverse stratification at a 50% increase in Q, due to increased surface warming from the inflow in winter and 64 ± 35 hours more inverse stratification at 50% decrease in Q.

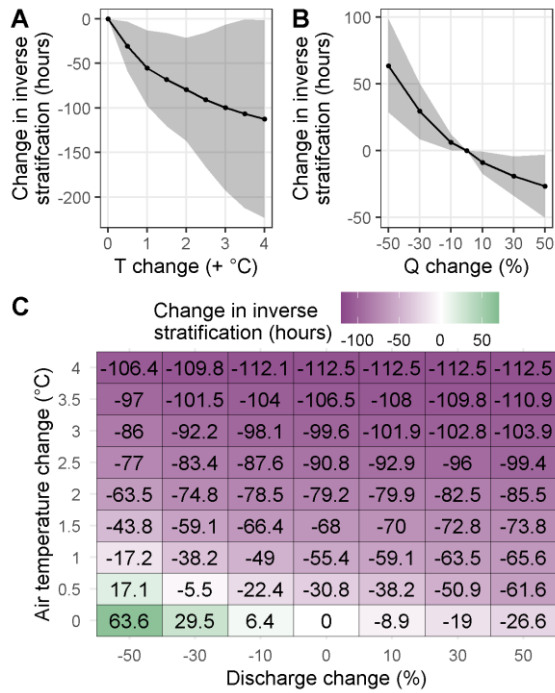


Figure 7.8 Change in inverse stratification occurrence (number of hours) for each A) air temperature (T) change, individually, B) discharge (Q) changes, individually and C) the combined effect of air temperature and discharge changes. Values represent the difference from unmodified air temperature and flow conditions. Grey shading on A) and B) show ± 1 standard deviation around the mean

7.4.4 Mixed depth

Summer mixed depth showed a shallowing with air temperature warming, although the magnitude of change was dependent on the method and definition used (Figure 7.9). The mixed depth shallowing was more than two times using Method 1 (rLakeAnalyzer) compared to Method 2 (0.1 kg m⁻³ density difference) – 0.6 m compared to 0.3 m at 4 °C warming. Changes to discharge had little effect on mixed depth, regardless of the method used (Figure 7.9), shallowing by 0.18 m at a 50% discharge reduction and deepening by 0.14 m with a 50% discharge increase. When Method 2 is used, no change in mixed depth in response to discharge changes is produced at any air temperature change.

Using Method 1, reductions in discharge compounded the shallowing of the mixed depth caused by air temperature increases and the effect of discharge change was more important at lower rates of air temperature warming (Figure 7.9). For example, at 1 °C air temperature warming, a 50% reduction in discharge resulted in another 0.16 \pm 0.1 m shallowing, whereas as at +3 °C air temperature, the same reduction in discharge only shallowed the mixed depth by an additional 0.07 \pm 0.01 m.

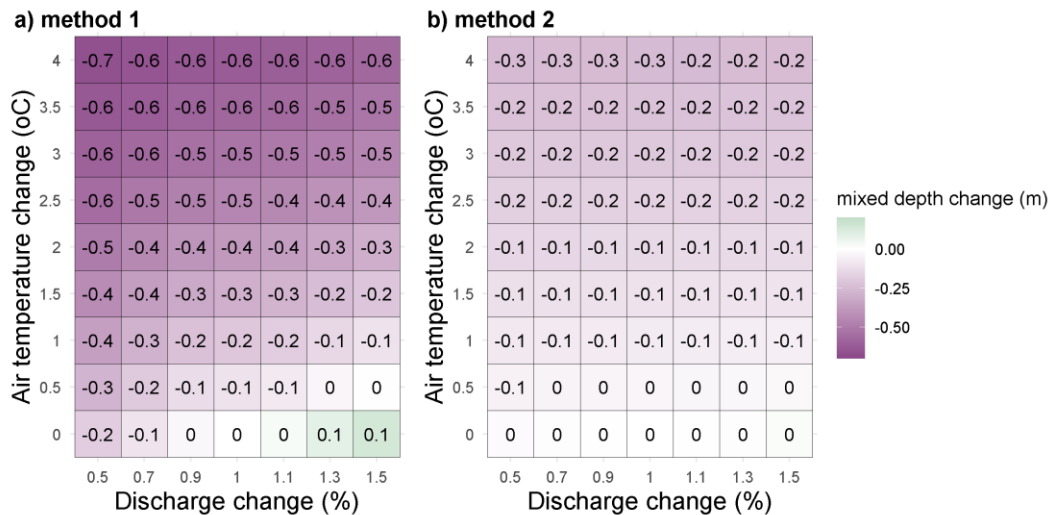


Figure 7.9 Change in summer mixed depth across different temperature and discharge scenarios using two different methods. Method 1 uses a modified version of LakeAnalyzer and Method 2 uses a density difference of 0.1 kg m^{-3} to define the mixed depth. Negative values indicate a shallowing of the mixed depth and positive values a deepening.

7.4.5 Inflow temperature importance

The air temperature and discharge scenarios were then rerun without the air temperature warming changing the inflow temperature. The effect of air temperature warming on SWT was less when the warming of the inflow was not considered. The inflow warming contributed about 25% of the warming effect in summer and >50% of the effect in winter (Figure 7.10). At 1.5 °C air temperature warming, including the inflow warming increased the effect by 0.3 °C. Including the inflow warming also moderated the effect of changing discharge, reducing the cooling effect of increased discharge in the summer, especially at higher air temperature changes (Figure 7.10). For example, the cooling effect of a 50% increase in discharge was 0.3 °C less at + 4 °C air temperature warming when inflow warming was included (0.4 °C compared to 0.7 °C). Similarly, warming effects of reduced discharge during summer were compounded when inflow warming is accounted for. At +2 °C air temperature warming, there was an additional 0.2 °C of SWT increase in summer with a 50% Q reduction when inflow warming was included (Figure 7.10a). In winter, this inflow warming effect was more important, accounting for > 40% of the warming effect of air temperature increase on SWT (Figure 7.10b). At 1.5 °C air temperature increase, the warming effect of a 50% increase in discharge was almost doubled from 0.8 °C to 1.5 °C, with the effect increasing at higher air temperature changes. By including inflow temperature effects there was a decrease in the cooling effect of reducing discharge in winter, but there is less impact on the warming effect of increasing discharge.

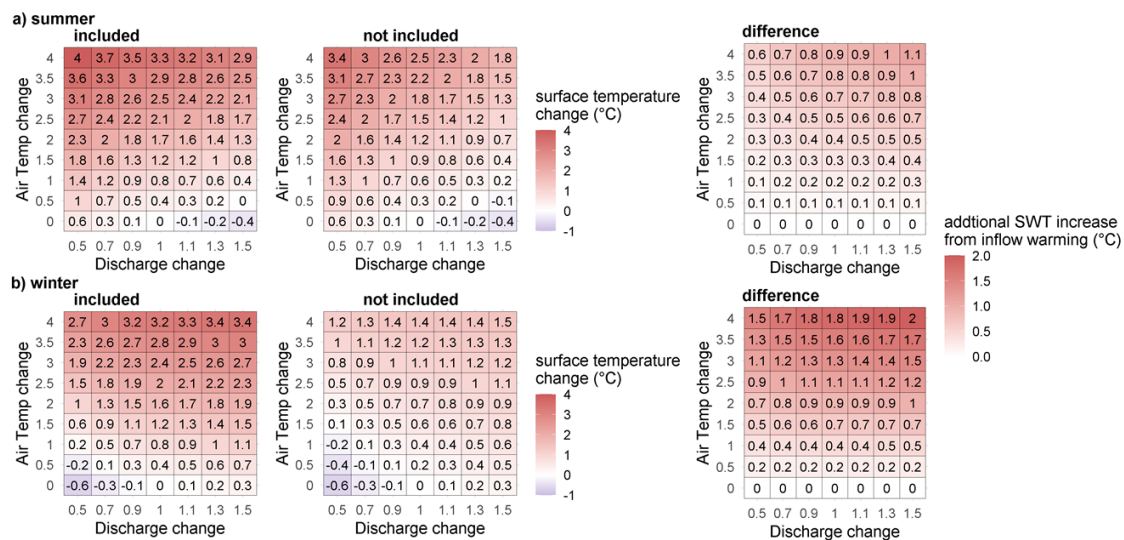


Figure 7.10 Comparison of changes in lake surface water temperatures with and without the inclusion of changes to the inflow temperature in a) summer and b) winter. Difference represents the additional warming when the inflow temperature warming is included.

7.5 Discussion

7.5.1 Discharge effects

This study investigated the sensitivity of lake thermal structure to the combined climate change impacts of increasing air temperatures and river flow changes. With 75% of the landmass expecting significant increases or decreases in discharge (van Vliet et al., 2013), a large number of lakes are likely to be affected. Our results show that impacts from discharge changes are non-negligible and can cause warming in lakes equivalent to changes caused by more than 0.5 °C of air temperature warming. Decreasing discharge by 50% increased summer SWTs by 0.6 °C, an equivalent change to that caused by 0.7 °C of air temperature warming. This lake warming is also equivalent to two to five decades of historic in-lake warming (Magnuson et al., 1997; O'Reilly et al., 2015). Lake warming of this magnitude will have direct effects on metabolic processes, which increase exponentially with linear temperature change (Kraemer et al., 2017). Higher water temperatures will also reduce oxygen saturation values by approximately 0.02 mg L⁻¹ per 0.1 °C (Jane et al., 2021; Lee et al., 2018). Warmer bottom waters will also have greater rates of sediment microbial metabolism and internal nutrient loading (Gudasz et al., 2010; Pettersson, 1998).

Warming of summer SWT with reduced flow is seen in observational (Beaver et al., 2013; Obertegger et al., 2010) and modelling studies (Bayer et al., 2013; Christianson et al., 2020; Valerio et al., 2015). Although observations are often from short-term events such as droughts, which can co-occur with water-level change decrease and increased sunshine, making the

separation of co-variate impacts difficult. Using an incremental method in this study demonstrates the importance of changes to river flow in isolation. In reality, these changes may co-occur at both long-term and short-term timescales (Allan et al., 2020; Berg et al., 2009; Park and Min, 2017), where a future warmer atmosphere is likely to intensify the water cycle and change rates of evaporation and precipitation in lake catchments. By using incremental changes and decoupling air temperature and flow changes, we have been able to identify and quantify some of the processes impacted by these co-occurring climate drivers. These results also provide insight into the sensitivity of particular systems and time periods to change in river flow, previously overlooked in the literature.

We also investigated the sensitivity of winter thermal conditions. The effect of increasing discharge by 50% resulted in winter SWTs increasing by as much as another 0.5 °C of air temperature warming, approximately equal to an additional decade of air temperature warming (O'Reilly et al., 2015; Rogora et al., 2018; Woolway et al., 2019b). Warming during winter is important for ice formation (Niedrist et al., 2018; Woolway et al., 2019b), crucial for many ecosystem processes (Sharma et al., 2019).

Discharge changes also affected the stability of the water column and the length of stratification. The increase in water column stability in summer caused by a 50% discharge reduction was equivalent to the change caused by an air temperature rise of > 0.7 °C. In stratifying lakes, increased stability reduces hypolimnetic oxygen concentrations (Foley et al., 2012; Rogora et al., 2018), through earlier and longer stratification (North et al., 2014; Smucker et al., 2021; Snorheim et al., 2017) and higher rates of oxygen depletion (Foley et al., 2012). Coupled with increased water column temperatures this can limit habitat for cold water species (Darko et al., 2019; Elliott and Bell, 2011). Reductions in hypolimnetic oxygen concentrations and shallower anoxic layer (Komatsu et al., 2007) will also promote redox conditions conducive to internal nutrient loading from lake sediments (Komatsu et al., 2007; North et al., 2014).

The impacts of flow on in-lake temperatures showed distinct seasonality due to the difference in inflow and outflow temperature (assumed to be equal to lake surface temperature). In Elterwater during summer, inflow temperature is less than outflow temperature (Figure S 7.7.4-1) so the advective heat flux is cooling, whereas in the winter inflow temperatures often exceed outflow temperature, so the advective heat flux is warming. Therefore, changes to the inflow discharge, which modified the magnitude of the advective heat flux, affected the thermal structure of the lake differently depending on the season. In systems with different

relationships between inflow and outflow temperature, the effect of changing discharge could show a different pattern. One particular difference would be in snowmelt fed systems, where changes to the timing and magnitude of snowmelt are likely to induce advective flux changes (Flaim et al., 2019; Shrestha et al., 2012). Changes to snowfall extent and snowmelt timing are important contributors to lake surface temperature changes, alongside air temperature warming (Flaim et al., 2019), with the rate of snow precipitation accounting for 90% of the variation in mean summer lake temperature (Sadro et al., 2019).

7.5.2 Interaction of discharge changes and air temperature warming

In the northwest of England, climate projections are for increases in seasonality; increased flow in winter and reduced flow in summer (Fowler and Kilsby, 2007; Prudhomme et al., 2013). Our results suggest that the projected increase in winter flow will result in warming of the lake in the winter. Lower flow in summer would result in decreased cooling from the inflow in the summer, promoting warmer SWTs and stronger stratification. The combined impacts of the seasonality of the advective heat flux (warming in winter, cooling in summer) and future projections (wetter winters, drier summers) will act to compound warming effects of air temperature rises (Råman Vinnå et al., 2018; Valerio et al., 2015) in this region at both times of year. Increased flow seasonality is projected for around one third of the global land-surface by 2070, including much of eastern and western North America, central South America, northern Europe, southern Asia, southern Africa, and Australia (van Vliet et al., 2013), further exacerbating air temperature warming in these regions. When considering dangerous levels of climate warming for lakes, the additional warming effects from discharge changes that exacerbate lake warming need to be included when determining the likely climate change impacts of air temperature warming on lakes.

In contrast, for some regions, changes to discharge may act to buffer the impacts of climate warming. Projections for the high northern latitudes and monsoon regions are for increases in discharge (van Vliet et al., 2013), which our results suggest could buffer up to 0.8 °C of warming depending on the magnitude of the flow change and the inflow-lake temperature difference. Management could also help mitigate possible temperature changes through management of water use and restricting abstraction upstream of lakes and reservoirs to limit climate impacts. Similarly, management to increase throughflow in the summer, where inflows are cooler than the lake in summer, may buffer some of the lake warming induced by air temperature rises (Bayer et al., 2013; Christianson et al., 2020; Råman Vinnå et al., 2018), especially at lower levels (0-2 °C) of air temperature change.

7.5.3 Air temperature effects

Our results show that around 80% of air temperature warming is converted into surface water temperature increases. This rate of SWT increase, 0.8 °C per 1 °C of air temperature warming, is similar to the warming seen in other studies (Bayer et al., 2013; Komatsu et al., 2007; Lee et al., 2018), although there is evidence in some lakes of faster warming than local air temperatures (Komatsu et al., 2007; O'Reilly et al., 2015). Air temperature warming also increased water column stability, as seen in other studies (Magee and Wu, 2017; Woolway and Merchant, 2019), due to larger rates of warming at the surface compared to the bottom (Niedrist et al., 2018; Taner et al., 2011; Valerio et al., 2015). Air temperature warming also increased the length of the stratified period, and stratification occurrence overall increased by 8-10 days per 0.5 °C of air temperature change. The relationship between air temperature increase, increased stability and length of the stratified period is a phenomena occurring in lakes globally (Woolway et al., 2021b).

Air temperature warming also affects lakes indirectly through warming of inflows, which is likely to be occurring at a different rate to lake temperatures (Fink et al., 2014a; Jonkers and Sharkey, 2016). Our results showed that the change to the inflow temperature contributed 25% of the lake warming effect in summer, and without accounting for inflow temperature effects, the extent of lake warming would be underestimated (Valerio et al., 2015). Evidence suggests in some regions rivers are warming at a faster rate than lakes (Jonkers and Sharkey, 2016), although the exact rate depends on local drivers such as discharge changes and riparian shading (Garner et al., 2017b; van Vliet et al., 2013). Faster warming of the inflow relative to the lake would reduce the cooling effect of inflows in summer, intensifying the warming caused by reduced flow, as we have shown.

The uncertainty in inflow temperature was relatively large (RMSE = 1.30 °C, R-squared = 0.87, Figure S 7.7.2-2), and potentially larger than the magnitude of change, so the exact impact of inflow warming on in-lake conditions should be inferred with caution. Given the uncertainty of the inflow temperature, the direction and magnitude of the advective heat flux, and the impact of flow on in-lake temperatures, may be being under- or over-estimated. However, the results demonstrate the sensitivity of lake temperatures to possible inflow warming/cooling and therefore require additional consideration in future studies. Using an ensemble of river temperature predictions or applying a process-based model will more effectively capture likely future river temperature, under a warming climate, than regression-based approaches (Arismendi et al., 2014).

7.5.4 Global relevance

The results from this study suggest that a large number of lakes globally are likely to be sensitive to changes in throughflow. Elterwater-IB, the lake basin modelled in this study, is small (0.03 km²) and has short-residence time. Small lakes, are likely to be most impacted by WRT changes and represent the majority of lake globally (Downing et al., 2006; Messenger et al., 2016; Verpoorter et al., 2014). The smallest class of lakes (0.1 – 1 km) were estimated to account for 87 % of lakes (> 1.2 million) in the HydroLAKES database (Messenger et al., 2016), using geo-spatial methods. Smaller lakes (<0.1 km), which are not counted in this method, may represent an even greater number of freshwater systems. Verpoorter et al. (2014) estimated that even smaller lakes (0.002 – 0.01 km²) make up 77% of lakes globally (90 million). Given the importance of this effect on small lakes, this is likely to be globally relevant. The residence time of Elterwater-IB is very short (annual WRT approximately 9 days). However, recent modelling showed that even at annual WRT of ≤100 days, simulations of lake temperatures neglecting inflow and outflow effects had statistically significant deviation from observations, and highlighted the importance of inflow-outflow dynamics at WRTs of this magnitude (Almeida et al., 2022). Globally, lakes with an annual WRT of ≤100 days account for 1 in 4 lakes (Messenger et al., 2016). Besides these short residence time systems, larger, longer residence time lakes have also shown the importance of inflows on lake dynamics. Lake Iseo, Italy has a WRT of 4.3 years and modelling showed that when inflow cooling effects were neglected modelled epilimnetic temperature was 3 °C warmer (Valerio et al., 2015). Lakes northern temperate thermal region, in which Elterwater-IB is located (Maberly et al., 2020), accounts for 11% of lakes globally and 13% of global landmass, are estimated to increase in number by 166% under future climate (Maberly et al., 2020), showing again the global relevance of this study.

7.5.5 Future work

Our results have shown that understanding the direction and magnitude of discharge changes is important to get accurate projections of in-lake thermal conditions, as failing to account for these changes may fail to capture the full range of climate impacts. In this study, the difference in summer SWT between a 50% increase and a 50% decrease in discharge was 1 °C, more than the warming impact of +1.5 °C air temperature change. Currently there is considerable uncertainty in the predictions of river flow under future climate, inhibiting their use in their use in management and for projecting future lake conditions (Lee et al., 2018). There is a clear need for increased modelling of future river flow to inform climate impact studies on lakes, using up-to-date regional climate projections (Kay et al., 2020), especially for smaller

freshwater systems, which are understudied and may be more susceptible to discharge changes.

In this study, the focus was on quantifying discharge effects on lake thermal structure and potential interactions with air temperature, the “headline” impact of climate change (IPCC, 2014), by using incremental changes. Using this method, including the decoupling of air temperature and flow effects, we have been able to investigate the processes affected by each of the variables in isolation and in combination. Using a range of synthetic future scenarios gives an idea of how lakes may respond to climate change and management intervention on a broader scale than would be possible when using regional climate projections. However, this study has not included other possible changes in local climate and hydrology that may be important for thermal structure, such as changes to wind speed (Magee and Wu, 2017; Stetler et al., 2020; Woolway et al., 2019a), solar radiation/cloud cover (O’Reilly et al., 2015; Schmid and Köster, 2016), water clarity (Butcher et al., 2015; Pilla et al., 2018), and lake levels (Fink et al., 2014a; Lee et al., 2018; Rimmer et al., 2011). These changes may be more or less important depending on lake morphometry and size (Kraemer et al., 2015; Magee and Wu, 2017). To gain a detailed understanding of likely future thermal conditions in individual lakes probabilistic scenarios, that use downscaled regional climate projections and integrate the effects of multiple climate and catchment stressors, will be required.

7.6 Conclusions

In this study, we have shown that thermal conditions in lakes are sensitive to modifications in river flow and that discharge changes had seasonal impacts on lake thermal structure due to the lake-inflow temperature difference. Our results showed that changes to discharge can cause changes to the lakes thermal structure equivalent to 0.8 °C of air temperature warming and could be important for a large proportion of lakes globally. Furthermore, the warming of the inflow contributes significantly (>25 %) to the discharge effect on lake thermal structure. Overall, the impact of discharge changes on lake temperatures has the potential to exacerbate or buffer the impacts of air temperature rises, depending on the direction of change and the relationship between inflow and in-lake temperatures. Future work should include projections of river flow to capture fully lake conditions under future climate.

7.7 Supplementary information for Chapter 7

7.7.1 Protocol for processing Blelham meteorological data

7.7.1.1 Gap filling protocol for meteorological data (2012-2019)

- Gaps of less than 24 hours were filled using linear interpolation, for solar radiation maximum gap = 6 hours
- For the gaps that remained we used comparisons between Blelham and Windermere buoy meteorological data and fitted linear models between the sites (Table S 7.7.1-1). Windermere’s automatic water quality monitoring buoy measures the same meteorological data as Blelham and is situated on the south basin, approximately 2 km to the E of Blelham

Table S 7.7.1-1 Linear regression between Blelham and Windermere buoy data variables

Variable	% missing before	% missing after	Intercept	Slope	<i>p</i>	Adjusted r-squared
Air temperature	6.8	0	-0.978	1.056	< 0.001	0.957
Wind speed	4.4	0.3	0.090	0.548	< 0.001	0.572
Solar radiation	1.9	0	3.913	0.931	< 0.001	0.895
Relative humidity	4.2	1.3	-1.809	1.024	< 0.001	0.863
Surface water temperature	4.3	0.04	-0.639	1.047	< 0.001	0.924

For the remaining missing values the following protocol was used:

1. Wind speed – average wind speed 24 hours previous and 1 week after the timestep.
2. Relative humidity – linear regression with between Blelham and Esthwaite Water automated water quality monitoring buoy weather station data (intercept = -5.917, slope =1.07, *p* < 0.001, adjusted R-squared = 0.915).
3. Surface water temp – linear interpolation.

7.7.1.2 Solar radiation and cloud cover calculations

R packages `suncalc` (Thieurmél & Elmarhraoui, 2019) and `insol` (Corripio, 2019)

1. The time steps before sunrise and after sunset (i.e. at night) were set to 0
2. We then calculated clear sky solar radiation. Clear sky solar radiation is dependent on the time of day and the day of the year.
3. The clear sky solar radiation was compared with the observed solar radiation to estimate the cloud cover (between 0 and 1)

$$cloud\ cover = 1 - \frac{observed}{max\ possible}$$

4. Night-time cloud cover was estimated as the mean cloud cover for the previous day

Thieurmél, B. & Elmarhraoui, A. (2019). `suncalc`: Compute Sun Position, Sunlight Phases, Moon Position and Lunar Phase. R package version 0.5.0. <https://CRAN.R-project.org/package=suncalc>

Corripio, J. G. (2019). insol: Solar Radiation. R package version 1.2.1. <https://CRAN.R-project.org/package=insol>

7.7.2 Estimating pipeline discharge and inflow temperature during unmeasured periods

7.7.2.1 Inflow discharge estimates

Using the measurements from the diversion (Jan 2016 to Dec 2019) a workflow was developed to estimate the discharge where there are gaps in the measurements (274 missing values, < 1% of data), based on the gauged discharge in the River Brathay (lake outflow). The maximum discharge through the pipeline, based on Environment Agency defined abstraction limits is $0.122 \text{ m}^3\text{s}^{-1}$. The minimum discharge in the source river when abstraction is permitted, is $0.383 \text{ m}^3\text{s}^{-1}$. The 95th percentile of measured source discharge that produced the maximum (capped) diversion discharge ($0.122 \text{ m}^3\text{s}^{-1}$) was calculated. When this discharge was exceeded in the source it was assumed the diversion discharge would be maximised ($0.122 \text{ m}^3\text{s}^{-1}$). Where the source discharge dropped below $0.383 \text{ m}^3\text{s}^{-1}$ the diversion would be $0 \text{ m}^3\text{s}^{-1}$. Between these flows a general additive model was fitted between the source and diversion discharges. The smooth was significant at $p < 0.01$ and the model had an R-squared of 0.528. The gam.check function was used to visually check model fit. Despite a relatively poor fit, < 1% of the data is estimated in this way we accepted any errors.

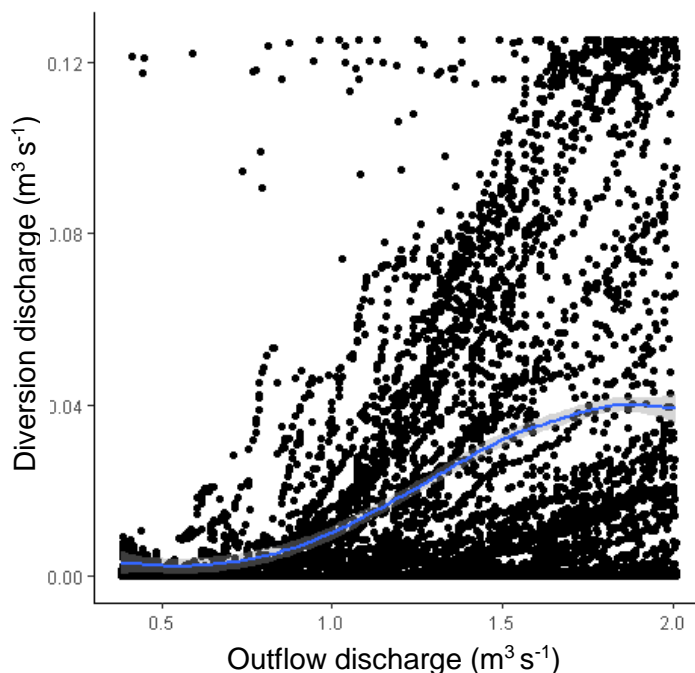


Figure S 7.7.2-1 observations (points) and model fit (line) outflow and piped discharge

```
mod <- mgcv::gam(data = comparisons, Q_m3_s.t ~ s(Q_m3_s.JK, k = 20), bs="cs")
mgcv::gam.check(mod)
summary(mod)
```

```
#use the gam to predict these values
missing_dat$t_gam <- mgcv::predict.gam(mod, missing_dat[,2:3])
```

```
> summary(mod)

Family: gaussian
Link function: identity

Formula:
Q_m3_s.t ~ s(Q_m3_s.JK, k = 20)

Parametric coefficients:
              Estimate Std. Error t value Pr(>|t|)
(Intercept) 0.0576170  0.0002488   231.6  <2e-16 ***
---
Signif. codes:  0 '***' 0.001 '**' 0.01 '*' 0.05 '.' 0.1 ' ' 1

Approximate significance of smooth terms:
              edf Ref.df    F p-value
s(Q_m3_s.JK) 16.68  18.26 1314  <2e-16 ***
---
Signif. codes:  0 '***' 0.001 '**' 0.01 '*' 0.05 '.' 0.1 ' ' 1

R-sq.(adj) = 0.534  Deviance explained = 53.5%
GCV = 0.0012972  Scale est. = 0.0012961  n = 20937
```

7.7.2.2 Inflow temperature estimates

A relationship between the mean of the previous 12 hours air temperature and water temperature was developed using the measurements taken of air temperature and inflow temperature between July 2017 and Dec 2019. This relationship was used to estimate inflow temperature prior to these measurements (2012-June 2017). A linear regression with an intercept of 3.2 and a slope of 0.67 produced an R-squared of 0.880 and a RMSE of 1.30 °C. Assumptions of the model were checked and confirmed visually.

```
> summary(lmnear_ma)

Call:
lm(formula = merge$pipe_T ~ merge$AT_ma)

Residuals:
    Min       1Q   Median       3Q      Max
-4.0825 -0.8289  0.0215  0.8135  4.7420

Coefficients:
            Estimate Std. Error t value Pr(>|t|)
(Intercept)  3.227604   0.019197   168.1  <2e-16 ***
merge$AT_ma  0.671351   0.001718   390.9  <2e-16 ***
---
Signif. codes:  0 '***' 0.001 '**' 0.01 '*' 0.05 '.' 0.1 ' ' 1

Residual standard error: 1.297 on 20911 degrees of freedom
(11 observations deleted due to missingness)
Multiple R-squared:  0.8796,    Adjusted R-squared:  0.8796
F-statistic: 1.528e+05 on 1 and 20911 DF,  p-value: < 2.2e-16
```

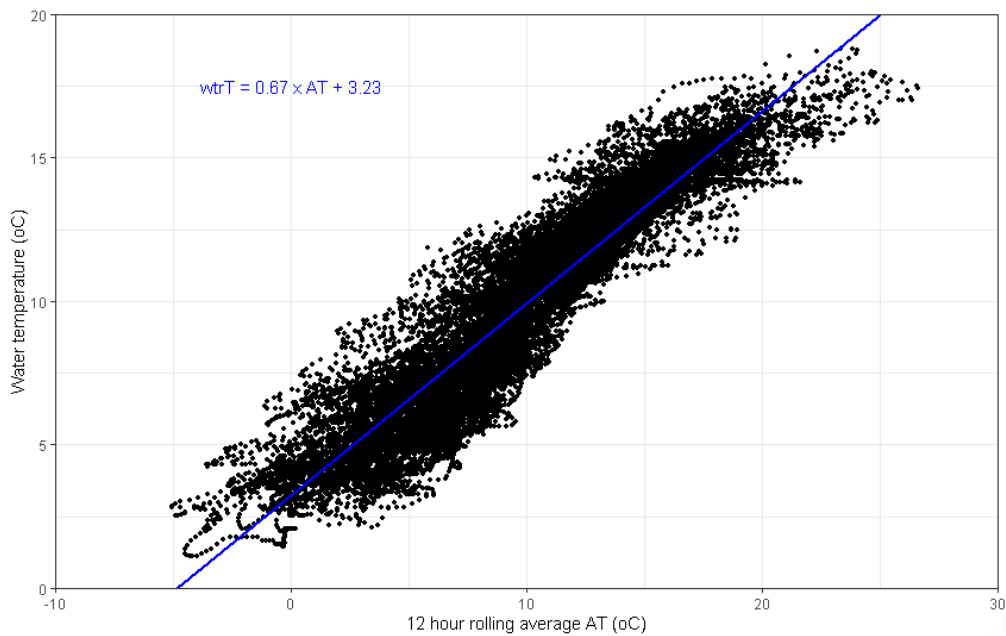


Figure S 7.7.2-2 Prediction of water temperature based on the 12 hour rolling average air temperature. Points show observations and blue line the fitted linear model

7.7.3 Future Flows predictions for the River Brathay catchment

Season	maximum	minimum	median	mean
winter	35	-3	15	14
spring	30	-13	-0.6	0.4
summer	6	-61	-30	-25
autumn	21	-25	-4	-2
Total period	9	-7	0.3	0.2

Future river flow for the Brathay catchment is predicted in the Future Flows dataset (Prudhomme et al., 2013). Future flow predictions show uncertainty based on the ensemble of 11 future predictions. The direction and magnitude of the predictions are variable – especially in the shoulder seasons where the direction of change is more uncertain

- Spring ranges from +30 to –13% change, although the central estimates (median and mean) are small (around <1% reductions)
- Autumn similarly shows a +21 to –25% change, although the central estimates are also small reductions (2-4%)
- The mean change for the whole period is small compared to the potential changes in each season. The reductions in summer and largely compensated for by increases in winter flow

Monthly summaries

Month	Maximum	Minimum	range	median	mean
Jan	50	-17	67	17	18
Feb	40	-15	55	13	15
Mar	69	-24	93	-6	0.3
Apr	35	-32	67	8	3
May	54	-22	76	-4	2
Jun	42	-55	97	-17	-9
Jul	33	-55	88	-31	-19
Aug	8	-74	82	-34	-37
Sep	1	-60	61	-30	-26
Oct	24	-26	50	5	0.1
Nov	57	-2	59	3	12
Dec	39	-8	47	11	11

- Monthly changes generally show the pattern observed in the seasonal data (reduction in Jun/Jul/Aug/Sep, increases in Nov/Dec/Jan/Feb)
- Estimates for June predictions range from a 53% increase to a 61% increase but all months show a large possible range of changes – highlighting the importance of looking at a range possibilities in the study

7.7.4 Lake-Inflow temperature difference

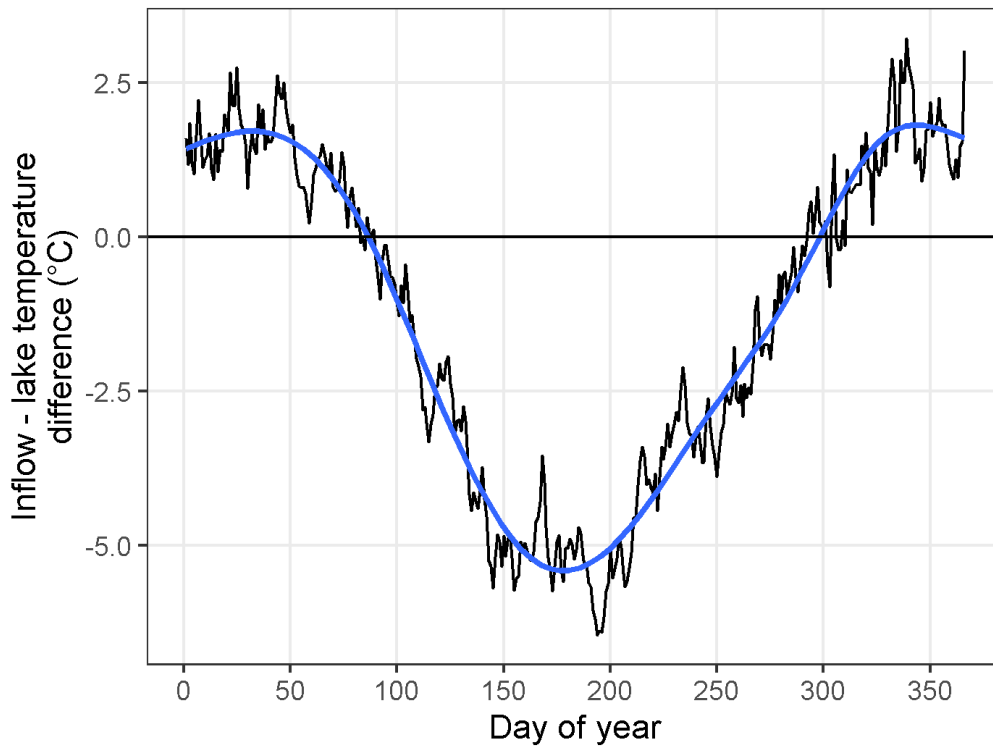


Figure S 7.7.4-1 Lake-Inflow temperature difference. Negative values are where the surface lake temperature is greater than the inflow temperature; positive values are where the inflow temperature is greater than the surface temperature. Data show are averages values for each day of the year using 2012-2019 data. Blue line is a fitted general additive model to highlight the general pattern.

Chapter 8 Discussion

This thesis has set out to investigate how changes to water residence time (WRT) impact the functioning of short-residence time lake systems, with particular focus on the thermal structure and deep-water oxygen dynamics. Investigating this topic in small/short residence time lakes is important because the global distribution of lakes is dominated by small lakes. Small, short-residence time lakes (< 100 days) make up more than one fifth of lakes (Messenger et al., 2016), and are those that will be most impacted by changes to WRTs. Ecosystem dynamics in small lakes remain under-researched considering their prevalence and their worldwide importance for biogeochemical cycling and regional biodiversity (Downing et al., 2006; Holgerson and Raymond, 2016; Scheffer et al., 2006). Eutrophication threatens lake ecosystems, prompting management interventions. Changes to WRT from the direct management of river flow have been considered as a novel restoration method, reducing WRT to inhibit stratification and seasonal anoxia that drives internal nutrient loading. Using whole-lake experiments to provide robust assessments of the effectiveness of new methods, is crucial to establish if the method can be applied more frequently as a means to restore eutrophic lakes. Climate change is also likely to impact these lakes and intensify the need for management as well as complicating the application of management actions. In addition to warming air temperatures, future climate projections show changes to evaporation and precipitation patterns (IPCC, 2014), impacting river flows. Future projections of river flow show that >80% of the global landmass is expected to experience changes in river flow (Arnell and Gosling, 2013), which will affect lake residence times. As well as changes to climate, there is potential increased pressure on water resources due to greater abstraction requirements for irrigation under warming climate (Döll et al., 2009; Rio et al., 2018), further modifying the inflow rates into lakes.

Elterwater presents an ideal case study to explore WRT changes, both WRT intervention for managing water quality as well as the global climate situation, owing to a combination of factors. Firstly, it is a rare example of WRT intervention taking place with the intention of impacting stratification dynamics. The site benefits from previous monitoring efforts, providing historical information and data. Finally, meteorological stations on nearby lakes provide high resolution meteorological data and the catchment has long-term gauged streams providing essential discharge information, which enable process-based analysis and modelling to be carried out.

The findings of this thesis contribute to our improved understanding of WRT impacts on lake systems. This discussion synthesises the evidence generated in Chapters 4-7 (Figure 8.1) of the impact of WRT changes on lake ecosystem functioning, focussing on the impacts on in-lake temperatures, stratification, and deep-water oxygen concentrations (Section 8.1). These findings will be related to lake restoration and the potential for WRT manipulations to improve lake water quality (Section 8.2). Additionally, the management of lake WRTs will be considered in the context of a changing climate, identifying the potential implications of climate-related inflow discharge changes on lake temperatures and the interaction with management action (Section 8.3). Finally, the chapter will highlight how the combined methodological approach, using fieldwork and modelling, long-term and high-frequency data, can be most useful in inferring process-based understanding (Section 8.4).

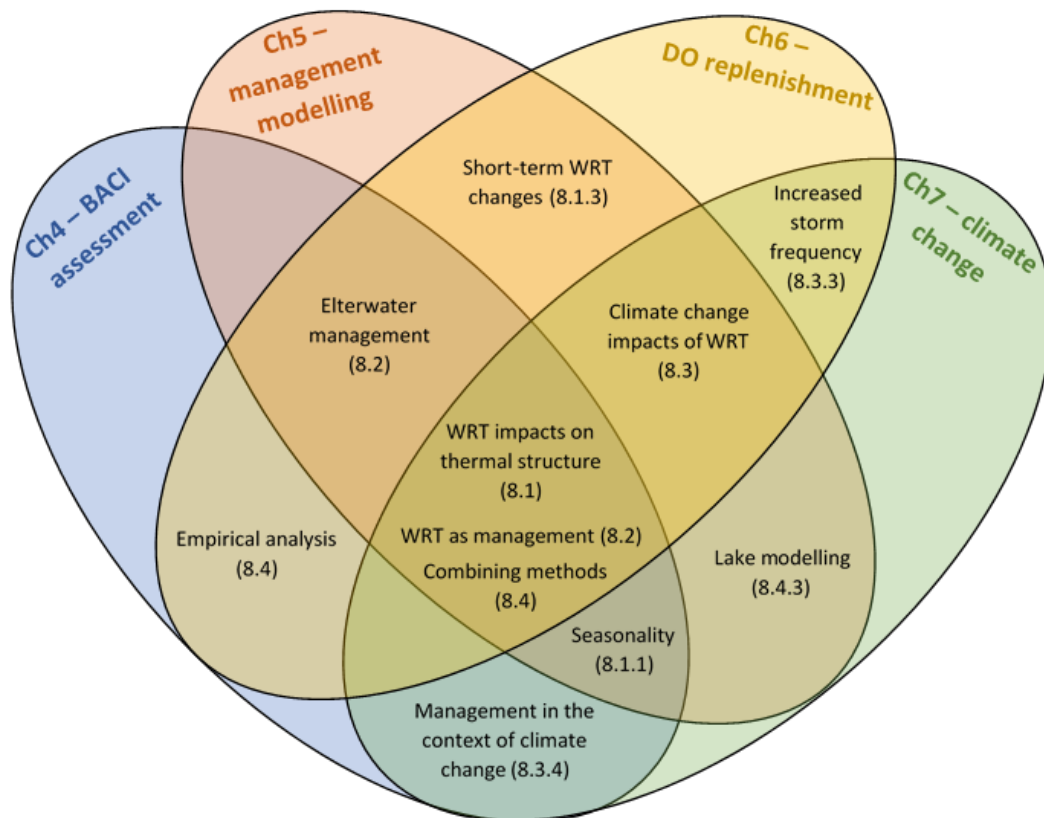


Figure 8.1 Common themes between data Chapters 4-7 and the understanding generated from the conclusions of each. Numbers in brackets correspond to the sections of the discussion in which these themes are primarily discussed.

8.1 WRT impacts on lake thermal dynamics

This thesis has investigated the impact of changes to WRT, through inflow modifications, on in-lake temperatures and stratification dynamics. By understanding the dynamics of the heat budget, and the influence of inflow discharge changes, the response of deep-water oxygen

dynamics and other lake functions is inferred (Figure 8.2). Using this understanding, the individual and combined impact of management and climate change can be investigated.

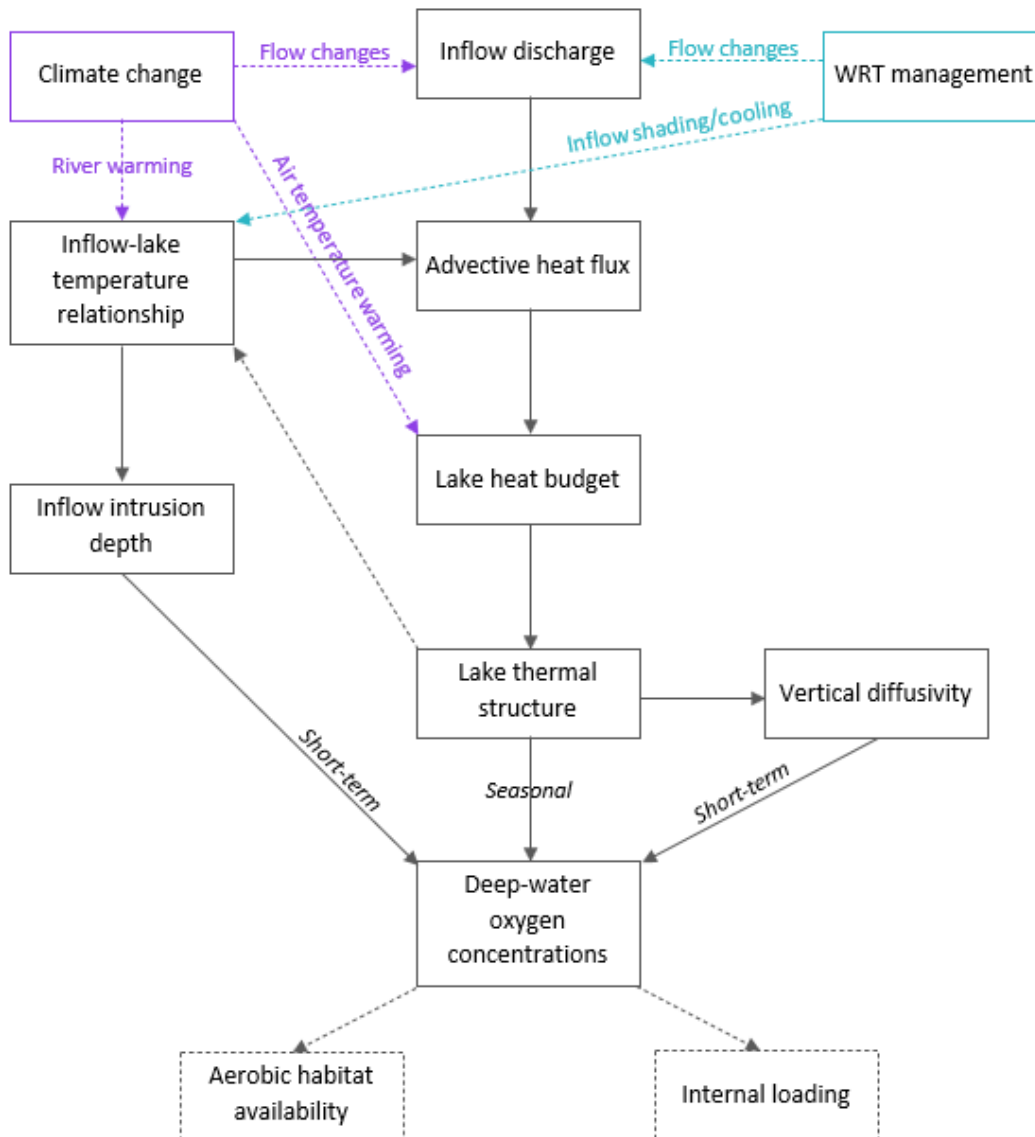


Figure 8.2 Theoretical impact of inflow discharge changes investigated in this thesis on lake functioning through its impact on the advective heat flux and lake heat budget. The theoretical system is shown in black with inferred responses (dashed). The processes impacted by management (blue) and climate change (purple) are also shown.

8.1.1 Seasonality of WRTs, the advective heat flux and its contribution to lakes heat budgets

The advective heat flux (Q_{adv}) via inflows contributes to the lake heat budget (Livingstone and Imboden, 1989). The combination of all heat fluxes determines the heat balance of the lake and subsequent lake temperatures – an important control of lake process and function. However, Q_{adv} has often been considered a minor element of the heat budget and has been frequently overlooked in previous studies, which have, instead, focused only on the surface

heat fluxes. In smaller, short-residence time lakes, Q_{adv} is likely to be more important than in larger or longer-residence time lakes and may be an important driver of thermal dynamics. Results from Chapters 4, 5 and 7 in this thesis have shown that changes to WRT, through changes in throughflow, have quantifiable and significant implications for Q_{adv} , sufficient in this short-residence time lake to have a major influence on the lake heat budget and the thermal structure, demonstrating the importance of considering this lake process in future studies.

The contribution of Q_{adv} to the heat budget, in both its magnitude and direction, is seasonal as demonstrated in Chapter 5. The seasonality in direction is caused by the difference in temperature between the inflowing and the outflowing water, meaning the throughflow is importing water with a different temperature than is being exported from the lake surface (Livingstone and Imboden, 1989). A cooling advective flux in summer is common in temperate lakes, including Elterwater, as inflowing water tends to be cooler than lake surface water (Carmack, 1979; Colomer et al., 1996), and therefore water which is exported from the lake via a surface outflow (see Figure 5.3). Conversely, in winter, inflows in north-west England can be warmer than the resident lake water inducing a warming flux (Colomer et al., 1996).

The seasonality in the magnitude of Q_{adv} is determined in part by the size of the inflow-lake temperature difference but also the discharge of the throughflow. Therefore, the lake WRT also determines the magnitude of the heat flux with larger discharge, increasing the magnitude of the heat flux (Chapter 5). WRTs exhibited a seasonal cycle due to changes in local and regional climate conditions (Chapter 4 and 5). In Elterwater, WRTs were generally longest during the summer when precipitation was low, and higher temperatures increase evapotranspiration in the catchment, thus reducing river flows (Figure 5.3) – typical of temperate lakes. High flow in winter increased the importance of Q_{adv} at this time of year despite smaller temperature differences (Chapter 4 and 5). Furthermore, during the winter lower incoming short-wave radiation increases the importance of inflow as a key heating flux. Previously identified in under-ice (Smits et al., 2020), this finding reiterates the important contribution of lake inflow heating to the lake heat budget during the winter for warm monomictic lakes.

The seasonality of the heat budget, the direction and magnitude of Q_{adv} and whether it is acting against or in addition to the surface heat fluxes, will determine the response of lake temperature to WRT changes. Natural or management-induced changes to WRT can amplify or diminish the cooling or warming advective heat flux. In other systems, different seasonal

dynamics in the direction and magnitude of Q_{adv} occur due to the distinct inflow-lake temperatures relationship. For example, in snowmelt regions large cooling fluxes can occur as a result of snow melt in early spring (Flaim et al., 2019; Shrestha et al., 2012). Changes to nival and pluvial precipitation in these regions have been shown to be modifying the timing of inflow discharge and the direction of Q_{adv} (Flaim et al., 2019; Roberts et al., 2018).

8.1.2 Changes to AWRT change the magnitude of the advective heat flux and lake water temperatures

Inflow discharge determines the magnitude of Q_{adv} , therefore modifications to WRT, through management action or from climate change, would be expected to modify the magnitude of Q_{adv} and thus in-lake temperatures, on a seasonal basis (Chapter 4, 5, and 7). WRT reductions (increased flow) caused decreased lake temperatures in the summer and increased lake temperatures in the winter, whereas increased WRT caused increased lake temperatures in the summer and decreased lake temperatures in the winter (Chapter 4, 5, and 7). Chapter 4 described how reductions in WRT, brought about by a water diversion, modified water temperatures throughout the year, cooling the lake by 0.7 °C in summer and warming the lake by 0.5 °C in winter. Further investigations in Chapter 5, showed that incremental changes in WRT had considerable impacts on lake temperatures, reaching to more than 2 °C of cooling in summer with ten times increased annual flow. At other times of year, the impact of WRT reductions was less pronounced, although marginal warming and marginal cooling were evident in spring and autumn, respectively. Previously modelling to investigate the impact of WRT changes on temperatures and stratification (Huang et al., 2016; Li et al., 2018; Straškraba and Hocking, 2002) used constant flow discharge or only looked at two contrasting scenarios (“high” vs “low” flow), which limits the realism of their results. No previous studies have integrated heat budget calculations and systematic modelling of annual WRTs, yet this work has shown the value of this method to determine impacts of flow changes to lake temperatures and therefore their potential use in managing water quality.

Changes to annual WRT were important for winter thermal conditions, which has only received limited attention in previous studies. The increased warming flux under shorter WRTs increased water temperature, caused transient normal stratification, and reduced inverse stratification occurrence (Chapters 4 and 5). These changes could have important implications for ecosystem function during the winter. Warming in winter may inhibit ice formation (Woolway et al., 2019b), promote winter phytoplankton blooms (Weyhenmeyer, 2001), and increase the occurrence of incomplete mixing (meromixis) of deeper lakes (Boehrer and Schultze, 2008; Woolway and Merchant, 2019). Climate impacts of air temperature include

winter warming and ice loss in lakes (Piccolroaz et al., 2020; Sharma et al., 2019; Woolway et al., 2019b) and additional warming due to flow changes could further exacerbate the warming trend in lakes, but this has yet to be investigated.

The cooling effect of inflows in summer, magnified by WRT reductions, affected lake summer stratification dynamics. Additional cooling at shorter WRTs, reduced the length and the strength of the summer stratified period (Chapters 4, 5 & 7; Straškraba & Hocking, 2002; Li et al., 2018), particularly expediting overturn in the autumn (Huang et al., 2014; Li et al., 2018; Wang et al., 2012). The impact of additional advective cooling at shorter WRTs, did not completely inhibit stratification at any annual WRT scenario tested (Chapter 5). This highlighted the importance of surface heat fluxes and how the interaction of advective and surface heat fluxes ultimately controls the lake thermal structure, which supports ideas from Straškraba & Hocking (2002). However, water column stability was reduced, which may prevent toxic cyanobacterial blooms (e.g. Mitrovic et al., 2011) and reduce rates of oxygen depletion in the hypolimnion (Foley et al., 2012), both important water quality parameters targeted by intervention measures. Indeed, evidence from Chapter 6 showed that short-term reductions in water column stability were associated with increased vertical mixing sufficient for oxygen replenishment in the hypolimnion.

The reduced summer cooling flux from longer WRTs, as projected under future climate (Chapter 7), lengthened and strengthened the stratified period (Chapters 5 and 7). Longer and more stable stratification can drive earlier spring bloom formation (Meis et al., 2009; Thackeray et al., 2008; Winder and Schindler, 2004), favour the growth of buoyant cyanobacteria species (Carey et al., 2012; Paerl and Huisman, 2009), and cause later and longer autumn and winter blooms (Weyhenmeyer, 2001). Furthermore, longer and more stable stratification driven by WRT changes has implications for oxygen dynamics, as the hypolimnion remains isolated from the air-water interface for longer, driving greater duration and extent of anoxia (Jane et al., 2021; North et al., 2014). Increased anoxia may increase rates of internal loading of nutrients, such as phosphorus, and metals (Komatsu et al., 2007; North et al., 2014; Nürnberg, 1987).

Previously, inflows have predominantly been considered in ecological studies as a means of loading nutrients and organic matter, with the heating and turbulent energy secondarily considered or omitted entirely. This study suggests that for short-residence time lakes, of which there are a large number globally, the impact on the heat budget should be included in considerations of inflow effects, alongside the impact of direct flushing of algal cells (Havens

et al., 2017; Padišák et al., 1999; Rennella and Quirós, 2006) and dilution and loading of nutrients (Elliott et al., 2009; Jones and Elliott, 2007), important for water quality.

8.1.3 Short term changes in WRT also impact water column stability and lake mixing dynamics

In many studies, annual WRTs are quoted for lakes, but this does not tell the full story of the impact of inflows on lake processes. As discussed above, the sub-annual understanding is important when determining how to manage WRTs for improved water quality and in determining climate impacts. At even shorter timescales (daily), WRT varies considerably. Instantaneous WRT for one year of the study (2018) varied by more than two orders of magnitude from > 500 days, to < 1 day (Chapter 5), impacting the magnitude and overall contribution of Q_{adv} .

In Chapter 6, the sub-seasonal dynamics of inflow discharge were shown to impact on lake water column stability. High discharge inflow events, lasting as short as one day, were associated with reduced water column stability and increased vertical mixing and subsequent replenishment of dissolved oxygen to the deep-water during the stratified period. Previous work suggested that vertical mixing and stability are mainly driven by surface cooling and increased wind speeds (Imberger, 2013; Saber et al., 2018) but this may not be the case for lakes such as Elterwater where inflow discharge were strongly correlated to vertical mixing (Chapter 6).

This research has demonstrated that during the stratified periods, in a shallow temperate lake, deep-water oxygen dynamics were not stationary. Previous research has focused on seasonal anoxia developing in productive lakes, linked to the length of summer stratification (Foley et al., 2012; Mackay et al., 2014a; Snorheim et al., 2017). The effect of inflows on oxygen dynamics has previously focused on the impact of cold plunging inflows in deep alpine lakes and reservoirs (Fink et al., 2016; Liu et al., 2020; Marcé et al., 2010) or the impact of multi-feature storms (reduced solar radiation, increased wind speed, high precipitation) (M. R. Andersen et al., 2020; Liu et al., 2020). However, this thesis shows that for smaller, short residence time lakes, inflow could be an important source of turbulence and mixing, contributing to short-term oxygen dynamics. Implications for redox related internal loading and aerobic habitat availability are not well understood and further investigations using high-frequency data would enable an assessment of the importance of these short-term oxygen replenishment events for biogeochemical cycling and aerobic habitat availability and highlight a potential mechanism of increasing the oxygen flux into the hypolimnion during the stratified period (see Section 8.1).

This thesis reveals that quantification of annual, seasonal, and short-term WRT changes are important for understanding lake processes and there is a need to consider WRTs at shorter timescales to improve our system understanding of how inflows impact lake ecosystems. In this thesis a lake's heat budget was quantified, determining the seasonality of the surface and advective heat flux. This methodology provided insights into the potential impacts of WRT changes for lake water temperatures, allowing lake managers to use WRT manipulations most effectively or to quantify climate change impacts. Other studies which have modelled WRT impacts on lake stratification (Liu et al., 2019; Straškraba and Hocking, 2002) have not quantified the heat budget and thus the importance of Q_{adv} in controlling stratification, therefore have failed to understand the importance of Q_{adv} to the overall heat budget. The contribution of the findings from this thesis, especially Chapters 4, 5, and 7, to the understanding of the importance of inflow to annual lake heat budgets, demonstrates that it should not be discounted as negligible, but included in the consideration of management and climate responses in future lake studies.

The results of this thesis show why quantifying the heat fluxes throughout the year is essential for determining actual and potential impacts of WRT on the lake thermal structure and determine how manipulations of flow could provide a 'nature-based solution' to current water quality problems (see Section 8.1). This work has shown WRT impacts are seasonal as well as the importance of short-term changes in WRT on thermal structure. Consequently, effective management actions should consider the seasonal or sub-seasonal impacts of WRT changes.

8.2 WRT as a management tool

Eutrophication is a prevalent and widespread problem for lake managers, resulting in high phytoplankton concentrations that can produce toxins dangerous for animal and human health (Kalff, 2002). In turn, the high oxygen consumption in the hypolimnion due to increased metabolism of organic matter, can cause widespread anoxia (Bouffard et al., 2013; Cooke et al., 2005), triggering the release of nutrients and heavy metals from enriched lake sediments (Kalff, 2002; Mortimer, 1942; Nürnberg, 1984). The combined impacts of eutrophication on lake quality, and the degradation of ecosystem services lakes provide, continues to motivate widespread application of in-lake measures alongside catchment-scale reductions in nutrient loading (Birk et al., 2020). In-lake methods are increasingly used to target internal loading of nutrients (Abell et al., 2020; Lürling et al., 2020), seen in many lakes to be slowing the recovery from eutrophication following successful catchment nutrient load reductions (Does et al., 1992; Søndergaard et al., 2003; Van Liere and Gulati, 1992).

Problems can persist in lakes decades after external nutrient reductions (McCrackin et al., 2017) as internal loading maintains water column nutrient concentrations (Huser et al., 2016b; Lürling and Mucci, 2020). Methods to control internal loading are varied in their theoretical approach, by either targeting hypolimnetic anoxia or sediment nutrient retention, and in their long-term efficacy (Bormans et al., 2016; Huser et al., 2016b; Lürling and Mucci, 2020). Sediment nutrient retention methods include targeting sediment through dredging (e.g. Bormans et al., 2016; Does et al., 1992) and chemical inactivation (e.g. Lang et al., 2016; Mackay et al., 2014; Spears et al., 2016), and hypolimnetic anoxia is targeted by using aeration and oxygenation (e.g. Preece et al., 2019; Toffolon et al., 2013). Successful implementation of in-lake internal loading management is not guaranteed, or always long-lasting, and different methods lend themselves to different lake types. Therefore, the novel method to target WRTs investigated in this thesis (Chapters 4 and 5), will provide further options to control internal loading, whether used alone or in combination with other existing methods (Jeppesen et al., 2017). For example, WRT reductions that target stratification duration and improved oxygen conditions may be supplemented with P-binding methods. Increased oxygenation of the water column may not be sufficient to prevent internal P loading, if there is not sufficient sediment retention capacity (Jilbert et al., 2020), so could be applied in combination with P-binding material such as aluminium, lanthanum, or iron compounds (Dunalska and Wiśniewski, 2016; Engstrom, 2005). Economic arguments for restoration may also promote WRT manipulation if efficacy can be optimised in individual lake systems. Methods to control internal loading can have high upfront costs (e.g. dredging, application of binding materials) and be only temporarily effective (Huser et al., 2016a; Mackay et al., 2014b). Others require constant application to be effective (e.g. bubblers, oxygenation), and therefore incur running and maintenance costs over many decades (Preece et al., 2019). Unlike other methods, WRT changes in the way implemented at Elterwater, although with high upfront capital costs, has low maintenance costs, and could continue to operate for many years.

At Elterwater, management action was taken to try and improve water quality by reducing WRTs. It was hoped that through increased flow, stratification could be inhibited, and anoxia prevented. In this thesis, the use of WRT manipulations, as a means to control internal nutrient load through targeting changes to the thermal structure of the lake, has been investigated systematically using a combination of long-term monitoring data, high frequency in-lake profiles in a whole-lake investigation (Chapter 4) and hydrodynamic modelling (Chapter 5). Previous modelling of WRT changes in lake management has assumed constant flow rates in reservoirs, potentially achieved using pumping systems, when flow management is more likely

(Li et al., 2018; Straškraba and Hocking, 2002), rather than understanding how a system could work with the natural seasonality of WRTs. This thesis investigated the potential for using WRT manipulation by enhancing natural flow regimes, in keeping with the current focus for working with natural processes to create 'nature-based solutions' in management (Seddon et al., 2020; Tickner et al., 2020).

Chapter 4 described the small, but quantifiable, impact of the restoration at Elterwater on water temperatures and water column stability, in which WRT was reduced through means of a flow diversion that reduced annual WRT by around 40% (8 days). Despite changes to the lakes physical functioning, no observable impact was found on lake chlorophyll *a* concentrations or phosphorus (as total or soluble reactive), primary indicators of eutrophication. This robust statistical assessment showed that the restoration, in its current form, was insufficient to induce the water quality improvements anticipated when the restoration was implemented. However, the change in water temperatures estimated to be caused by the intervention (0.7 °C cooling in summer), may buffer approximately 0.9 °C of air temperature warming, therefore could alleviate climate change impacts of air temperature warming, providing a climate mitigation co-benefit of the management action.

Utilising a 1-D hydrodynamic model, Chapter 5 applied a systematic modelling approach to investigate how WRT changes, on an annual scale, could cause changes to lake stratification length and strength. Chapter 5 suggested that sub-seasonal management of WRT presents the most potential for controlling stratification to limit internal loading, based on the advective and surface heat fluxes contributing to Elterwater's heat budget. Targeting the start and end of stratification as periods of lower stability, is likely to be the most effective means of limiting stratification (Chapter 5). This proposal to manage WRTs differently throughout the year is a novel contribution to the lake management literature where previous work has looked at estimating the required flow rate to disturb stratification (Mitrovic et al., 2011, 2006; Webster et al., 2000) or the impact of a constant flow on stratification dynamics rate in managed reservoirs (Li et al., 2018; Straškraba and Hocking, 2002).

Chapter 4 and 5 also modelled water temperatures throughout the year and highlighted that management actions for the summer (aiming to inhibit stratification) could be having secondary effects at other times of year (winter surface warming) that has the potential to cause problems for the lake water quality. By using the insights from the hydrodynamic modelling, quantification of the heat budget and an understanding of annual dynamics of WRTs at Elterwater and other lakes, the management measure could be optimised to increase

the efficacy of the intervention whilst limiting potential unintended consequence at other times of year as well as considering future climate change (Janssen et al., 2019b; Ladwig et al., 2018; Tanner-McAllister et al., 2017). Future implementation of WRT manipulation as a management strategy should learn from the lessons at Elterwater, evidenced by the research carried out for Chapters 4 and 5. These findings suggest that a thorough pre-intervention assessment of WRTs and heat flux dynamics should be carried out to assess whether the aim, to inhibit fully stratification in the lake of interest, is possible (Figure 8.3).

Although not originally part of the planned management strategy at Elterwater, Chapter 6 showed that WRT management could work to inhibit internal loading on a shorter timescale by using short-term reductions in WRT to induce DO replenishment in the hypolimnion. This additional possible impact of WRT management, which weakens stratification to enhance vertical mixing rather than fully mixing the water column, should be explored more in the future. Pulses of inflow during the stratified period induced vertical mixing, increasing the downwards flux of oxygen to potentially inhibit redox-related internal loading, although additional work on the implications of reoxygenation on internal loading would be needed. Some lake restoration schemes have used direct injection of oxygenated water to the hypolimnion using piped inflows direct to the deep-waters as a means to relieve anoxic conditions (Beutel and Horne, 1999; Dunalska and Wiśniewski, 2016; Preece et al., 2019). Results here present a process that works with the natural functioning of the lake.

Flow changes have been previously used in the management of water quality. Previous work on small, impounded rivers showed that pulsed inflows were able to reduce water column stability (Mitrovic et al., 2011; Webster et al., 2000), and disturb blooms of buoyant cyanobacteria (Bormans and Ford, 2002; Mitrovic et al., 2011). On larger lakes and reservoirs, flow has been modelled to suppress or disturb phytoplankton blooms through direct flushing of algal cells (Bormans and Ford, 2002; Lundgren et al., 2013; Mitrovic et al., 2006), although the rates of throughflow required to inhibit growth were variable between systems. This thesis has brought additional insights that, as well as the impact on thermal structure and phytoplankton blooms, pulse inflow events are linked to the replenishment of oxygen concentrations during the seasonal anoxic period. Using a modelling approach, the WRT reduction required at Elterwater was estimated to determine how management could use short-term changes in WRT to reduce stratification and potentially induce longer oxygen replenishment (Chapter 5). The findings in Chapter 6, show that it is possible to replenish, and potentially maintain, dissolved oxygen concentrations at depth, without completely inhibiting stratification, by inducing vertical mixing from oxygen-rich water at the surface or where a

chlorophyll *a* maxima exists in the metalimnion with super-saturated water. In Elterwater, a sub-surface maxima of chlorophyll *a* exists between 2 and 5 m throughout the summer (Figure 6.13). High productivity increases oxygen concentrations at depth (Kalff, 2002; Wilkinson et al., 2015), and may also provide an oxygen source in closer proximity to the hypolimnion. This could be beneficial where mixing is induced below the surface, by an interflow, even if the surface layers remain more strongly stratified.

Utilising the inflow as a direct source of reoxygenation, WRT manipulation could also be used to add directly oxygenated water to depth. Inflowing water can intrude below the surface where the density of the inflow is higher, due to cooler water temperatures and increased solute concentrations, than the surface water (Liu et al., 2020; MacIntyre et al., 2006; Wetzel, 2001a). As shown in Chapters 4, 5, and 7, the inflow in summer can be considerably cooler than the surface lake water, but warmer than the bottom and is therefore likely to be intruding as an interflow (Wetzel, 2001a). Management could utilise this knowledge of intrusion depths to add water of a particular temperature (and estimated intrusion depth) into the lake, thus adding oxygenated water to a specific depth. By increasing shading (Garner et al., 2017b; Ishikawa et al., 2021) or using heat pumps to extract heat from the inflowing water (Gaudard et al., 2019), inflow temperature could be cooled to induce a deeper inflow intrusion to the most anoxic parts of the lake (Ishikawa et al., 2021). The advective flux of the cooler inflow would also contribute to cooling and convective mixing in the lake, bringing increased vertical mixing as well (Brand et al., 2008; Kimura et al., 2014). With ever growing pressure to decarbonise global energy and heating demands (BEIS, 2017; Gielen et al., 2019) the opportunity for synergistic water resources management that integrates zero-carbon heating and water quality improvements should be considered further.

8.2.1 Optimising future management strategies

Based on the lessons learnt and the understanding gained from this thesis, and from the investigations at Elterwater, a workflow for future management is proposed (Figure 8.3). Future management to utilise WRT manipulations should first consider the aim of the restoration. Then using information on lake and inflow temperatures, the heat budget and intrusion depths can be used to identify periods of interest to achieve the management aim. Subsequently, modelling methods can be employed to investigate different annual, seasonal, and pulsed WRT scenarios on lake thermal structure and anoxia. Implementation of the restoration should include sufficient pre- and post-restoration monitoring in order to assess, robustly, the intervention success. Following this assessment, the strategy should then be adapted in order to optimise the management outcomes.

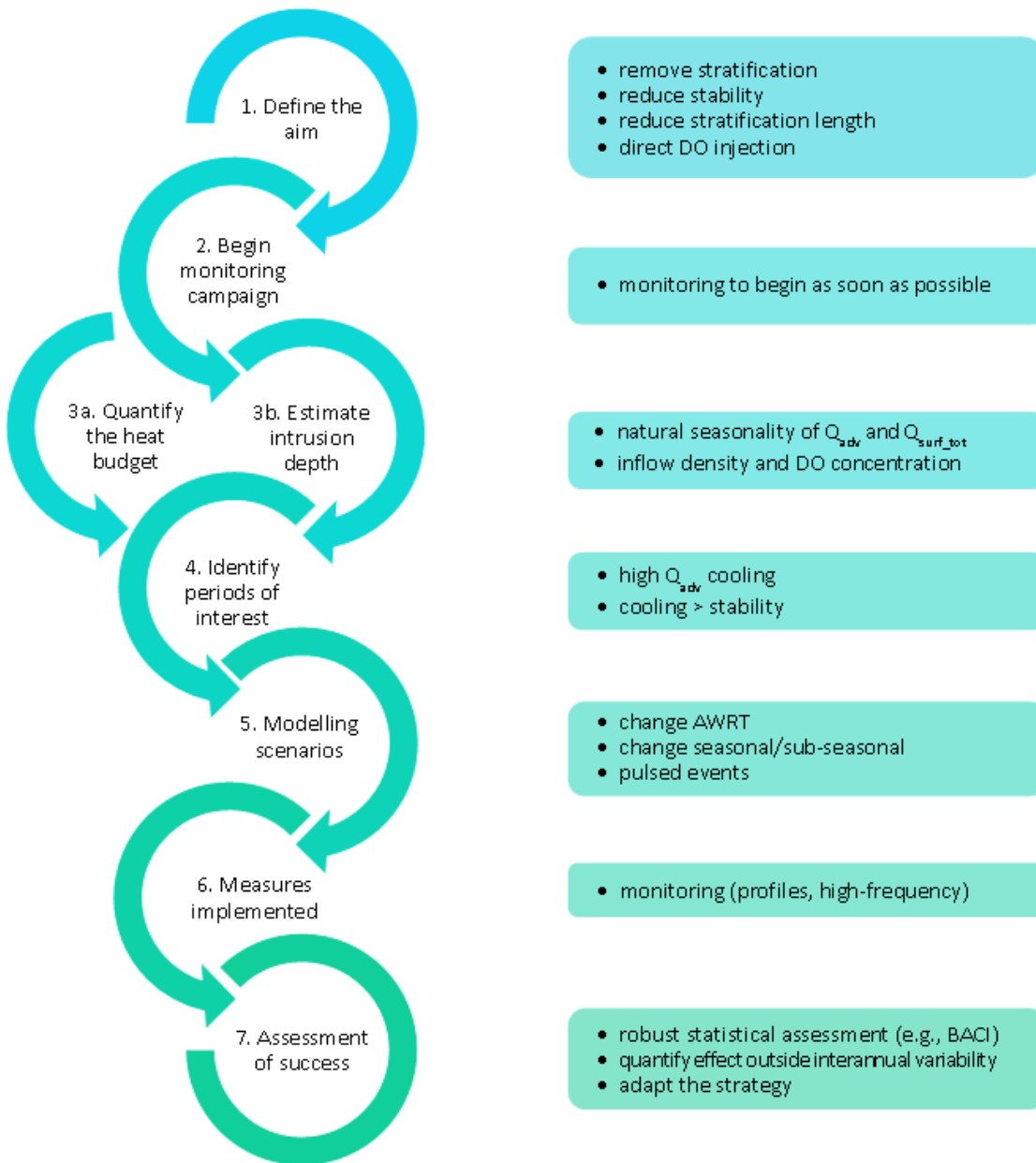


Figure 8.3 Suggested workflow to investigate and implement a success WRT manipulation restoration scheme, based on lessons learned in this thesis.

8.3 Impacts of climate change on lake temperatures

The effects of climate change are having a long-term impact on the physical structure of lakes including increased surface water temperature (O'Reilly et al., 2015) and stratification duration and stability (Kraemer et al., 2015; Woolway et al., 2021b). Climate change impact research primarily considers widespread air temperature rises, however, air temperature warming is not the only projected change in global climate under future scenarios. Future projections of global climate also show changes to precipitation and evaporation (IPCC, 2014), which both have implications for lake ecosystems. The interaction of precipitation and

evaporation changes, as well as future abstraction pressure, will impact global river flows (Arnell and Gosling, 2013; van Vliet et al., 2013), a key determinant of lake WRT.

8.3.1 Climate change induced WRT modification

The findings from this thesis has shown that climate-related changes in WRT are important in small residence time lakes (Chapter 7), contributing to lake warming at a magnitude greater than an additional 0.5 °C of air temperature warming. Lakes are already showing warming trends in surface temperatures (Dokulil et al., 2021; O'Reilly et al., 2015; Piccolroaz et al., 2020; Woolway et al., 2020, 2019b), primarily attributed to warming air temperatures (Winslow et al., 2017) and future modelling suggests this trend will continue (Woolway et al., 2021a; Woolway and Maberly, 2020) as the planet continues to warm. The results of Chapter 7 showed that for a significant proportion of global lakes WRT changes could also be further contributing to a warming trend. 50% reductions in discharge, not implausible for some regions (Arnell and Gosling, 2013; van Vliet et al., 2013), caused warming of summer lake surface temperatures at Elterwater equivalent to the impact of an addition 0.7 °C air temperature rise (SWT increase by 0.6 °C). The lake temperature changes associated with 50% reductions in flow caused warming equivalent to multi-decadal trends in surface temperatures (Magnuson et al., 1997; O'Reilly et al., 2015). Previous research showed that Blelham Tarn, a small stratifying lake 5 km from Elterwater, has a warming trend in mean summer temperature of approximately 0.2 °C decade⁻¹ (Woolway et al., 2019b). Therefore, under the most extreme flow scenarios projected for the region (80% reductions; Fowler and Kilsby, 2007; Prudhomme et al., 2013), warming rates due to flow reductions could exceed 40 years of lake warming. As 75% of global landmass is projected to experience changes to river flows (Döll and Zhang, 2010; van Vliet et al., 2013), failing to account for discharge impacts on lakes will be increasing the inaccuracy of future lake temperatures projections, especially in short residence time lakes.

In addition, future changes to WRT may not impact seasons equally, with many regions likely to see exacerbation of present flow seasonality (Prudhomme et al., 2013; van Vliet et al., 2013). River flow modelling suggests around one third of the global land-surface by 2070 will experience increased river flow seasonality (van Vliet et al., 2013). For example, projections for the northwest of England are for reduced river flows in summer, already the driest season, and increased river flow in winter, the period of highest discharge (Arnell et al., 2015; Fowler and Kilsby, 2007; Prudhomme et al., 2013), amplifying the existing seasonality. Reduced summer flow and increased winter flow are likely to increase lake warming in both seasons in Elterwater (Chapter 7). However, in other regions, such as high northern latitudes and

monsoon regions where projections are for higher discharges during summer (van Vliet et al., 2013), changes may be buffering air temperature rises (Bayer et al., 2013), although the impact will depend on the temperature of the inflowing water. The difference between the impacts of diverse discharge changes across regions may explain some of the discrepancy in lake surface water temperature trends (O'Reilly et al., 2015; Råman Vinnå et al., 2018; Woolway et al., 2020). Chapter 7 discusses how the changes to seasonality will have profound implications for in-lake temperatures and highlights the need for understanding the seasonal and sub-seasonal impacts of WRT changes to fully understand the implications for lake functioning.

Vertical mixing from the destabilising cooling effect of inflows (Chapter 6) is likely to be reduced under scenarios of lower inflow discharge, reducing the replenishment of DO into the hypolimnion. Although the impact of WRT changes on water column stability is smaller than that of air temperature changes (Chapter 7), reductions in inflow could additionally impact anoxia through reductions in the direct injection of oxygenated flow as interflows and reduced vertical mixing. Evidence from Chapter 6 shows that during stratification inflows could be providing important sources of oxygen to the hypolimnion of lakes during the anoxic period, which would reduce under future climate projections of lower summer flow.

8.3.2 Climate impacts on river temperatures

The impacts of inflows on stratification and deep-water anoxia need to consider how future air temperature rises will impact river water temperatures. In Chapter 7, the results showed that in summer 25% of the warming impact of inflow reductions was due to the warming impact on the inflow temperature, with the other 75% of the impact due to lower inflow. Modifying the lake-inflow temperature relationship, and thus the advective heat flux, will be an important impact of air temperature warming in lakes, especially those with short WRTs, something that has not been widely considered before. In Lake Constance, the river inflow (River Rhine) is warming at a slower rate than the lake, reducing the advective flux during parts of the year (Fink et al., 2014a). If rivers warm at a different rate to lakes, as seen in some regions (Jonkers and Sharkey, 2016), further impacted by discharge or abstraction changes (Döll et al., 2009; Fink et al., 2014a; van Vliet et al., 2013), then the relationship between inflow and lake temperatures will be modified and the advective flux changed (Fink et al., 2014a). For example, the cooling advective flux would be reduced in summer under lower flows, in which rivers warm faster than lakes (Figure 8.4).

Coupled with the reduced cooling effect on lake temperatures, warming of rivers has implications for the intrusion of inflows into the water column (see Figure 8.4). Warmer inflows, relative to lakes, will cause shallowing of the intrusion into the water column (Figure

8.4), when coupled with reduced flow, this will provide less direct injection of oxygen into the hypolimnion. From current conditions (Figure 8.4a) more warming of the inflow, relative to the lake, will have the dual consequences of reduce the inflow-lake temperature difference (from 10 to 9 °C) and the advective flux and shallowing the intrusion depth (Figure 8.4b). If differential warming is also accompanied by reduced flow (Figure 8.4c), the river is likely to undergo additional warming. This has the impact of reducing the advective flux through reduced flow and reduced inflow-lake temperature difference, and even greater shallowing of the river intrusion. Therefore, this existing supplementary benefit of inflows for deep-water oxygen, direct injection, could be lost, important for determining the potential effectiveness of WRT management.

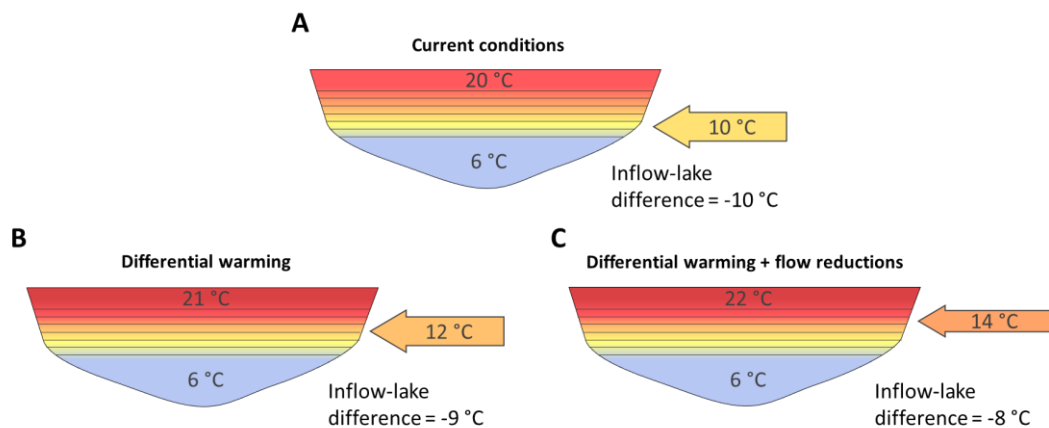


Figure 8.4 Example of how differential warming of lakes and rivers and reduced flow could impact the temperature difference between the lake and its inflow (arrow) and the potential depth of neutral buoyancy (depth of river intrusion).

8.3.3 Episodic flow changes

Under future climate, despite the reductions projected for baseline summer flow, projections also suggest increased rates of extreme episodic events (IPCC, 2014). High discharge episodic inflow associated with extreme events, may continue to intrude into the warming water column and induce additional cooling and vertical mixing of oxygen. In Chapter 6, all discharge events above $0.3 \text{ m}^3 \text{ s}^{-1}$ were associated with DO replenishment events, suggesting that more large inflow events may increase the frequency of replenishment. Furthermore, the depth of intrusion will depend on the impact of the long-term warming and discharge trends on water column temperatures and the magnitude and temperature of storm-related inflows. More understanding of the complicated interactions of future discharge changes is needed to quantify how future flow will influence deep-water oxygen during the stratified period.

8.3.4 WRT interventions in the context of climate change

Future management using WRT changes needs to be considered in the context of climate change (Jeppesen et al., 2017). If the aim is to reduce stratification length and strength then under future climate, more flow may be needed to influence increasingly stable stratification. This is particularly important given the possibility of additional inflow warming relative to lakes (Jonkers and Sharkey, 2016), which could reduce the inflow-lake temperature difference and therefore the magnitude of the advective heat flux (Figure 8.4). Even greater changes in WRT will be needed to induce the same impact on water temperatures under a warmer climate, where the inflow-lake temperature difference is reduced.

However, changes of the magnitude required may be even less easy to attain in areas with reduced precipitation and river flows in the summer (Arnell et al., 2015; Fowler and Kilsby, 2007; Prudhomme et al., 2013) reducing the water available in the catchment for this type of restoration measure. In future, it may be harder to rely on natural flow regimes for management purposes, so potentially additional pumped flows could be needed or 'intelligent' interventions that target specific periods (Chapter 5). The potential of cooling the inflow to induce the same advective cooling flux with lower discharge may present an alternative or complimentary option to induce equivalent impacts on the lake's temperature (see Section 8.2) where additional flow is not available or feasibly attained. In order to optimise any type of management under future climate, understanding how the measures interact with climate change (Ladwig et al., 2018; Radbourne et al., 2019; Tanner-McAllister et al., 2017), both air temperature warming and river discharge changes, is crucial to achieving long-term success of the measures.

Further developing an understanding of the impact of river flow changes on lakes will help inform how lake managers can use WRT changes to buffer or ameliorate the impacts of air temperature warming. For example, in a UK context, managing water use from rivers upstream of lakes so as to maintain flows into lakes during summer, when reductions in discharge will increase lake warming, and potentially abstracting water in winter, when increased flow will contribute to lake warming, could help mitigate some of the warming trend. Also, reductions in WRT, proposed to improve water quality could have secondary impacts of buffering climate induced warming. Rimmer *et al.*, (2011) suggested that management changes in Lake Kinneret, particularly water level drawdown and upstream pumping, were having a greater effect on lake temperatures than either air temperature warming or natural inflow changes, highlighting another potential impact on lake thermal structure.

8.4 Methods

This research has applied a range of methods to investigate WRT effects on lake stratification and oxygen dynamics on different temporal scales. This section discusses the benefits and limitations of the methods implemented to elucidate the processes impacted by WRT changes and to understand management implications of WRT changes. Within this thesis long-term monitoring data, high-frequency sensor data, process-based modelling, and inferential statistics of empirical data have been combined to understand WRT impacts at different spatial and temporal scales.

8.4.1 Long-term data

Routine lake sampling has been carried out in the English Lake District for more than 70 years and regular monitoring continues through the UK Centre for Ecology & Hydrology and via regulatory monitoring by the Environment Agency for the Water Framework Directive. Long-term data sets are an invaluable asset for scientific research, providing insights into long-term changes from nutrient pollution and climate change (Foley et al., 2012; Meis et al., 2009; Reynolds et al., 2012; Thackeray et al., 2008). The eight years of data from two Lake District lakes, used in Chapter 4, helped to disentangle inter-annual variability from restoration impacts at Elterwater. Without this scale of data, incorrect conclusions may have been reached in which true impacts were missed or inter-annual variability in values assumed to be the result of restoration impacts (Smokorowski and Randall, 2017; Underwood, 1994). Despite using the eight years of monitoring data available from Elterwater (impact) and Blelham (control), subtle changes caused by the intervention may have been missed due to the large variability naturally occurring at Elterwater, such as the large inter-annual variability in chlorophyll *a* concentrations (see Chapter 4).

Missing from the long-term records was any spatially differentiated sampling of the water column. Integrated samples of the top part of the water column collected at both lakes, fails to account for the vertical heterogeneity present in the lake. Although some profile data were included in the analysis in Chapter 4, to highlight the anoxia present, the BACI analysis was not able to consider any changes affecting water quality at different depths. For example, nutrients and phytoplankton are frequently distributed heterogeneously in the water column (Hamilton et al., 2010; Obrador et al., 2014), potentially impacted by changes to WRT that would not be detected using integrated sampling methods, such as the development or disruption of deep-water maxima of chlorophyll *a* concentrations. Had long-term monitoring incorporated vertical profiles of nutrients and biota, as occurs with some temperature and oxygen sampling, a more complete picture of long-term trends and intervention impacts

would have been possible. Sampling of vertical profiles will be aided by the development of more robust, inexpensive, and sufficiently sensitive sensors for nutrients and biota, to help supplement time-consuming laboratory analysis with higher resolution data (e.g. Chowdhury et al., 2020). Furthermore, planning restoration projects needs to ensure that the monitoring carried out is appropriate for the intended purpose, such that proper assessment of the management intervention can be carried out. Frequently, due to a lack of this type of data, data collected for other purposes are used which doesn't necessarily allow the success of a measure to be evaluated comprehensively.

8.4.2 High-frequency data

Traditional lake sampling used in long-term monitoring can fail to capture episodic events and the fine detail of processes occurring on short-time scales, which are important for resolving process changes in lake functioning. Advancement of sensor technology provides the opportunity to monitor lakes at higher frequency through the deployment of water quality monitoring buoys (Hamilton et al., 2015; Marcé et al., 2016; McBride and Rose, 2018). High-frequency sensors were deployed at the deepest point in Elterwater-IB to measure water temperature and oxygen at 4 and 15 minutely time intervals respectively, providing information on dynamics and processes not detectable using traditional sampling frequency of weekly to monthly samples. Chapter 6, especially, utilises high-frequency temperature and oxygen data, as well as daily flow data collected by the Environment Agency, to elucidate the processes acting within the lake at daily timescales, enabling the identification and investigation of events not previously studied. Using high-frequency data, Chapter 6 was able to demonstrate a relationship between high-discharge inflow events and short-lived (1-3 days) oxygen replenishment in the hypolimnion, which would not have been possible with weekly sampling, where these types of events would be missed or impacts misjudged (Aguilera et al., 2016). The temperature sensors had excellent accuracy (± 0.002 °C) and precision (< 0.00005 °C), allowing small changes in water temperature to be detected and reliable calculation of vertical diffusivity values, at the appropriate timescale to be relevant to lake dynamics (Chapter 6). This analysis would have been difficult with lower accuracy or lower resolution data.

High-frequency data have been used in lake research to develop understanding of lake temperature dynamics (Liu et al., 2019; Woolway et al., 2015a), lake metabolism (Fernández Castro et al., 2021; Staehr et al., 2010), responses to episodic events (Jennings et al., 2012; Perga et al., 2018), and to detect and forecast cyanobacterial blooms (Rousso et al., 2020; Zhang et al., 2022). Tools have also been developed to deal with the rapid expansion of high-

frequency data accrual, such as Lake Analyzer (Read et al., 2011), used in all Chapters to calculate stability metrics, Lake Heat Flux Analyzer (Woolway et al., 2015b), used in Chapters 5 and 6 to calculate the total surface heat flux and wind power, and Lake Metabolizer (Winslow et al., 2016).

Despite the knowledge gained from the high-frequency observations in this study, additional oxygen sensors deployed at a finer vertical spatial scale would have improved the accuracy of the conclusions reached in Chapter 6. Due to lack of high-frequency data at more depths, the estimation of the dissolved oxygen concentration at 4 m, between the sensors at 3 and 5 m, may have under or over-estimated the flux of oxygen to the deep-water. The cost of sensors can restrict adequate sensors deployment at a resolution that would be most informative. Sensors also require regular maintenance, checking, and replacement. High-frequency measurements of DO at the surface stopped mid-summer 2019 due to sensor failure, but could not be replaced, highlighting a drawback of such measurements, where budgets are limited. Deployment of additional sensors on increased spatial resolution will further the understanding, especially of short-term processes as described in Chapter 6, and determine the horizontal and vertical heterogeneity of biogeochemical distributions.

High-resolution data were also invaluable for validating and calibrating the GOTM model for Chapters 4, 5, and 7. High-frequency meteorological data were used to drive the model and in-lake measurements of water temperature were compared with modelled temperatures to modify parameters (calibration) to determine the goodness-of-fit of the model (validation). Validation with data independent of the calibration period can avoid model overfitting and identify the predictive ability of the model (Hipsey et al., 2020). Proper calibration and validation of the model, using high quality observations, gives greater strength to the conclusions formed using modelling approaches for scenario or hypothesis testing (Hipsey et al., 2020; Robson, 2014). The high-frequency observations of water temperature ensured that the processes acting in the lake were being sufficiently represented by the model in a way in which scenario testing could be applied with confidence.

8.4.3 Modelling

Process-based modelling is a useful tool for limnologists (Janssen et al., 2015; Mooij et al., 2010), enabling the testing of hypotheses and scenarios (Chapter 5), quantification of process effects (Chapters 4 and 7), and disentanglement of feedbacks and co-occurring drivers (Chapter 7). Particularly useful is the opportunity for using models *a priori* to understand potential responses to future events, both large scale climate changes and management

action. In management, modelling prior to the event could help to optimise the management action ensuring cost-effectiveness and efficacy (Janssen et al., 2015; Mooij et al., 2010) of the actions such as nutrient load reductions (e.g. T. K. Andersen et al., 2020; Janse et al., 2008) and biomanipulation (e.g. Hilt et al., 2018). In Elterwater, Chapter 4 demonstrated that the changes to WRT were insufficient to cause the changes to the lake physical structure that were desired and modelling in Chapter 5 further showed that no changes to annual WRT that were tested would have inhibited stratification entirely in this lake. Scenario modelling of this nature, prior to implementing management action at Elterwater would have highlighted the potential outcomes of the restoration and would have enabled WRT manipulation to be optimised to achieve water quality targets.

This thesis has demonstrated that a hydrodynamic lake model can be set-up, calibrated and validated with commonly collected observational data (water temperatures and meteorological data), sufficient to investigate management actions. More complex lake ecosystem models can model more components of the ecology, although require greater parameterisation, additional calibration and validation data and potentially have increased uncertainty (Hellweger, 2017). For example, the PCLake model was specifically designed to understand state-changes and critical nutrient loads in shallow lakes in response to management (nutrient reductions and biomanipulation) (Janse et al., 2010, 2008), bridging lake function theory and application of management action (Janssen et al., 2019a). Good practice of using modelling to investigate potential implications of management action has been evident in some cases (e.g. Hilt et al., 2018; Hupfer et al., 2016; Ladwig et al., 2018; Li et al., 2011) and future work to utilise WRT manipulations should consider a modelling approach for individual lakes to determine potential efficacy before implementation.

Chapter 7 also used lake modelling to investigate the sensitivity of lake temperatures to the interactive effects of air temperature and inflow discharge changes. Likely acting concurrently under future climate, the individual and compound impacts of air temperature and discharge change were quantified for a short-residence time lake, highlighting a potentially important, but often neglected, impact for lake systems. Previous work that has modelled discharge changes has considered fewer scenarios (e.g. Bayer et al., 2013; Christianson et al., 2020) or has looked at specific regional projections for specific lakes (e.g. Komatsu et al., 2007; Rogora et al., 2018; Taner et al., 2011), where less general messages can be inferred.

Modelling does have limitations which should be considered when the outputs are used in decision making (Hipsey et al., 2020; Robson, 2014). To make models computationally usable

and relevant for a wide range of systems and scenarios, often the processes, ecosystem functions, and interactions between compartments are simplified and assumptions made, especially when rates are unknown or highly changeable, particularly in biogeochemical models (Janssen et al., 2015). Issues have been raised in the modelling community of using single parameter sets that do not consider the non-uniqueness of the output, termed *equifinality* (see Beven, 2006). The suggestion that multiple parameter sets produce equally good output, raises the question of which is the “right” parameter set. Discussion in the literature suggests that ensemble modelling of lake systems, using a range of acceptable parameter sets in the same model (e.g. GLUE method) or a multi-model ensemble, will support the identification of methodological and technical differences and weaknesses in the different models and cover a broader set of parameterisations (see Moore et al., 2021).

Making assumptions and simplifications is necessary but the uncertainty produced should be considered when using the output from any model and adequate observational data for calibration and validation are essential. For example, GOTM, as a one-dimensional model, assumes homogeneous structure in the horizontal plane and further detailed understanding of horizontal mixing processes would require a more complex hydrodynamic model. For small to moderate sized lakes, the vertical thermal gradients are typically much larger than the horizontal thermal gradients and are not affected by the Coriolis acceleration or other horizontal transport processes (Patterson et al., 1984). Finally, the version of GOTM used in this thesis, does not include an ice module, so dynamics of ice-cover cannot be considered.

8.4.4 Inferential statistics

As well as process-based modelling, this thesis employed statistical analysis of empirical data (Chapter 4). Determining the success of management and restoration through robust statistical methods is crucial if novel management actions are to be more widely employed and the method optimised in future. Using robust statistical assessment is necessary when observed ecological data are complex (missing data, highly skewed) and treatments are non-repeatable and non-random (targeted management). Before-After-Control-Impact (BACI) statistical designs have been proposed as a means to draw inference about impacts from management and restoration actions (e.g. Lang et al., 2016; Liu et al., 2018; McGowan et al., 2005). Impact and control sites are paired and treated as fixed effects with sampling conducted synchronously before and after perturbation (Stewart-Oaten et al., 1986; Underwood, 1994). The treatment effect is estimated as the mean difference between impact and control sites before and after restoration ($d_{\text{impact-control after}} - d_{\text{treatment-control before}}$) (Stewart-Oaten et al., 1986).

The strengths of BACI designs are demonstrated in their ability to detect treatment effects that other, simpler design such as Before-After or Control-Impact, have failed to detect (Christie et al., 2019; Smokorowski and Randall, 2017) or drawn false conclusions (Mahlum et al., 2018). BACI designs account for inter-annual variability and changes due to other stochastic environmental factors, such as particularly warm or wet years (Smokorowski and Randall, 2017; Underwood, 1994). Furthermore, by using multiple years of observation, temporally confounding effects can be avoided (Underwood, 1994). Missing data can be problematic for statistical assessment, but BACI designs, and the formal statistical methods used, can be modified to account for unbalanced designs (e.g. Smokorowski and Randall, 2017). Moreover, formal BACI statistical tests can also be used alongside descriptive statistics and high-frequency data (such as in Chapter 4) to give a more comprehensive picture of current conditions (Kerr et al., 2019), which can identify whether an impact site has met thresholds or pre-defined criteria, such as WFD regulations, even when changes cannot be detected statistically.

Despite the strengths of BACI methods, limitations need to be acknowledged to ensure any bias is recognised and caution employed when drawing conclusions based on statistical inference. Firstly, "control" sites used in BACI designs to evaluate the impacts of "natural experiments", such as this whole-lake restoration, are not true controls comparable to those possible in a laboratory setting (Kerr et al., 2019), but do provide some level of comparison to be able to identify local climate effects (Schwartz, 2015; Smith, 2006). It is acknowledged that no two systems will respond entirely the same to external stimulus but in field conditions, using whole lake experiments is one of the optimal solutions to assess restoration. It is also possible that large amounts of inter-annual variability may mask more subtle treatment effects (Sit and Taylor, 1998). For example, the large inter-annual variability in chlorophyll *a* concentrations in Elterwater may have masked smaller changes caused by the restoration intervention, despite the four years pre- and post-intervention data used. The requirement for long-term data, more of which may have helped to untangle the inter-annual variability, can limit the usefulness of the method, as data of the right quantity and quality to assess changes robustly are not often collected (see Section 8.4.1). In order to utilise BACI methods, assumptions of additivity and spatial and temporal independence must be met (Kerr et al., 2019; Stewart-Oaten et al., 1992, 1986). Issues with temporal autocorrelation can be accounted for using defined error structures and additional temporal parameters (Sit and Taylor, 1998; Stewart-Oaten et al., 1986). Finally, the BACI method does not formally test the effect of the intervention on changes to variability, but on mean values (Schwartz, 2015;

Underwood, 1994), so the impact of the restoration on this aspect of the data was not tested. Frequentist methods are most commonly applied (GLM, ANOVAs, t-tests; Smith, 2006), however more recently Bayesian modelling has become more widely employed to answer study questions of “How much impact did a management action or natural perturbation have?” (Conner et al., 2015) and to estimate the effect size, often producing results that are readily reportable to managers and stakeholders (Conner et al., 2015).

8.4.5 Combining methods

Combining the different approaches of modelling, high-frequency data collection, and long-term monitoring is the key to untangling the process of WRT on different spatial and temporal scales (Hampton et al., 2019). Using complimentary techniques helps to alleviate the limitations of individual methods, such as supplementing long-term monitoring and statistical modelling with high-frequency data collection and using process-based modelling to fill data gaps or forecast future conditions based on known processes and current conditions (Janssen et al., 2015; Page et al., 2018). Models present a particularly useful tool that when used alongside monitoring and high-frequency data (Chapter 4) can be used to infer processes and responses to management not possible with observational data alone.

Chapter 9 Conclusions and future work

This thesis has explored the impact of WRT changes on lake thermal structure at different timescales, in the context of lake restoration and management and under future climate. These conclusions will return to the aims outlined in Chapter 1 and identify the main conclusions relating to these aims as well as outlining potential areas of future research prompted by these findings.

9.1 Thesis conclusions

9.1.1 Aim 1: Understand how changes to WRT on different timescales impact the thermal structure of a short-residence time lake and subsequent deep-water oxygen dynamics

The impact of WRT changes on lake thermal structure has been investigated on annual, seasonal, and sub-seasonal time scales using both observational data (Chapter 6) and modelling scenarios (Chapter 4, 5 and 7). By combining these methods, this thesis has shown that through modifications to the advective heat flux, WRT changes can modify lake water temperatures and the length and strength of the stratified period. Shorter WRTs were linked to increased lake cooling in summer and increased lake warming in the winter, due to the difference in water temperature between the inflow and outflow at different times of year. This seasonality caused water temperature and stratification changes in the lake, which are important for broader lake functioning, including the duration and extent of seasonal anoxia. At shorter timescales, reductions in WRT during the seasonal stratified period were associated with short-term declines in lake water column stability and increased vertical mixing related to oxygen replenishment in the hypolimnion.

9.1.2 Aim 2: Investigate how WRT manipulations could be used in the management of eutrophic lake systems

The impacts of eutrophication are a widespread and persistent problem in lakes worldwide, increasingly requiring in-lake methods to manage and restore impacted systems. Changes to WRT, managed at a sub-seasonal timescale, present a potential method to modify the thermal structure and deep-water anoxia that is linked to problematic internal nutrient loading. Targeting the beginning and the end of the stratified periods presents the most likely times for WRT changes to modify the length of the stratified period, while reductions in WRT during the peak summer period only reduced water column stability (Chapter 5). However, short-term reductions in stability during the stratified period, caused by episodic WRT reductions were shown to be associated with oxygen replenishment during the stratified period and

suggest that short-term pulses of inflow may be a useful management action. Further, inflows may also be bringing highly oxygenated water directly to the metalimnion or hypolimnion, providing a secondary benefit to reducing WRT as a management strategy for stratification change. Modelling and heat budget estimates for individual lake systems will further highlight when and how WRT manipulations will be most effective in improving deep-water oxygen conditions and subsequent management of internal loading.

9.1.3 Aim 3: Explore how climate-related change in river discharge, and consequent lake WRT, might interact with rising air temperature to impact lake temperatures

River flow is projected to change under future climate. However, the direction and magnitude of these projected changes varies by region, catchment, and season. In Elterwater, projections are for increased flow in winter and decreased flow in summer exacerbating lake warming caused by air temperature rises with WRT reductions of 50% having the equivalent warming impact of up to an additional 0.8 °C air temperature rise (Chapter 7). Furthermore, river temperature warming was an important effect of climate change on lake temperatures, modifying the inflow-lake temperature relationship and contributing more than 40% of the observed discharge-related at certain times of year. With three-quarters of global rivers predicted to show changes to river flow, failing to account for changes to inflow discharge and temperature could mean underestimating the impact of climate change on lake temperatures globally, especially in short-residence time lakes (1 in 5 lakes).

9.2 Areas of potential future research

9.2.1 Additional modelling to optimise WRT manipulations under a changing climate

Evidence from Chapter 4 and 5 suggests that the current management at Elterwater has not been effective at limiting stratification, anoxia, and internal loading. Using methods similar to those implemented in Chapter 5, additional modelling studies could be performed to test further WRT scenarios. For example, Chapter 5 outlines a scheme to investigate the rates and timing of WRT changes that would be most effective in controlling stratification. Lessons learned from this research show that an understanding of a lake's heat budget and annual WRT dynamics are crucial prior to implementing WRT changes. Furthering this understanding will help optimise management at Elterwater and other lakes. Modelling could also be used to investigate how the restoration will be impacted by regional climate change, including the impact on the advective heat flux, and the WRT changes required necessary to inhibit or shorten stratification in a warming climate.

9.2.2 WRT impacts on lake temperatures in different climate regions

Chapters 4, 5 and 7 reveal that the impact of WRT changes are determined by the relationship between inflow and lake temperature. In turn, these drove the seasonality in the lake temperature response. We would therefore expect that lakes outside of the temperate zone, such as in alpine or tropical locations, would exhibit different responses to WRT changes. It would also be expected that lakes with different inflow-lake temperature relationships would require different optimised WRT management to impact lake stratification. Using observations or modelling methods, similar to those implemented in Chapter 5 and 7, future studies could look at the response of lake temperatures to WRT changes, either relating to management techniques or due to climate change.

9.2.3 Global scale assessment of discharge impacts on lakes

Chapter 7 demonstrated that for Elterwater's inner basin – a small, short-residence time system – the impact of WRT changes driven by climate change may contribute the equivalent of an air temperature rise of 0.8 °C to lake warming. Rising lake temperatures has consequences for the availability of thermal habitats, gas solubility, and metabolic processes. Given that small, short-residence time lakes, like Elterwater, represent a considerable proportion of global lakes, and many regions are likely to be impacted by large river discharge changes, a global-scale analysis of the impact of climate change-induced lake WRT changes should be conducted. From this, using up-to-date climate projections of precipitation,

evaporation and potential abstraction pressure, a global-scale analysis could be run that integrates projected river flow changes and climate models. An extension of chapter 7 could also implement a multi-model ensemble to investigate the uncertainty in future climate projections of lake temperatures driven by flow changes.

9.2.4 WRT impacts on different spatial scales

The work in this thesis was concerned with the WRT impacts within the lake, primarily at the deepest point where samples and measurements were taken. However, future research could widen our understanding by exploring the impact of WRT at different locations and over different spatial scales. For example, the downstream impacts in the source river due to reductions in discharge; or in shallower regions of the lake that are important for macrophyte cover and resuspension of sediment. These littoral zones are important for lake biogeochemical cycling and as habitat for aquatic species.

9.2.5 Deep water oxygen dynamics driven by short-term changes in inflow discharge

Chapter 6 showed that short-term changes in inflow discharge were correlated with increased vertical mixing, which induced dissolved oxygen replenishment during the seasonal anoxic period in a small monomictic lake. With high-frequency oxygen measurements becoming increasingly available, future research could be used to investigate this relationship between inflow and hypolimnetic oxygen dynamics on sub-seasonal timescales in other lake systems. Furthermore, high-spatial resolution sensor deployment within the water column (0.5 – 1 m scale) would help to elucidate the processes driving oxygen replenishment in the hypolimnion by distinguishing between vertical mixing and direct injection of oxygenated water from the inflows. Understanding this phenomenon is important for informing process-based models of flow impacts that enable us to test hypotheses on WRT impact on lake oxygen dynamics. Further research is also needed on how these short-term fluctuations in oxygen in the hypolimnion effect biogeochemical cycling at the water-sediment interface and aerobic habitat availability.

Bibliography

- Abdo, K.S., Fiseha, B.M., Rientjes, T.H.M., Gieske, A.S.M., Haile, A.T., 2009. Assessment of climate change impacts on the hydrology of Gilgel Abay catchment in Lake Tana basin, Ethiopia. *Hydrol. Process.* 23, 3661–3669. doi:10.1002/hyp.7363
- Abell, J.M., Özkundakci, D., Hamilton, D.P., Reeves, P., 2020. Restoring shallow lakes impaired by eutrophication: Approaches, outcomes, and challenges. *Crit. Rev. Environ. Sci. Technol.* 1–48. doi:10.1080/10643389.2020.1854564
- Adrian, R., O'Reilly, C.M., Zagarese, H., Baines, S.B., Hessen, D.O., Keller, W., Livingstone, D.M., Sommaruga, R., Straile, D., Van Donk, E., Weyhenmeyer, G.A., Winder, M., 2009. Lakes as sentinels of climate change. *Limnol. Oceanogr.* 54, 2283–2297. doi:10.4319/lo.2009.54.6_part_2.2283
- Aguilera, R., Livingstone, D.M., Marcé, R., Jennings, E., Piera, J., Adrian, R., 2016. Using dynamic factor analysis to show how sampling resolution and data gaps affect the recognition of patterns in limnological time series. *Int. Waters* 6, 284–294. doi:10.5268/IW-6.3.948
- Alabaster, J.S., Lloyd, R., 1982. Dissolved Oxygen, in: *Water Quality Criteria for Freshwater Fish*. Butterworths, London, pp. 127–142.
- Allan, R.P., Barlow, M., Byrne, M.P., Cherchi, A., Douville, H., Fowler, H.J., Gan, T.Y., Pendergrass, A.G., Rosenfeld, D., Swann, A.L.S., Wilcox, L.J., Zolina, O., 2020. Advances in understanding large-scale responses of the water cycle to climate change. *Ann. N. Y. Acad. Sci.* 1472, 49–75. doi:10.1111/nyas.14337
- Almeida, M.C., Shevchuk, Y., Kirillin, G., Soares, P.M., Cardoso, R.M.A. de P., Matos, J.P., Rebelo, R.M., Rodrigues, A.P.N.C., Coelho, P.M. da H.S., 2022. Modeling reservoir surface temperatures for regional and global climate models: a multi-model study on the inflow and level variation effects. *Geosci. Model Dev.* 1–37. doi:10.5194/gmd-2021-64
- Ambrosetti, W., Barbanti, L., Sala, N., 2003. Residence time and physical processes in lakes. *J. Limnol.* 62, 1–15. doi:10.4081/jlimnol.2003.s1.1
- Andersen, M.R., Eyto, E. De, Dillane, M., Poole, R., Jennings, E., 2020. 13 years of storms : An analysis of the effects of storms on lake physics on the Atlantic fringe of Europe. *Water* 12, 1–21. doi:10.3390/w12020318
- Andersen, T.K., Nielsen, A., Jeppesen, E., Hu, F., Bolding, K., Liu, Z., Søndergaard, M.,

- Johansson, L.S., Trolle, D., 2020. Predicting ecosystem state changes in shallow lakes using an aquatic ecosystem model: Lake Hinge, Denmark, an example. *Ecol. Appl.* 30. doi:10.1002/eap.2160
- Andradóttir, H.Ó., Rueda, F.J., Armengol, J., Marcé, R., 2012. Characterization of residence time variability in a managed monomictic reservoir. *Water Resour. Res.* 48, 1–16. doi:10.1029/2012WR012069
- APEM, 2012. Elterwater phosphorus and algal bloom assessment. Warrington.
- Arismendi, I., Safeeq, M., Dunham, J.B., Johnson, S.L., 2014. Can air temperature be used to project influences of climate change on stream temperature? *Environ. Res. Lett.* 9, 1–13. doi:10.1088/1748-9326/9/8/084015
- Arnell, N.W., Gosling, S.N., 2013. The impacts of climate change on river flow regimes at the global scale. *J. Hydrol.* 486, 351–364. doi:10.1016/j.jhydrol.2013.02.010
- Arnell, N.W., Halliday, S.J., Battarbee, R.W., Skeffington, R.A., Wade, A.J., 2015. The implications of climate change for the water environment in England. *Prog. Phys. Geogr.* 39, 93–120. doi:10.1177/0309133314560369
- Austin, J.A., Colman, S.M., 2007. Lake Superior summer water temperatures are increasing more rapidly than regional temperatures: A positive ice-albedo feedback. *Geophys. Res. Lett.* 34. doi:10.1029/2006GL029021
- Ayala, A.I., Moras, S., Pierson, D.C., 2020. Simulations of future changes in thermal structure of Lake Erken: Proof of concept for ISIMIP2b lake sector local simulation strategy. *Hydrol. Earth Syst. Sci.* 24, 3311–3330. doi:10.5194/hess-24-3311-2020
- Barontini, S., Grossi, G., Kouwen, N., Maran, S., Scaroni, P., Ranzi, R., 2009. Impacts of climate change scenarios on runoff regimes in the southern Alps. *Hydrol. Earth Syst. Sci. Discuss.* 6, 3089–3141. doi:10.5194/hessd-6-3089-2009
- Bayer, T.K., Burns, C.W., Schallenberg, M., 2013. Application of a numerical model to predict impacts of climate change on water temperatures in two deep, oligotrophic lakes in New Zealand. *Hydrobiologia* 713, 53–71. doi:10.1007/s10750-013-1492-y
- Beattie, L., Gize, I., Berry, S., Webster, R., Fletcher, A., Hartland, A., 1996. A study of the water and sediment chemistry of key Cumbrian Lakes, Elterwater.
- Beaver, J.R., Jensen, D.E., Casamatta, D.A., Tausz, C.E., Scotese, K.C., Buccier, K.M., Teacher,

- C.E., Rosati, T.C., Minerovic, A.D., Renicker, T.R., 2013. Response of phytoplankton and zooplankton communities in six reservoirs of the middle Missouri River (USA) to drought conditions and a major flood event. *Hydrobiologia* 705, 173–189. doi:10.1007/s10750-012-1397-1
- BEIS, 2017. The Clean Growth Strategy: Leading the way to a low carbon future [WWW Document]. BEIS. doi:10.1021/ac00297a029
- Beklioglu, M., Romo, S., Kagalou, I., Quintana, X., Bécares, E., 2007. State of the art in the functioning of shallow Mediterranean lakes: Workshop conclusions, in: *Hydrobiologia*. pp. 317–326. doi:10.1007/s10750-007-0577-x
- Berg, P., Haerter, J.O., Thejll, P., Piani, C., Hagemann, S., Christensen, J.H., 2009. Seasonal characteristics of the relationship between daily precipitation intensity and surface temperature. *J. Geophys. Res.* 114, 18102. doi:10.1029/2009JD012008
- Beutel, M.W., Horne, A.J., 1999. A review of the effects of hypolimnetic oxygenation on lake and reservoir water quality. *Lake Reserv. Manag.* 15, 285–297. doi:10.1080/07438149909354124
- Beven, K., 2006. A manifesto for the equifinality thesis. *J. Hydrol.* 320, 18–36. doi:10.1016/j.jhydrol.2005.07.007
- Birk, S., Chapman, D., Carvalho, L., Spears, B.M., Andersen, H.E., Argillier, C., Auer, S., Baattrup-Pedersen, A., Banin, L., Beklioglu, M., Bondar-Kunze, E., Borja, A., Branco, P., Bucak, T., Buijse, A.D., Cardoso, A.C., Couture, R.M., Cremona, F., de Zwart, D., Feld, C.K., Ferreira, M.T., Feuchtmayr, H., Gessner, M.O., Gieswein, A., Globevnik, L., Graeber, D., Graf, W., Gutiérrez-Cánovas, C., Hanganu, J., Işkın, U., Järvinen, M., Jeppesen, E., Kotamäki, N., Kuijper, M., Lemm, J.U., Lu, S., Solheim, A.L., Mischke, U., Moe, S.J., Nöges, P., Nöges, T., Ormerod, S.J., Panagopoulos, Y., Phillips, G., Posthuma, L., Pouso, S., Prudhomme, C., Rankinen, K., Rasmussen, J.J., Richardson, J., Sagouis, A., Santos, J.M., Schäfer, R.B., Schinegger, R., Schmutz, S., Schneider, S.C., Schülting, L., Segurado, P., Stefanidis, K., Sures, B., Thackeray, S.J., Turunen, J., Uyarra, M.C., Venohr, M., von der Ohe, P.C., Willby, N., Hering, D., 2020. Impacts of multiple stressors on freshwater biota across spatial scales and ecosystems. *Nat. Ecol. Evol.* 4, 1060–1068. doi:10.1038/s41559-020-1216-4
- Boehrer, B., Schultze, M., 2008. Stratification of lakes. *Rev. Geophys.* 46, 1–27. doi:10.1029/2006RG000210.1.INTRODUCTION

- Bolding, K., Bruggeman, J., 2017. ACPy [WWW Document]. URL <https://bolding-bruggeman.com/portfolio/acpy/> (accessed 10.14.19).
- Börger, T., Campbell, D., White, M.P., Elliott, L.R., Fleming, L.E., Garrett, J.K., Hattam, C., Hynes, S., Lankia, T., Taylor, T., 2021. The value of blue-space recreation and perceived water quality across Europe: A contingent behaviour study. *Sci. Total Environ.* doi:10.1016/j.scitotenv.2021.145597
- Bormans, M., Ford, P., 2002. Setting flow levels for controlling cyanobacterial blooms in tropical weir pools. *Lake Reserv. Manag.* 18, 275–284. doi:10.1080/07438140209353933
- Bormans, M., Maršálek, B., Jančula, D., 2016. Controlling internal phosphorus loading in lakes by physical methods to reduce cyanobacterial blooms: a review. *Aquat. Ecol.* 50, 407–422. doi:10.1007/s10452-015-9564-x
- Boström, B., Andersen, J.M., Fleischer, S., Jansson, M., 1988. Exchange of phosphorus across the sediment-water interface. *Hydrobiologia* 170, 229–244. doi:10.1007/978-94-009-3109-1_14
- Bouffard, D., Ackerman, J.D., Boegman, L., 2013. Factors affecting the development and dynamics of hypoxia in a large shallow stratified lake: Hourly to seasonal patterns. *Water Resour. Res.* 49, 2380–2394. doi:10.1002/wrcr.20241
- Brand, A., Bruderer, H., Oswald, K., Guggenheim, C., Schubert, C.J., Wehrli, B., 2016. Oxygenic primary production below the oxycline and its importance for redox dynamics. *Aquat. Sci.* 78, 727–741. doi:10.1007/s00027-016-0465-4
- Brand, A., McGinnis, D.F., Wehrli, B., Wüest, A., 2008. Intermittent oxygen flux from the interior into the bottom boundary of lakes as observed by eddy correlation. *Limnol. Oceanogr.* 53, 1997–2006. doi:10.4319/lo.2008.53.5.1997
- Brasil, J., Attayde, J.L., Vasconcelos, F.R., Dantas, D.D.F., Huszar, V.L.M., 2016. Drought-induced water-level reduction favors cyanobacteria blooms in tropical shallow lakes. *Hydrobiologia* 770, 145–164. doi:10.1007/s10750-015-2578-5
- Burchard, H., Bolding, K., Kühn, W., Meister, A., Neumann, T., Umlauf, L., 2006. Description of a flexible and extendable physical–biogeochemical model system for the water column. *J. Mar. Syst.* 61, 180–211. doi:10.1016/J.JMARSYS.2005.04.011
- Burchard, H., Bolding, K., Ruiz-Villarreal, M., 1999. GOTM, a general ocean turbulence model. Theory, implementation and test cases 1–104.

- Burke, S.A., Wik, M., Lang, A., Contosta, A.R., Palace, M., Crill, P.M., Varner, R.K., 2019. Long-term measurements of methane ebullition from thaw ponds. *J. Geophys. Res. Biogeosciences* 124, 2208–2221. doi:10.1029/2018JG004786
- Butcher, J.B., Nover, D., Johnson, T.E., Clark, C.M., 2015. Sensitivity of lake thermal and mixing dynamics to climate change. *Clim. Change* 129, 295–305. doi:10.1007/s10584-015-1326-1
- Carey, C.C., Ibelings, B.W., Hoffmann, E.P., Hamilton, D.P., Brookes, J.D., 2012. Ecophysiological adaptations that favour freshwater cyanobacteria in a changing climate. *Water Res.* 46, 1394–1407. doi:10.1016/j.watres.2011.12.016
- Carmack, E.C., 1979. Combined influence of inflow and lake temperatures on spring circulation in a riverine lake. *J. Phys. Oceanogr.* 9, 422–434. doi:10.1175/1520-0485(1979)009<0422:ccioial>2.0.co;2
- Carmack, E.C., Gray, C.B.J., Pharo, C.H., Daley, R.J., 1979. Importance of lake-river interaction on seasonal patterns in the general circulation of Kamloops Lake, British Columbia. *Limnol. Oceanogr.* 24, 634–644. doi:10.4319/lo.1979.24.4.0634
- Carmack, E.C., Wiegand, R.C., Daley, R.J., Gray, C.B.J., Jasper, S., Pharo, C.H., 1986. Mechanisms influencing the circulation and distribution of water mass in a medium residence-time lake. *Limnol. Oceanogr.* 31, 249–265. doi:10.4319/lo.1986.31.2.0249
- Castellano, L., Ambrosetti, W., Barbanti, L., Rolla, A., 2010. The residence time of the water in Lago Maggiore (N. Italy): First results from an Eulerian-Lagrangian approach. *J. Limnol.* 69, 15–28. doi:10.3274/JL10-69-1-02
- Catalán, N., Marcé, R., Kothawala, D.N., Tranvik, L.J., 2016. Organic carbon decomposition rates controlled by water retention time across inland waters. *Nat. Geosci.* 9, 501–504. doi:10.1038/ngeo2720
- Chen, W., Nielsen, A., Andersen, T.K., Hu, F., Chou, Q., Søndergaard, M., Jeppesen, E., Trolle, D., 2020. Modeling the ecological response of a temporarily summer-stratified lake to extreme heatwaves. *Water* 12, 94. doi:10.3390/w12010094
- Chowdhury, R.I., Wahid, K.A., Nugent, K., Baulch, H., 2020. Design and development of low-cost, portable, and smart chlorophyll-a sensor. *IEEE Sens. J.* 20, 7362–7371. doi:10.1109/JSEN.2020.2978758
- Christianson, K.R., Johnson, B.M., Hooten, M.B., 2020. Compound effects of water clarity,

- inflow, wind and climate warming on mountain lake thermal regimes. *Aquat. Sci.* 82, 1–17. doi:10.1007/s00027-019-0676-6
- Christie, A.P., Amano, T., Martin, P.A., Shackelford, G.E., Simmons, B.I., Sutherland, W.J., 2019. Simple study designs in ecology produce inaccurate estimates of biodiversity responses. *J. Appl. Ecol.* 56, 2742–2754. doi:10.1111/1365-2664.13499
- Clark, N.E., Eber, L., Laurs, R.M., Renner, J.A., Saur, J.F.T., 1974. Heat exchange between ocean and atmosphere in the eastern North Pacific for 1961-71. NOAA Tech. Rep. NMFS SSRF 632–682.
- Collen, B., Whitton, F., Dyer, E.E., Baillie, J.E.M., Cumberlidge, N., Darwall, W.R.T., Pollock, C., Richman, N.I., Soulsby, A.M., Böhm, M., 2014. Global patterns of freshwater species diversity, threat and endemism. *Glob. Ecol. Biogeogr.* 23, 40–51. doi:10.1111/geb.12096
- Colomer, J., Roget, E., Casamitjana, X., 1996. Daytime heat balance for estimating non-radiative fluxes of Lake Banyoles, Spain. *Hydrol. Process.* 10, 721–726. doi:10.1002/(SICI)1099-1085(199605)10:5<721::AID-HYP314>3.0.CO;2-0
- Conner, M.M., Saunders, W.C., Bouwes, N., Jordan, C., 2015. Evaluating impacts using a BACI design, ratios, and a Bayesian approach with a focus on restoration. *Environ. Monit. Assess.* 188, 555. doi:10.1007/s10661-016-5526-6
- Cooke, G.D., Welch, E.B., Peterson, S.A., Nichols, S.A., 2005. *Restoration and Management of Lakes and Reservoirs*, 3rd ed. Taylor & Francis Group, Boca Raton, Florida.
- Coppens, J., Özen, A., Tavşanoğlu, T.N., Erdoğan, Ş., Levi, E.E., Yozgatligil, C., Jeppesen, E., Beklioğlu, M., 2016. Impact of alternating wet and dry periods on long-term seasonal phosphorus and nitrogen budgets of two shallow Mediterranean lakes. *Sci. Total Environ.* 563–564, 456–467. doi:10.1016/j.scitotenv.2016.04.028
- Cornett, R.J., Rigler, F.H., 1987. Transport of oxygen into the hypolimnion of lakes. *Can. J. Fish. Aquat. Sci.* 44, 852–858.
- Corripio, J.G., 2019. *insol: Solar Radiation*. R Packag. version 1.2.1.
- Cortés, A., Forrest, A.L., Sadro, S., Stang, A.J., Swann, M., Framsted, N.T., Thirkill, R., Sharp, S.L., Schladow, S.G., 2021. Prediction of hypoxia in eutrophic polymictic lakes. *Water Resour. Res.* 57, 1–19. doi:10.1029/2020wr028693
- Coutant, C., 1985. Striped bass, temperature, and dissolved oxygen: a speculative hypothesis

- for environmental risk. *Trans. Am. Fish. Soc.* 114, 31–61.
- Crossman, J., Futter, M.N., Elliott, J.A., Whitehead, P.G., Jin, L., Dillon, P.J., 2018. Optimizing land management strategies for maximum improvements in lake dissolved oxygen concentrations. *Sci. Total Environ.* 652, 382–397. doi:10.1016/j.scitotenv.2018.10.160
- Dai, J., Wu, S., Wu, X., Lv, X., Sivakumar, B., Wang, F., Zhang, Y., Yang, Q., Gao, A., Zhao, Y., Yu, L., Zhu, S., 2020. Impacts of a large river-to-lake water diversion project on lacustrine phytoplankton communities. *J. Hydrol.* 587. doi:10.1016/j.jhydrol.2020.124938
- Darko, D., Trolle, D., Asmah, R., Bolding, K., Adjei, K.A., Odai, S.N., 2019. Modeling the impacts of climate change on the thermal and oxygen dynamics of Lake Volta. *J. Great Lakes Res.* 45, 73–86. doi:10.1016/j.jglr.2018.11.010
- Davis, J.C., 1975. Minimal dissolved oxygen requirements of aquatic life with emphasis on Canadian species: a review. *J. Fish. Res. Board Canada* 32, 2295–2332. doi:10.1139/f75-268
- de Eyto, E., Jennings, E., Ryder, E., Sparber, K., Dillane, M., Dalton, C., Poole, R., 2016. Response of a humic lake ecosystem to an extreme precipitation event: physical, chemical, and biological implications. *Int. Waters* 6, 483–498. doi:10.1080/iw-6.4.875
- De La Fuente, A., 2014. Heat and dissolved oxygen exchanges between the sediment and water column in a shallow salty lagoon. *J. Geophys. Res. Biogeosciences* 119, 596–613. doi:10.1002/2013JG002413
- Deines, A.M., Bunnell, D.B., Rogers, M.W., Bennion, D., Woelmer, W., Sayers, M.J., Grimm, A.G., Shuchman, R.A., Raymer, Z.B., Brooks, C.N., Mychek-Londer, J.G., Taylor, W., Beard, T.D., 2017. The contribution of lakes to global inland fisheries harvest. *Front. Ecol. Environ.* 15, 293–298. doi:10.1002/fee.1503
- Does, J., Verstraelen, P., Boers, P., Roestel, J., Roijackers, R., Moser, G., 1992. Lake restoration with and without dredging of phosphorus-enriched upper sediment layers. *Hydrobiologia* 233, 197–210. doi:10.1007/BF00016108
- Dokulil, M.T., Eyto, E. De, Maberly, S.C., Weyhenmeyer, G.A., Woolway, R.I., May, L., 2021. Increasing maximum lake surface temperature under climate change. *Clim. Change* 165, 1–17.
- Döll, P., Fiedler, K., Zhang, J., 2009. Global-scale analysis of river flow alterations due to water withdrawals and reservoirs. *Hydrol. Earth Syst. Sci.* 13, 2413–2432. doi:10.5194/hess-13-

2413-2009

- Döll, P., Zhang, J., 2010. Impact of climate change on freshwater ecosystems: A global-scale analysis of ecologically relevant river flow alterations. *Hydrol. Earth Syst. Sci.* 14, 783–799. doi:10.5194/hess-14-783-2010
- Doubek, J.P., Carey, C.C., Lavender, M., Winegardner, A.K., Beaulieu, M., Kelly, P.T., Pollard, A.I., Straile, D., Stockwell, J.D., 2019. Calanoid copepod zooplankton density is positively associated with water residence time across the continental United States. *PLoS One* 14, 1–22. doi:10.1371/journal.pone.0209567
- Douglas, G.B., Hamilton, D.P., Robb, M.S., Pan, G., Spears, B.M., Lurling, M., 2016. Guiding principles for the development and application of solid-phase phosphorus adsorbents for freshwater ecosystems. *Aquat. Ecol.* 50, 385–405. doi:10.1007/s10452-016-9575-2
- Downing, J.A., 2010. Emerging global role of small lakes and ponds: Little things mean a lot. *Limnetica* 29, 9–24. doi:10.23818/limn.29.02
- Downing, J.A., Polasky, S., Olmstead, S.M., Newbold, S.C., 2021. Protecting local water quality has global benefits. *Nat. Commun.* 12, 2709. doi:10.1038/s41467-021-22836-3
- Downing, J.A., Prairie, Y.T., Cole, J.J., Duarte, C.M., Tranvik, L.J., Striegl, R.G., McDowell, W.H., Kortelainen, P., Caraco, N.F., Melack, J.M., Middelburg, J.J., 2006. The global abundance and size distribution of lakes, ponds, and impoundments. *Limnol. Oceanogr.* 51, 2388–2397. doi:10.4319/lo.2006.51.5.2388
- Dunalska, J.A., Wiśniewski, G., 2016. Can we stop the degradation of lakes? Innovative approaches in lake restoration. *Ecol. Eng.* 95, 714–722. doi:10.1016/j.ecoleng.2016.07.017
- Elliott, J.A., 2010. The seasonal sensitivity of Cyanobacteria and other phytoplankton to changes in flushing rate and water temperature. *Glob. Chang. Biol.* 16, 864–876. doi:10.1111/j.1365-2486.2009.01998.x
- Elliott, J.A., Bell, V.A., 2011. Predicting the potential long-term influence of climate change on vendace (*Coregonus albula*) habitat in Bassenthwaite Lake, U.K. *Freshw. Biol.* 56, 395–405. doi:10.1111/j.1365-2427.2010.02506.x
- Elliott, J.A., Defew, L., 2012. Modelling the response of phytoplankton in a shallow lake (Loch Leven, UK) to changes in lake retention time and water temperature. *Hydrobiologia* 681, 105–116. doi:10.1007/s10750-011-0930-y

- Elliott, J.A., Jones, I.D., Page, T., 2009. The importance of nutrient source in determining the influence of retention time on phytoplankton: An explorative modelling study of a naturally well-flushed lake. *Hydrobiologia* 627, 129–142. doi:10.1007/s10750-009-9720-1
- Elliott, J.A., Jones, I.D., Thackeray, S.J., 2006. Testing the sensitivity of phytoplankton communities to changes in water temperature and nutrient load, in a temperate lake. *Hydrobiologia* 559, 401–411. doi:10.1007/s10750-005-1233-y
- Engstrom, D.R., 2005. Long-term changes in iron and phosphorus sedimentation in Vadnais Lake, Minnesota, resulting from ferric chloride addition and hypolimnetic aeration. *Lake Reserv. Manag.* 21, 95–105. doi:10.1080/07438140509354417
- Environment Agency, 2000. Elterwater: The Lakes Business Plan.
- Evans, C.D., Futter, M.N., Moldan, F., Valinia, S., Frogbrook, Z., Kothawala, D.N., 2017. Variability in organic carbon reactivity across lake residence time and trophic gradients. *Nat. Geosci.* 10, 832–835. doi:10.1038/NGEO3051
- Fadel, A., Atoui, A., Lemaire, B.J., Vinçon-Leite, B., Slim, K., 2015. Environmental factors associated with phytoplankton succession in a Mediterranean reservoir with a highly fluctuating water level. *Environ. Monit. Assess.* 187, 633. doi:10.1007/s10661-015-4852-4
- Fairall, C.W., Bradley, E.F., Godfrey, J.S., Wick, G.A., Edson, J.B., Young, G.S., 1996a. Cool-skin and warm-layer effects on sea surface temperature. *J. Geophys. Res. C Ocean.* 101, 1295–1308. doi:10.1029/95JC03190
- Fairall, C.W., Bradley, E.F., Rogers, D.P., Edson, J.B., Young, G.S., 1996b. Bulk parameterization of air-sea fluxes for tropical ocean-atmosphere coupled-ocean atmosphere response experiment. *J. Geophys. Res. C Ocean.* 101, 3747–3764. doi:10.1029/95JC03205
- Fang, X., Stefan, H.G., 1998. Temperature variability in lake sediments. *Water Resour. Res.* 34, 717–729.
- Fenocchi, A., Rogora, M., Sibilla, S., Ciampittiello, M., Dresti, C., 2018. Forecasting the evolution in the mixing regime of a deep subalpine lake under climate change scenarios through numerical modelling (Lake Maggiore, Northern Italy/Southern Switzerland). *Clim. Dyn.* 51, 3521–3536. doi:10.1007/s00382-018-4094-6

- Fenocchi, A., Rogora, M., Sibilla, S., Dresti, C., 2017. Relevance of inflows on the thermodynamic structure and on the modeling of a deep subalpine lake (Lake Maggiore, Northern Italy/Southern Switzerland). *Limnologica* 63, 42–56. doi:10.1016/j.limno.2017.01.006
- Fernández Castro, B., Chmiel, H.E., Minaudo, C., Krishna, S., Perolo, P., Rasconi, S., Wüest, A., 2021. Primary and net ecosystem production in a large lake diagnosed from high-resolution oxygen measurements. *Water Resour. Res.* 57, 1–24. doi:10.1029/2020WR029283
- Fink, G., Schmid, M., Wahl, B., Wolf, T., Wüest, A., 2014a. Heat flux modifications related to climate-induced warming of large European lakes. *Water Resour. Res.* 50, 2072–2085. doi:10.1002/2013WR014448
- Fink, G., Schmid, M., Wüest, A., 2014b. Large lakes as sources and sinks of anthropogenic heat: Capacities and limits. *Water Resour. Res.* 50, 7285–7301. doi:10.1002/2014WR015509
- Fink, G., Wessels, M., Wüest, A., 2016. Flood frequency matters: Why climate change degrades deep-water quality of peri-alpine lakes. *J. Hydrol.* 540, 457–468. doi:10.1016/j.jhydrol.2016.06.023
- Flaim, G., Nishri, A., Camin, F., Corradini, S., Obertegger, U., 2019. Shift from nival to pluvial recharge of an aquifer-fed lake increases water temperature. *Int. Waters* 9, 261–274. doi:10.1080/20442041.2019.1582958
- Foley, B., Jones, I.D., Maberly, S.C., Rippey, B., 2012. Long-term changes in oxygen depletion in a small temperate lake: Effects of climate change and eutrophication. *Freshw. Biol.* 57, 278–289. doi:10.1111/j.1365-2427.2011.02662.x
- Fowler, H.J., Kilsby, C.G., 2007. Using regional climate model data to simulate historical and future river flows in northwest England. *Clim. Change* 80, 337–367. doi:10.1007/s10584-006-9117-3
- Gächter, R., Müller, B., 2003. Why the phosphorus retention of lakes does not necessarily depend on the oxygen supply to their sediment surface. *Limnol. Oceanogr.* 48, 929–933. doi:10.4319/LO.2003.48.2.0929
- Gächter, R., Wehrli, B., 1998. Ten years of artificial mixing and oxygenation: No effect on the internal phosphorus loading of two eutrophic lakes. *Environ. Sci. Technol.* 32, 3659–3665. doi:10.1021/es980418l

- Garner, G., Hannah, D.M., Watts, G., 2017a. Climate change and water in the UK: Recent scientific evidence for past and future change. *Prog. Phys. Geogr.* 41, 154–170. doi:10.1177/0309133316679082
- Garner, G., Malcolm, I.A., Sadler, J.P., Hannah, D.M., 2017b. The role of riparian vegetation density, channel orientation and water velocity in determining river temperature dynamics. *J. Hydrol.* 553, 471–485. doi:10.1016/j.jhydrol.2017.03.024
- Gaudard, A., Wüest, A., Schmid, M., 2019. Using lakes and rivers for extraction and disposal of heat: Estimate of regional potentials. *Renew. Energy* 134, 330–342. doi:10.1016/j.renene.2018.10.095
- George, D.G., Hurley, M.A., 2003. Using a continuous function for residence time to quantify the impact of climate change on the dynamics of thermally stratified lakes. *J. Limnol.* 62, 21–26. doi:10.4081/jlimnol.2003.s1.21
- Gerling, A.B., Browne, R.G., Gantzer, P.A., Mobley, M.H., Little, J.C., Carey, C.C., 2014. First report of the successful operation of a side stream supersaturation hypolimnetic oxygenation system in a eutrophic, shallow reservoir. *Water Res.* 67, 129–143. doi:10.1016/j.watres.2014.09.002
- Gielen, D., Boshell, F., Saygin, D., Bazilian, M.D., Wagner, N., Gorini, R., 2019. The role of renewable energy in the global energy transformation. *Energy Strateg. Rev.* 24, 38–50. doi:10.1016/j.esr.2019.01.006
- Goldsmith, B.J., Luckes, S.J., Bennion, H., Carvalho, L., Hughes, M., Appleby, P.G., Sayer, C.D., 2003. Feasibility Studies on the Restoration Needs of Four Lake SSSIs: Final Report To English Nature. Environmental Change Research Centre, University College London.
- Gołdyn, R., Podsiadłowski, S., Dondajewska, R., Kozak, A., 2014. The sustainable restoration of lakes-towards the challenges of the water framework directive. *Ecohydrol. Hydrobiol.* 14, 68–74. doi:10.1016/j.ecohyd.2013.12.001
- Golub, M., Thiery, W., Marcé, R., Pierson, D., Vanderkelen, I., Mercado, D., Woolway, R.I., Grant, L., Jennings, E., Schewe, J., Zhao, F., Frieler, K., Mengel, M., Bogomolov, V.Y., Bouffard, D., Couture, R.-M., Debolskiy, A., Droppers, B., Gal, G., Guo, M., Janssen, A.B.G., Kirillin, G., Ladwig, R., Magee, M.R., Moore, T., Perroud, M., Piccolroaz, S., Råman Vinnå, L., Schmid, M., Shatwell, T., Stepanenko, V., Tan, Z., Yao, H., Adrian, R., Allan, M., Anneville, O., Arvola, L., Atkins, K., Boegman, L., Carey, C.C., Christianson, K.R., De Eyto,

- E., DeGasperi, C.L., Grechushnikova, M., Hejzlar, J., Joehnk, K.D., Jones, I.D., Laas, A., Mackay, E.B., Mammarella, I., Markensten, H., McBride, C., Özkundakci, D., Potes, M., Rinke, K., Robertson, D.M., Rusak, J.A., Salgado, R., van den Linden, L., Verburg, P., Wain, D., Ward, N.K., Wollrab, S., Zdorovenova, G., n.d. A framework for ensemble modelling of climate change impacts on lakes worldwide: the ISIMIP Lake Sector [Preprint], Geoscientific Model Development. doi:<https://doi.org/10.5194/gmd-2021-433>, in review, 2022
- Gophen, M., 2003. Water quality management in Lake Kinneret (Israel): Hydrological and food web perspectives. *J. Limnol.* 62, 91–101. doi:10.4081/jlimnol.2003.s1.91
- Gorham, E., Boyce, F.M., 1989. Influence of lake surface area and depth upon thermal stratification and the depth of the summer thermocline. *J. Great Lakes Res.* 15, 233–245. doi:10.1016/S0380-1330(89)71479-9
- Gray, E., Elliott, J.A., Mackay, E.B., Folkard, A.M., Keenan, P.O., Jones, I.D., 2019. Modelling lake cyanobacterial blooms: Disentangling the climate-driven impacts of changing mixed depth and water temperature. *Freshw. Biol.* 64, 2141–2155. doi:10.1111/fwb.13402
- Gray, E., Mackay, E.B., Elliott, J.A., Folkard, A.M., Jones, I.D., 2020. Wide-spread inconsistency in estimation of lake mixed depth impacts interpretation of limnological processes. *Water Res.* 168, 115136. doi:10.1016/j.watres.2019.115136
- Gudasz, C., Bastviken, D., Steger, K., Premke, K., Sobek, S., Tranvik, L.J., 2010. Temperature-controlled organic carbon mineralization in lake sediments. *Nature* 466, 478–481. doi:10.1038/nature09186
- Gudmundsson, L., Boulange, J., Do, H.X., Gosling, S.N., Grillakis, M.G., Koutroulis, A.G., Leonard, M., Liu, J., Schmied, H.M., Papadimitriou, L., Pokhrel, Y., Seneviratne, S.I., Satoh, Y., Thiery, W., Westra, S., Zhang, X., Zhao, F., 2021. Globally observed trends in mean and extreme river flow attributed to climate change. *Science* (80-). 371, 1159–1162. doi:10.1126/science.aba3996
- Hamilton, D.P., Carey, C.C., Arvola, L., Arzberger, P., Brewer, C., Cole, J.J., Gaiser, E., Hanson, P.C., Ibelings, B.W., Jennings, E., Kratz, T.K., Lin, F.P., McBride, C.G., Marques, D. de M., Muraoka, K., Nishri, A., Qin, B., Read, J.S., Rose, K.C., Ryder, E., Weathers, K.C., Zhu, G., Trolle, D., Brookes, J.D., 2015. A Global lake ecological observatory network (GLEON) for synthesising high-frequency sensor data for validation of deterministic ecological models. *Int. Waters* 5, 49–56. doi:10.5268/IW-5.1.566

- Hamilton, D.P., O'Brien, K.R., Burford, M.A., Brookes, J.D., McBride, C.G., 2010. Vertical distributions of chlorophyll in deep, warm monomictic lakes. *Aquat. Sci.* 72, 295–307. doi:10.1007/s00027-010-0131-1
- Hampton, S.E., Scheuerell, M.D., Church, M.J., Melack, J.M., 2019. Long-term perspectives in aquatic research. *Limnol. Oceanogr.* 64, S2–S10. doi:10.1002/lno.11092
- Hanson, P.C., Carpenter, S.R., Armstrong, D.E., Stanley, E.H., Kratz, T.K., 2006. Lake dissolved inorganic carbon and dissolved oxygen: Changing drivers from days to decades. *Ecol. Monogr.* 76, 343–363. doi:10.1890/0012-9615(2006)076[0343:ldicad]2.0.co;2
- Harrison, J.A., Maranger, R.J., Alexander, R.B., Giblin, A.E., Jacinthe, P.A., Mayorga, E., Seitzinger, S.P., Sobota, D.J., Wollheim, W.M., 2009. The regional and global significance of nitrogen removal in lakes and reservoirs. *Biogeochemistry* 93, 143–157. doi:10.1007/s10533-008-9272-x
- Havens, K.E., Fulton, R.S., Beaver, J.R., Samples, E.E., Colee, J., 2016. Effects of climate variability on cladoceran zooplankton and cyanobacteria in a shallow subtropical lake. *J. Plankton Res.* 38, 418–430. doi:10.1093/plankt/fbw009
- Havens, K.E., Ji, G., Beaver, J.R., Fulton, R.S., Teacher, C.E., 2017. Dynamics of cyanobacteria blooms are linked to the hydrology of shallow Florida lakes and provide insight into possible impacts of climate change. *Hydrobiologia* 1–17. doi:10.1007/s10750-017-3425-7
- Haworth, E., de Boer, G., Evans, I., Osmaston, H., Pennington, W., Smith, A., Storey, P., Ware, B., 2003. *Tarns of the Central Lake District*. Brathay Exploration Group Trust Ltd.
- Heinz, G., Ilmberger, J., Schimmele, M., 1990. Vertical mixing in Überlinger See, western part of Lake Constance. *Aquat. Sci.* 52, 256–268. doi:10.1007/BF00877283
- Hellweger, F.L., 2017. 75 years since Monod: It is time to increase the complexity of our predictive ecosystem models (opinion). *Ecol. Modell.* 346, 77–87. doi:10.1016/j.ecolmodel.2016.12.001
- Hilt, S., Alirangues Nuñez, M.M., Bakker, E.S., Blindow, I., Davidson, T.A., Gillefalk, M., Hansson, L.-A., Janse, J.H., Janssen, A.B.G., Jeppesen, E., Kabus, T., Kelly, A., Köhler, J., Lauridsen, T.L., Mooij, W.M., Noordhuis, R., Phillips, G., Rucker, J., Schuster, H.-H., Søndergaard, M., Teurlincx, S., van de Weyer, K., van Donk, E., Waterstraat, A., Willby, N., Sayer, C.D., 2018. Response of submerged macrophyte communities to external and internal restoration

- measures in north temperate shallow lakes. *Front. Plant Sci.* 9, 194. doi:10.3389/fpls.2018.00194
- Hipsey, M.R., Gal, G., Arhonditsis, G.B., Carey, C.C., Elliott, J.A., Frassl, M.A., Janse, J.H., de Mora, L., Robson, B.J., 2020. A system of metrics for the assessment and improvement of aquatic ecosystem models. *Environ. Model. Softw.* 128, 104697. doi:10.1016/j.envsoft.2020.104697
- Holgerson, M.A., Raymond, P.A., 2016. Large contribution to inland water CO₂ and CH₄ emissions from very small ponds. *Nat. Geosci.* 9, 222–226. doi:10.1038/ngeo2654
- Hosper, H., Meyer, M.L., 1986. Control of phosphorus loading and flushing as restoration methods for Lake Veluwe, The Netherlands. *Hydrobiol. Bull.* 20, 183–194. doi:10.1007/BF02291162
- Huang, J., Yan, R., Gao, J., Zhang, Z., Qi, L., 2016. Modeling the impacts of water transfer on water transport pattern in Lake Chao, China. *Ecol. Eng.* 95, 271–279. doi:10.1016/j.ecoleng.2016.06.074
- Huang, T., Li, X., Rijnaarts, H., Grotenhuis, T., Ma, W., Sun, X., Xu, J., 2014. Effects of storm runoff on the thermal regime and water quality of a deep, stratified reservoir in a temperate monsoon zone, in Northwest China. *Sci. Total Environ.* 485–486, 820–827. doi:10.1016/j.scitotenv.2014.01.008
- Hupfer, M., Lewandowski, J., 2008. Oxygen controls the phosphorus release from lake sediments - A long-lasting paradigm in limnology. *Int. Rev. Hydrobiol.* 93, 415–432. doi:10.1002/iroh.200711054
- Hupfer, M., Reitzel, K., Kleeberg, A., Lewandowski, J., 2016. Long-term efficiency of lake restoration by chemical phosphorus precipitation: Scenario analysis with a phosphorus balance model. *Water Res.* 97, 153–161. doi:10.1016/j.watres.2015.06.052
- Huser, B.J., Egemose, S., Harper, H., Hupfer, M., Jensen, H., Pilgrim, K.M., Reitzel, K., Rydin, E., Futter, M., 2016a. Longevity and effectiveness of aluminum addition to reduce sediment phosphorus release and restore lake water quality. *Water Res.* 97, 122–132. doi:10.1016/j.watres.2015.06.051
- Huser, B.J., Futter, M., Lee, J.T., Perniel, M., 2016b. In-lake measures for phosphorus control: The most feasible and cost-effective solution for long-term management of water quality in urban lakes. *Water Res.* 97, 142–152. doi:10.1016/j.watres.2015.07.036

- Hutchinson, G.E., Loffler, H., 1956. The thermal classification of lakes. *Proc. Natl. Acad. Sci.* 42, 84–86. doi:10.1073/pnas.42.2.84
- Idso, S.B., 1973. On the concept of lake stability. *Limnol. Oceanogr.* 18, 681–683.
- Imberger, J., 2013. *Environmental Fluid Dynamics: Flow Processes, Scaling, Equations of Motion, and Solutions to Environmental Flows*. Academic Press, Oxford.
- Imberger, J., 1985. Thermal characteristics of standing waters: an illustration of dynamic processes. *Hydrobiologia* 125, 7–29. doi:10.1007/BF00045923
- Imberger, J., Patterson, J.C., 1989. *Physical Limnology*. *Adv. Appl. Mech.* 27, 303–475. doi:10.1016/S0065-2156(08)70199-6
- IPCC, 2014. *Climate Change 2014: Synthesis Report. Contribution of Working Groups I, II and III to the Fifth Assessment Report of the Intergovernmental Panel on Climate Change*, IPCC. Gian-Kasper Plattner, Geneva.
- Ishikawa, M., Haag, I., Krumm, J., Teltscher, K., Lorke, A., 2021. The effect of stream shading on the inflow characteristics in a downstream reservoir. *River Res. Appl.* 1–12. doi:10.1002/rra.3821
- Ito, Y., Momii, K., 2015. Impacts of regional warming on long-term hypolimnetic anoxia and dissolved oxygen concentration in a deep lake. *Hydrol. Process.* 29, 2232–2242. doi:10.1002/hyp.10362
- Jagtman, E., Van der Molen, D.T., Vermij, S., 1992. The influence of flushing on nutrient dynamics, composition and densities of algae and transparency in Veluwemeer, The Netherlands. *Hydrobiologia* 233, 187–196.
- Jane, S.F., Hansen, G.J.A., Kraemer, B.M., Leavitt, P.R., Mincer, J.L., North, R.L., Pilla, R.M., Stetler, J.T., Williamson, C.E., Woolway, R.I., Arvola, L., Chandra, S., DeGasperis, C.L., Diemer, L., Dunalska, J., Erina, O., Flaim, G., Grossart, H.-P., Hambright, K.D., Hein, C., Hejzlar, J., Janus, L.L., Jenny, J.-P., Jones, J.R., Knoll, L.B., Leoni, B., Mackay, E., Matsuzaki, S.-I.S., McBride, C., Müller-Navarra, D.C., Paterson, A.M., Pierson, D., Rogora, M., Rusak, J.A., Sadro, S., Saulnier-Talbot, E., Schmid, M., Sommaruga, R., Thiery, W., Verburg, P., Weathers, K.C., Weyhenmeyer, G.A., Yokota, K., Rose, K.C., 2021. Widespread deoxygenation of temperate lakes. *Nature* 594, 66–70. doi:10.1038/s41586-021-03550-y
- Janse, J.H., De Senerpont Domis, L.N., Scheffer, M., Lijklema, L., Van Liere, L., Klinge, M., Mooij,

- W.M., 2008. Critical phosphorus loading of different types of shallow lakes and the consequences for management estimated with the ecosystem model PCLake. *Limnologica* 38, 203–219. doi:10.1016/j.limno.2008.06.001
- Janse, J.H., Scheffer, M., Lijklema, L., Van Liere, L., Sloot, J.S., Mooij, W.M., 2010. Estimating the critical phosphorus loading of shallow lakes with the ecosystem model PCLake: Sensitivity, calibration and uncertainty. *Ecol. Modell.* 221, 654–665. doi:10.1016/j.ecolmodel.2009.07.023
- Janssen, A.B.G., Arhonditsis, G.B., Beusen, A., Bolding, K., Bruce, L., Bruggeman, J., Couture, R.M., Downing, A.S., Alex Elliott, J., Frassl, M.A., Gal, G., Gerla, D.J., Hipsey, M.R., Hu, F., Ives, S.C., Janse, J.H., Jeppesen, E., Jöhnk, K.D., Kneis, D., Kong, X., Kuiper, J.J., Lehmann, M.K., Lemmen, C., Özkundakci, D., Petzoldt, T., Rinke, K., Robson, B.J., Sachse, R., Schep, S.A., Schmid, M., Scholten, H., Teurlincx, S., Trolle, D., Troost, T.A., Van Dam, A.A., Van Gerven, L.P.A., Weijerman, M., Wells, S.A., Mooij, W.M., 2015. Exploring, exploiting and evolving diversity of aquatic ecosystem models: a community perspective. *Aquat. Ecol.* 49, 513–548. doi:10.1007/s10452-015-9544-1
- Janssen, A.B.G., Teurlincx, S., Beusen, A.H.W., Huijbregts, M.A.J., Rost, J., Schipper, A.M., Seelen, L.M.S., Mooij, W.M., Janse, J.H., 2019a. PCLake+: A process-based ecological model to assess the trophic state of stratified and non-stratified freshwater lakes worldwide. *Ecol. Modell.* 396, 23–32. doi:10.1016/J.ECOLMODEL.2019.01.006
- Janssen, A.B.G., van Wijk, D., van Gerven, L.P.A., Bakker, E.S., Brederveld, R.J., DeAngelis, D.L., Janse, J.H., Mooij, W.M., 2019b. Success of lake restoration depends on spatial aspects of nutrient loading and hydrology. *Sci. Total Environ.* 679, 248–259. doi:10.1016/j.scitotenv.2019.04.443
- Jennings, E., Jones, S., Arvola, L., Staehr, P.A., Gaiser, E., Jones, I.D., Weathers, K.C., Weyhenmeyer, G.A., Chiu, C.Y., De Eyto, E., 2012. Effects of weather-related episodic events in lakes: an analysis based on high-frequency data. *Freshw. Biol.* 57, 589–601. doi:10.1111/j.1365-2427.2011.02729.x
- Jensen, H.S., Andersen, F.O., 1992. Importance of temperature, nitrate, and pH for phosphate release from aerobic sediments of four shallow, eutrophic lakes. *Limnol. Oceanogr.* 37, 577–589. doi:10.4319/LO.1992.37.3.0577
- Jeppesen, E., Brucet, S., Naselli-Flores, L., Papastergiadou, E., Stefanidis, K., Nöges, T., Nöges, P., Attayde, J.L., Zohary, T., Coppens, J., Bucak, T., Menezes, R.F., Freitas, F.R.S., Kernan,

- M., Søndergaard, M., Beklioglu, M., 2015. Ecological impacts of global warming and water abstraction on lakes and reservoirs due to changes in water level and related changes in salinity. *Hydrobiologia* 750, 201–227. doi:10.1007/s10750-014-2169-x
- Jeppesen, E., Søndergaard, M., Liu, Z., 2017. Lake restoration and management in a climate change perspective: An introduction. *Water (Switzerland)*. doi:10.3390/w9020122
- Jilbert, T., Couture, R.M., Huser, B.J., Salonen, K., 2020. Preface: Restoration of eutrophic lakes: current practices and future challenges. *Hydrobiologia* 847, 4343–4357. doi:10.1007/s10750-020-04457-x
- Jöhnk, K.D., Huisman, J., Sharples, J., Sommeijer, B., Visser, P.M., Stroom, J.M., 2008. Summer heatwaves promote blooms of harmful cyanobacteria. *Glob. Chang. Biol.* 14, 495–512. doi:10.1111/j.1365-2486.2007.01510.x
- Jones, C.A., Welch, E.B., 1990. Internal phosphorus loading related to mixing and dilution in a dendritic, shallow prairie lake. *Res. J. Water Pollut. Control Fed.* 62, 847–852.
- Jones, I.D., Elliott, J.A., 2007. Modelling the effects of changing retention time on abundance and composition of phytoplankton species in a small lake. *Freshw. Biol.* 52, 988–997. doi:10.1111/j.1365-2427.2007.01746.x
- Jones, I.D., Page, T., Elliott, J.A., Thackeray, S.J., Heathwaite, A.L., 2011. Increases in lake phytoplankton biomass caused by future climate-driven changes to seasonal river flow. *Glob. Chang. Biol.* 17, 1809–1820. doi:10.1111/j.1365-2486.2010.02332.x
- Jones, L., Fitch, A., Evans, C., Stephen, T., Spears, B., Gunn, I., Carvalho, L., May, L., Schonrogge, K., Clilverd, H., Mitchell, Z., Garbutt, A., Taylor, P., Fletcher, D., Gorst, A., Smale, R., Giam, G., Aron, J., Elliott, J., Illman, H., Ray, D., Fung, F., Tinker, J., Berenice-Wilmes, S., King, N., Malham, S., 2020. Climate driven threshold effects in the natural environment. Report to the Climate Change Committee.
- Jonkers, A.R.T., Sharkey, K.J., 2016. The differential warming response of Britain's rivers (1982–2011). *PLoS One* 11, e0166247. doi:10.1371/journal.pone.0166247
- Jørgensen, S.E., 2002. The application of models to find the relevance of residence time in lake and reservoir management. *Educ. J. Limnol* 62, 16–20. doi:10.4081/jlimnol.2003.s1.16
- Kalff, J., 2002. *Limnology: Inland water ecosystems*. Prentice Hall, Upper Saddle River, NJ.
- Kalinin, A., Covino, T., McGlynn, B., 2016. The influence of an in-network lake on the timing,

- form, and magnitude of downstream dissolved organic carbon and nutrient flux. *Water Resour. Res.* 52, 8668–8684. doi:10.1002/2016WR018977. Received
- Kay, A.L., Watts, G., Wells, S.C., Allen, S., 2020. The impact of climate change on U. K. river flows: A preliminary comparison of two generations of probabilistic climate projections. *Hydrol. Process.* 34, 1081–1088. doi:10.1002/hyp.13644
- Kerimoglu, O., Jacquet, S., Vinçon-Leite, B., Lemaire, B.J., Rimet, F., Soullignac, F., Trévisan, D., Anneville, O., 2017. Modelling the plankton groups of the deep, peri-alpine Lake Bourget. *Ecol. Modell.* 359, 415–433. doi:10.1016/J.ECOLMODEL.2017.06.005
- Kerr, L.A., Kritzer, J.P., Cadrin, S.X., 2019. Strengths and limitations of before-after-control-impact analysis for testing the effects of marine protected areas on managed populations. *ICES J. Mar. Sci.* 76, 1039–1051. doi:10.1093/icesjms/fsz014
- Kettle, A.J., Hughes, C., Unazi, G.A., Birch, L., Mohie-El-Din, H., Jones, M.R., 2012. Role of groundwater exchange on the energy budget and seasonal stratification of a shallow temperate lake. *J. Hydrol.* 470–471, 12–27. doi:10.1016/j.jhydrol.2012.07.004
- Kimura, N., Liu, W.C., Chiu, C.Y., Kratz, T.K., 2014. Assessing the effects of severe rainstorm-induced mixing on a subtropical, subalpine lake. *Environ. Monit. Assess.* 186, 3091–3114. doi:10.1007/s10661-013-3603-7
- Kirillin, G., Shatwell, T., Kasprzak, P., 2013. Consequences of thermal pollution from a nuclear plant on lake temperature and mixing regime. *J. Hydrol.* 496, 47–56. doi:10.1016/j.jhydrol.2013.05.023
- Kirillin, G., Wen, L., Shatwell, T., 2017. Seasonal thermal regime and climatic trends in lakes of the Tibetan highlands. *Hydrol. Earth Syst. Sci.* 21, 1895–1909. doi:10.5194/hess-21-1895-2017
- Kirk, J.T.O., 2010. *Light and photosynthesis in aquatic ecosystems*. Cambridge University Press. doi:10.1017/CBO9781139168212
- Klapper, H., 2007. The Assessment, Management and Reversal of Eutrophication, in: O’Sullivan, P.E., Reynolds, C.S. (Eds.), *The Lakes Handbook, Volume 2: Lake Restoration and Rehabilitation*. Blackwell Science Ltd, Oxford, UK, pp. 438–461.
- Klaus, M., Karlsson, J., Seekell, D., 2021. Tree line advance reduces mixing and oxygen concentrations in arctic-alpine lakes through wind sheltering and organic carbon supply. *Glob. Chang. Biol.* gcb.15660. doi:10.1111/gcb.15660

- Knoll, L.B., Williamson, C.E., Pilla, R.M., Leach, T.H., Brentrup, J.A., Fisher, T.J., 2018. Browning-related oxygen depletion in an oligotrophic lake. *Int. Waters* 8, 255–263. doi:10.1080/20442041.2018.1452355
- Komatsu, E., Fukushima, T., Harasawa, H., 2007. A modeling approach to forecast the effect of long-term climate change on lake water quality. *Ecol. Modell.* 209, 351–366. doi:10.1016/j.ecolmodel.2007.07.021
- Kopáček, J., Borovec, J., Hejzlar, J., Ulrich, K.U., Norton, S.A., Amirbahman, A., 2005. Aluminum control of phosphorus sorption by lake sediments. *Environ. Sci. Technol.* 39, 8784–8789. doi:10.1021/es050916b
- Kraemer, B.M., Anneville, O., Chandra, S., Dix, M., Kuusisto, E., Livingstone, D.M., Rimmer, A., Schladow, S.G., Silow, E., Sitoki, L.M., Tamatamah, R., Vadeboncoeur, Y., McIntyre, P.B., 2015. Morphometry and average temperature affect lake stratification responses to climate change. *Geophys. Res. Lett.* 42, 4981–4988. doi:10.1002/2015GL064097
- Kraemer, B.M., Chandra, S., Dell, A.I., Dix, M., Kuusisto, E., Livingstone, D.M., Schladow, S.G., Silow, E., Sitoki, L.M., Tamatamah, R., McIntyre, P.B., 2017. Global patterns in lake ecosystem responses to warming based on the temperature dependence of metabolism. *Glob. Chang. Biol.* 23, 1881–1890. doi:10.1111/gcb.13459
- Kuster, A.C., Kuster, A.T., Huser, B.J., 2020. A comparison of aluminum dosing methods for reducing sediment phosphorus release in lakes. *J. Environ. Manage.* 261, 110195. doi:10.1016/j.jenvman.2020.110195
- Ladwig, R., Furusato, E., Kirillin, G., Hinkelmann, R., Hupfer, M., 2018. Climate change demands adaptive management of urban lakes: Model-based assessment of management scenarios for Lake Tegel (Berlin, Germany). *Water* 10, 1–23. doi:10.3390/w10020186
- Ladwig, R., Hanson, P.C., Dugan, H.A., Carey, C.C., Zhang, Y., Shu, L., Duffy, C.J., Cobourn, K.M., 2021. Lake thermal structure drives interannual variability in summer anoxia dynamics in a eutrophic lake over 37 years. *Hydrol. Earth Syst. Sci.* 25, 1009–1032. doi:10.5194/hess-25-1009-2021
- Lang, P., Meis, S., Procházková, L., Carvalho, L., Mackay, E.B., Woods, H.J., Pottie, J., Milne, I., Taylor, C., Maberly, S.C., Spears, B.M., 2016. Phytoplankton community responses in a shallow lake following lanthanum-bentonite application. *Water Res.* 97, 55–68. doi:10.1016/j.watres.2016.03.018

- Laval, B.E., Vagle, S., Potts, D., Morrison, J., Sentlinger, G., James, C., McLaughlin, F., Carmack, E.C., 2012. The joint effects of riverine, thermal, and wind forcing on a temperate fjord lake: Quesnel Lake, Canada. *J. Great Lakes Res.* 38, 540–549. doi:10.1016/j.jglr.2012.06.007
- Lee, R.M., Biggs, T.W., Fang, X., 2018. Thermal and hydrodynamic changes under a warmer climate in a variably stratified hypereutrophic reservoir. *Water* 10, 1284. doi:10.3390/w10091284
- León, J.G., Beamud, S.G., Temporetti, P.F., Atencio, A.G., Diaz, M.M., Pedrozo, F.L., 2016. Stratification and residence time as factors controlling the seasonal variation and the vertical distribution of chlorophyll-a in a subtropical irrigation reservoir. *Int. Rev. Hydrobiol.* 101, 36–47. doi:10.1002/iroh.201501811
- Lewis, W.M., 1983. A revised classification of lakes based on mixing. *Can. J. Fish. Aquat. Sci.* 40, 1779–1787.
- Lewtas, K., Paterson, M., Venema, H.D., Roy, D., 2015. Manitoba Prairie Lakes: Eutrophication and in-lake remediation treatments literature review.
- Li, Y., Acharya, K., Yu, Z., 2011. Modeling impacts of Yangtze River water transfer on water ages in Lake Taihu, China. *Ecol. Eng.* 37, 325–334. doi:10.1016/j.ecoleng.2010.11.024
- Li, Y., Huang, T.L., Zhou, Z.Z., Long, S.H., Zhang, H.H., 2018. Effects of reservoir operation and climate change on thermal stratification of a canyon-shaped reservoir, in northwest China. *Water Sci. Technol. Water Supply* 18, 418–429. doi:10.2166/ws.2017.068
- Liu, Miao, Zhang, Yunlin, Shi, K., Zhang, Yibo, Zhou, Y., Zhu, M., Zhu, G., Wu, Z., Liu, Mingliang, 2020. Effects of rainfall on thermal stratification and dissolved oxygen in a deep drinking water reservoir. *Hydrol. Process.* 34, 3387–3399. doi:10.1002/hyp.13826
- Liu, Miao, Zhang, Yunlin, Shi, K., Zhu, G., Wu, Z., Liu, Mingliang, Zhang, Yibo, 2019. Thermal stratification dynamics in a large and deep subtropical reservoir revealed by high-frequency buoy data. *Sci. Total Environ.* 651, 614–624. doi:10.1016/j.scitotenv.2018.09.215
- Liu, Z., Hu, J., Zhong, P., Zhang, X., Ning, J., Larsen, S.E., Chen, D., Gao, Y., He, H., Jeppesen, E., 2018. Successful restoration of a tropical shallow eutrophic lake: Strong bottom-up but weak top-down effects recorded. *Water Res.* 146, 88–97. doi:10.1016/j.watres.2018.09.007

- Livingstone, D.M., Imboden, D.M., 1989. Annual heat balance and equilibrium temperature of Lake Aegeri, Switzerland. *Aquat. Sci.* 51, 351–369. doi:10.1007/BF00877177
- Londe, L.R., Novo, E.M.L.M., Barbosa, C., Araujo, C.A.S., 2016. Water residence time affecting phytoplankton blooms: study case in Ibitinga Reservoir (São Paulo, Brazil) using Landsat/TM images. *Brazilian J. Biol.* 76, 664–672. doi:10.1590/1519-6984.23814
- Lucas, L. V., Thompson, J.K., Brown, L.R., 2009. Why are diverse relationships observed between phytoplankton biomass and transport time? *Limnol. Oceanogr.* 54, 381–390. doi:10.4319/lo.2009.54.1.0381
- Lundgren, V.M., Roelke, D.L., Grover, J.P., Brooks, B.W., Prosser, K.N., Scott, W.C., Laws, C.A., Umphres, G.D., 2013. Interplay between ambient surface water mixing and manipulated hydraulic flushing: Implications for harmful algal bloom mitigation. *Ecol. Eng.* 60, 289–298. doi:10.1016/j.ecoleng.2013.07.063
- Lürling, M., Mackay, E., Reitzel, K., Spears, B.M., 2016. Editorial – A critical perspective on geo-engineering for eutrophication management in lakes. *Water Res.* 97, 1–10. doi:10.1016/j.watres.2016.03.035
- Lürling, M., Mucci, M., 2020. Mitigating eutrophication nuisance: in-lake measures are becoming inevitable in eutrophic waters in the Netherlands. *Hydrobiologia* 847, 4447–4467. doi:10.1007/s10750-020-04297-9
- Lürling, M., Smolders, A.J.P., Douglas, G., 2020. Methods for the management of internal phosphorus loading in lakes, in: Spears, B., Steinman, A.D. (Eds.), *Internal Phosphorus Loading in Lakes : Causes, Case Studies, and Management*. J. Ross Publishing, Chicago, pp. 77–107.
- Lynch, A.J., Cooke, S.J., Deines, A.M., Bower, S.D., Bunnell, D.B., Cowx, I.G., Nguyen, V.M., Nohner, J., Phouthavong, K., Riley, B., Rogers, M.W., Taylor, W.W., Woelmer, W., Youn, S.J., Beard, T.D., 2016. The social, economic, and environmental importance of inland fish and fisheries. *Environ. Rev.* doi:10.1139/er-2015-0064
- Maberly, S.C., de Ville, M.M., Thackeray, S.J., Ciar, D., Clarke, M., Fletcher, J.M., James, J.B., Keenan, P., Mackay, E.B., Patel, M., Tanna, B., Winfield, I.J., Bell, K., Clark, R., Jackson, A., Muir, J., Ramsden, P., Thompson, J., Titterton, H., Webb, P., 2016. A survey of the lakes of the English Lake District : The Lakes Tour 2015.
- Maberly, S.C., O'Donnell, R.A., Woolway, R.I., Cutler, M.E.J., Gong, M., Jones, I.D., Merchant,

- C.J., Miller, C.A., Politi, E., Scott, E.M., Thackeray, S.J., Tyler, A.N., 2020. Global lake thermal regions shift under climate change. *Nat. Commun.* 11, 1–9. doi:10.1038/s41467-020-15108-z
- MacIntyre, S., Romero, J.R., Kling, G.W., 2002. Spatial-temporal variability in surface layer deepening and lateral advection in an embayment of Lake Victoria, East Africa. *Limnol. Oceanogr.* 47, 656–671. doi:10.4319/lo.2002.47.3.0656
- MacIntyre, S., Sickman, J.O., Goldthwait, S.A., Kling, G.W., 2006. Physical pathways of nutrient supply in a small, ultraoligotrophic arctic lake during summer stratification. *Limnol. Oceanogr.* 51, 1107–1124. doi:10.4319/lo.2006.51.2.1107
- Mackay, E.B., Folkard, A.M., Jones, I.D., 2014a. Interannual variations in atmospheric forcing determine trajectories of hypolimnetic soluble reactive phosphorus supply in a eutrophic lake. *Freshw. Biol.* 59, 1646–1658. doi:10.1111/fwb.12371
- Mackay, E.B., Maberly, S.C., Pan, G., Reitzel, K., Bruere, A., Corker, N., Douglas, G., Egemose, S., Hamilton, D., Hatton-Ellis, T., Huser, B., Li, W., Meis, S., Moss, B., Lürling, M., Phillips, G., Yasseri, S., Spears, B.M., 2014b. Geoengineering in lakes: Welcome attraction or fatal distraction? *Int. Waters* 4, 349–356. doi:10.5268/IW-4.4.769
- Mackay, E.B., Ville, M.M. De, James, J.B., Dodd, B., Hunt, A., Chetiu, N., Keenan, P., 2020. Phosphorus composition of the surface sediments of Elterwater 2019.
- Magee, M.R., Wu, C.H., 2017. Response of water temperatures and stratification to changing climate in three lakes with different morphometry. *Hydrol. Earth Syst. Sci.* 21, 6253–6274. doi:10.5194/hess-21-6253-2017
- Magnuson, J.J., Webster, K.E., Assel, R.A., Bowser, C.J., Dillon, P.J., Eaton, J.G., Evans, H.E., Fee, E.J., Hall, R.I., Mortsch, L.R., Schindler, D.W., Quinn, F.H., 1997. Potential effects of climate changes on aquatic systems: Laurentian Great Lakes and Precambrian Shield region. *Hydrol. Process.* 11, 825–871. doi:10.1002/(SICI)1099-1085(19970630)11:8<825::AID-HYP509>3.0.CO;2-G
- Mahlum, S., Cote, D., Wiersma, Y.F., Pennell, C., Adams, B., 2018. Does restoration work? It depends on how we measure success. *Restor. Ecol.* 26, 952–963. doi:10.1111/rec.12649
- Marcé, R., George, G., Buscarinu, P., Deidda, M., Dunalska, J., De Eyto, E., Flaim, G., Grossart, H.P., Istvanovics, V., Lenhardt, M., Moreno-Ostos, E., Obrador, B., Ostrovsky, I., Pierson, D.C., Potužák, J., Poikane, S., Rinke, K., Rodríguez-Mozaz, S., Staehr, P.A., Šumberová, K.,

- Waajen, G., Weyhenmeyer, G.A., Weathers, K.C., Zion, M., Ibelings, B.W., Jennings, E., 2016. Automatic high frequency monitoring for improved lake and reservoir management. *Environ. Sci. Technol.* 50, 10780–10794. doi:10.1021/acs.est.6b01604
- Marcé, R., Moreno-Ostos, E., López, P., Armengol, J., 2008. The role of allochthonous inputs of dissolved organic carbon on the hypolimnetic oxygen content of reservoirs. *Ecosystems* 11, 1035–1053. doi:10.1007/s10021-008-9177-5
- Marcé, R., Rodríguez-Arias, M.À., García, J.C., Armengol, J.O.A.N., 2010. El Niño Southern Oscillation and climate trends impact reservoir water quality. *Glob. Chang. Biol.* 16, 2857–2865. doi:10.1111/j.1365-2486.2010.02163.x
- Marsden, M.W., 1989. Lake restoration by reducing external phosphorus loading: the influence of sediment phosphorus release. *Freshw. Biol.* 21, 139–162. doi:10.1111/j.1365-2427.1989.tb01355.x
- Martinsen, K.T., Andersen, M.R., Sand-Jensen, K., 2019. Water temperature dynamics and the prevalence of daytime stratification in small temperate shallow lakes. *Hydrobiologia* 826, 247–262. doi:10.1007/s10750-018-3737-2
- Matthews, K.R., Berg, N.H., 1997. Rainbow trout responses to water temperature and dissolved oxygen stress in two southern California stream pools. *J. Fish Biol.* 50, 50–67. doi:10.1111/j.1095-8649.1997.tb01339.x
- McBride, C.G., Rose, K.C., 2018. Automated High-frequency Monitoring and Research, in: Hamilton, D.P., Collier, K.J., Quinn, J., Howard-Williams, C. (Eds.), *Lake Restoration Handbook*. Springer, pp. 419–461. doi:10.1007/978-3-319-93043-5_13
- McCrackin, M.L., Jones, H.P., Jones, P.C., Moreno-Mateos, D., 2017. Recovery of lakes and coastal marine ecosystems from eutrophication: A global meta-analysis. *Limnol. Oceanogr.* 62, 507–518. doi:10.1002/lno.10441
- McFadden, D., 1974. The measurement of urban travel demand. *J. Public Econ.* 3, 303–328. doi:10.1016/0047-2727(74)90003-6
- McGowan, S., Leavitt, P.R., Hall, R.I., 2005. A whole-lake experiment to determine the effects of winter droughts on shallow lakes. *Ecosystems* 8, 694–708. doi:10.1007/s10021-003-0152-x
- McVicar, T.R., Roderick, M.L., Donohue, R.J., Li, L.T., Van Niel, T.G., Thomas, A., Grieser, J., Jhajharia, D., Himri, Y., Mahowald, N.M., Mescherskaya, A. V., Kruger, A.C., Rehman, S.,

- Dinpashoh, Y., 2012. Global review and synthesis of trends in observed terrestrial near-surface wind speeds: Implications for evaporation. *J. Hydrol.* 416–417, 182–205. doi:10.1016/j.jhydrol.2011.10.024
- Mehner, T., Diekmann, M., Gonsiorczyk, T., Kasprzak, P., Koschel, R., Krienitz, L., Rumpf, M., Schulz, M., Wauer, G., 2008. Rapid recovery from eutrophication of a stratified lake by disruption of internal nutrient load. *Ecosystems* 11, 1142–1156. doi:10.1007/s10021-008-9185-5
- Meis, S., Thackeray, S.J., Jones, I.D., 2009. Effects of recent climate change on phytoplankton phenology in a temperate lake. *Freshw. Biol.* 54, 1888–1898. doi:10.1111/j.1365-2427.2009.02240.x
- Mendonça, R., Müller, R.A., Clow, D., Verpoorter, C., Raymond, P., Tranvik, L.J., Sobek, S., 2017. Organic carbon burial in global lakes and reservoirs. *Nat. Commun.* 8, 1–6. doi:10.1038/s41467-017-01789-6
- Mesman, J.P., Ayala, A.I., Adrian, R., De Eyto, E., Frassl, M.A., Goyette, S., Kasparian, J., Perroud, M., Stelzer, J.A.A., Pierson, D.C., Ibelings, B.W., 2020. Performance of one-dimensional hydrodynamic lake models during short-term extreme weather events. *Environ. Model. Softw.* 133, 104852. doi:10.1016/j.envsoft.2020.104852
- Mesman, J.P., Stelzer, J.A.A., Dakos, V., Goyette, S., Jones, I.D., Kasparian, J., McGinnis, D.F., Ibelings, B.W., 2021. The role of internal feedbacks in shifting deep lake mixing regimes under a warming climate. *Freshw. Biol.* doi:10.1111/fwb.13704
- Messenger, M.L., Lehner, B., Grill, G., Nedeva, I., Schmitt, O., 2016. Estimating the volume and age of water stored in global lakes using a geo-statistical approach. *Nat. Commun.* 7, 13603. doi:10.1038/ncomms13603
- Milly, P.C.D., Dunne, K.A., Vecchia, A. V., 2005. Global pattern of trends in streamflow and water availability in a changing climate. *Nature* 438, 347–350. doi:10.1038/nature04312
- Missaghi, S., Hondzo, M., Herb, W., 2017. Prediction of lake water temperature, dissolved oxygen, and fish habitat under changing climate. *Clim. Change* 141, 747–757. doi:10.1007/s10584-017-1916-1
- Mitrovic, S.M., Chessman, B.C., Bowling, L.C., Cooke, R.H., 2006. Modelling suppression cyanobacterial blooms by flow management in a lowland river. *River Res. Appl.* 22, 109–114. doi:10.1002/rra.875

- Mitrovic, S.M., Hardwick, L., Dorani, F., 2011. Use of flow management to mitigate cyanobacterial blooms in the Lower Darling River, Australia. *J. Plankton Res.* 33, 229–241. doi:10.1093/plankt/fbq094
- Monsen, N.E., Cloern, J.E., Lucas, L. V., Monismith, S.G., 2002. A comment on the use of flushing time, residence time, and age as transport time scales. *Limnol. Oceanogr.* 47, 1545–1553. doi:10.4319/lo.2002.47.5.1545
- Mooij, W.M., Trolle, D., Jeppesen, E., Arhonditsis, G., Belolipetsky, P. V., Chitamwebwa, D.B.R., Degermendzhy, A.G., DeAngelis, D.L., De Senerpont Domis, L.N., Downing, A.S., Elliott, J.A., Fragoso, C.R., Gaedke, U., Genova, S.N., Gulati, R.D., Håkanson, L., Hamilton, D.P., Hipsey, M.R., 't Hoen, J., Hülsmann, S., Los, F.H., Makler-Pick, V., Petzoldt, T., Prokopkin, I.G., Rinke, K., Schep, S.A., Tominaga, K., van Dam, A.A., van Nes, E.H., Wells, S.A., Janse, J.H., 2010. Challenges and opportunities for integrating lake ecosystem modelling approaches. *Aquat. Ecol.* 44, 633–667. doi:10.1007/s10452-010-9339-3
- Moore, T., Mesman, J., Ladwig, R., Feldbauer, J., Olsson, F., Pilla, R.M., Shatwell, T., Venkiteswaran, J.J., Delany, A.D., Dugan, H., Rose, K.C., Read, J.S., 2021. LakeEnsemblR : An R package that facilitates ensemble modelling of lakes. *Environ. Model. Softw.* 0–36.
- Moras, S., Ayala, A.I., Pierson, D.C., 2019. Historical modelling of changes in Lake Erken thermal conditions. *Hydrol. Earth Syst. Sci.* 23, 5001–5016. doi:10.5194/hess-23-5001-2019
- Mortimer, C.H., 1942. The Exchange of Dissolved Substances between Mud and Water in Lakes. *J. Ecol.* 30, 147. doi:10.2307/2256691
- Morton, D., Rowland, C., Wood, C., Meek, C., Marston, C., Smith, G., Wadsworth, R., Simpson, I., 2011. Final report for LCM2007 - the new UK land cover map. Countryside Survey Technical Report No 11/07.
- Moss, B., Kosten, S., Meerhoff, M., Battarbee, R.W., Jeppesen, E., Mazzeo, N., Havens, K., Lacerot, G., Liu, Z., De Meester, L., Paerl, H., Scheffer, M., 2011. Allied attack: climate change and eutrophication. *Int. Waters* 1, 101–105. doi:10.5268/iw-1.2.359
- Müller, B., Bryant, L.D., Matzinger, A., Wüest, A., 2012. Hypolimnetic oxygen depletion in eutrophic lakes. *Environ. Sci. Technol.* 46, 9964–9971. doi:10.1021/es301422r
- Müller, B., Steinsberger, T., Schwefel, R., Gächter, R., Sturm, M., Wüest, A., 2019. Oxygen consumption in seasonally stratified lakes decreases only below a marginal phosphorus threshold. *Sci. Rep.* 9, 1–7. doi:10.1038/s41598-019-54486-3

- Murphy, J., Riley, J.P., 1962. A modified single solution method for the determination of phosphate in natural waters. *Anal. Chim. Acta* 27, 31–36. doi:10.1016/S0003-2670(00)88444-5
- Myers, B.J.E., Lynch, A.J., Bunnell, D.B., Chu, C., Falke, J.A., Kovach, R.P., Krabbenhoft, T.J., Kwak, T.J., Paukert, C.P., 2017. Global synthesis of the documented and projected effects of climate change on inland fishes. *Rev. Fish Biol. Fish.* 27, 339–361. doi:10.1007/s11160-017-9476-z
- Neal, C., Watts, C., Williams, R.J., Neal, M., Hill, L., Wickham, H., 2002. Diurnal and longer term patterns in carbon dioxide and calcite saturation for the River Kennet, south-eastern England. *Sci. Total Environ.* 282–283, 205–231. doi:10.1016/S0048-9697(01)00952-4
- Niedrist, G.H., Psenner, R., Sommaruga, R., 2018. Climate warming increases vertical and seasonal water temperature differences and inter-annual variability in a mountain lake. *Clim. Change* 151, 473–490. doi:10.1007/s10584-018-2328-6
- Nöges, P., Nöges, T., Ghiani, M., Sena, F., Fresner, R., Friedl, M., Mildner, J., 2011. Increased nutrient loading and rapid changes in phytoplankton expected with climate change in stratified South European lakes: Sensitivity of lakes with different trophic state and catchment properties. *Hydrobiologia* 667, 255–270. doi:10.1007/s10750-011-0649-9
- North, R.P., North, R.L., Livingstone, D.M., Köster, O., Kipfer, R., 2014. Long-term changes in hypoxia and soluble reactive phosphorus in the hypolimnion of a large temperate lake: Consequences of a climate regime shift. *Glob. Chang. Biol.* 20, 811–823. doi:10.1111/gcb.12371
- Nurnberg, G.K., 1988. Prediction of phosphorus release rates from total and reductant-soluble phosphorus in anoxic lake sediments. *Can. J. Fish. Aquat. Sci.* 45, 453–462. doi:10.1139/f88-054
- Nürnberg, G.K., 2019. Hypolimnetic withdrawal as a lake restoration technique: determination of feasibility and continued benefits. *Hydrobiologia*. doi:10.1007/s10750-019-04094-z
- Nürnberg, G.K., 1987. A comparison of internal phosphorus loads in lakes with anoxic hypolimnia: Laboratory incubation versus in situ hypolimnetic phosphorus accumulation. *Limnol. Oceanogr.* doi:10.4319/lo.1987.32.5.1160
- Nürnberg, G.K., 1984. The prediction of internal phosphorus load in lakes with anoxic hypolimnia. *Limnol. Oceanogr.* 29, 111–124. doi:10.4319/lo.1984.29.1.0111

- O'Reilly, C.M., Sharma, S., Gray, D.K., Hampton, S.E., Read, J.S., Rowley, R.J., Schneider, P., Lenters, J.D., McIntyre, P.B., Kraemer, B.M., Weyhenmeyer, G.A., Straile, D., Dong, B., Adrian, R., Allan, M.G., Anneville, O., Arvola, L., Austin, J., Bailey, J.L., Baron, J.S., Brookes, J.D., De Eyto, E., Dokulil, M.T., Hamilton, D.P., Havens, K., Hetherington, A.L., Higgins, S.N., Hook, S., Izmet'eva, L.R., Joehnk, K.D., Kangur, K., Kasprzak, P., Kumagai, M., Kuusisto, E., Leshkevich, G., Livingstone, D.M., MacIntyre, S., May, L., Melack, J.M., Mueller-Navarra, D.C., Naumenko, M., Noges, P., Noges, T., North, R.P., Plisnier, P.D., Rigosi, A., Rimmer, A., Rogora, M., Rudstam, L.G., Rusak, J.A., Salmaso, N., Samal, N.R., Schindler, D.E., Schladow, S.G., Schmid, M., Schmidt, S.R., Silow, E., Soylu, M.E., Teubner, K., Verburg, P., Voutilainen, A., Watkinson, A., Williamson, C.E., Zhang, G., 2015. Rapid and highly variable warming of lake surface waters around the globe. *Geophys. Res. Lett.* 42, 10773–10781. doi:10.1002/2015GL066235
- Obertegger, U., Borsato, A., Flaim, G., 2010. Rotifer-crustacean interactions in a pseudokarstic lake: Influence of hydrology. *Aquat. Ecol.* 44, 121–130. doi:10.1007/s10452-009-9285-0
- Obertegger, U., Flaim, G., Braioni, M.G., Sommaruga, R., Corradini, F., Borsato, A., 2007. Water residence time as a driving force of zooplankton structure and succession. *Aquat. Sci.* 69, 575–583. doi:10.1007/s00027-007-0924-z
- Obertegger, U., Obrador, B., Flaim, G., 2017. Dissolved oxygen dynamics under ice: Three winters of high-frequency data from Lake Tovel, Italy. *Water Resour. Res.* 53, 7234–7246. doi:10.1002/2017WR020599
- Obrador, B., Staehr, P.A., Christensen, J.P.C., 2014. Vertical patterns of metabolism in three contrasting stratified lakes. *Limnol. Oceanogr.* 59, 1228–1240. doi:10.4319/lo.2014.59.4.1228
- Ockenden, M.C., Tych, W., Beven, K.J., Collins, A.L., Evans, R., Falloon, P.D., Forber, K.J., Hiscock, K.M., Hollaway, M.J., Kahana, R., Macleod, C.J.A., Villamizar, M.L., Wearing, C., Withers, P.J.A., Zhou, J.G., Benskin, C.M.W.H., Burke, S., Cooper, R.J., Freer, J.E., Haygarth, P.M., 2017. Prediction of storm transfers and annual loads with data-based mechanistic models using high-frequency data. *Hydrol. Earth Syst. Sci.* 21, 6425–6444. doi:10.5194/hess-21-6425-2017
- Olsson, F., Mackay, E.B., Barker, P., Davies, S., Hall, R., Spears, B., Exley, G., Thackeray, S.J., Jones, I.D., 2022. Can reductions in water residence time be used to disrupt seasonal stratification and control internal loading in a eutrophic monomictic lake? *J. Environ.*

- Manage. 304. doi:10.1016/j.jenvman.2021.114169
- Özen, A., Karapinar, B., Kucuk, I., Jeppesen, E., Beklioglu, M., 2010. Drought-induced changes in nutrient concentrations and retention in two shallow Mediterranean lakes subjected to different degrees of management. *Hydrobiologia* 646, 61–72. doi:10.1007/s10750-010-0179-x
- Padisák, J., Kohler, J., Hoeg, S., 1999. The effect of changing flushing rates on development of late summer *Aphanizomenon* and *Microcystis* populations in a shallow lake, Müggelsee, Berlin, Germany. *Theor. Reserv. Ecol. its Appl.* 411–423.
- Paerl, H.W., Gardner, W.S., Havens, K.E., Joyner, A.R., McCarthy, M.J., Newell, S.E., Qin, B., Scott, J.T., 2016. Mitigating cyanobacterial harmful algal blooms in aquatic ecosystems impacted by climate change and anthropogenic nutrients. *Harmful Algae* 54, 213–222. doi:10.1016/j.hal.2015.09.009
- Paerl, H.W., Huisman, J., 2009. Climate change: A catalyst for global expansion of harmful cyanobacterial blooms. *Environ. Microbiol. Rep.* doi:10.1111/j.1758-2229.2008.00004.x
- Paerl, H.W., Huisman, J., 2008. Blooms like it hot. *Science* (80-.). 320, 57–58. doi:10.1126/science.1155398
- Page, T., Smith, P.J., Beven, K.J., Jones, I.D., Elliott, J.A., Maberly, S.C., Mackay, E.B., De Ville, M., Feuchtmayr, H., 2018. Adaptive forecasting of phytoplankton communities. *Water Res.* 134, 74–85. doi:10.1016/j.watres.2018.01.046
- Palmer, M.J., Chételat, J., Jamieson, H.E., Richardson, M., Amyot, M., 2021. Hydrologic control on winter dissolved oxygen mediates arsenic cycling in a small subarctic lake. *Limnol. Oceanogr.* 66, S30–S46. doi:10.1002/lno.11556
- Papst, M.H., Mathias, J.A., Barica, J., 1980. Relationship between thermal stability and summer oxygen depletion in a prairie pothole lake. *Can. J. Fish. Aquat. Sci.* 37, 1433–1438. doi:10.1139/f80-183
- Park, I.H., Min, S.K., 2017. Role of convective precipitation in the relationship between subdaily extreme precipitation and temperature. *J. Clim.* 30, 9527–9537. doi:10.1175/JCLI-D-17-0075.1
- Patterson, J.C., Hamblin, P.F., Imberger, J., 1984. Classification and dynamic simulation of the vertical density structure of lakes. *Limnol. Oceanogr.* 29, 845–861. doi:10.4319/LO.1984.29.4.0845

- Perga, M.E., Bruel, R., Rodriguez, L., Guénand, Y., Bouffard, D., 2018. Storm impacts on alpine lakes: Antecedent weather conditions matter more than the event intensity. *Glob. Chang. Biol.* 24, 5004–5016. doi:10.1111/gcb.14384
- Pettersson, K., 1998. Mechanisms for internal loading of phosphorus in lakes, in: *Hydrobiologia*. Springer, pp. 21–25. doi:10.1007/978-94-011-5266-2_2
- Piccolroaz, S., Toffolon, M., Majone, B., 2015. The role of stratification on lakes' thermal response: The case of Lake Superior. *Water Resour. Res.* 51, 7878–7894. doi:10.1111/j.1752-1688.1969.tb04897.x
- Piccolroaz, S., Woolway, R.I., Merchant, C.J., 2020. Global reconstruction of twentieth century lake surface water temperature reveals different warming trends depending on the climatic zone. *Clim. Change* 160, 427–442. doi:10.1007/s10584-020-02663-z
- Pilla, R.M., Williamson, C.E., Adamovich, B. V., Adrian, R., Anneville, O., Chandra, S., Colom-Montero, W., Devlin, S.P., Dix, M.A., Dokulil, M.T., Gaiser, E.E., Girdner, S.F., Hambright, K.D., Hamilton, D.P., Havens, K., Hessen, D.O., Higgins, S.N., Huttula, T.H., Huuskonen, H., Isles, P.D.F., Joehnk, K.D., Jones, I.D., Keller, W.B., Knoll, L.B., Korhonen, J., Kraemer, B.M., Leavitt, P.R., Lepori, F., Luger, M.S., Maberly, S.C., Melack, J.M., Melles, S.J., Müller-Navarra, D.C., Pierson, D.C., Pislegina, H. V., Plisnier, P.D., Richardson, D.C., Rimmer, A., Rogora, M., Rusak, J.A., Sadro, S., Salmaso, N., Saros, J.E., Saulnier-Talbot, É., Schindler, D.E., Schmid, M., Shimaraeva, S. V., Silow, E.A., Sitoki, L.M., Sommaruga, R., Straile, D., Strock, K.E., Thiery, W., Timofeyev, M.A., Verburg, P., Vinebrooke, R.D., Weyhenmeyer, G.A., Zadereev, E., 2020. Deeper waters are changing less consistently than surface waters in a global analysis of 102 lakes. *Sci. Rep.* 10, 1–15. doi:10.1038/s41598-020-76873-x
- Pilla, R.M., Williamson, C.E., Zhang, J., Smyth, R.L., Lenters, J.D., Brentrup, J.A., Knoll, L.B., Fisher, T.J., 2018. Browning-related decreases in water transparency lead to long-term increases in surface water temperature and thermal stratification in two small lakes. *J. Geophys. Res. Biogeosciences* 123, 1651–1665. doi:10.1029/2017JG004321
- Pilotti, M., Simoncelli, S., Valerio, G., 2014. A simple approach to the evaluation of the actual water renewal time of natural stratified lakes. *Water Resour. Res.* 50, 2830–2849. doi:10.1002/2013WR014471
- Preece, E.P., Moore, B.C., Skinner, M.M., Child, A., Dent, S., 2019. A review of the biological and chemical effects of hypolimnetic oxygenation. *Lake Reserv. Manag.* 35, 229–246.

doi:10.1080/10402381.2019.1580325

- Prudhomme, C., Haxton, T., Crooks, S., Jackson, C., Barkwith, A., Williamson, J., Kelvin, J., Mackay, J., Wang, L., Young, A., Watts, G., 2013. Future Flows Hydrology: An ensemble of daily river flow and monthly groundwater levels for use for climate change impact assessment across Great Britain. *Earth Syst. Sci. Data* 5, 101–107. doi:10.5194/essd-5-101-2013
- Prudhomme, C., Young, A., Watts, G., Haxton, T., Crooks, S., Williamson, J., Davies, H., Dadson, S., Allen, S., 2012. The drying up of Britain? A national estimate of changes in seasonal river flows from 11 Regional Climate Model simulations. *Hydrol. Process.* 26, 1115–1118. doi:10.1002/hyp.8434
- Radbourne, A.D., Ryves, D.B., Madgwick, G., Anderson, N.J., 2019. The influence of climate change on the restoration trajectory of a nutrient-rich deep lake. *Ecosystems*. doi:10.1007/s10021-019-00442-1
- Råman Vinnå, L., Medhaug, I., Schmid, M., Bouffard, D., 2021. The vulnerability of lakes to climate change along an altitudinal gradient. *Commun. Earth Environ.* 2, 35. doi:10.1038/s43247-021-00106-w
- Råman Vinnå, L., Wüest, A., Bouffard, D., 2017. Physical effects of thermal pollution in lakes. *Water Resour. Res.* 53, 3968–3987. doi:10.1002/2016WR019686
- Råman Vinnå, L., Wüest, A., Zappa, M., Fink, G., Bouffard, D., 2018. Tributaries affect the thermal response of lakes to climate change. *Hydrol. Earth Syst. Sci.* 22, 31–51. doi:10.5194/hess-22-31-2018
- Rangel, L.M., Silva, L.H.S., Rosa, P., Roland, F., Huszar, V.L.M., 2012. Phytoplankton biomass is mainly controlled by hydrology and phosphorus concentrations in tropical hydroelectric reservoirs. *Hydrobiologia* 693, 13–28. doi:10.1007/s10750-012-1083-3
- Raven, J.A., Kübler, J.E., Beardall, J., 2000. Put out the light, and then put out the light. *J. Mar. Biol. Assoc. United Kingdom*. doi:10.1017/S0025315499001526
- Raymond, P.A., Hartmann, J., Lauerwald, R., Sobek, S., McDonald, C., Hoover, M., Butman, D., Striegl, R., Mayorga, E., Humborg, C., Kortelainen, P., Dürr, H., Meybeck, M., Ciais, P., Guth, P., 2013. Global carbon dioxide emissions from inland waters. *Nature* 503, 355–359. doi:10.1038/nature12760
- Read, J.S., Hamilton, D.P., Desai, A.R., Rose, K.C., MacIntyre, S., Lenters, J.D., Smyth, R.L.,

- Hanson, P.C., Cole, J.J., Staehr, P.A., Rusak, J.A., Pierson, D.C., Brookes, J.D., Laas, A., Wu, C.H., 2012. Lake-size dependency of wind shear and convection as controls on gas exchange. *Geophys. Res. Lett.* 39, n/a-n/a. doi:10.1029/2012GL051886
- Read, J.S., Hamilton, D.P., Jones, I.D., Muraoka, K., Winslow, L.A., Kroiss, R., Wu, C.H., Gaiser, E., 2011. Derivation of lake mixing and stratification indices from high-resolution lake buoy data. *Environ. Model. Softw.* 26, 1325–1336. doi:10.1016/j.envsoft.2011.05.006
- Rennella, A.M., Quirós, R., 2006. The effects of hydrology on plankton biomass in shallow lakes of the Pampa Plain. *Hydrobiologia* 556, 181–191. doi:10.1007/s10750-005-0318-y
- Reynaud, A., Lanzanova, D., 2017. A global meta-analysis of the value of ecosystem services provided by lakes. *Ecol. Econ.* 137, 184–194. doi:10.1016/j.ecolecon.2017.03.001
- Reynolds, C.S., Lund, J.W.G., 1988. The phytoplankton of an enriched, soft-water lake subject to intermittent hydraulic flushing (Grasmere, English Lake District), North West Water. doi:10.1111/j.1365-2427.1988.tb00359.x
- Reynolds, C.S., Maberly, S.C., Parker, J.E., de Ville, M.M., 2012. Forty years of monitoring water quality in Grasmere (English Lake District): Separating the effects of enrichment by treated sewage and hydraulic flushing on phytoplankton ecology. *Freshw. Biol.* 57, 384–399. doi:10.1111/j.1365-2427.2011.02687.x
- Richards, J., Moore, R.D., Forrest, A.L., 2012. Late-summer thermal regime of a small proglacial lake. *Hydrol. Process.* 26, 2687–2695. doi:10.1002/hyp.8360
- Richardson, D.C., Melles, S.J., Pilla, R.M., Hetherington, A.L., Knoll, L.B., Williamson, C.E., Kraemer, B.M., Jackson, J.R., Long, E.C., Moore, K., Rudstam, L.G., Rusak, J.A., Saros, J.E., Sharma, S., Strock, K.E., Weathers, K.C., Wigdahl-Perry, C.R., 2017. Transparency, geomorphology and mixing regime explain variability in trends in lake temperature and stratification across Northeastern North America (1975-2014). *Water (Switzerland)* 9, 442. doi:10.3390/w9060442
- Rimmer, A., Gal, G., Opher, T., Lechinsky, Y., Yacobi, Y.Z., 2011. Mechanisms of long-term variations in the thermal structure of a warm lake. *Limnol. Oceanogr.* 56, 974–988. doi:10.4319/lo.2011.56.3.0974
- Rio, M., Rey, D., Prudhomme, C., Holman, I.P., 2018. Evaluation of changing surface water abstraction reliability for supplemental irrigation under climate change. *Agric. Water Manag.* 206, 200–208. doi:10.1016/j.agwat.2018.05.005

- Roberts, D.C., Forrest, A.L., Sahoo, G.B., Hook, S.J., Schladow, S.G., 2018. Snowmelt timing as a determinant of lake inflow mixing. *Water Resour. Res.* 54, 1237–1251. doi:10.1002/2017WR021977
- Robson, B.J., 2014. When do aquatic systems models provide useful predictions, what is changing, and what is next? *Environ. Model. Softw.* 61, 287–296. doi:10.1016/j.envsoft.2014.01.009
- Roderick, M.L., Sun, F., Lim, W.H., Farquhar, G.D., 2014. A general framework for understanding the response of the water cycle to global warming over land and ocean. *Hydrol. Earth Syst. Sci.* 18, 1575–1589. doi:10.5194/hess-18-1575-2014
- Rodgers, G.K., 1987. Time of onset of full thermal stratification in Lake Ontario in relation to lake temperatures in winter. *Can. J. Fish. Aquat. Sci.* 44, 2225–2229. doi:10.1139/f87-273
- Rogora, M., Buzzi, F., Dresti, C., Leoni, B., Lepori, F., Mosello, R., Patelli, M., Salmaso, N., 2018. Climatic effects on vertical mixing and deep-water oxygen content in the subalpine lakes in Italy. *Hydrobiologia* 824, 33–50. doi:10.1007/s10750-018-3623-y
- Rolighed, J., Jeppesen, E., Søndergaard, M., Bjerring, R., Janse, J.H., Mooij, W.M., Trolle, D., 2016. Climate change will make recovery from eutrophication more difficult in shallow Danish Lake Søbygaard. *Water (Switzerland)* 8, 459. doi:10.3390/w8100459
- Romo, S., Soria, J., Fernández, F., Ouahid, Y., Barón-Solá, Á., 2013. Water residence time and the dynamics of toxic cyanobacteria. *Freshw. Biol.* 58, 513–522. doi:10.1111/j.1365-2427.2012.02734.x
- Rose, K.C., Greb, S.R., Diebel, M., Turner, M.G., 2017. Annual precipitation regulates spatial and temporal drivers of lake water clarity: *Ecol. Appl.* 27, 632–643. doi:10.1002/eap.1471
- Rousso, B.Z., Bertone, E., Stewart, R., Hamilton, D.P., 2020. A systematic literature review of forecasting and predictive models for cyanobacteria blooms in freshwater lakes. *Water Res.* 115959. doi:10.1016/j.watres.2020.115959
- Rueda, F., Moreno-Ostos, E., Armengol, J., 2006. The residence time of river water in reservoirs. *Ecol. Modell.* doi:10.1016/j.ecolmodel.2005.04.030
- Rueda, F.J., MacIntyre, S., 2009. Flow paths and spatial heterogeneity of stream inflows in a small multibasin lake. *Limnol. Oceanogr.* 54, 2041–2057. doi:10.4319/lo.2009.54.6.2041
- Rueda Valdivia, F., 2006. Basin scale transport in stratified lakes and reservoirs: Towards the

- knowledge of freshwater ecosystems. *Limnetica* 25, 33–56.
- Saber, A., James, D.E., Hayes, D.F., 2018. Effects of seasonal fluctuations of surface heat flux and wind stress on mixing and vertical diffusivity of water column in deep lakes. *Adv. Water Resour.* 119, 150–163. doi:10.1016/j.advwatres.2018.07.006
- Sadro, S., Melack, J.M., Sickman, J.O., Skeen, K., 2019. Climate warming response of mountain lakes affected by variations in snow. *Limnol. Oceanogr. Lett.* 4, 9–17. doi:10.1002/lo.10099
- Saito, M., Onodera, S.-I., Shiimizu, Y., 2013. Effects of residence time and nutrient load on eutrophic conditions and phytoplankton variations in agricultural reservoirs, in: *Understanding Freshwater Quality Problems in a Changing World*. IAHS Publ, pp. 197–203.
- Schallenberg, M., De Winton, M.D., Verburg, P., Kelly, D.J., Hamill, K.D., Hamilton, D.P., 2013. Ecosystem Services of Lakes, in: *Ecosystem Services in New Zealand - Conditions and Trends*. pp. 203–225.
- Scheffer, M., Van Geest, G.J., Zimmer, K., Jeppesen, E., Søndergaard, M., Butler, M.G., Hanson, M.A., Declerck, S., De Meester, L., 2006. Small habitat size and isolation can promote species richness: Second-order effects on biodiversity in shallow lakes and ponds. *Oikos*. doi:10.1111/j.0030-1299.2006.14145.x
- Schindler, D.W., 2009. Lakes as sentinels and integrators for the effects of climate change on watersheds, airsheds, and landscapes. *Limnol. Oceanogr.* 54, 2349–2358. doi:10.4319/lo.2009.54.6_part_2.2349
- Schindler, D.W., 2006. Recent advances in the understanding and management of eutrophication. *Limnol. Oceanogr.* 51, 356–363. doi:10.4319/lo.2006.51.1_part_2.0356
- Schmid, M., Köster, O., 2016. Excess warming of a Central European lake driven by solar brightening. *Water Resour. Res.* 52, 8103–8116. doi:10.1002/2016WR018651
- Schmid, M., Read, J., 2021. Heat Budget of Lakes, in: *Earth Systems and Environmental Sciences. Encyclopedia of Inland Waters*. p. 7. doi:10.1016/b978-0-12-819166-8.00011-6
- Schwartz, C.J., 2015. Analysis of BACI experiments. *Course Notes Begin. Intermed. Stat.* 614–705.

- Schwefel, R., Gaudard, A., Wüest, A., Bouffard, D., 2016. Effects of climate change on deepwater oxygen and winter mixing in a deep lake (Lake Geneva): Comparing observational findings and modeling. *Water Resour. Res.* 52, 8811–8826. doi:10.1002/2016WR019194
- Seddon, N., Daniels, E., Davis, R., Chausson, A., Harris, R., Hou-Jones, X., Huq, S., Kapos, V., Mace, G.M., Rizvi, A.R., Reid, H., Roe, D., Turner, B., Wicander, S., 2020. Global recognition of the importance of nature-based solutions to the impacts of climate change. *Glob. Sustain.* 3. doi:10.1017/sus.2020.8
- Seitzinger, S., Harrison, J.A., Böhlke, J.K., Bouwman, A.F., Lowrance, R., Peterson, B., Tobias, C., Van Drecht, G., 2006. Denitrification across landscapes and waterscapes: A synthesis. *Ecol. Appl.* 16, 2064–2090. doi:10.1890/1051-0761(2006)016[2064:DALAWA]2.0.CO;2
- Sharma, S., Blagrove, K., Magnuson, J.J., O'Reilly, C.M., Oliver, S., Batt, R.D., Magee, M.R., Straile, D., Weyhenmeyer, G.A., Winslow, L., Woolway, R.I., 2019. Widespread loss of lake ice around the Northern Hemisphere in a warming world. *Nat. Clim. Chang.* doi:10.1038/s41558-018-0393-5
- Shatwell, T., Thiery, W., Kirillin, G., 2019. Future projections of temperature and mixing regime of European temperate lakes. *Hydrol. Earth Syst. Sci.* 23, 1533–1551. doi:10.5194/hess-23-1533-2019
- Shiklomanov, I. a., 1998. World Water Resources- A new Appraisal and Assessment for the 21st century, Report. doi:10.4314/wsa.v30i4.5101
- Shrestha, R.R., Dibike, Y.B., Prowse, T.D., 2012. Modelling of climate-induced hydrologic changes in the Lake Winnipeg watershed. *J. Great Lakes Res.* 38, 83–94. doi:10.1016/j.jglr.2011.02.004
- Sit, V., Taylor, B., 1998. Statistical methods for adaptive management studies, in: *Land Management Handbook*. pp. 279–300. doi:10.1191/096228098677382724
- Smith, E.P., 2006. BACI Design, in: *Encyclopedia of Environmetrics*. pp. 141–148. doi:10.1002/9780470057339.vab001
- Smith, V.H., Schindler, D.W., 2009. Eutrophication science: where do we go from here? *Trends Ecol. Evol.* doi:10.1016/j.tree.2008.11.009
- Smits, A.P., Gomez, N.W., Dozier, J., Sadro, S., 2021. Winter climate and lake morphology control ice phenology and under-ice temperature and oxygen regimes in mountain lakes.

- J. Geophys. Res. Biogeosciences 1–20. doi:10.1029/2021jg006277
- Smits, A.P., MacIntyre, S., Sadro, S., 2020. Snowpack determines relative importance of climate factors driving summer lake warming. *Limnol. Oceanogr. Lett.* 5, 271–279. doi:10.1002/lol2.10147
- Smokorowski, K.E., Randall, R.G., 2017. Cautions on using the Before-After-Control-Impact design in environmental effects monitoring programs. *FACETS* 2, 212–232. doi:10.1139/facets-2016-0058
- Smucker, N.J., Beaulieu, J.J., Nietch, C.T., Young, J.L., 2021. Increasingly severe cyanobacterial blooms and deep water hypoxia coincide with warming water temperatures in reservoirs. *Glob. Chang. Biol.* 1–13. doi:10.1111/gcb.15618
- Snorheim, C.A., Hanson, P.C., McMahon, K.D., Read, J.S., Carey, C.C., Dugan, H.A., 2017. Meteorological drivers of hypolimnetic anoxia in a eutrophic, north temperate lake. *Ecol. Modell.* 343, 39–53. doi:10.1016/j.ecolmodel.2016.10.014
- Soares, L.M.V., Calijuri, M. do C., 2021. Deterministic modelling of freshwater lakes and reservoirs: Current trends and recent progress. *Environ. Model. Softw.* 144. doi:10.1016/j.envsoft.2021.105143
- Soares, M.C.S., Marinho, M.M., Azevedo, S.M.O.F., Branco, C.W.C.W., Huszar, V.L.L.M., 2012. Eutrophication and retention time affecting spatial heterogeneity in a tropical reservoir. *Limnologica* 42, 197–203. doi:10.1016/j.limno.2011.11.002
- Søndergaard, M., Jensen, J.P., Jeppesen, E., 2003. Role of sediment and internal loading of phosphorus in shallow lakes. *Hydrobiologia* 506–509, 135–145. doi:10.1023/B
- Søndergaard, M., Jeppesen, E., Lauridsen, T.L., Skov, C., Van Nes, E.H., Roijackers, R., Lammens, E., Portielje, R., 2007. Lake restoration: Successes, failures and long-term effects. *J. Appl. Ecol.* 44, 1095–1105. doi:10.1111/j.1365-2664.2007.01363.x
- Spears, B.M., Carvalho, L., Paterson, D.M., 2007. Phosphorus partitioning in a shallow lake: Implications for water quality management. *Water Environ. J.* 21, 47–53. doi:10.1111/j.1747-6593.2006.00045.x
- Spears, B.M., Chapman, D., Carvalho, L., Rankinen, K., Stefanidis, K., Ives, S., Vuorio, K., Birk, S., Spears, B.M., Chapman, D., Carvalho, L., Rankinen, K., Stefanidis, K., Ives, S., Vuorio, K., Birk, S., Spears, B.M., Chapman, D., Carvalho, L., Rankinen, K., 2021. Assessing multiple stressor effects to inform climate change management responses in three European

- catchments. *Inl. Waters* 1–13. doi:10.1080/20442041.2020.1827891
- Spears, B.M., Maberly, S.C., Pan, G., Mackay, E., Bruere, A., Corker, N., Douglas, G., Egemose, S., Hamilton, D., Hatton-Ellis, T., Huser, B., Li, W., Meis, S., Moss, B., Lüring, M., Phillips, G., Yasseri, S., Reitzel, K., 2014. Geo-Engineering in Lakes: A Crisis of Confidence? *Environ. Sci. Technol.* 48, 9977–9979. doi:10.1021/ES5036267
- Spears, B.M., Mackay, E.B., Yasseri, S., Gunn, I.D.M., Waters, K.E., Andrews, C., Cole, S., De Ville, M., Kelly, A., Meis, S., Moore, A.L., Nürnberg, G.K., van Oosterhout, F., Pitt, J.A., Madgwick, G., Woods, H.J., Lüring, M., 2016. A meta-analysis of water quality and aquatic macrophyte responses in 18 lakes treated with lanthanum modified bentonite (Phoslock®). *Water Res.* 97, 111–121. doi:10.1016/j.watres.2015.08.020
- Staeher, P.A., Bade, D., van de Bogert, M.C., Koch, G.R., Williamson, C., Hanson, P., Cole, J.J., Kratz, T., 2010. Lake metabolism and the diel oxygen technique: State of the science. *Limnol. Oceanogr. Methods* 8, 628–644. doi:10.4319/lom.2010.8.0628
- Standing Committee of Analysts, 1980. Phosphorus in waters, effluents and sewages, in: *Methods for the Examination of Waters and Associated Materials*. HMSO, London.
- Stetler, J.T., Girdner, S., Mack, J., Winslow, L.A., Leach, T.H., Rose, K.C., 2020. Atmospheric stilling and warming air temperatures drive long-term changes in lake stratification in a large oligotrophic lake. *Limnol. Oceanogr.* 66, 954–964. doi:10.1002/lno.11654
- Stewart-Oaten, A., Bence, J.R., Osenberg, C.W., 1992. Assessing effects of unreplicated perturbations: no simple solutions. *Ecology* 73, 1396–1404. doi:10.2307/1940685
- Stewart-Oaten, A., Murdoch, W.W., Parker, K.R., 1986. Environmental impact assessment: “pseudoreplication” in time? *Ecology* 67, 929–940.
- Stockdale, J.M., 1991. *A Study of the Hydrology and Water Quality of Elterwater, Cumbria*. Imperial College, University of London.
- Stockwell, J.D., Doubek, J.P., Adrian, R., Anneville, O., Carey, C.C., Carvalho, L., De Senerpont Domis, L.N., Dur, G., Frassl, M.A., Grossart, H.P., Ibelings, B.W., Lajeunesse, M.J., Lewandowska, A.M., Llamas, M.E., Matsuzaki, S.I.S., Nodine, E.R., Nöges, P., Patil, V.P., Pomati, F., Rinke, K., Rudstam, L.G., Rusak, J.A., Salmaso, N., Selmann, C.T., Straile, D., Thackeray, S.J., Thiery, W., Urrutia-Cordero, P., Venail, P., Verburg, P., Woolway, R.I., Zohary, T., Andersen, M.R., Bhattacharya, R., Hejzlar, J., Janatian, N., Kpodonu, A.T.N.K., Williamson, T.J., Wilson, H.L., 2020. Storm impacts on phytoplankton community

- dynamics in lakes. *Glob. Chang. Biol.* 26, 2756–2784. doi:10.1111/gcb.15033
- Storn, R., Price, K., 1997. Differential Evolution - A Simple and Efficient Heuristic for Global Optimization over Continuous Spaces. *J. Glob. Optim.* 11, 341–359. doi:10.1023/A:1008202821328
- Straškraba, M., Hocking, G., 2002. The effect of theoretical retention time on the hydrodynamics of deep river valley reservoirs. *Int. Rev. Hydrobiol.* 87, 61–83. doi:10.1002/1522-2632(200201)87:1<61::AID-IROH61>3.0.CO;2-4
- Strayer, D.L., Dudgeon, D., 2010. Freshwater biodiversity conservation: Recent progress and future challenges. *J. North Am. Benthol. Soc.* 29, 344–358. doi:10.1899/08-171.1
- Stroom, J.M., Kardinaal, W.E.A., 2016. How to combat cyanobacterial blooms: strategy toward preventive lake restoration and reactive control measures. *Aquat. Ecol.* 50, 541–576. doi:10.1007/s10452-016-9593-0
- Talling, J.F., 1974. Photosynthetic pigments: general outline of spectrophotometric methods; specific procedures, in: Vollenweider, R.A. (Ed.), *A Manual on Methods of Measuring Primary Production in Aquatic Environments*. Blackwell Publishing Ltd, pp. 22–26.
- Tammeorg, O., Möls, T., Niemistö, J., Holmroos, H., Horppila, J., 2017. The actual role of oxygen deficit in the linkage of the water quality and benthic phosphorus release: Potential implications for lake restoration. *Sci. Total Environ.* 599–600, 732–738. doi:10.1016/j.scitotenv.2017.04.244
- Tanentzap, A.J., Yan, N.D., Keller, B., Girard, R., Heneberry, J., Gunn, J.M., Hamilton, D.P., Taylor, P.A., 2008. Cooling lakes while the world warms: Effects of forest regrowth and increased dissolved organic matter on the thermal regime of a temperate, urban lake. *Limnol. Oceanogr.* 53, 404–410. doi:10.4319/lo.2008.53.1.0404
- Taner, M.Ü., Carleton, J.N., Wellman, M., 2011. Integrated model projections of climate change impacts on a North American lake. *Ecol. Modell.* 222, 3380–3393. doi:10.1016/j.ecolmodel.2011.07.015
- Tanner-McAllister, S.L., Rhodes, J., Hockings, M., 2017. Managing for climate change on protected areas: An adaptive management decision making framework. *J. Environ. Manage.* 204, 510–518. doi:10.1016/j.jenvman.2017.09.038
- Tarczyńska, M., Romanowska-Duda, Z., Jurczak, T., Zalewski, M., 2001. Toxic cyanobacterial blooms in a drinking water reservoir-causes, consequences and management strategy.

- Water Sci. Technol. Water Supply 1, 237–246. doi:10.2166/ws.2001.0043
- Thackeray, S.J., Jones, I.D., Maberly, S.C., 2008. Long-term change in the phenology of spring phytoplankton: species-specific responses to nutrient enrichment and climatic change. *J. Ecol.* 96, 523–535. doi:10.1111/J.1365-2745.2008.01355.X
- Thieurmel, B., Elmarhraoui, A., 2019. suncal: Compute sun position, sunlight phases moon position and lunar phase.
- Thornton, K.W., Kimmel, B.L., Payne, F.E., 1990. *Reservoir Limnology: Ecological Perspectives*. John Wiley & Sons, Ltd, New York.
- Threlkeld, S., 1982. Water renewal effects on reservoir zooplankton communities. *Can. Water Resour. J.* 7, 151–167. doi:10.4296/cwrj0701151
- Tickner, D., Opperman, J.J., Abell, R., Acreman, M., Arthington, A.H., Bunn, S.E., Cooke, S.J., Dalton, J., Darwall, W., Edwards, G., Harrison, I., Hughes, K., Jones, T., Leclère, D., Lynch, A.J., Leonard, P., McClain, M.E., Muruven, D., Olden, J.D., Ormerod, S.J., Robinson, J., Tharme, R.E., Thieme, M., Tockner, K., Wright, M., Young, L., 2020. Bending the curve of global freshwater biodiversity loss: an emergency recovery plan. *Bioscience*. doi:10.1093/biosci/biaa002
- Toffolon, M., Piccolroaz, S., Calamita, E., 2020. On the use of averaged indicators to assess lakes' thermal response to changes in climatic conditions. *Environ. Res. Lett.* 15, 034060. doi:10.1088/1748-9326/ab763e
- Toffolon, M., Ragazzi, M., Righetti, M., Teodoru, C.R., Tubino, M., Defrancesco, C., Pozzi, S., 2013. Effects of artificial hypolimnetic oxygenation in a shallow lake. Part 1: Phenomenological description and management. *J. Environ. Manage.* 114, 520–529. doi:10.1016/j.jenvman.2012.10.062
- Toming, K., Kotta, J., Uemaa, E., Sobek, S., Kutser, T., Tranvik, L.J., 2020. Predicting lake dissolved organic carbon at a global scale. *Sci. Rep.* 10, 1–8. doi:10.1038/s41598-020-65010-3
- Tong, Y., Li, J., Qi, M., Zhang, X., Wang, M., Liu, X., Zhang, W., Wang, X., Lu, Y., Lin, Y., 2019. Impacts of water residence time on nitrogen budget of lakes and reservoirs. *Sci. Total Environ.* 646, 75–83. doi:10.1016/j.scitotenv.2018.07.255
- UK Lakes Portal, 2020. Elter Water or Elterwater [WWW Document]. URL <https://eip.ceh.ac.uk/apps/lakes/detail.html#wbid=29222> (accessed 11.13.20).

- Umlauf, L., Burchard, H., 2005. Second-order turbulence closure models for geophysical boundary layers. A review of recent work. *Cont. Shelf Res.* 25, 795–827. doi:10.1016/J.CSR.2004.08.004
- Umlauf, L., Burchard, H., Bolding, K., 2005. GOTM - Sourcecode and Test Case Documentation.
- Underwood, A.J., 1994. On beyond BACI: Sampling designs that might reliably detect environmental disturbances. *Ecol. Appl.* 4, 3–15.
- Uttormark, P.D., Hutchins, M.L., 1980. Input-output models as decision aids for lake restoration. *Water Resour. Bull.* 16, 494–500. doi:10.1111/j.1752-1688.1980.tb03903.x
- Valerio, G., Pilotti, M., Barontini, S., Leoni, B., 2015. Sensitivity of the multiannual thermal dynamics of a deep pre-alpine lake to climatic change. *Hydrol. Process.* 29, 767–779. doi:10.1002/hyp.10183
- Van Liere, L., Gulati, R.D., 1992. Restoration and recovery of shallow eutrophic lake ecosystems in The Netherlands: epilogue. *Hydrobiologia* 233, 283–287. doi:10.1007/978-94-011-2432-4
- van Vliet, M.T.H., Franssen, W.H.P., Yearsley, J.R., Ludwig, F., Haddeland, I., Lettenmaier, D.P., Kabat, P., 2013. Global river discharge and water temperature under climate change. *Glob. Environ. Chang.* 23, 450–464. doi:10.1016/j.gloenvcha.2012.11.002
- Verpoorter, C., Kutser, T., Seekell, D.A., Tranvik, L.J., 2014. A global inventory of lakes based on high-resolution satellite imagery. *Geophys. Res. Lett.* 41, 6396–6402. doi:10.1002/2014GL060641
- Verspagen, J.M.H., Passarge, J., Jöhnk, K.D., Visser, P.M., Peperzak, L., Boers, P., Laanbroek, H.J., Huisman, J., 2006. Water management strategies against toxic *Microcystis* blooms in the Dutch delta. *Ecol. Appl.* 16, 313–327. doi:10.1890/04-1953
- Visser, P.M., Ibelings, B.W., Bormans, M., Huisman, J., 2016. Artificial mixing to control cyanobacterial blooms: a review. *Aquat. Ecol.* 50, 423–441. doi:10.1007/s10452-015-9537-0
- Vollenweider, R.A., 1976. Advances in defining critical loading levels for phosphorus in lake eutrophication. *Mem. dell'Istituto Ital. di Idrobiol.* 33, 53–83.
- Vollenweider, R.A., 1975. Input-output models with special reference to the phosphorus loading concept in limnology. *Schweizerische Zeitschrift für Hydrol.* 37, 53–82.

doi:10.1007/BF02505178

- Wagner, I., Zalewski, M., 2000. Effect of hydrological patterns of tributaries on biotic processes in a lowland reservoir - Consequences for restoration. *Ecol. Eng.* 16, 79–90. doi:10.1016/S0925-8574(00)00092-6
- Wang, S., Qian, X., Han, B.P., Luo, L.C., Hamilton, D.P., 2012. Effects of local climate and hydrological conditions on the thermal regime of a reservoir at Tropic of Cancer, in southern China. *Water Res.* 46, 2591–2604. doi:10.1016/j.watres.2012.02.014
- Wang, W., Lee, X., Xiao, W., Liu, S., Schultz, N., Wang, Y., Zhang, M., Zhao, L., 2018. Global lake evaporation accelerated by changes in surface energy allocation in a warmer climate. *Nat. Geosci.* 11, 410–414. doi:10.1038/s41561-018-0114-8
- Webster, I.T., Sherman, B.S., Bormans, M., Jones, G., 2000. Management strategies for cyanobacterial blooms in an impounded lowland river. *Regul. Rivers-Research Manag.* 16, 513–525. doi:10.1002/1099-1646(200009/10)16:5<513::AID-RRR601>3.0.CO;2-B
- Weinke, A.D., Biddanda, B.A., 2019. Influence of episodic wind events on thermal stratification and bottom water hypoxia in a Great Lakes estuary. *J. Great Lakes Res.* 45, 1103–1112. doi:10.1016/j.jglr.2019.09.025
- Welch, E.B., 1981. The dilution/flushing technique in lake restoration. *J. Am. Water Resour. Assoc.* 17, 558–564. doi:10.1111/j.1752-1688.1981.tb01260.x
- Welch, E.B., Barbiero, R.P., Bouchard, D., Jones, C.A., 1992. Lake trophic state change and constant algal composition following dilution and diversion. *Ecol. Eng.* 1, 173–197. doi:10.1016/0925-8574(92)90001-I
- Welch, E.B., Patmont, C.R., 1980. Lake restoration by dilution: Moses lake, Washington. *Water Res.* 14, 1317–1325. doi:10.1016/0043-1354(80)90192-X
- Wetzel, R.G., 2001a. Water Economy, in: *Limnology: Lake and River Ecosystems*. Academic Press, London, pp. 46–48.
- Wetzel, R.G., 2001b. Fate of Heat, in: *Limnology: Lake and River Ecosystems*. pp. 71–92. doi:10.1016/b978-0-08-057439-4.50010-1
- Wetzel, R.G., 2001c. Oxygen, in: *Limnology: Lake and River Ecosystems*. Academic Press, San Diego, pp. 151–168. doi:10.1016/B978-0-08-057439-4.50013-7
- Weyhenmeyer, G.A., 2001. Warmer winters: Are planktonic algal populations in Sweden's

- largest lakes affected? *Ambio* 30, 565–571. doi:10.1579/0044-7447-30.8.565
- Wilhelm, S., Adrian, R., 2008. Impact of summer warming on the thermal characteristics of a polymictic lake and consequences for oxygen, nutrients and phytoplankton. *Freshw. Biol.* 53, 226–237. doi:10.1111/j.1365-2427.2007.01887.x
- Wilkinson, G.M., Cole, J.J., Pace, M.L., Johnson, R.A., Kleinhans, M.J., 2015. Physical and biological contributions to metalimnetic oxygen maxima in lakes. *Limnol. Oceanogr.* 60, 242–251. doi:10.1002/lno.10022
- Williams, R.J., Boorman, D.B., 2012. Modelling in-stream temperature and dissolved oxygen at sub-daily time steps: An application to the River Kennet, UK. *Sci. Total Environ.* 423, 104–110. doi:10.1016/j.scitotenv.2012.01.054
- Wilson, H., Ayala, A., Jones, I., Rolston, A., Pierson, D., de Eyto, E., Grossart, H.-P., Perga, M.-E., Woolway, R.I., Jennings, E., 2020. Variability in epilimnion depth estimations in lakes. *Hydrol. Earth Syst. Sci. Discuss.* 24, 1–26. doi:10.5194/hess-2020-222
- Winder, M., Schindler, D.E., 2004. Climatic effects on the phenology of lake processes. *Glob. Chang. Biol.* 10, 1844–1856. doi:10.1111/j.1365-2486.2004.00849.x
- Winder, M., Sommer, U., 2012. Phytoplankton response to a changing climate. *Hydrobiologia* 698, 5–16. doi:10.1007/s10750-012-1149-2
- Winslow, L.A., Read, J.S., Hansen, G.J.A., Hanson, P.C., 2015. Small lakes show muted climate change signal in deepwater temperatures. *Geophys. Res. Lett.* 42, 355–361. doi:10.1002/2014GL062325.Received
- Winslow, L.A., Read, J.S., Hansen, G.J.A., Rose, K.C., Robertson, D.M., 2017. Seasonality of change: Summer warming rates do not fully represent effects of climate change on lake temperatures. *Limnol. Oceanogr.* 62, 2168–2178. doi:10.1002/lno.10557
- Winslow, L.A., Zwart, J.A., Batt, R.D., Dugan, H.A., Woolway, R.I., Corman, J.R., Hanson, P.C., Read, J.S., 2016. LakeMetabolizer: an R package for estimating lake metabolism from free-water oxygen using diverse statistical models. *Int. Waters* 6, 622–636. doi:10.1080/iw-6.4.883
- Winter, T.C., 2004. The Hydrology of Lakes, in: Reynolds, C.S., O’Sullivan, P.E. (Eds.), *The Lakes Handbook*, Volume 1. Blackwell Publishing Ltd, Oxford, UK, pp. 61–78. doi:10.1002/9780470999271.ch3

- Wood, S.N., 2011. Fast stable restricted maximum likelihood and marginal likelihood estimation of semiparametric generalized linear models. *J. R. Stat. Soc.* 73, 3–36.
- Woolway, R.I., Jennings, E., Shatwell, T., Golub, M., Pierson, D.C., Maberly, S.C., 2021a. Lake heatwaves under climate change. *Nature* 589, 402–407. doi:10.1038/s41586-020-03119-1
- Woolway, R.I., Jones, I.D., Feuchtmayr, H., Maberly, S.C., 2015a. A comparison of the diel variability in epilimnetic temperature for five lakes in the English Lake District. *Int. Waters* 5, 139–154. doi:10.5268/IW-5.2.748
- Woolway, R.I., Jones, I.D., Hamilton, D.P., Maberly, S.C., Muraoka, K., Read, J.S., Smyth, R.L., Winslow, L.A., 2015b. Automated calculation of surface energy fluxes with high-frequency lake buoy data. *Environ. Model. Softw.* 70, 191–198. doi:10.1016/j.envsoft.2015.04.013
- Woolway, R.I., Kraemer, B.M., Lenters, J.D., Merchant, C.J., O'Reilly, C.M., Sharma, S., 2020. Global lake responses to climate change. *Nat. Rev. Earth Environ.* 1, 388–403. doi:10.1038/s43017-020-0067-5
- Woolway, R.I., Maberly, S.C., 2020. Climate velocity in inland standing waters. *Nat. Clim. Chang.* 10, 1124–1129. doi:10.1038/s41558-020-0889-7
- Woolway, R.I., Meinson, P., Nöges, P., Jones, I.D., Laas, A., 2017a. Atmospheric stilling leads to prolonged thermal stratification in a large shallow polymictic lake. *Clim. Change* 141, 759–773. doi:10.1007/s10584-017-1909-0
- Woolway, R.I., Merchant, C.J., 2019. Worldwide alteration of lake mixing regimes in response to climate change. *Nat. Geosci.* 12, 271–276. doi:10.1038/s41561-019-0322-x
- Woolway, R.I., Merchant, C.J., 2017. Amplified surface temperature response of cold, deep lakes to inter-annual air temperature variability. *Sci. Rep.* 7, 0–8. doi:10.1038/s41598-017-04058-0
- Woolway, R.I., Merchant, C.J., Van Den Hoek, J., Azorin-Molina, C., Nöges, P., Laas, A., Mackay, E.B., Jones, I.D., 2019a. Northern hemisphere atmospheric stilling accelerates lake thermal responses to a warming world. *Geophys. Res. Lett.* 46, 11983–11992. doi:10.1029/2019GL082752
- Woolway, R.I., Sharma, S., Weyhenmeyer, G.A., Debolskiy, A., Golub, M., Mercado-Bettín, D., Perroud, M., Stepanenko, V., Tan, Z., Grant, L., Ladwig, R., Mesman, J., Moore, T.N.,

- Shatwell, T., Vanderkelen, I., Austin, J.A., DeGasperi, C.L., Dokulil, M., La Fuente, S., Mackay, E.B., Geoffrey Schladow, S., Watanabe, S., Marcé, R., Pierson, D.C., Thiery, W., Jennings, E., 2021b. Phenological shifts in lake stratification under climate change. *Nat. Commun.* 12, 1–19. doi:10.1038/s41467-021-22657-4
- Woolway, R.I., Simpson, J.H., Spiby, D., Feuchtmayr, H., Powell, B., Maberly, S.C., 2018. Physical and chemical impacts of a major storm on a temperate lake: a taste of things to come? *Clim. Change* 151, 333–347. doi:10.1007/s10584-018-2302-3
- Woolway, R.I., Verburg, P., Merchant, C.J., Lenters, J.D., Hamilton, D.P., Brookes, J., Kelly, S., Hook, S., Laas, A., Pierson, D., Rimmer, A., Rusak, J.A., Jones, I.D., 2017b. Latitude and lake size are important predictors of over-lake atmospheric stability. *Geophys. Res. Lett.* 44, 8875–8883. doi:10.1002/2017GL073941
- Woolway, R.I., Weyhenmeyer, G.A., Schmid, M., Dokulil, M.T., de Eyto, E., Maberly, S.C., May, L., Merchant, C.J., 2019b. Substantial increase in minimum lake surface temperatures under climate change. *Clim. Change* 155, 81–94. doi:10.1007/s10584-019-02465-y
- Wüest, A., Piepke, G., van Senden, D.C., 2000. Turbulent kinetic energy balance as a tool for estimating vertical diffusivity in wind-forced stratified waters. *Limnol. Oceanogr.* 45, 1388–1400.
- Xing, Z., Fong, D.A., Tan, K.M., Lo, E.Y.M., Monismith, S.G., 2012. Water and heat budgets of a shallow tropical reservoir. *Water Resour. Res.* 48, 6532. doi:10.1029/2011WR011314
- Yang, X., Li, Y., Wang, B., Xiao, J., Yang, M., Liu, C.Q., 2020. Effect of hydraulic load on thermal stratification in karst cascade hydropower reservoirs, Southwest China. *J. Hydrol. Reg. Stud.* 32. doi:10.1016/j.ejrh.2020.100748
- Yang, Y., Stenger-Kovács, C., Padisák, J., Pettersson, K., 2016. Effects of winter severity on spring phytoplankton development in a temperate lake (Lake Erken, Sweden). *Hydrobiologia* 780, 47–57. doi:10.1007/s10750-016-2777-8
- Yankova, Y., Neuenschwander, S., Köster, O., Posch, T., 2017. Abrupt stop of deep water turnover with lake warming: Drastic consequences for algal primary producers. *Sci. Reports* 2017 71 7, 1–9. doi:10.1038/s41598-017-13159-9
- Zamparas, M., Zacharias, I., 2014. Restoration of eutrophic freshwater by managing internal nutrient loads. A review. *Sci. Total Environ.* 496, 551–562. doi:10.1016/j.scitotenv.2014.07.076

- Zhang, M., Shen, Y., 2015. Determination of water flushing characteristics and their influencing factors on the Dahuofang Reservoir in China using an improved ECOMSED model. *Front. Earth Sci.* 9, 394–411. doi:10.1007/s11707-014-0437-8
- Zhang, M., Zhang, Yunlin, Deng, J., Liu, M., Zhou, Y., Zhang, Yibo, Shi, K., Jiang, C., 2022. High-resolution temporal detection of cyanobacterial blooms in a deep and oligotrophic lake by high-frequency buoy data. *Environ. Res.* 203, 111848. doi:10.1016/j.envres.2021.111848
- Zhang, Y., Wu, Z., Liu, M., He, J., Shi, K., Zhou, Y., Wang, M., Liu, X., 2015. Dissolved oxygen stratification and response to thermal structure and long-term climate change in a large and deep subtropical reservoir (Lake Qiandaohu, China). *Water Res.* 75, 249–258. doi:10.1016/j.watres.2015.02.052
- Zinger-Gize, I., Hartland, a, Saxby-Rouen, K.J., Beattie, L., 1999. Protecting the oligotrophic lakes of the English Lake District. *Hydrobiologia* 396, 265–280.
- Zwart, J.A., Sebestyen, S.D., Solomon, C.T., Jones, S.E., 2017. The influence of hydrologic residence time on lake carbon cycling dynamics following extreme precipitation events. *Ecosystems* 20, 1000–1014. doi:10.1007/s10021-016-0088-6